

LONG TERM EVAPORATION PAN DATA TO ESTIMATE POTENTIAL EVAPORATION DURING THE
WARM SEASON ON THE ALASKAN NORTH SLOPE: IMNAVAIT CREEK BASIN

By

John Paul Mumm, B.S.

A Thesis Submitted in Partial Fulfillment of the Requirements

for the Degree of

Master of Science

in

Hydrology-Interdisciplinary

University of Alaska Fairbanks

December 2017

APPROVED:

Dr. Douglas L. Kane, Committee Chair

Dr. Horacio Toniolo, Committee Member

Dr. William Schnabel, Committee Member

Dr. Leroy Hulsey, Chair

Department of Civil and Environmental Engineering

Dr. Douglas Goering, Dean

College of Engineering and Mines

Dr. Michael Castellini, *Dean of the Graduate School*

ABSTRACT

Evapotranspiration plays a significant role in the hydrologic cycle of all basins, yet is only occasionally measured in the Arctic. One simple index method to evaluate evapotranspiration is the evaporation pan. The energy environment surrounding the simple evaporation pan varies considerably from that of the natural environment. Yet, an evaporation pan is a sound way to determine and estimate the potential evapotranspiration, and actual evapotranspiration can be estimated from evaporation pan data by determining and employing a pan coefficient.

An evaporation pan was initially installed in 1986 in the northern foothills of the Brooks Range on the North Slope of Alaska in Imnavait Creek Basin, collecting data for 22 years. The total summer maximum, average, minimum and standard deviation of pan evaporation were 34.9 cm, 29.9 cm, 19.7 cm and 9.3 cm, respectively from 1986 to 2008 (1989 missing). Both, the seasonal water balance and the Priestley-Taylor method for the 2.2 km² Imnavait Creek catchment were used to produce seasonal estimates of actual evapotranspiration. When used in conjunction with the evaporation pan measurements, an average pan coefficient of 0.58 was found in both cases, which was very similar to what was found in an earlier study on Imnavait Creek Basin. The evaporation pan results can also be correlated effectively with other measured variables (such as thawing degree days, air temperature, net radiation, vapor pressure deficit, precipitation, wind speed, and wind direction); this is a method that allows one to predict potential evapotranspiration in areas where it is not measured at broader spatial scales.

Table of Contents

	Page
TITLE PAGE	i
Abstract	iii
Table of Contents	v
List of Figures	vii
List of Tables	ix
List of Equations	xi
List of Appendices	xiii
<i>Chapter 1-Introduction</i>	<i>1</i>
1.1 Literature Review	3
1.2 Site Description	10
1.3 Evaporation Pan	14
1.4 Potential and Actual Evapotranspiration	16
1.5 Spatial Scale Measurements	19
<i>Chapter 2-Methods.....</i>	<i>23</i>
2.1 Data Collection: Evaporation Pan and Met Station	23
2.2 Data Processing	26
<i>Chapter 3-Results</i>	<i>29</i>
3.1 Evaporation Pan	29
3.2 Priestley-Taylor and Coefficient.....	36
3.3 Variable Comparison	39
<i>Chapter 4-Analysis.....</i>	<i>55</i>
4.1 Evaporation Pan	55
4.2 Priestly-Taylor/Coefficient	57
4.3 Variable Comparison/Calculated Potential Evaporation	58
<i>Chapter 5-Discussion</i>	<i>61</i>
<i>Chapter 6-Conclusions</i>	<i>65</i>

REFERENCES.....	67
APPENDICES.....	73

List of Figures

	Page
Figure 1: Location of Kuparuk Basin, Alaskan North Slope (Trochim, 2009).	10
Figure 2: Left panel is The Upper Kuparuk Basin (yellow line is the boundary for the entire Kuparuk watershed) and the right panel shows details of smaller Imnavait Creek Basin (outlined in blue) where evaporation pan was located at the Imnavait B site (Trochim, 2009).	11
Figure 3: Imnavait Creek Basin's beaded stream (white lines) with pools that can reach 1.5m to 3 m deep.	13
Figure 4: Evaporation pan (Type A) used at Imnavait Creek Basin.	15
Figure 5: Arctic Hydrologic Cycle (Kane and Yang, 2004)	18
Figure 6: Instruments used in the Imnavait Creek Basin during the summer of 2009.	19
Figure 7: Meteorological Station at B site in Imnavait Creek Basin	24
Figure 8: 2009 view of the Meteorological Station at B site in Imnavait Creek with Wyoming gauge after a summer snow storm in early July.	25
Figure 9- Cumulative Monthly (June, July, August) pan evaporation (cm).	29
Figure 10- Total Summer summation of evaporation pan and Priestley-Taylor estimates.	30
Figure 11- An example of summer accumulation of pan evaporation.	35
Figure 12- Potential evaporation measured with the evaporation pan vs. actual evapotranspiration calculated using Priestly-Taylor equation.	36
Figure 13- Yearly summation of summer (June, July, August) months of net radiation for 22 years at Imnavait Creek, North Slope, Alaska.	40
Figure 14- Yearly summation of summer (June, July, August) months of thawing degree days for 22 years at Imnavait Creek, North Slope, Alaska.	41
Figure 15- Comparison of Monthly thawing degree days vs. Monthly Sum of evaporation pan measurements.	43
Figure 16- Relationship between the 2008 thawing degree days vs Cumulative pan evaporation.	44
Figure 17- The thawing degree days was used to produce a potential evaporation that is calculated. This shows the close relationship between the measured potential and calculated potential using only TDD.	44
Figure 18- Comparison between the 2008 Warm Season Cumulative net radiation vs. the Cumulative evaporation pan measurements.	45
Figure 19- The net radiation was used to produce a potential evaporation that is calculated. This shows the close relationship between the measured potential and Calculated potential only using Rnet.	45
Figure 20- Comparison between the 2008 Warm Season cumulative vapor pressure deficit vs. the cumulative evaporation pan measurements.	46
Figure 21- The vapor pressure deficit (VPD) was used to produce potential evaporation that is calculated. This figure shows the close relationship between the measured potential and Calculated potential evapotranspiration using only VPD.	46
Figure 22- 22 Years of relationship between cumulative pan evaporation and cumulative thawing degree days, producing linear best-fit equation.	47
Figure 23- 22 Years of relationship between cumulative pan evaporation and cumulative net radiation, producing linear best-fit equation.	47
Figure 24- 2 Years of relationship between cumulative pan evaporation and cumulative vapor pressure deficit, producing linear best-fit equation.	48
Figure 25- 22 years of summer cumulative pan ET vs. Priestley-Taylor calculated ET.	53
Figure 26- 2008 relationship between potential ET and actual ET.	53

List of Tables

	Page
<i>Table 1- June cumulative monthly pan evaporation, average daily pan evaporation, maximum daily pan evaporation, and minimum daily pan evaporation for 22 years at Imnavait Creek, North Slope, Alaska.....</i>	31
<i>Table 2- July cumulative monthly pan evaporation, average daily pan evaporation, maximum daily pan evaporation, and minimum daily pan evaporation for 22 years at Imnavait Creek, North Slope, Alaska.....</i>	32
<i>Table 3- August cumulative monthly pan evaporation, average daily pan evaporation, maximum daily pan evaporation, and minimum daily pan evaporation for 22 years at Imnavait Creek, North Slope, Alaska.....</i>	33
<i>Table 4- Total cumulative warm season pan evaporation, average daily pan evaporation, maximum daily pan evaporation, and minimum daily pan evaporation for 22 years at Imnavait Creek, North Slope, Alaska.....</i>	34
<i>Table 5- Yearly June, July, and August Priestley-Taylor Actual ET and the ET pan coefficient for 22 years at Imnavait Creek, North Slope, Alaska, 1989 missing.</i>	37
<i>Table 6- Total cumulative warm season (June, July, August) potential evaporation, actual evaporation, and ET pan coefficient for 22 years at Imnavait Creek, North Slope, Alaska.....</i>	38
<i>Table 7- Total warm season (June, July, August) 22 year average potential ET calculated using TDD and Rnet. Total warm season (June, July, August) 2 year average potential ET calculated using VPD. The percent difference between the summer (June, July, August) total pan evaporation and the calculated variable potential ET.</i>	39
<i>Table 8- June yearly potential evaporation measured and calculated totals using TDD, RNET, and VPD.....</i>	49
<i>Table 9- July yearly potential evaporation measured and calculated totals using TDD, RNET, and VPD.</i>	50
<i>Table 10- August yearly potential evaporation measured and calculated totals using TDD, RNET, and VPD.....</i>	51
<i>Table 11- Yearly Summer Totals for yearly potential evaporation measured and calculated totals using TDD, RNET, and VPD.</i>	52

List of Equations

	Page
Equation 1- Pan Coefficient equation	16
Equation 2- Priestley-Taylor equation	16
Equation 3- Slope of the temperature-saturated vapor pressure curve in $\text{Pa}^\circ\text{C}^{-1}$	16
Equation 4- psychometric constant in Pa°C	17
Equation 5- Energy balance component	17
Equation 6- Best fit line equation	27
Equation 7- Slope of line equation	27
Equation 8- Line Intercept equation	28
Equation 9- Best fit equation between TDD and pan evaporation	42
Equation 10- Best fit equation between R_{net} and pan evaporation	42
Equation 11- Best fit equation between VPD and pan evaporation	43

List of Appendices

	Page
<i>Appendix A: Warm Season Cumulative pan evaporation 1986-2008.....</i>	<i>73</i>
<i>Appendix B: Warm Season Cumulative Priestley-Taylor calculated evapotranspiration 1986-2008.....</i>	<i>84</i>
<i>Appendix C: Warm Season Cumulative pan evaporation and Priestley-Taylor evapotranspiration 1986-2008.....</i>	<i>95</i>
<i>Appendix D: Warm Season thawing degree days versus times, 1986-2008.</i>	<i>106</i>
<i>Appendix E: Warm Season Comparison (relationship) between thawing degree days and pan evaporation (potential evaporation) 1986-2008.</i>	<i>117</i>
<i>Appendix F: Warm Season Cumulative Calculated potential evaporation using thawing degree days measurements 1986-2008.....</i>	<i>128</i>
<i>Appendix G: Warm Season Cumulative measured pan evaporation (potential evaporation) and Calculated potential evaporation using thawing degree days 1986-2008.</i>	<i>139</i>
<i>Appendix H: Warm Season Comparison between measured and calculated potential evaporation using thawing degree days and pan evaporation 1986-2008.....</i>	<i>150</i>
<i>Appendix I: Warm Season Cumulative net radiation 1986-2008.....</i>	<i>161</i>
<i>Appendix J: Warm Season Comparison (relationship) between net radiation and pan evaporation (potential evaporation) 1986-2008.</i>	<i>172</i>
<i>Appendix K: Warm Season Cumulative Calculated potential evaporation using net radiation measurements 1986-2008.....</i>	<i>183</i>
<i>Appendix L: Warm Season Cumulative measured pan evaporation (potential evaporation) and Calculated potential evaporation using net radiation 1986-2008.</i>	<i>194</i>
<i>Appendix M: Warm Season Comparison between measured and calculated potential evaporation using net radiation and pan evaporation 1986-2008.....</i>	<i>205</i>
<i>Appendix N: Warm Season Cumulative vapor pressure deficit 2007-2008.....</i>	<i>216</i>
<i>Appendix O: Warm Season Comparison (relationship) between vapor pressure deficit and pan evaporation (potential evaporation) 2007-2008.</i>	<i>217</i>
<i>Appendix P: Warm Season Cumulative Calculated potential evaporation using vapor pressure deficit measurements 2007-2008.....</i>	<i>218</i>
<i>Appendix Q: Warm Season Cumulative measured pan evaporation (potential evaporation) and Calculated potential evaporation using vapor pressure deficit 2007-2008.</i>	<i>219</i>
<i>Appendix R: Warm Season Comparison between measured and calculated potential evaporation using vapor pressure deficit and pan evaporation 2007-2008.....</i>	<i>220</i>
<i>Appendix S: Total warm season calculated potential evaporation using an environmental variable (TDD, Rnet, VPD) and measured pan evaporation.....</i>	<i>221</i>

Chapter 1-Introduction

Hydrology is the study of the movement, distribution, and quality of water in the environment, and how the physical environmental changes are affected by the influence of water (Perlman, 2015). Evapotranspiration (ET) plays an important role in the hydrologic cycle of all basins, yet is only occasionally measured in the Arctic. There is actual ET (AET) and potential evapotranspiration (PET). AET is the true amount of both combined transpiration and evaporation, while PET is the estimated amount of transpiration and evaporation that would emit from the basin if there was an unlimited amount of moisture. ET is a significant component of the Arctic hydrologic cycle; as it is one of the major pathways for water to exit basins. When a water balance was completed for Imnavait Creek Basin on the North Slope of Alaska, 74% of the summer precipitation or 50% of the annual precipitation was found to exit the basin due to ET (Kane et al., 1990).

ET measurements at high latitudes are often confounded by considerable variability observed over relatively short distances (Kane et al., 1990). Simple models are used to estimate ET because of the lack of data, and thus do not capture all of the variability. Past studies in the Arctic show that using different methods (Priestley-Taylor method, water balance equation, etc.) produce estimates that can be used to develop an idea on what the ET should be in high latitude locations if there is limited energy and water at the surface (Kane et al., 2004, Mendez et al., 1998, Reid and Faria, 2004, and Rouse and Stewart, 1976). Potential ET can be measured by using a simple instrument such as an evaporation pan. Since potential ET overestimates the actual amount of water that leaves a basin, actual ET is calculated from measurements done by instruments such as the Large Aperture Scintillometer (LAS) and Sonic Anemometer Eddy-Covariance Tower. Both LAS and Eddy-Covariance methods have a much larger foot print than the evaporation pan. Actual ET could also be estimated by water balance averaged over a watershed, or using a pan coefficient. The use of satellites could also be another way of estimating the ET over an entire catchment. By using variables that have a strong relationship to ET, and measuring that variable using the satellite imagery, one could obtain estimates over that catchment.

In the Alaskan Arctic, variables such as the continuous permafrost, lack of trees, vegetation variations, and large seasonal and diurnal effects significantly impact the regional hydrology. Presently, the majority of basic hydrological information on the North Slope of Alaska comes from the Kuparuk River and tributary basins. An enduring environmental monitoring program spans over as long as thirty years in some areas and it is the only designated Long-Term Ecological Research (LTER) area in the Alaskan Arctic. In the near vicinity, the Sagavanirktok and Putuligayuk Rivers have also been meteorologically instrumented and gauged, but less intensively in both spatial and temporal perspectives (McNamara et al., 1998).

In the study by Kane et al. (1990), the use of the evaporation pan was only one of several ways that ET was estimated. The many methods of measuring ET generate challenges with making comparisons; using data at different scales (due to variations in vegetation, soils, and soil moisture availability) also make comparisons difficult. The evaporation pan if scaled up through relationships with other variables could allow for larger scale estimates of the potential evapotranspiration.

The main research objective of this thesis is to develop a technique to estimate ET from basins at larger scales (than at point scale) in the Alaskan Arctic. Since the mid-1980s, the evaporation pan data in Imnavait Creek basin, a small headwater basin and a tributary of the Kuparuk River, was collected. The long-term records from the meteorological station and evaporation pan were used in expanding our understanding what variables have strong relationships with the evaporation pan and which ones can be used to estimate ET at a larger scale.

Hypothesis:

It is hypothesized that one can get quality estimates of PET with an evaporation pan and that one can correlate the measured pan evaporation data with other environmental variables (like vapor pressure deficit, thawing degree days, net radiation, etc.) such that estimates of PET can be made for other areas (such as watershed scale) that are lacking the use of evaporation pans.

1.1 Literature Review

There have been numerous short term studies conducted in the Arctic environment related to the measurement and estimation of evapotranspiration. The methods used in these studies vary from estimations using equations and indirect measurements to actual measurements using eddy covariance, lysimeters, and evaporation pans.

One of the earliest studies performed in the North America Arctic on evapotranspiration was in June thru September 1956 at Barrow, Alaska by Clebsch and Shanks (1968). Using evapotranspirometers they discovered that the evapotranspiration rate increased from 1.08 mm/d to 1.49 mm/d from coastal to inland sites. They also observed that for the inland sites, at least 50% of evapotranspiration was from transpiration.

In 1957 and 1958 Mather and Thornthwaite (1958) performed a study in Barrow, Alaska during the summer (July and August) focusing on the tundra. Using evapotranspirometers and an aerodynamic flux profile method they obtained evapotranspiration rates. The evapotranspirometers had averages of 1.3 mm/d for both years, while the aerodynamic flux method had an average of 1.7 mm/d in 1957 and 0.8 mm/d in 1958. Even with the variations between the measured and calculated methods the comparison was still close. It was observed that evapotranspiration had greater rates in the low-lying wetter study site than the higher elevation drier study site. They found that only 40% of net radiation was used for evapotranspiration in the Arctic, while 80 to 90% is used in mid-latitude moist soil sites.

Weller and Holmgren (1974) conducted a study on the energy balance at a tundra site about 3 km from the coast near Barrow, Alaska in June, July, and August of 1971. The energy balance method gave them rates that compared well with pan evaporation measurements in the area. They observed that most of the latent heat flux that occurred during the snow melt happened from the change from snow to water and not evaporation. Evaporation rates during the snowmelt were 0.2 mm/d while the snow melt ablation rates were 9 mm/d, due to these results the energy balance method shouldn't be used during the snow melt period unless one accounts for the energy used for ablation. Evapotranspiration requires approximately eight times more energy for phase change than snowmelt.

Kane and Carlson (1973) performed a study on estimating the evaporation rate from a lake in the Putuligayuk River basin near Prudhoe Bay, Alaska during the summer months. They estimated the rate to be 2 mm/d using Kohler's equation which is based on lake temperatures and meteorological variables. While the pan evaporation rate in the area was 2.4 mm/d. They observed in late August that the lake level decline was less than the calculated evaporation rate using the Kohler's equation due to possible late-summer subsurface flow entering the lake during maximum depth of thaw of active layer.

From 1969 to 1972 Ohmura (1982) conducted a study on evaporation in the high Arctic tundra at Axel Heiberg Island, Canada. Using the Bowen ratio energy balance (BREB) during the snow free period of the summer the average evaporation rate for all three years was 1.5 mm/d. It was noted that the greatest daily evaporation occurred during the periods of higher solar elevation. The study concluded that 80% of annual precipitation left the area through evaporation

In 1978 in northern Quebec, Wright (1981) conducted a water balance study using the Priestley-Taylor method during the thaw period thru summer months into winter freeze. The method produced average rates of 1.8 mm/d at tundra sites while the average rate from ponds was 2.8 mm/d. Priestley-Taylor uses a constant α which is dependent on the surface wetness. Using a value of 0.74 for dry tundra and 1.26 for saturated surfaces, the rates compared well with evaporation pan and lysimeter measurements.

Rouse (1982a and 1982b) performed a water balance and energy balance study at upland tundra sites near Churchill, Manitoba during 1978 and 1979. Using the Priestley-Taylor method during the snow free period of the summer, evapotranspiration rates calculated out as 1.4 mm/d for both years. Using an α constant of 0.94, the method performed well in many different climatic situations when comparing the rates to estimates from the BREB method. It was reinforced that the constant α is dependent on soil moisture and net radiation. Also it was noted that the highest evapotranspiration rates are after snowmelt period and decrease through the summer due to the maximum solar radiation in late June which decreases throughout the remainder of the summer.

Lafleur and Rouse (1988) conducted a study, on the influence of surface cover and climate on evaporation near southern James Bay, Canada in 1985. They observed that the wetter marsh site experienced large latent heat fluxes and smaller Bowen ratios (Bowen ratio (β) is the ratio between sensible and latent energy fluxes) values than the dry raised backshore sedge meadow site during pre-vegetation growth period. The marsh had higher evaporation rates of 3.6 mm/d while the backshore sedge meadow site had 2.4 mm/d rates. This was due to the dry cover of dead grasses over the underlying soil slowing down the evaporation rate. During the growing period the marsh still had higher evapotranspiration rates with 2.9 mm/d and the backshore sedge meadow having 2.6 mm/d. It was found that the canopy resistance was highest during drier offshore wind conditions. They observed that evapotranspiration increased during the higher canopy resistance due to the large vapor pressure deficit.

During a 5-year period (1982-1986) Marsh and Bigras (1988) studied the evaporation from two different lakes in the Mackenzie River Delta, N.W.T., Canada. Using the Priestley-Taylor method with a constant of 1.26 they compared it to the water balance evaporation rates. 70% of the time the calculated rates were within 15% of the water balance estimates. From 1984-1986 Priestley-Taylor method overestimated cumulative evapotranspiration by 7%.

Kane et al. (1990) and Hinzman et al. (1996) performed a study at Imnavait Creek basin using the energy balance, water balance, and Priestley-Taylor methods to study evapotranspiration. Their study covered a four year span from 1987 to 1990 and having an average evapotranspiration rate of 1.5 mm/d using the energy balance method for the summer months (May thru August) with June having the greatest monthly evapotranspiration rates right after snowmelt. The latent heat flux over the four years was an important energy variable for the area using between 38 and 65% of the net radiation. During the study different methods were compared (water balance, energy balance, Priestley-Taylor, and pan evaporation). They observed that the Priestley-Taylor method with a constant of $\alpha = 0.95$, produced good estimates of evapotranspiration with small amounts of data. Conclusions of the study being that the water balance method produced the best total evapotranspiration amounts over the summer, while the energy balance method produced the best daily evapotranspiration rates. Also, the

evaporation pan predicted sufficient total evapotranspiration amounts over the summer while using a pan coefficient of 0.49.

A study of the hydrology of the tundra wetland complex near Prudhoe Bay, Alaska in 1992 and 1993 by Rovaneck et al. (1996) produced results that showed that evapotranspiration after the snowmelt was the major variable in the water balance equation, with the highest rates in June and July. Over the two summers, evapotranspiration had higher rates than the precipitation in the ponds and wetlands. The Priestley-Taylor method was used to calculate the evapotranspiration rate. The α constant of this equation varied over the wetlands because of the changing soil moisture conditions and transpiration rates. The α value was consistent for the ponds and drier uplands, with the ponds having an $\alpha = 2$ and the drier uplands $\alpha = 0.95$. All the constants were backcalculated by using the water balance method to produce an evapotranspiration estimate. Also the eddy correlation method using the vapor fluxes measured in August backcalculated the Priestley-Taylor method; this produced a constant $\alpha = 1.13$ for the wetlands. Over the study, annually evapotranspiration of wetlands and ponds had higher rates than precipitation (snow water equivalent and summer precipitation), which means that the snowmelt runoff in the area kept the wetlands and ponds filled at the beginning of the warm season. They observed that the overall evaporation amounts from the ponds were greater than the overall evapotranspiration amounts from wetlands.

Mendez et al. (1998) conducted a multi-year study of evapotranspiration in an Arctic coastal wetland using multiple methods; Bowen ratio energy balance, Priestley-Taylor, Penman-Montieth, Penman Combination, energy balance, water balance, eddy correlation, and water balance based on time domain reflectometry (for soil moisture) at Prudhoe Bay, Alaska. The results showed ET during the summer (snow-free) period in the watershed averaged 1.45 mm/day using the BREB method. Evapotranspiration rates were very high right after the snowmelt averaging 3.11 mm/day using the water balance. Evaporation rates from the measured ponds were twice that of the tundra measurements. They concluded that latent heat flux was the dominant energy sink in wetlands and ponds, and where the sensible heat flux was most dominant in the drier upland tundra. The study observed that all models gave

similar results on cumulative and daily model comparisons, with the energy based models (BREB, PT, PM, and EB) comparing best with independent values of ET from the water balance and eddy correlation methods. It was noted that Priestley-Taylor model is best to use to estimate ET from wetland tundra, and if you don't want to measure different variables such as vapor pressure and wind speed.

The hydrological cycle on the North Slope of Alaska was studied in Kane et al. (2004); they focused on hydrological data collected since 1985 for Imnavait Creek and 1996 for the Upper Kuparuk River. These data were used to perform water balance calculations. The two small basins receive about one-third of their annual precipitation as snow and two-thirds as summer precipitation. The most significant hydrological event each year is usually the snowmelt period, producing the highest annual runoff. Yet the largest floods of record are from rainfall or rain/snow mixed summer events. It was observed that the water leaving Imnavait Creek basin is about 50% evaporation and 50% runoff. While for the Upper Kuparuk it is estimated that 64% leaves the basin as runoff and 36% as evapotranspiration. This might be due to the higher terrain, steeper slopes, and extensive bedrock outcrops. Kane et al. also noted that the evaporation pan coefficient averaged out as 0.55.

Reid and Faria (2004) conducted a study on evaporation in small Northwestern Territory, Canada watersheds. They focused on using the water balance studies to provide evaporation data for water management at mine sites. The collected evaporation data were used in different models such as Penman, Priestley-Taylor, and water balance equation to produce evapotranspiration rates. Their study focused on the similar results between using the Penman and Priestley-Taylor methods and how the equations use different variables to calculate the evaporation rates. It was observed that the water balance calculations had much different evaporation results compared to the two other methods used; it was concluded that since the water balance equation doesn't consider some hydrologic processes, such as soil moisture recharge and antecedent moisture conditions, this would explain the differences.

Kane and Yang (2004) conducted an overview of water balance determinations for high latitude watersheds. They compiled results from numerous scattered circumpolar watersheds by

scrutinizing water balance case studies sets that exist. This is a region where such statistics are severely lacking. From the collection of the water balance data for the high latitude regions (Kane and Yang, 2004) it was observed that with increasing latitude there is a decrease in precipitation, although this trend is not as true in coastal regions. The precipitation may decrease but the ratio of runoff to precipitation increases as one proceeds north. This is due to the high runoff and significant precipitation events occurring during the summer with limited surface and subsurface storage due to seasonal frost and permafrost. Also evapotranspiration parallels precipitation and decreases with higher latitudes, due to lack of energy and lack of moisture.

Shutov et al. (2006) conducted a review of methods used to study high latitude evaporation in various environments from boreal forest to the Arctic. The methods focused on both direct (eddy correlation, lysimeter observation) and indirect (energy balance, Priestley-Taylor, Penman). The review paid attention to the principles of each method, especially the ones developed in Russia as they are much different from the methods used elsewhere. Many studies from high latitude locations from Russia, Japan, Canada, and Alaska show the differences in evaporation rates are caused by differences in the method approach and variation in vegetation. A full region summary was formulated to analyze the relationship between evaporation, precipitation, and radiation energy showing similarities with a correlation plot having a value of $r=0.85$. The review observed that evaporation rates decreased from south to north due to a decrease in energy availability and decreased near coastal areas due to low vapor pressure deficit. They also observed that evaporation is greatest at lower elevation and in boreal forest compared to tundra, and that evaporation is strongly controlled by soil moisture levels and incoming solar radiation. Variables such as vegetation type, humidity and wind speed are secondary controlling factors to evaporation.

Liljedahl et al. (2011) conducted a study on nonlinear controls of evapotranspiration in the Arctic coastal wetlands. They focused on defining the controls on evapotranspiration which is the major mechanism of water loss for the coastal wetland systems. Over the multi-year study using the eddy covariance method, near-surface soil moisture and atmospheric vapor pressure

deficit were found to have nonlinear effects on evapotranspiration rates. The value of vapor pressure deficit allowing the latent heat flux to exceed the sensible heat flux was near 0.3 kPa. The dry soils increased surface resistance (water limited) while wet soils favored ground heat flux which limited the available energy for latent and sensible heat fluxes (evaporation). Midday evapotranspiration was suppressed by both dry and wet soils. It was concluded that much of the potential evapotranspiration being suppressed was caused by the low ability of mosses to transfer moisture. The controlling factors (net radiation, vapor pressure, surface moisture, etc.) on midday evapotranspiration on coastal wetlands resulted in an average evapotranspiration rate 75% of the potential evapotranspiration rate. These limitations on the rates can moderate the annual variation of evapotranspiration and reduce the excessive water loss in a warmer climate.

The many studies in the Arctic focusing on evapotranspiration use several different methods in many different environments (all are high latitude) with different vegetation, soil moisture regimes, and climate. They also demonstrate a large variation temporally and spatially, yet they all focus on evapotranspiration in the high latitude environments; comparisons can be made with some conclusions. Evapotranspiration rates are higher in wetter soil moisture locations and lower in tundra and drier environments because of the amount of available water. The evapotranspiration rates in general become lower as latitude increases.

Evapotranspiration has its highest rates in June and decreases over the summer months due to the decreasing availability of water after snowmelt and the decreasing amounts of incoming net radiation after the June solstice. Evapotranspiration mainly occurs during the summer months (May thru September) and barely happens during the winter. Both, the Priestley-Taylor and Bowen ratio energy balance methods are best when comparing to independent values of ET rates (Mendez et al., 1998).

Overall, these studies have compiled decades of evapotranspiration data to quantify evapotranspiration in the Arctic and how to best estimate and measure it.

1.2 Site Description

The Imnavait Creek Basin is a small headwater basin of approximately 2.2 km², located in the northern foothills of the Brooks Range (68°30'N, 149°15'W), 250 km south of the Arctic Ocean (Figure 1). Imnavait Creek flows parallel to the Kuparuk River for 12 km before it joins the Kuparuk River that eventually drains into the Arctic Ocean (Figure 2). The elevation in this area ranges from 880 m at the outlet to 960 m in the headwaters (Kane et al., 1989).

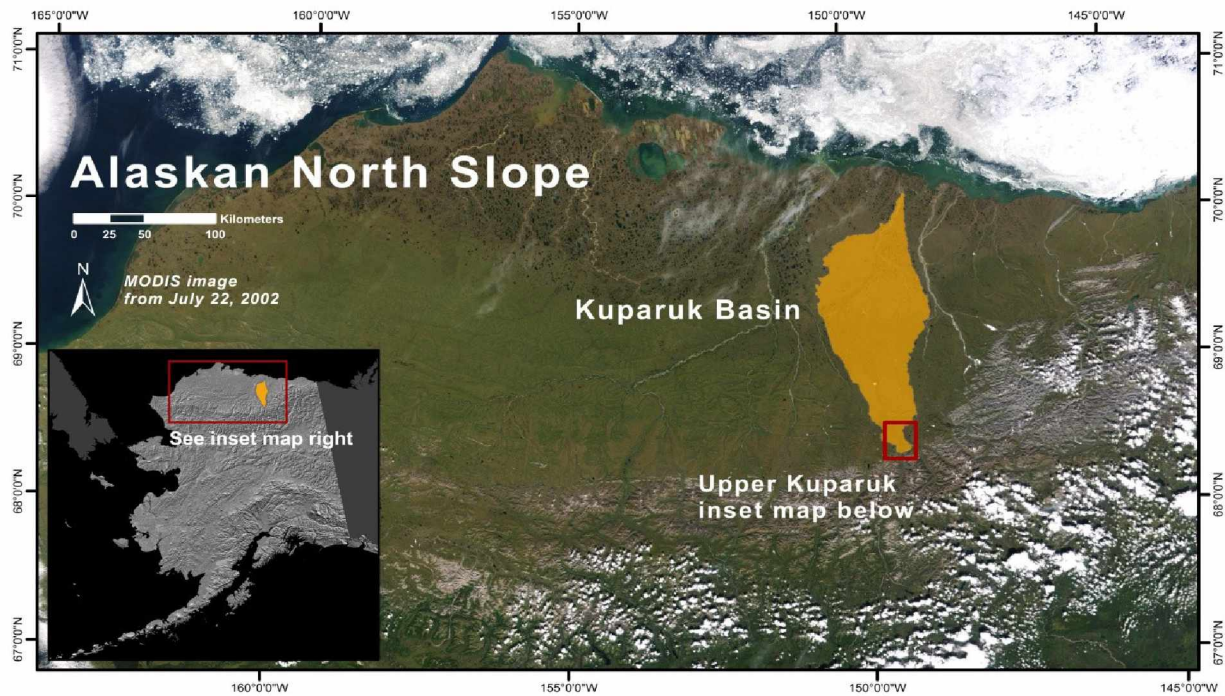


Figure 1: Location of Kuparuk Basin, Alaskan North Slope (Trochim, 2009).

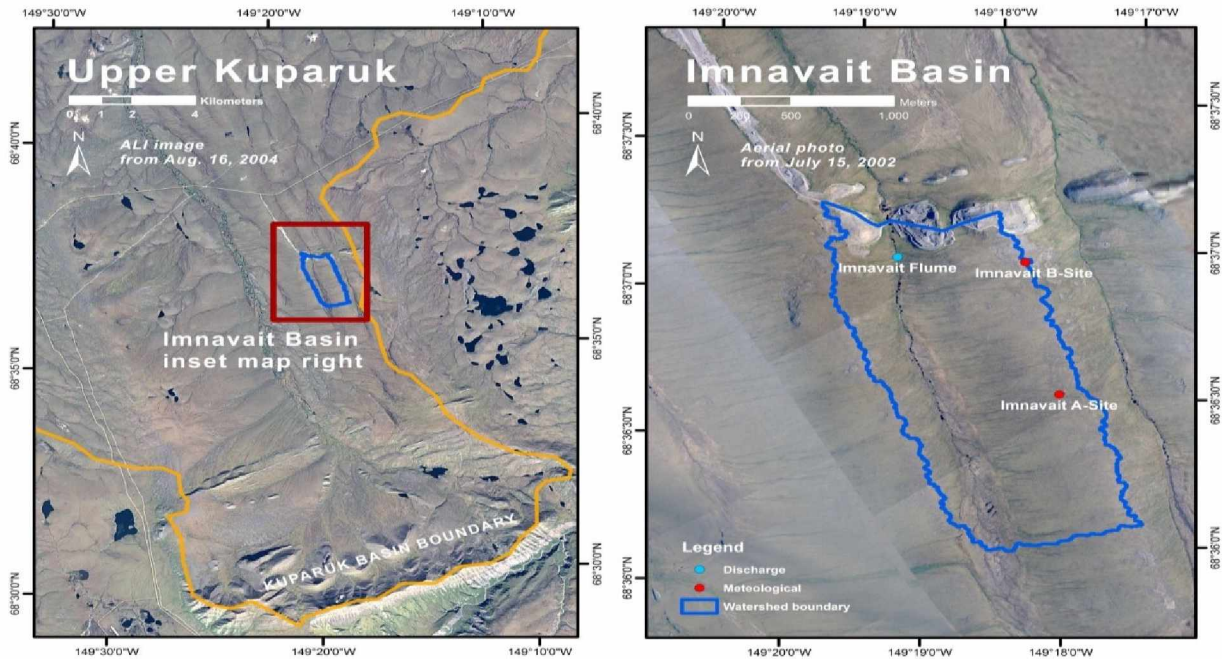


Figure 2: Left panel is The Upper Kupaaruk Basin (yellow line is the boundary for the entire Kupaaruk watershed) and the right panel shows details of smaller Imnavait Creek Basin (outlined in blue) where evaporation pan was located at the Imnavait B site (Trochim, 2009).

The dimensions of the Imnavait Creek Basin are approximately 1 km (width) by 2 km (length) (Kane et al., 1990). The slopes range from 1% to greater than 13%. There are two ridges; the west-facing slope takes up 78% of the basin's area, while the eastern facing slope takes up 22% (Kane et al., 1989).

The Imnavait Creek Basin has continuous permafrost that reaches depths of 250 to 300 m deep (Osterkamp and Payne, 1981). The glacial till and foothills were formed during middle Pleistocene glaciations (Walker et al., 1994). The soils in Imnavait Creek Basin are classified as Histic Pergelic Cryaquepts, which are shallow and variable (Hinzman et al., 1991). Typically, the first 10 cm of the soil consists of both live and dead organic matter. The next 5 to 10 cm is a mix of decomposed organic matter and silt, and the remainder of the profile is composed of glacial till. (Walker et al., 1989). The parent material is a silty colluvium in the basin (Hinzman et al., 1991). The soil has an active layer (a zone above the permafrost that has annual freeze/thaw cycles) that penetrates through the organic layer. This depth of thaw at the end of

summer can typically average 40 to 50 cm but can extend to depths of 100 cm in drier well-drained sites (McNamara et al., 1999). Thaw depths are affected by different factors such as soil type, slope, aspect and soil moisture (Hinzman et al., 1991). Organic soils in the valley bottoms are generally deeper (Hinzman et al., 1991). The geology that dominates the region is known as Cretaceous sedimentary rocks which form east-forming open folds (Black, 1969).

The vegetation in the basin is dominated by acidic tussock tundra. Tussock tundra is much more variable than assumed, having variation in species and growth-form dominance due to factors such as soil pH, snow regime, site stability, and hydrological regime (Walker et al., 1994). The vegetation has five different varieties: dry acidic, moist acidic snowbeds, moist non-acidic snowbeds, moist acidic uplands, and moist non-acidic uplands (Walker et al., 1994). The variation and the distribution of plants in the basin give insight on the hydrological patterns that are affected by the vegetation type. Different plant species require different soil moisture conditions and a range of active layer depths for root viable systems.

The hydrologic characteristics in the basin are controlled by the topography, soils, geology, vegetation, and permafrost. This forces all water to exit the Imnaviat Creek basin through either runoff or ET (Hinzman et al., 1996). There are potentially two possible peak hydrological events in headwater streams, annual snow melt runoff and summer flooding. The discharge that is produced from melting snow is a significant hydrological event each year (Hinzman and Kane, 1991). The excess of water during snowmelt was highest when the spring was particularly warm, there was a deep snowpack which was present until June, or both. Evaporation during spring snowmelt was previously estimated to be up to 4 mm per day in the Imnavait basin measurements from 1985 through 1990 (Kane et al., 1991). Summer events, either rain, snow, or a combination have produced the highest recorded discharge of record in the basin (Kane et al., 2008). They are likely to occur in either July or August (Kane et al., 2003; Kane et al., 2004), but do not occur each year. Precipitation during the summer recharges soil moisture that has been depleted by ET (Kane et al., 1989). The organic layers of the soil profile have a higher hydraulic conductivity than underlying finer-grained mineral soils. If the organic

soil becomes saturated, water can rapidly move down slope through this layer towards the valley bottom. The organic layer can experience moisture content fluctuations of 10 to 90% by volume over the relatively impermeable permafrost (Hinzman et al., 1991). The mineral layer remains saturated through the warm season (except during extended drought periods) due to the permafrost near the surface (McNamara et al., 1997). Imnavait Creek is a beaded stream (Figure 3) made up of a string of ponds and connecting channels (ponds created when ice wedges thaw); organic material covers the stream bottom (McNamara et al., 1997).

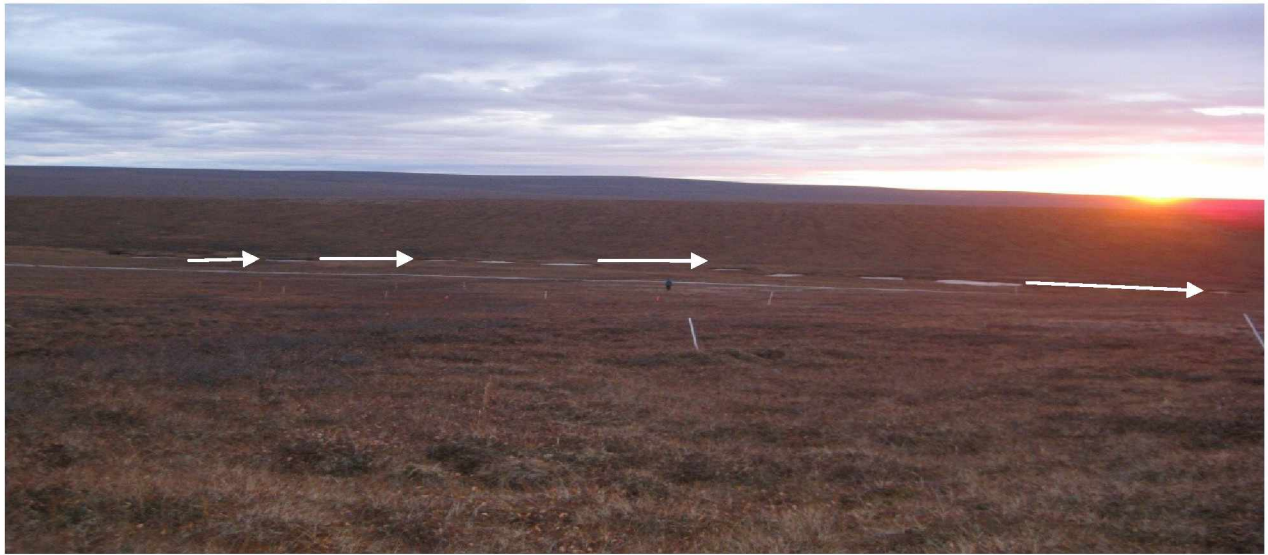


Figure 3: Imnavait Creek Basin's beaded stream (white lines) with pools that can reach 1.5m to 3 m deep.

1.3 Evaporation Pan

An evaporation pan is a simple instrument used for making estimates of potential evaporation. Potential evaporation is an estimate of the evaporation rate if there was a sufficient supply of water available (simulates open water evaporation such as from a pond with available energy). This allows for an estimate of actual evapotranspiration (ET) because we know actual ET is lower due to the varying amount of available water.

The evaporation pan must be used in areas where there is an open fetch or an area that is flat with no objects reaching above the level of the pan (Figure 4). The evaporation pan is slightly elevated above the ground and has a reflectance that is different from that of the surrounding soil and vegetation, causing the measurement to be a closer estimate of potential ET. Pans must be maintained because the albedo can affect the accuracy of the measurements. Evaporation can increase by as much as 10% in dirty pans with lower albedos (Hickox, 1944). Also, natural system ET takes place in an energy environment that is much different than what is happening around the evaporation pan. Transpiration occurs at the leaf surface where conditions can be much different in terms of energy fluxes when compared to that of the elevated evaporation pan. Yet, pan coefficients can be used to account for the soil temperature and climatic characteristics of the area (Kane et al., 1990). Pan coefficients are also used with the potential ET measurements to estimate the actual ET results when using the evaporation pan.

The standard American Class A evaporation pan was used (25.4 cm deep, 120.65 cm in diameter (Kane and Yang, 2004)) during this study. It has been located on the eastern ridge of the Imnavait Creek Basin (Figure 2) on the North Slope of Alaska (Figure 1) (Kane et al., 1990) since 1986. The evaporation pan measurements were taken hourly for 22 years during the summer months (warm season) in concert with precipitation and other meteorological variables. The evaporation pan is used as an index of potential ET over an area where the surface energy balance is uniform. Evaporation pan results deviate from actual ET, due to the impact of variation in soil moisture, vegetation, radiation, etc. Generally results are reported daily, but with updated electronics, sub-daily results can be obtained.

Evaporation rates depend on the supply of water and energy and the vapor pressure gradient, which all depend on meteorological variables such as air and soil temperature, solar radiation, wind speed, atmospheric pressure, and surface area (Xu and Singh, 1998) (Figure 5). Most techniques of estimating evaporation use more than one of these variables in the model, and allow for a close approximation with pan evaporation measurements (Chen et al., 2005). Different models suitable for estimating evaporation use temperature, relative humidity, and both mass-transfer and radiation methods. These methods have been compared with pan evaporation and the dominating variables that affect evaporation were shown to be solar radiation, maximum air temperature, and vapor pressure deficit (Gundalia and Dholakia, 2013). Using these different variables to estimate potential ET, comparisons with the evaporation pan results can be made.



Figure 4: Evaporation pan (Type A) used at Imnavait Creek Basin.

1.4 Potential and Actual Evapotranspiration

Actual ET (AET) is the true amount of combined transpiration and evaporation from a surface; it can range from all transpiration (heavily vegetated) to all evaporation (a lake) (Figure 5). The combination of these two, potential evapotranspiration (PET) and actual evapotranspiration (AET) can be used to estimate an evaporation pan coefficient. The evaporation pan coefficient is defined as:

$$\text{Pan Coefficient} = \frac{\text{Actual ET}}{\text{Potential ET}}.$$

Equation 1- Pan Coefficient equation

Once the pan coefficient is determined it can be used to get estimates of AET using measurements of evaporation pan PET. The coefficient is calculated from the relationship above by dividing the estimated Priestley-Taylor ET (or some other estimate or measurement of ET like the water balance equation) by the measured pan evaporation. Pan coefficients can be used to compensate for the spatial differences such as soil water availability, soil temperature characteristics, and climate variability (Kane et al., 1990). The Priestley-Taylor method of estimating ET over the summer always has a lower summer total than the measured PET from the evaporation pan. The variables necessary for the Priestley-Taylor equation are recorded at the nearby meteorological station located next to the evaporation pan in Imnavait Creek Basin (Figure 2).

Priestley-Taylor is a reliable method to estimate ET. This method uses a coefficient (α) to account for the effects of surface moisture, temperature and vegetation conditions:

$$ET = \alpha * (\Delta / (\Delta + \gamma)) E_R$$

Equation 2- Priestley-Taylor equation

(Reid and Faria, 2004). Where:

$$\Delta = 4098 * e_{as} / (237.3 + T)^2$$

Equation 3- Slope of the temperature-saturated vapor pressure curve in $\text{Pa } ^\circ\text{C}^{-1}$

$$\gamma = C_p * P_A / 0.622 * l_v$$

Equation 4- psychrometric constant in Pa °C

$$E_R = (R_n - H - G / l_v * \rho_w) \times (8.67 \times 10^7)$$

Equation 5- Energy balance component

Where:

ET = evapotranspiration (mm/day)

E_R = energy balance component (mm/day)

γ = psychrometric constant in Pa °C

e_{as} = saturated vapour pressure (Pa) at the air temperature (°C)

T = air temperature in Celsius (°C)

C_p = specific heat of air (J kg⁻¹ °C)

P_A = atmospheric pressure at 20°C (Pa)

R_n = net solar radiation (W m⁻²)

H = sensible heat flux (W m⁻²)

G = ground heat flux (W m⁻²)

l_v = latent heat of vaporization (J kg⁻¹)

ρ_w = water density at 10°C (kg m⁻³)

α = constant

The coefficient α is usually 1.26 in the sub-Arctic but it has been found to vary in the Arctic (Priestley and Taylor, 1972). It was determined that surface control factors for several different kinds of tundra and woodland surfaces in the Canadian sub-Arctic produced a lower coefficient of α = 0.95 (Rouse and Stewart, 1976). It has been found that the value of α is linked to the

Bowen ratio method, which depends on moisture from the evaporated surface (Shutov et al., 2006). Wet surfaces have a higher coefficient than dry surfaces (Eaton et al., 2000) since the Arctic is generally drier than the sub-Arctic, it is understandable to have a lower coefficient. The Priestley-Taylor method is commonly used when meteorological data are not abundant. Also, it doesn't require as much input data as other models (Mendez et al., 1998). The Priestley-Taylor method is used due to it being simpler than the Penman and being more comparable to other methods (Mendez et al., 1998); yet the α coefficient causes problems. For a better idea on what the coefficient should be for use in the equation, it can be produced by back calculating the coefficient from measured latent heat (measured pan evaporation) (Young et al., 1997).

The 22 years of data will allow many different looks at cumulative warm season (summer) and monthly pan evaporation. The comparison between the many different summer data curves will focus on cumulative summer plots. Cumulative ET curves allow for more of a visual means of comparing trends (Mendez et al., 1998). How different factors such as air temperature, radiation, and vapor pressure deficit affect the potential and actual ET can be seen through visual trends.

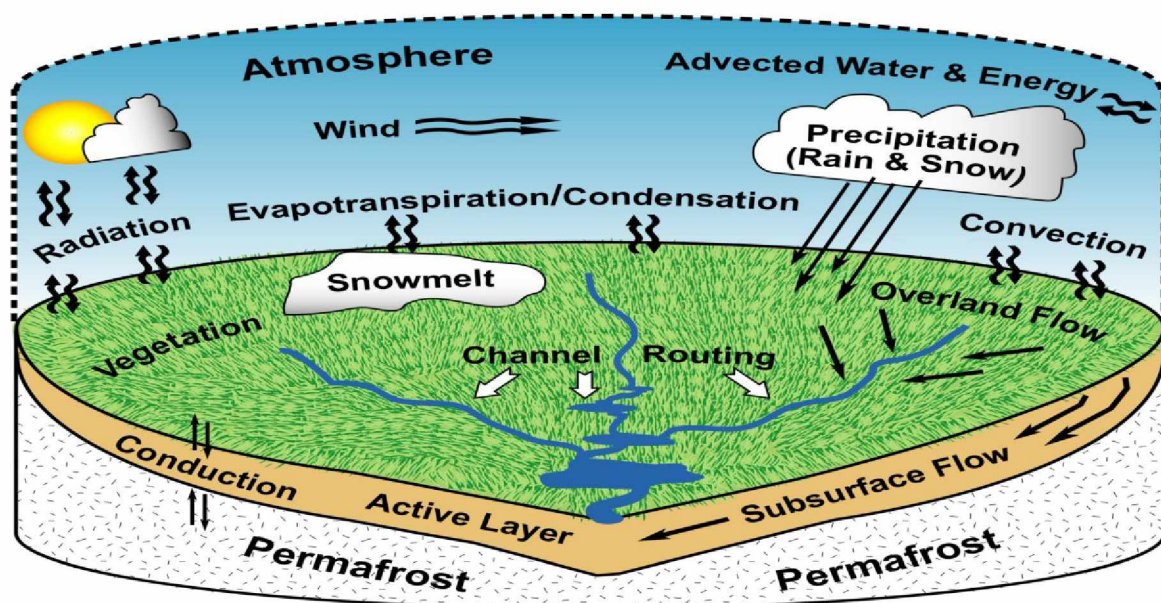
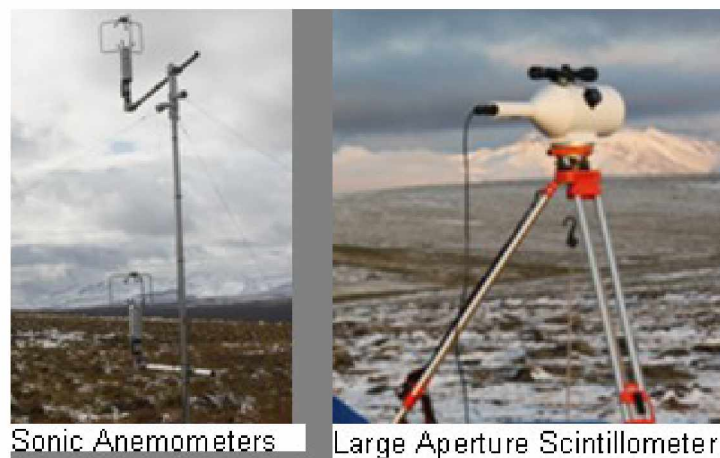


Figure 5: Arctic Hydrologic Cycle (Kane and Yang, 2004)

1.5 Spatial Scale Measurements

ET can be measured at different scales, ranging from point scale to regional scale. ET measurements can become more difficult to attain at increasing spatial scales because of increasing heterogeneity of soils, vegetation, topography and atmospheric variables. At larger scales, there is the additional challenge of the lack of innovative equipment suitable for measuring ET. The evaporation pan is a point measurement of potential ET which only reflects the micro-climate around the evaporation pan. These point estimates of ET are often utilized as the average over the surrounding area (small catchment); the question is how reliable is this procedure in catchments with considerable heterogeneity. The evaporation pan may only be a point measurement but so is the Priestley-Taylor method of calculated ET, which uses the variables from a meteorological station (in this case the one located on the eastern ridge of the Imnavait basin (Figure 2)). Other instruments such as the Large Aperture Scintillometer (LAS) or Sonic Anemometer (Eddy covariance towers) (Figure 6) both have larger measurement footprints than the point measurement of the evaporation pan and they both make actual ET estimates, but they still don't account for the entire large basins.

Figure 6: Instruments used in the Imnavait Creek Basin during the summer of 2009.



The LAS can measure the differences between vegetation and the soil moisture differences due to the sensible heat measurements in the path of the laser. The LAS allows for the measurement of ET at the small basin scale with more accuracy than the water balance equation (Hartogensis et al., 2003). The largest problem with the LAS is when it can be used and how it only covers a single path. The path can stretch across a basin but the soil moisture and sensible heat fluxes are different for other paths, so it is necessary to move the LAS throughout the basin, or have a few instrument sets (Chehbouni et al., 2000).

Eddy Covariance (EC) flux towers determine sensible and latent heat fluxes at 3 m above the canopy height. It has a larger footprint (approximately size of the upwind area which can range up to 400 meters distance from the tower) than meteorological stations (essentially point measurement), but is much smaller than the LAS (which can be up to two km in length). EC flux towers are equipped with a sonic anemometer, water vapor open-path sensor, and high-speed temperature sensor (Persson et al., 2002). The EC flux towers estimate water vapor fluxes and can be used to back calculate to see if the calculated methods such as Priestley-Taylor are coming up with reasonable estimates. It also can be used to determine constants in evaporation equations. The advantage of the EC flux towers to determine ET is having both the latent heat and sensible heat fluxes (Liu et al., 2009). The results can then be compared to variables that can be measured at larger scales such as surface temperature, net radiation, and vapor pressure deficit. By measuring both the relative humidity and the air temperature, the saturated vapor pressure and the actual vapor pressure can be calculated.

The use of satellite imagery to make an estimate of the potential ET is possible if there is some relevant measurement of a physical variable such as surface temperature. The use of remotely sensed imagery has the potential of estimating ET at larger scales using the simple idea of the close relationship between the potential ET from an evaporation pan and some characteristic of the imagery. The use of remote sensing at high latitude locations, especially up on the North Slope of Alaska, has many challenges. High latitudes have fewer satellites to provide data. Also, for locations with heavy cloud cover, the challenge of cloudless days can cause large periods where estimates need to be adjusted. The unique lengths of daylight in Alaska during

the summer and winter, also causes challenges with calculations that are commonly used in the contiguous United States (Bindschadler, 2003). Still, the challenges that come with using remote sensing at high latitudes (limited amounts of data and cloud coverage) can be partially corrected and ET can be predicted fairly accurately. Atmospheric corrections can be performed with the use of an algorithm that accounts for the percent of clouds in the air or a prediction of the soil moisture (Cristobal et al., 2009). Remote sensing using Landsat has been used for ET estimates for over 30 years. The advantage of remote sensing is the ability to measure parameters at scales that can't be covered by field instruments or where access to remote areas is a challenge. Landsat orbits overlap at high latitudes, thus increasing the amount of data coverage available. The largest challenge of using remote sensing is having cloudless days.

Chapter 2-Methods

2.1 Data Collection: Evaporation Pan and Met Station

Historically, evapotranspiration (ET) has been estimated on the North Slope of Alaska using many different methods such as: water balance, energy balance, Priestley-Taylor, Penman, and Thornwaite approaches using meteorological station data and hydrological data (Mendez et al., 1998). These different methods of calculation produce estimates that don't accurately account for spatial and temporal variability of soil moisture, topography, surface temperature, or heterogeneity of surface vegetation (Zhang et al., 2009). These calculations yield estimates of the actual ET that has occurred; while the evaporation pan method is an estimate of potential ET (Shutov et al., 2006).

The data collection occurred at one main location on the ridge of the west-facing slope known as B site (Figure 2). The meteorological station and evaporation pan are located both at B site which has been operational since 1985 (Figures 7 and 8). The meteorological station measures air temperature and relative humidity at heights of 1, 3, and 10 meters. Also measured is wind speed and direction at heights of 1 and 10 meters. Over time there have been a variety of other sensors used; currently the measurements are made using air temperature probes, humidity probes, and an anemometer. Soil temperature is measured using a thermistor along with a data logger. Radiation is measured using a net radiometer. Also, the use of multiple pyrgeometers, that measured the longwave and shortwave radiation both, incoming and outgoing are used.

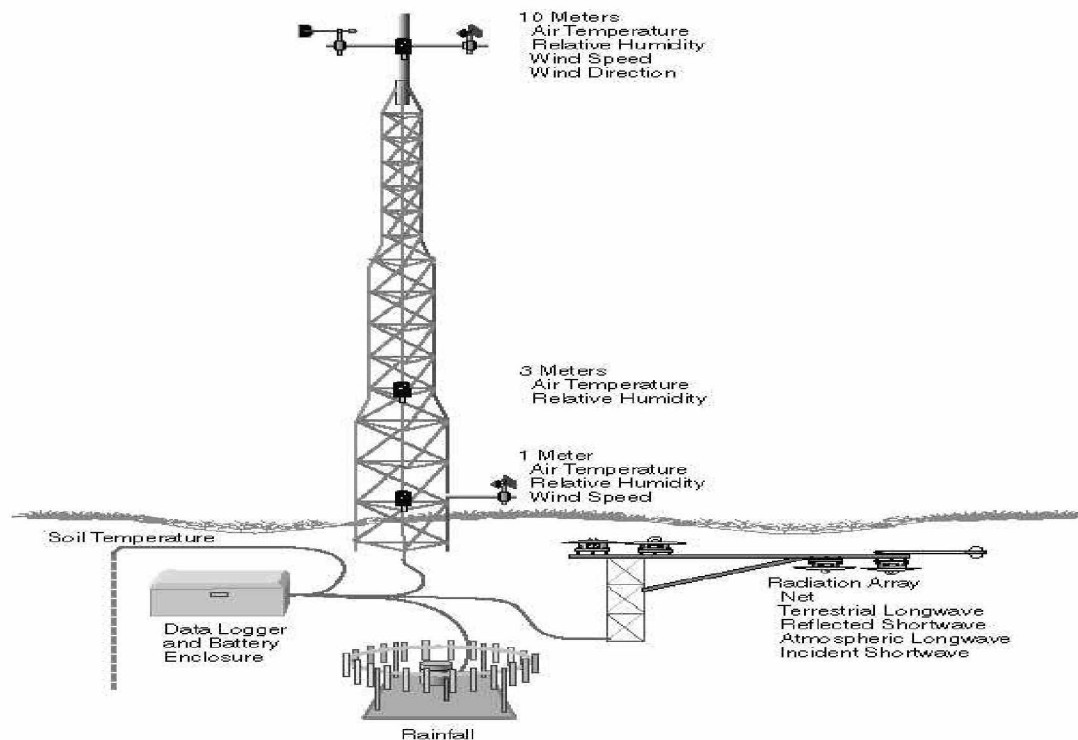


Figure 7: Meteorological Station at B site in Imnaviat Creek Basin

The evaporation pan was a class A evaporation pan that makes measurements from May till September (warm season) using a pressure transducer that measured water levels. An observer checked on the evaporation pan occasionally during the summer. Precipitation was measured using a tipping bucket at intervals of 0.3 mm with the gauge having an Alter shield. A Wyoming snow gauge was also located at B site to measure total precipitation, but mainly intended for cold season solid precipitation.

At Imnaviat Creek (Figure 2) there was a trapezoidal/v-notch weir that was used to measure the basin discharge. Before spring of 2011, stream-flow measurements were made twice a day during the spring break-up using either a cup type current meter or an Acoustic Doppler current meter to gather stream data for the water balance equation. Stream stage data was recorded at the weir using a pressure transducer, and this data was combined with the discharge data collected using the current meters to establish a rating curve.



Figure 8: 2009 view of the Meteorological Station at B site in Imnavait Creek with Wyoming gauge after a summer snow storm in early July.

Measuring ET from land surfaces in high latitude locations poses significant challenges in determining accurate estimates due to the remoteness of the measuring sites, difficulties of continuous measurements throughout the year and even summer measurements are not always possible, and instruments are powered by batteries or small generators that are not always reliable. ET is dependent on the variability of weather, soils, and vegetation. Therefore studies of long duration are preferred (Kane et al., 1990). Past studies by Kane et al. (1990 and 2004) in the Arctic have shown that using different methods (Priestley-Taylor, water balance equation, etc.) produce ET estimates that are not accurate at the basin scale. Instrumental error is common in high latitude environments due to extreme weather conditions and disturbances by animals.

2.2 Data Processing

The main data processed was the evaporation pan data that was collected for 22 years at B site in Imnaviat Creek Basin (Figure 2). The evaporation pan data was plotted as cumulative evaporation for the warm season each year. Since each year started and ended at different times due to variability of when break-up occurs and when winter is reinstated, the “summer” months were broken down into just June, July, and August. The lack of full months in May and September when temperatures were above freezing (evaporation pan with an ice cover) resulted in monthly estimates that were outliers.

Data was cleaned of breaks and negative evaporation pan measurements; meaning either there was an increase in water in the pan or fluctuations on the water level in the evaporation pan caused by wind, animal disturbance, precipitation, or some other error. Since these errors caused problems with cumulative evaporation totals for both summer total and monthly time amounts, negative numbers were zeroed and breaks were linearly interpolated. Missing data up to 12 hours were corrected by linear interpolation. The data were measured at an hourly rate over 22 years (during warm season for evaporation pan) of data collection; each day was converted into mean daily pan evaporation. Each day started at the 12:01 am and had a final measurement at midnight.

Monthly pan evaporation for 22 years is shown in Figure 9. Total warm season (June, July, and August) pan evaporation and Priestley-Taylor ET is shown in Figure 10. The Priestley-Taylor was used in this study as the method to calculate actual ET (Kane et al., 1990).

Once the evaporation pan data was set up for cumulative monthly and summer graphs and Priestley-Taylor comparisons, additional comparisons against variables were made. This additional data were also measured at the B site meteorological station. The different variables that the evaporation pan data were compared against were precipitation, thawing degree days (TDD), net radiation (RNet), and vapor pressure deficit (VPD). All data was from the 1 m height measurements at the meteorological station. Thawing degree days (air temperature) and net radiation are measured, while vapor pressure deficit is calculated from other variables measured. Air temperature and relative humidity are measured to calculate what the

saturated vapor pressure and the actual vapor pressure are. Vapor pressure deficit is calculated as the difference between the actual vapor pressure minus the saturated vapor pressure. The different variable data sets had more errors/missing data than the evaporation pan data. Missing data and erroneous data over 12 hours in duration wasn't corrected by using linear interpolation. First the 3 meter height was checked to see if that data was available, and then checked to see if there was a good correlation between the two heights. If data couldn't be used from the B site meteorological station, the Upper Kupařuk has a nearby meteorological station that collects similar data and this was substituted.

Correlations between the variables and the evaporation pan data were calculated to see how strong of a relationship there was between them. The variables that had high correlations for all 22 years (net radiation, thawing degree days, and vapor pressure deficit) against pan evaporation were examined (best fit) to see if that variable had a high probability of predicting potential ET assuming no evaporation pan is available.

The best regression fit line associated with the n points $(x_1, y_1), (x_2, y_2), \dots, (x_n, y_n)$ has the form

$$y = mx + b$$

Equation 6- Best fit line equation

where

y= potential evaporation (mm)

x= variable data (thawing degree days, net radiation, vapor pressure deficit)

$$\text{Slope} = m = \frac{n \sum xy - (\sum x)(\sum y)}{n \sum (x^2) - (\sum x)^2}$$

Equation 7- Slope of line equation

$$\text{Intercept} = b = \frac{\sum y - m(\sum x)}{n}$$

Equation 8- Line Intercept equation

(Waner, c2000-2008).

The regression line equation was used with the data variables listed above and compared against the cumulative evaporation pan data of each warm season.

Chapter 3-Results

3.1 Evaporation Pan

The evaporation pan results focused on monthly and total warm season cumulative potential evaporation (Figure 9 and 10). The results included data from 1986 to 2008 (1989 missing), June through August. The summer cumulative maximum, average, minimum and standard deviation of pan evaporation are 34.9 cm, 29.9 cm, 19.7 cm and 9.3 cm respectively.

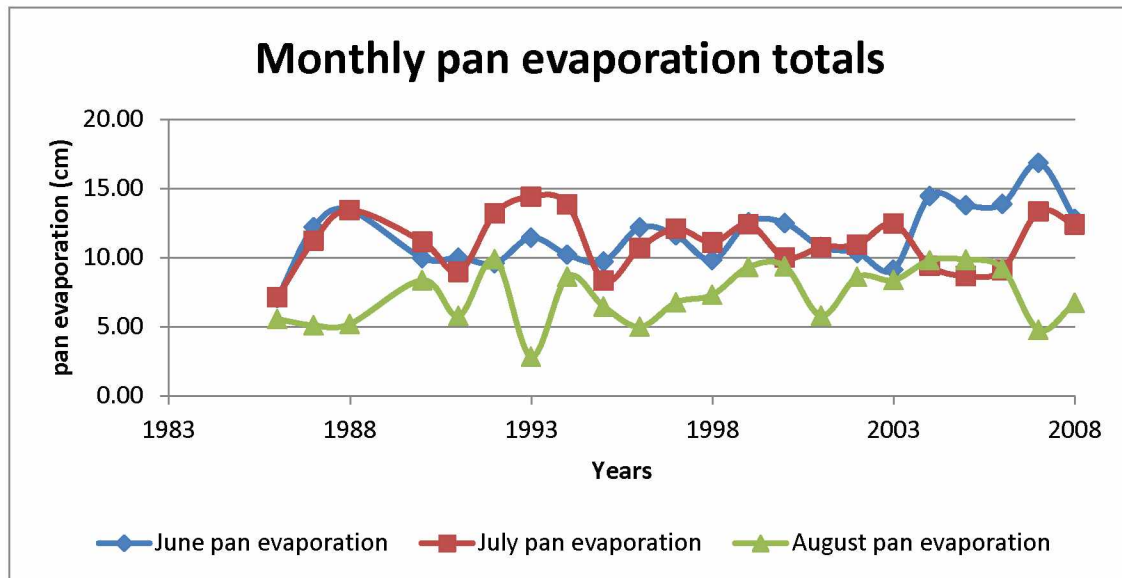


Figure 9- Cumulative Monthly (June, July, August) pan evaporation (cm).

June and July had the highest amounts of monthly evaporation (Figure 9). It varied over the 22 years of record which specific month had more pan evaporation, but overall June had the highest (Figure 9). Evaporation also has shown an increase over the last 22 years (Figure 10).

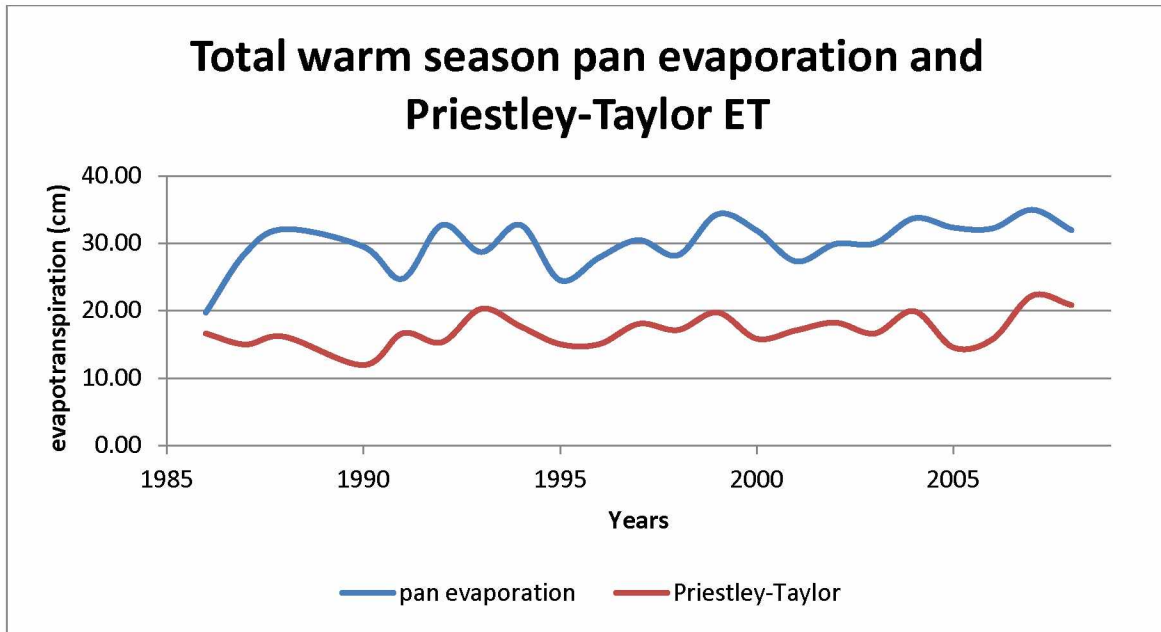


Figure 10- Total Summer summation of evaporation pan and Priestley-Taylor estimates.

Tables 1 - 3 show the cumulative pan evaporation monthly, daily average for that month and monthly daily maximum and minimum for each year throughout the summer. The warm season pan evaporation totals are shown in Table 4 which shows the cumulative warm season (June, July, and August) total, warm season daily average, daily maximum, and daily minimum measurements of pan evaporation.

Table 1- June cumulative monthly pan evaporation, average daily pan evaporation, maximum daily pan evaporation, and minimum daily pan evaporation for 22 years at Imnavait Creek, North Slope, Alaska.

years	June Monthly evaporation pan (cm)	June Daily Average (cm/day)	June Daily Max (cm/day)	June Daily Min. (cm/day)
1986	7.1	0.29	0.72	0.00
1987	12.2	0.41	1.27	0.00
1988	13.4	0.45	2.67	0.00
1990	10.0	0.33	0.65	0.00
1991	10.0	0.33	0.87	0.00
1992	9.6	0.42	0.99	0.00
1993	11.5	0.38	1.20	0.00
1994	10.2	0.34	0.98	0.00
1995	9.7	0.32	0.76	0.01
1996	12.2	0.41	1.08	0.00
1997	11.6	0.41	0.83	0.00
1998	9.8	0.33	1.00	0.00
1999	12.6	0.42	1.17	0.00
2000	12.5	0.45	0.91	0.00
2001	10.8	0.37	0.76	0.00
2002	10.3	0.34	0.86	0.00
2003	9.1	0.43	0.67	0.00
2004	14.5	0.48	0.73	0.02
2005	13.8	0.46	1.25	0.00
2006	13.9	0.46	1.19	0.00
2007	16.9	0.56	1.99	0.01
2008	12.8	0.43	1.39	0.00
Average	11.6	0.40	1.09	0.00
Standard Deviation	2.2	0.06	0.47	0.01

Table 2- July cumulative monthly pan evaporation, average daily pan evaporation, maximum daily pan evaporation, and minimum daily pan evaporation for 22 years at Imnavait Creek, North Slope, Alaska.

years	July Monthly evaporation pan (cm)	July Daily Average (cm/day)	July Daily Max (cm/day)	July Daily Min. (cm/day)
1986	7.1	0.23	0.83	0.00
1987	11.2	0.36	1.05	0.00
1988	13.4	0.43	1.48	0.00
1990	11.1	0.36	0.90	0.00
1991	9.0	0.29	0.77	0.00
1992	13.2	0.43	1.07	0.01
1993	14.4	0.46	0.99	0.00
1994	13.9	0.45	0.92	0.06
1995	8.3	0.27	0.72	0.00
1996	10.7	0.35	0.85	0.08
1997	12.1	0.39	0.73	0.00
1998	11.1	0.36	0.63	0.01
1999	12.4	0.40	0.76	0.01
2000	10.0	0.32	0.88	0.00
2001	10.7	0.35	1.20	0.00
2002	10.9	0.35	0.76	0.00
2003	12.5	0.40	0.97	0.00
2004	9.4	0.30	0.87	0.00
2005	8.7	0.28	1.29	0.00
2006	9.1	0.29	1.20	0.00
2007	13.3	0.43	1.27	0.00
2008	12.4	0.40	1.63	0.00
Average	11.1	0.36	0.99	0.01
Standard Deviation	2.0	0.06	0.26	0.02

Table 3- August cumulative monthly pan evaporation, average daily pan evaporation, maximum daily pan evaporation, and minimum daily pan evaporation for 22 years at Imnavait Creek, North Slope, Alaska.

years	August Monthly evaporation pan (cm)	August Daily Average (cm/day)	August Daily Max (cm/day)	August Daily Min (cm/day)
1986	5.5	0.22	0.77	0.03
1987	5.1	0.18	0.50	0.00
1988	5.2	0.21	0.81	0.00
1990	8.4	0.27	0.88	0.00
1991	5.8	0.19	0.53	0.00
1992	9.9	0.32	1.62	0.00
1993	2.8	0.17	0.69	0.00
1994	8.6	0.28	0.65	0.00
1995	6.5	0.21	0.55	0.00
1996	5.0	0.18	0.46	0.00
1997	6.8	0.22	0.72	0.00
1998	7.3	0.24	0.54	0.03
1999	9.3	0.30	0.59	0.04
2000	9.4	0.30	0.81	0.00
2001	5.8	0.19	1.23	0.00
2002	8.6	0.28	1.81	0.00
2003	8.4	0.27	0.67	0.00
2004	9.8	0.33	1.07	0.00
2005	9.9	0.32	0.84	0.00
2006	9.2	0.30	1.13	0.00
2007	4.8	0.15	0.68	0.00
2008	6.7	0.22	0.94	0.00
Average	7.2	0.24	0.84	0.00
Standard Deviation	2.0	0.06	0.35	0.01

Table 4- Total cumulative warm season pan evaporation, average daily pan evaporation, maximum daily pan evaporation, and minimum daily pan evaporation for 22 years at Imnavait Creek, North Slope, Alaska.

years	Total Warm Season evaporation pan (cm)	evaporation pan Daily Average (cm)	Max Daily (cm)	Min Daily (cm)
1986	19.7	0.25	0.83	0.00
1987	28.5	0.32	1.27	0.00
1988	32.1	0.37	2.67	0.00
1990	29.5	0.32	0.90	0.00
1991	24.7	0.27	0.87	0.00
1992	32.7	0.38	1.62	0.00
1993	28.7	0.37	1.20	0.00
1994	32.7	0.36	0.98	0.00
1995	24.5	0.27	0.76	0.00
1996	27.9	0.32	1.08	0.00
1997	30.4	0.34	0.83	0.00
1998	28.2	0.31	1.00	0.00
1999	34.3	0.37	1.17	0.00
2000	31.9	0.35	0.91	0.00
2001	27.3	0.30	1.23	0.00
2002	29.9	0.32	1.81	0.00
2003	30.0	0.36	0.97	0.00
2004	33.7	0.37	1.07	0.00
2005	32.3	0.35	1.29	0.00
2006	32.2	0.35	1.20	0.00
2007	34.9	0.38	1.99	0.00
2008	31.9	0.35	1.63	0.00
Total Average	29.9	0.34	1.24	0.00
Total Standard Deviation	3.6	0.04	0.46	5.64E-05

The graph of summer 2008 cumulative pan evaporation (Figure 11) is used as an illustrated example graph for the 22 years of data. The remainder of the cumulative evaporation pan graphs can be found in the Appendix A.

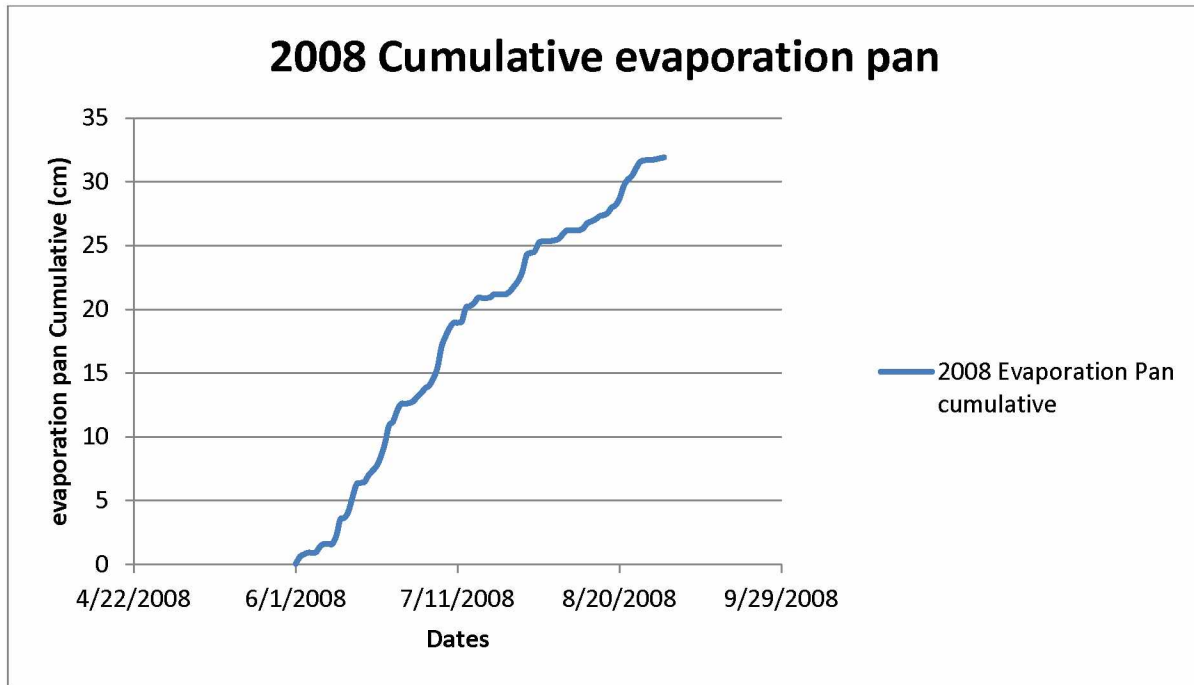


Figure 11- An example of summer accumulation of pan evaporation.

3.2 Priestley-Taylor and Coefficient

As explained earlier, the potential evaporation cumulative warm season total was higher than the actual evapotranspiration (AET) cumulative summer total (Figures 10 and 12). The remainder of the cumulative Priestley-Taylor and Priestley-Taylor vs evaporation pan graphs for other years can be found in the Appendices A, B, and C. The June, July, and August AET monthly cumulative totals and ET pan coefficient are published in Table 5. Table 6 is the summer cumulative yearly totals for the Priestley-Taylor calculated AET, measured evaporation pan potential evaporation, and the calculated pan coefficient. High pan coefficients result from high evaporation rates relative to the potential ET, and the low evaporation pan coefficient was when the Priestley-Taylor estimated ET was low relative to potential ET. The ET coefficient average over the 22 years is 0.58 (Table 6).

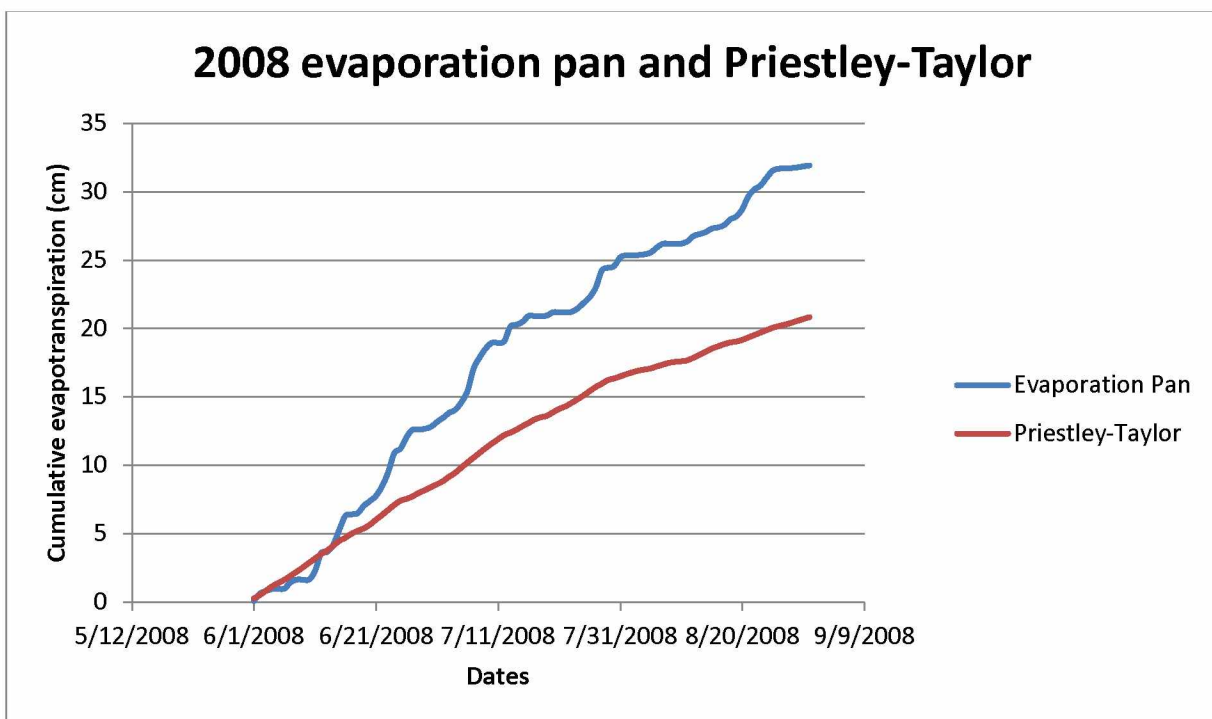


Figure 12- Potential evaporation measured with the evaporation pan vs. actual evapotranspiration calculated using Priestly-Taylor equation.

There were outliers (a value that is outside, much smaller or larger, than the rest of the data set) found in monthly and warm season total pan coefficients caused by instrumental error which is common in high latitude environments due to extreme weather conditions and disturbances by animals. Outliers were found in the 1986 June (Table 1), 1986 July (Table 2), and 1986 total ET pan coefficient (Table 6), 1990 August (Table 3) and 1990 total ET pan coefficient (Table 6), 1993 August (Table 3) and 1993 total ET pan coefficient (Table 6), and 2007 August monthly ET pan coefficient (Table 5).

Table 5- Yearly June, July, and August Priestley-Taylor Actual ET and the ET pan coefficient for 22 years at Imnavait Creek, North Slope, Alaska, 1989 missing.

years	June Priestley-Taylor (cm)	June ET pan coefficient	July Priestley-Taylor (cm)	July ET pan coefficient	August Priestley-Taylor (cm)	August ET pan coefficient
1986	7.2	1.02	6.4	0.89	3.1	0.55
1987	7.0	0.57	6.0	0.54	1.9	0.38
1988	7.0	0.52	6.4	0.47	2.8	0.53
1990	5.3	0.53	4.7	0.42	1.9	0.23
1991	7.5	0.75	6.0	0.66	3.2	0.56
1992	4.7	0.49	7.3	0.55	3.4	0.34
1993	8.2	0.72	9.2	0.64	2.8	1.01
1994	6.4	0.63	7.5	0.54	3.7	0.43
1995	6.0	0.61	5.9	0.70	3.2	0.50
1996	6.2	0.51	6.0	0.56	2.9	0.58
1997	7.6	0.65	6.7	0.55	3.8	0.56
1998	6.3	0.64	7.3	0.65	3.6	0.50
1999	7.9	0.62	7.3	0.59	4.6	0.50
2000	6.8	0.54	6.3	0.63	2.8	0.30
2001	6.8	0.64	6.3	0.58	4.0	0.69
2002	7.5	0.72	7.5	0.68	3.3	0.38
2003	7.4	0.81	5.6	0.45	3.6	0.43
2004	9.1	0.63	5.8	0.62	5.0	0.51
2005	6.1	0.44	5.1	0.58	3.4	0.34
2006	5.8	0.42	6.4	0.70	3.6	0.39
2007	8.8	0.52	8.5	0.64	4.9	1.03
2008	8.4	0.66	8.1	0.65	4.3	0.64
22 year Average	7.0	0.62	6.6	0.60	3.4	0.52

Table 6- Total cumulative warm season (June, July, August) potential evaporation, actual evaporation, and ET pan coefficient for 22 years at Imnavait Creek, North Slope, Alaska.

years	Total evaporation pan (cm)	Total Priestly-Taylor (cm)	ET coefficient
1986	19.7	16.6	0.84
1987	28.5	15.0	0.53
1988	32.1	16.1	0.50
1990	29.5	11.9	0.40
1991	24.7	16.7	0.67
1992	32.7	15.3	0.47
1993	28.7	20.3	0.71
1994	32.7	17.7	0.54
1995	24.5	15.0	0.61
1996	27.9	15.0	0.54
1997	30.4	18.1	0.59
1998	28.2	17.1	0.61
1999	34.3	19.8	0.58
2000	31.9	15.9	0.50
2001	27.3	17.1	0.63
2002	29.9	18.2	0.61
2003	30.0	16.6	0.55
2004	33.7	19.9	0.59
2005	32.3	14.6	0.45
2006	32.2	15.8	0.49
2007	34.9	22.2	0.64
2008	31.9	20.8	0.65
Total Average	29.9	17.1	0.58

3.3 Variable Comparison

The comparison between different individual environmental variables and pan evaporation produced strong relationships. Potential evaporation was estimated using individual environmental variables that could possibly estimate potential pan evaporation in areas that only have instruments to measure the different environmental variables but not an evaporation pan. Measured pan evaporation total cumulative average was compared to the total cumulative average estimated potential evaporation that was calculated using each of the environmental variables (thawing degree days, net radiation, and vapor pressure deficit) to produce a percent difference between the measured and calculated potential evaporation. The strongest relationship was between thawing degree days (TDD) and pan evaporation. Net radiation has a moderate relationship with pan evaporation, and vapor pressure deficit (VPD) has a moderately strong relationship with pan evaporation. The highest percent in summer cumulative total averages comparison between the calculated potential evaporation and measured potential evaporation was the thawing degree days (Table 7).

Table 7- Total warm season (June, July, August) 22 year average potential ET calculated using TDD and Rnet. Total warm season (June, July, August) 2 year average potential ET calculated using VPD. The percent difference between the summer (June, July, August) total pan evaporation and the calculated variable potential ET.

	Total average potential evaporation (cm)	Total average evaporation pan (cm)	Percent Difference between the measured pan evaporation and calculated variable potential ET (%)
Total average calculated TDD potential ET (cm)	29.3	29.9	2
Total average calculated RNET potential ET (cm)	21.2	29.9	29
Total average calculated VPD potential ET (cm)	32.6	33.4	3

Figures 13 and 14 show the rise in both thawing degree days and net radiation over the last 22 years at Imnaviat Creek basin.

Figures 15 and 16 show the strong correlation between cumulative pan evaporation and cumulative TDD, while Figure 17 shows the 2008 comparison of the calculated potential evaporation using TDD and the measured potential evaporation using pan evaporation. The calculated potential evaporation was based on the best fit equation set from 22 years of data.

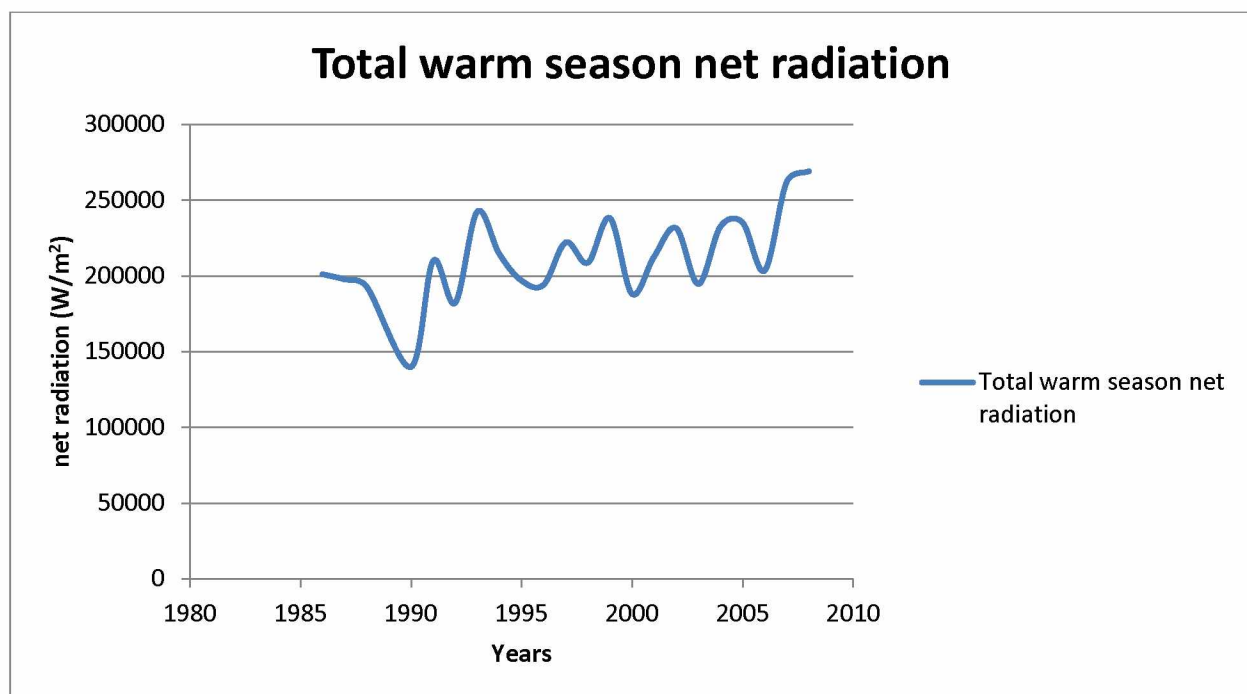


Figure 13- Yearly summation of summer (June, July, August) months of net radiation for 22 years at Imnaviat Creek, North Slope, Alaska.

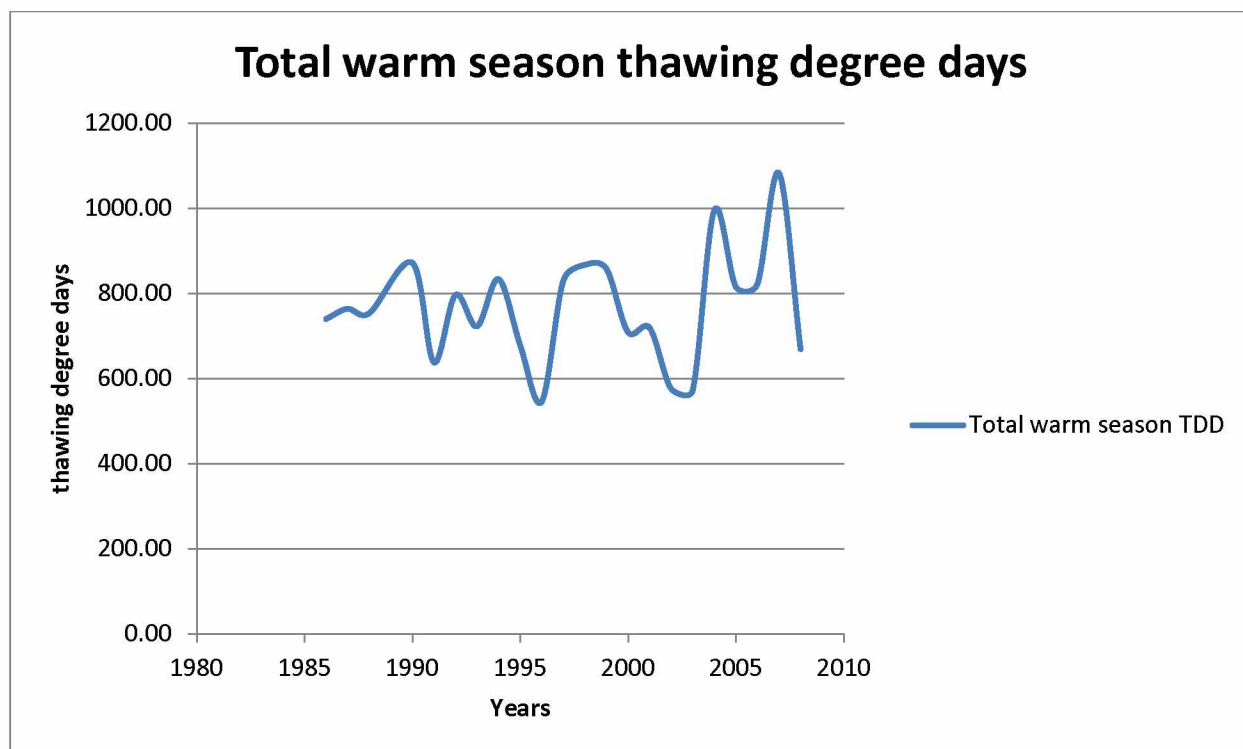


Figure 14- Yearly summation of summer (June, July, August) months of thawing degree days for 22 years at Imnaviat Creek, North Slope, Alaska.

The three different variables (thawing degree days $r^2=0.91$, net radiation $r^2=0.90$, and VPD $r^2=0.95$) had strong relationships with potential evaporation for the 22 years of data. Using the three equations generated from the three variables, estimates of potential evapotranspiration were made that could be compared with the measured pan evaporation. The rationale is that estimates of pan evaporation could be made for areas where the variables are measured, but evaporation pan data is lacking. The figures (Figures 15-21) only show the 2008 results, the rest of the 22 years of charts can be found in the Appendices (thawing degree days: Appendices D, E, F, G, H, and S; net radiation: Appendices I, J, K, L, M, and S; and vapor pressure deficit: Appendices N, O, P, Q, R, and S). The Appendices are arranged in this order:

- 1) Variable of interest (TDD, net radiation, and VPD) versus time each year.
- 2) Cumulative plot of variable of interest (TDD, net radiation, and VPD) versus pan evaporation for each year with best fit linear equation.
- 3) Estimate of potential evapotranspiration using variable of interest (TDD, net radiation, and VPD) versus time for each year.
- 4) Estimate of potential evapotranspiration using variable of interest (TDD, net radiation, and VPD) and pan evaporation versus time for each year.
- 5) Estimate of potential evapotranspiration using variable of interest (TDD, net radiation, and VPD) versus pan evaporation with best fit linear equation each year.
- 6) Estimate of potential evapotranspiration using variable of interest (TDD, net radiation, and VPD) cumulative warm season total and pan evaporation cumulative warm season total for the entire 22 years

The correlation between TDD and pan evaporation is extremely high with all 22 years summer total correlations being $r^2 > 0.91$ (see Figure 16 for an example; also refer to results in the Appendices D through H and S). The best fit equation between TDD and pan evaporation applied to all years' results averaged is:

$$y = 0.0348x + 2.5903$$

Equation 9- Best fit equation between TDD and pan evaporation

Where: Y = estimated potential evaporation (cm)

X = Cumulative thawing degree days

The correlation between Rnet and pan evaporation is also very high with $r^2 > 0.90$ (see Figure 18 for an example; refer to results in the Appendices I thru M, and S). The best fit equation between Rnet and pan evaporation applied to all years' results averaged is:

$$y = 0.0001x + 0.1021$$

Equation 10- Best fit equation between Rnet and pan evaporation

Where: Y = estimated potential evaporation (cm)

X = Cumulative net radiation (W/m^2)

Pan evaporation has a moderately strong linear relationship with VPD of $r^2 > 0.95$ for only two years (see Figure 20 for an example; refer to results in the Appendices N thru R, and S). The best fit equation used between VPD and pan evaporation is:

$$y = 0.0003x + 2.7337$$

Equation 11- Best fit equation between VPD and pan evaporation

Where: Y = estimated potential evaporation (cm)

X = Cumulative vapor pressure deficit (Pa)

Each equation was set up by compiling all 22 years of cumulative pan evaporation compared to 22 years of cumulative TDD and Rnet, and 2 years (2007 and 2008) of VPD, producing a graph of all the data and setting up a linear trend line that produced a best-fit equation (Figures 22-24).

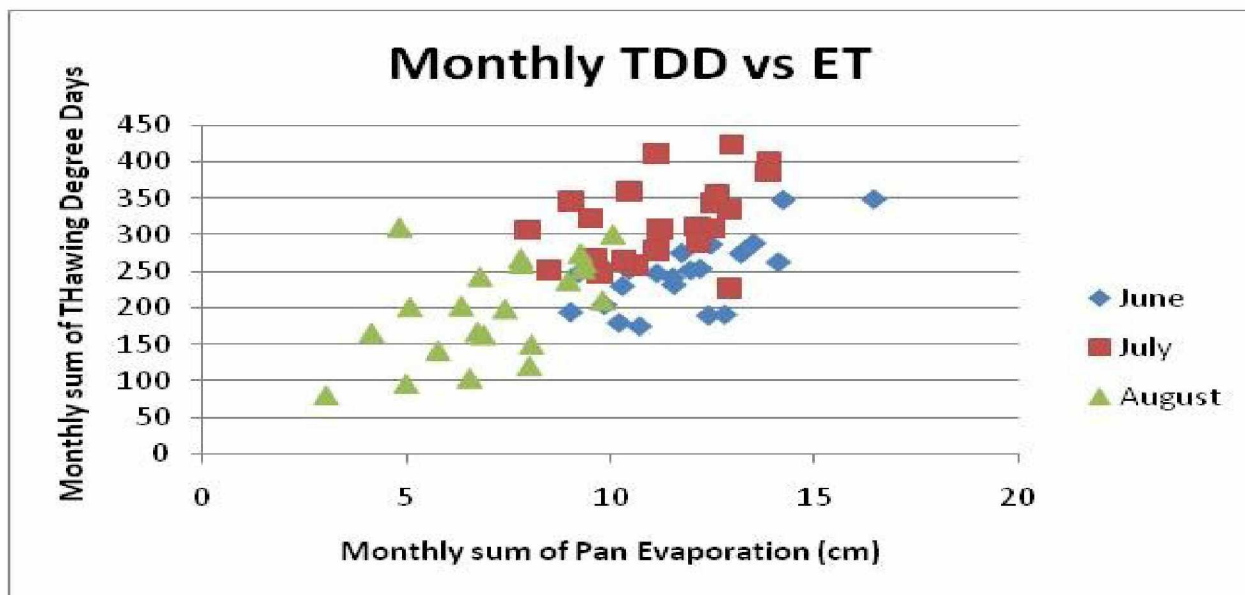


Figure 15- Comparison of Monthly thawing degree days vs. Monthly Sum of evaporation pan measurements.

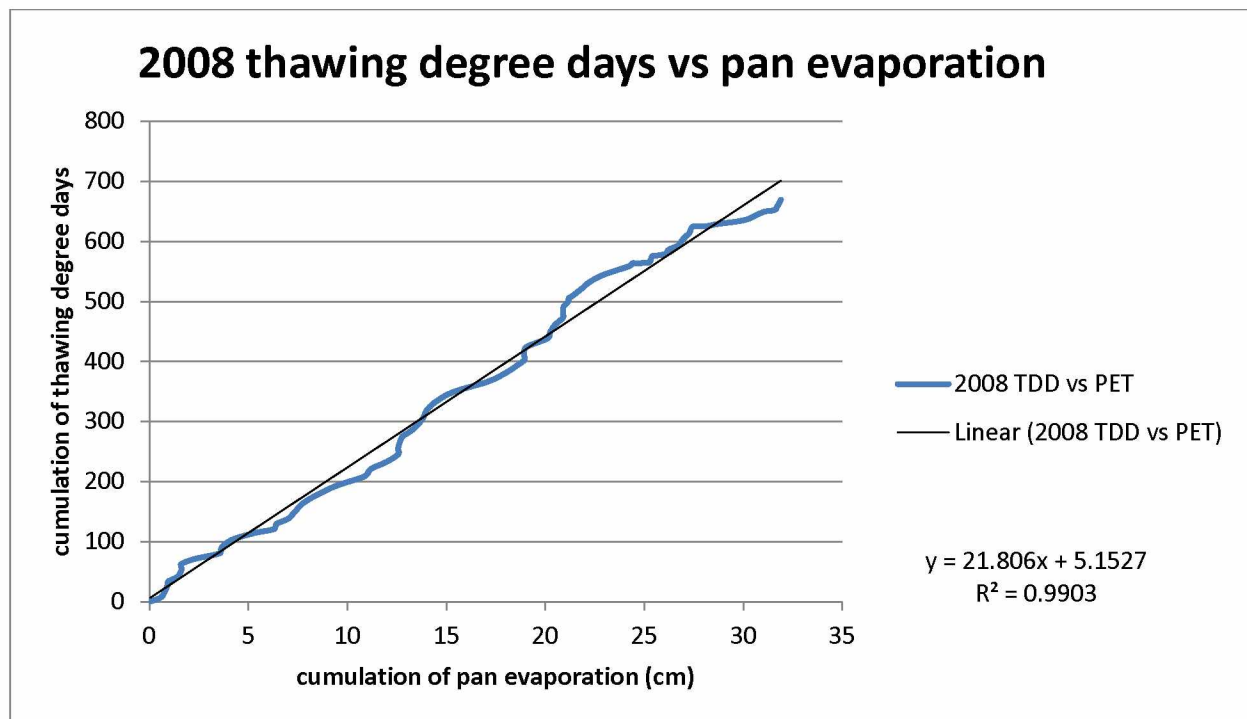


Figure 16- Relationship between the 2008 thawing degree days vs Cumulative pan evaporation.

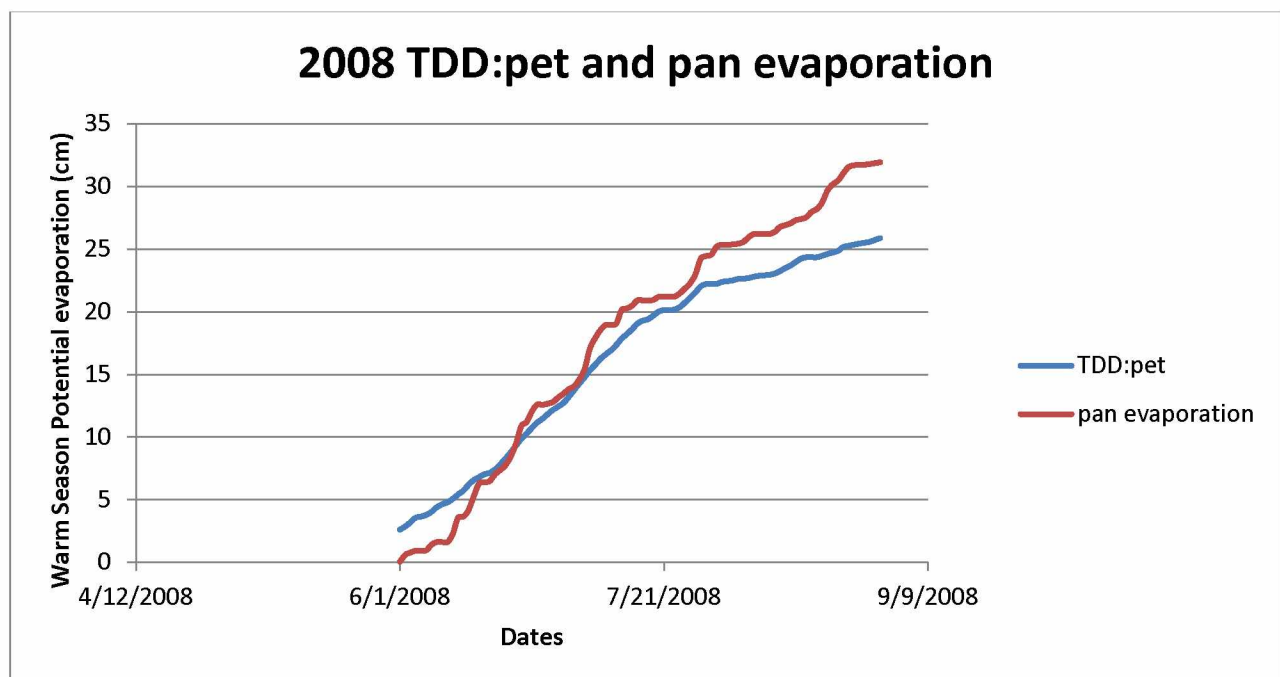


Figure 17- The thawing degree days was used to produce a potential evaporation that is calculated. This shows the close relationship between the measured potential and calculated potential using only TDD.

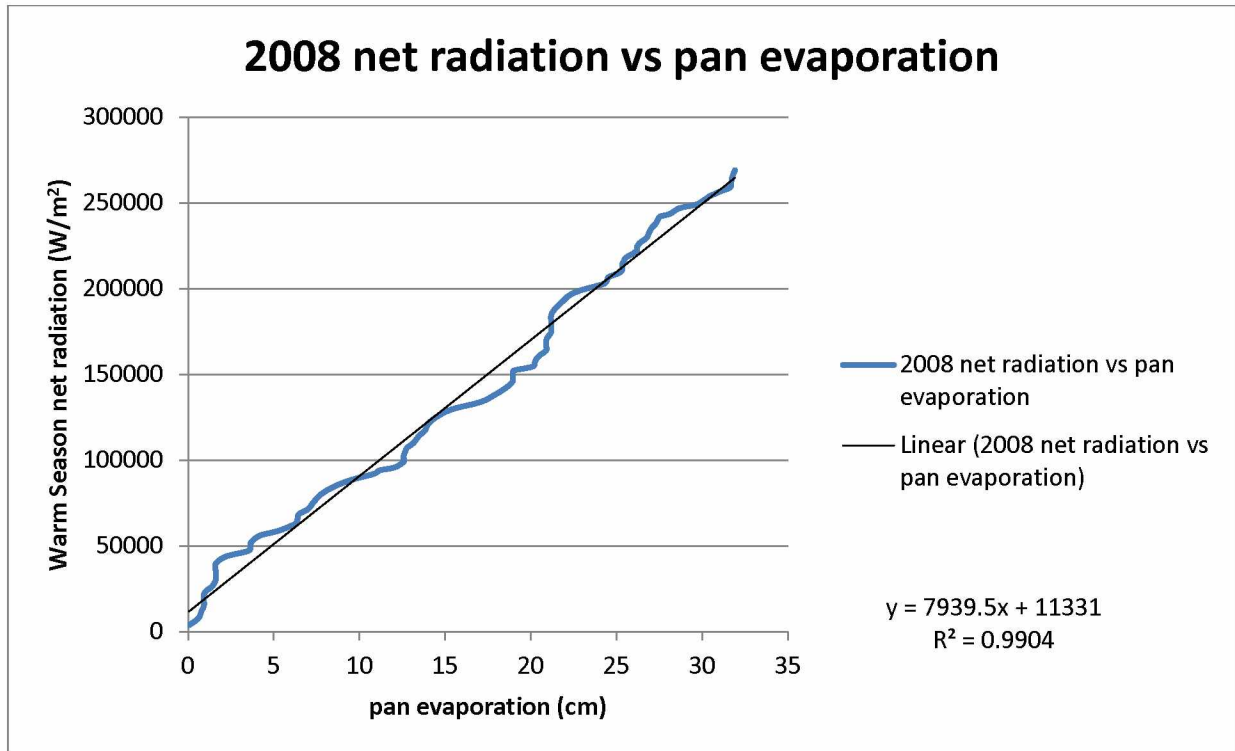


Figure 18- Comparison between the 2008 Warm Season Cumulative net radiation vs. the Cumulative evaporation pan measurements.

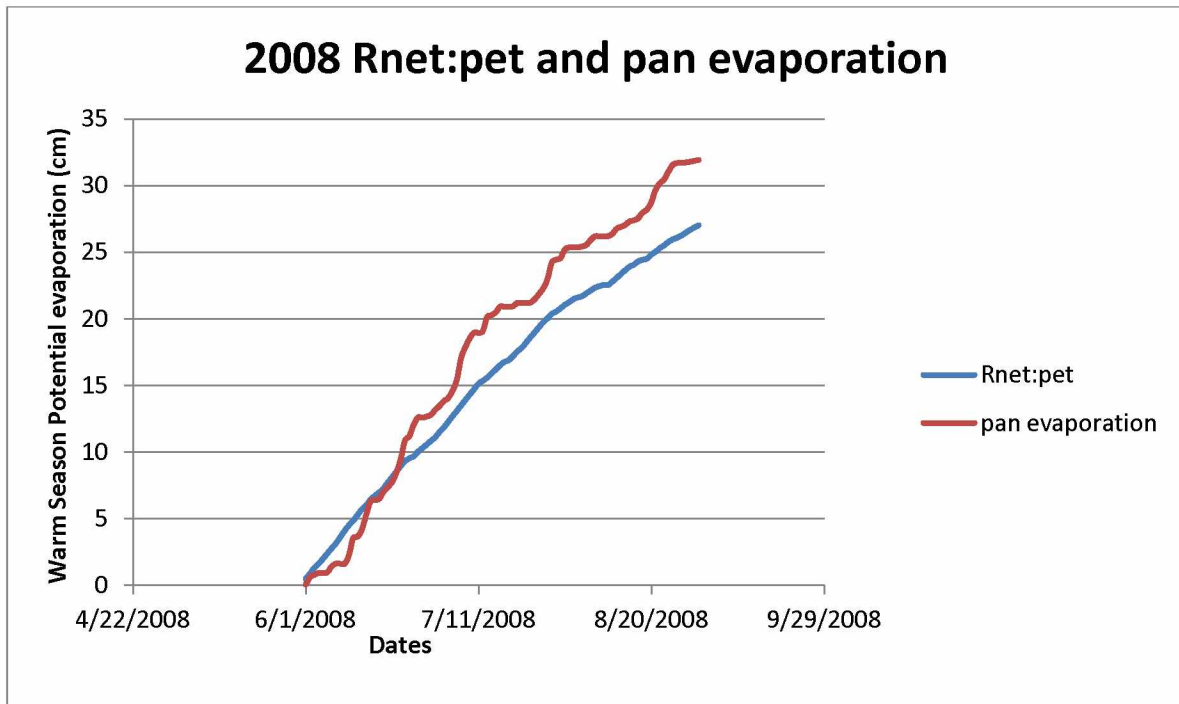


Figure 19- The net radiation was used to produce a potential evaporation that is calculated. This shows the close relationship between the measured potential and Calculated potential only using Rnet.

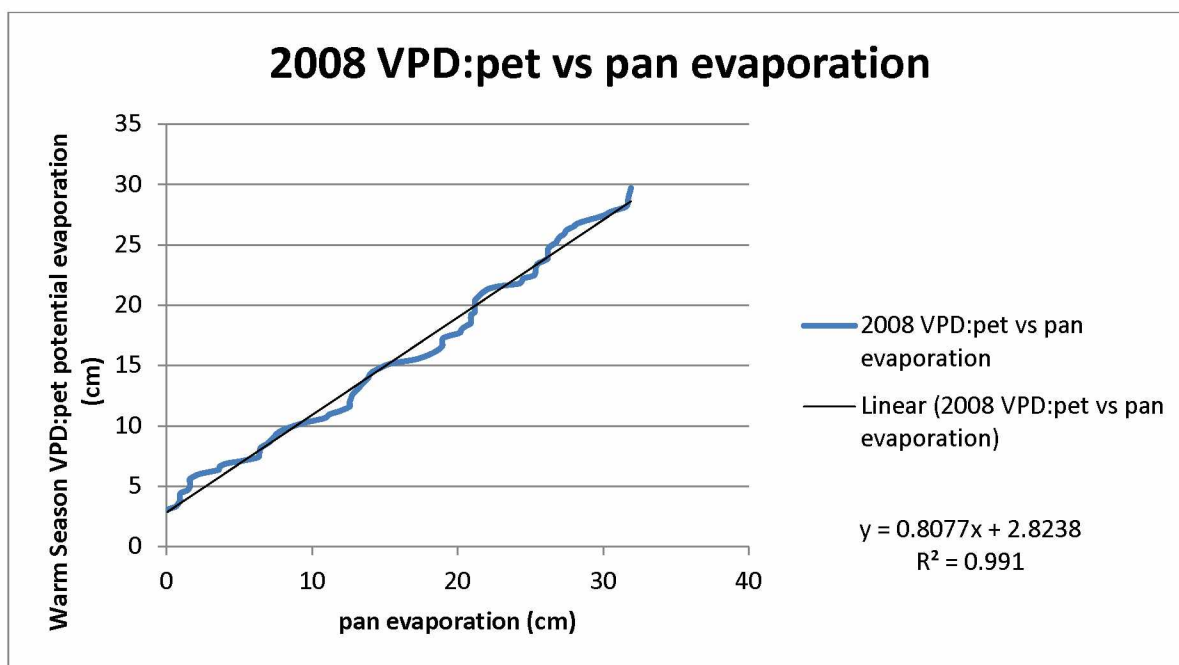


Figure 20- Comparison between the 2008 Warm Season cumulative vapor pressure deficit vs. the cumulative evaporation pan measurements.

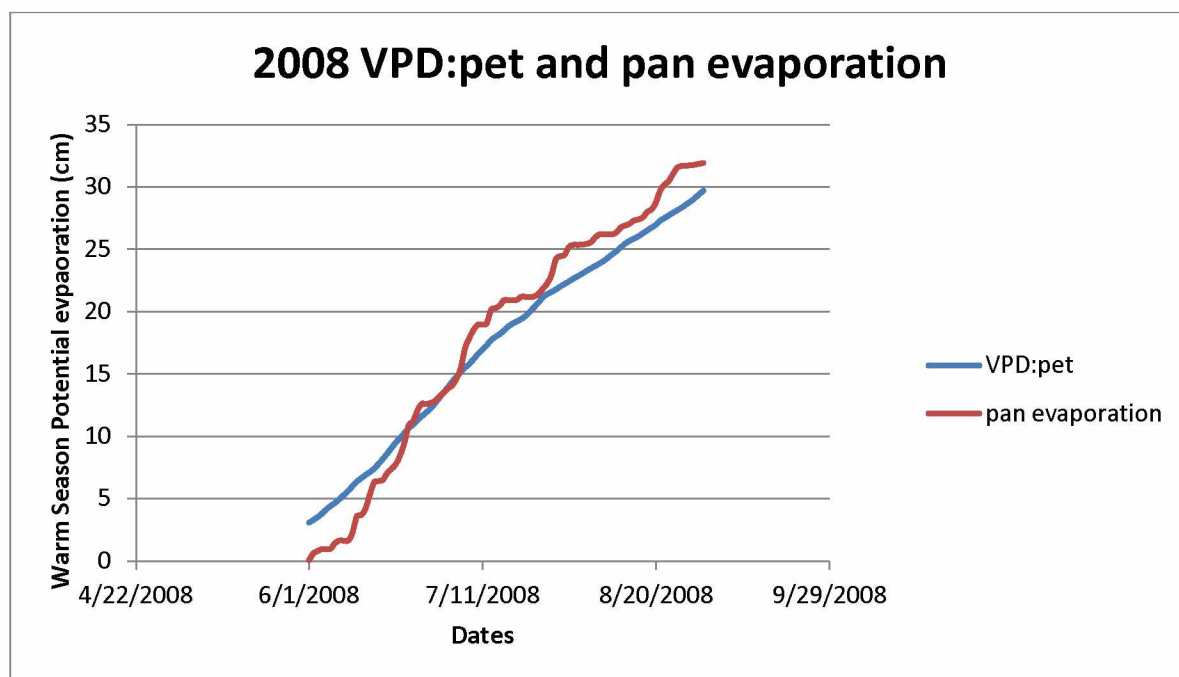


Figure 21- The vapor pressure deficit (VPD) was used to produce potential evaporation that is calculated. This figure shows the close relationship between the measured potential and Calculated potential evapotranspiration using only VPD.

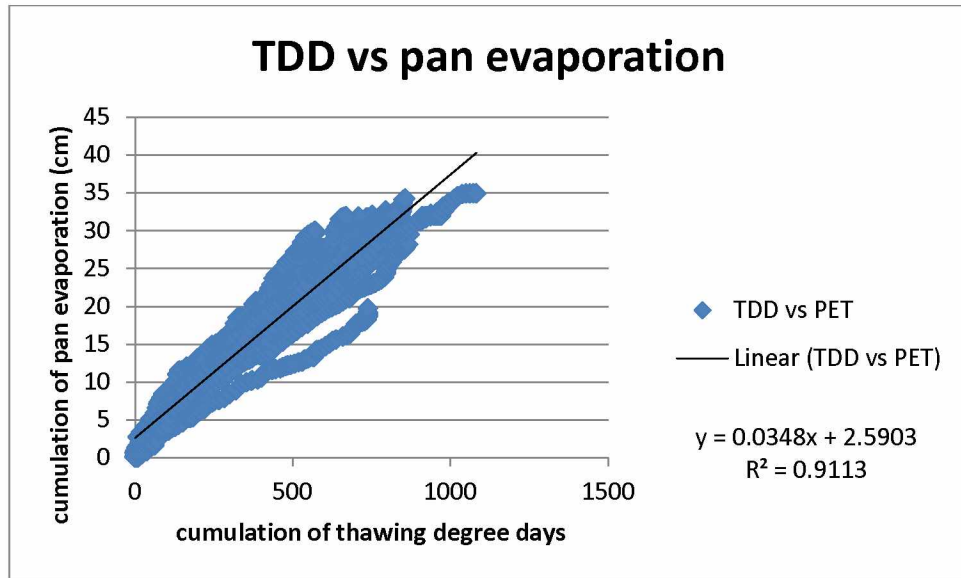


Figure 22- 22 Years of relationship between cumulative pan evaporation and cumulative thawing degree days, producing linear best-fit equation.

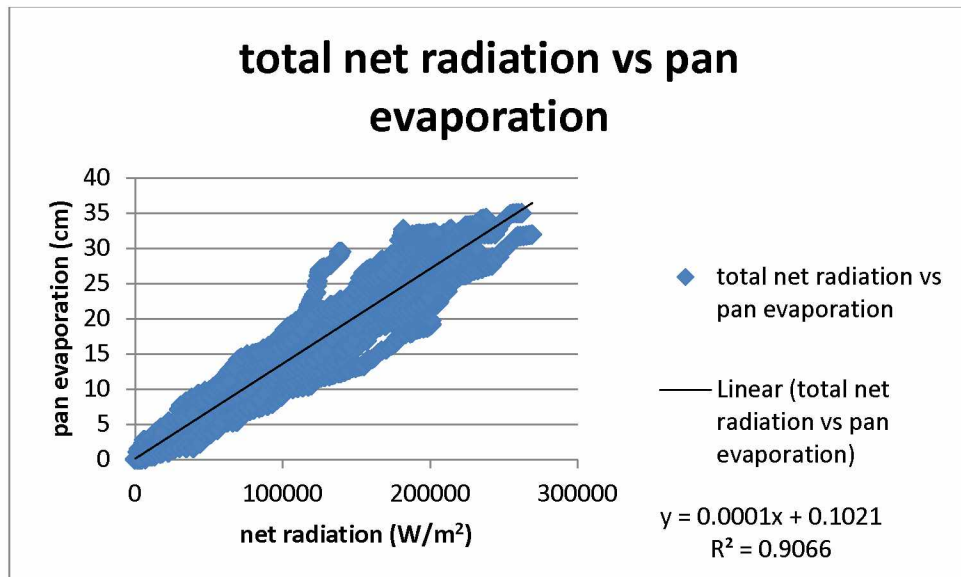


Figure 23- 22 Years of relationship between cumulative pan evaporation and cumulative net radiation, producing linear best-fit equation.

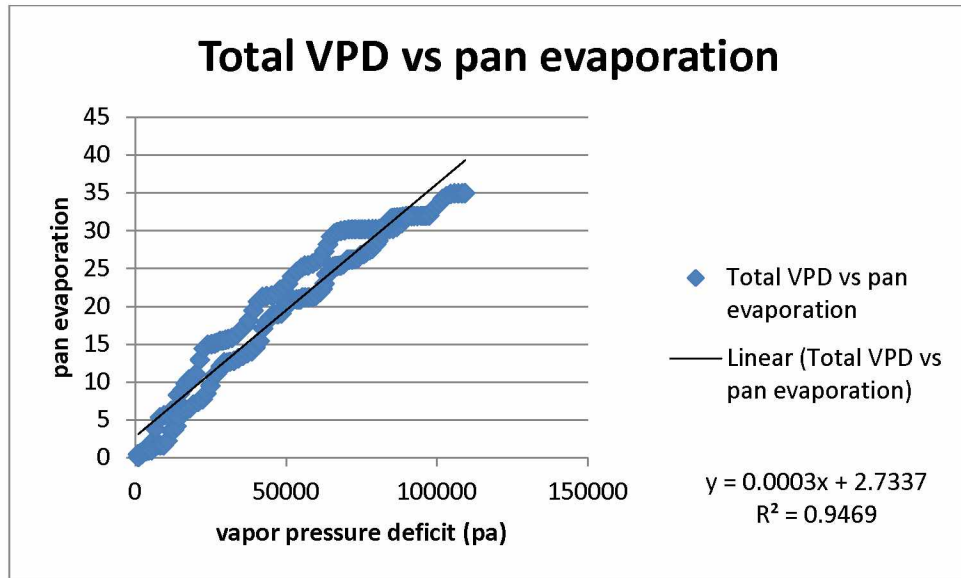


Figure 24- 2 Years of relationship between cumulative pan evaporation and cumulative vapor pressure deficit, producing linear best-fit equation.

For two years (2007 and 2008) vapor pressure deficit had a strong and close relationship and cumulative comparison between the measured and calculated potential evaporation (Figures 16, 18, 20). In Tables 8, 9, and 10, the monthly cumulative totals are listed for each year and Table 11 is the cumulative warm season totals. Due to large amounts of missing data there were only two summers of useable VPD data for the comparison of measured pan evaporation and calculated estimates based on VPD.

Table 8- June yearly potential evaporation measured and calculated totals using TDD, RNET, and VPD.

years	June evaporation pan (cm)	June calculated potential ET TDD (cm)	June calculated potential ET RNET (cm)	June calculated potential ET VPD (cm)
1986	7.1	10.7	8.0	
1987	12.2	11.4	8.5	
1988	13.4	11.4	8.5	
1990	10.0	11.4	6.4	
1991	10.0	11.2	9.3	
1992	9.6	10.6	6.6	
1993	11.5	11.0	10.2	
1994	10.2	8.9	8.6	
1995	9.7	9.7	7.9	
1996	12.2	9.2	8.1	
1997	11.6	12.2	9.4	
1998	9.8	11.6	8.0	
1999	12.6	12.6	9.6	
2000	12.5	9.3	7.7	
2001	10.8	11.2	8.7	
2002	10.3	8.7	9.9	
2003	9.1	9.4	7.8	
2004	14.5	14.7	10.8	
2005	13.8	12.7	10.0	
2006	13.9	11.7	7.5	
2007	16.9	14.7	10.5	13.3
2008	12.8	12.2	10.7	12.6

Table 9- July yearly potential evaporation measured and calculated totals using TDD, RNET, and VPD.

years	July evaporation pan (cm)	July calculated potential ET TDD (cm)	July calculated potential ET RNET (cm)	July calculated potential ET VPD (cm)
1986	7.1	12.0	7.8	
1987	11.2	11.5	8.0	
1988	13.4	12.3	7.7	
1990	11.1	13.2	3.6	
1991	9.0	9.2	8.9	
1992	13.2	12.3	6.7	
1993	14.4	14.2	12.3	
1994	13.9	11.6	9.1	
1995	8.3	9.7	7.3	
1996	10.7	7.5	7.5	
1997	12.1	12.3	9.5	
1998	11.1	15.2	8.1	
1999	12.4	12.7	10.1	
2000	10.0	7.8	7.4	
2001	10.7	9.9	8.2	
2002	10.9	7.7	11.0	
2003	12.5	6.6	6.6	
2004	9.4	16.1	9.5	
2005	8.7	10.7	10.2	
2006	9.1	12.3	7.6	
2007	13.3	18.8	12.2	12.0
2008	12.4	11.6	12.9	9.8

Table 10- August yearly potential evaporation measured and calculated totals using TDD, RNET, and VPD.

years	August evaporation pan (cm)	August calculated potential ET TDD (cm)	August calculated potential ET RNET (cm)	August calculated potential ET VPD (cm)
1986	5.5	5.7	4.3	
1987	5.1	7.0	3.8	
1988	5.2	5.8	3.6	
1990	8.4	9.1	2.3	
1991	5.8	5.0	4.0	
1992	9.9	7.3	3.5	
1993	2.8	2.8	3.9	
1994	8.6	9.3	4.3	
1995	6.5	5.8	4.4	
1996	5.0	3.4	3.9	
1997	6.8	8.5	4.7	
1998	7.3	6.9	4.8	
1999	9.3	9.1	5.6	
2000	9.4	8.8	3.4	
2001	5.8	7.1	5.1	
2002	8.6	4.2	4.1	
2003	8.4	5.3	4.8	
2004	9.8	10.5	5.7	
2005	9.9	9.6	5.3	
2006	9.2	8.3	4.7	
2007	4.8	10.8	5.9	10.3
2008	6.7	3.7	6.0	7.3

Table 11- Yearly Summer Totals for yearly potential evaporation measured and calculated totals using TDD, RNET, and VPD.

years	Total evaporation pan (cm)	Total calculated potential ET TDD (cm)	Total calculated potential ET RNET (cm)	Total calculated potential ET VPD (cm)
1986	19.7	28.3	20.1	
1987	28.5	29.2	19.8	
1988	32.1	28.8	19.3	
1990	29.5	32.9	14.0	
1991	24.7	24.8	21.0	
1992	32.7	30.3	18.2	
1993	28.7	27.7	24.2	
1994	32.7	31.6	21.4	
1995	24.5	26.2	19.7	
1996	27.9	21.6	19.4	
1997	30.4	31.5	22.2	
1998	28.2	32.8	20.9	
1999	34.3	32.4	23.8	
2000	31.9	27.3	18.2	
2001	27.3	27.6	21.3	
2002	29.9	22.6	23.1	
2003	30.0	22.5	19.5	
2004	33.7	37.2	23.3	
2005	32.3	31.0	23.5	
2006	32.2	31.2	20.3	
2007	34.9	40.3	26.2	35.6
2008	31.9	25.9	26.9	29.7

Figures 25 and 26 show the relationship between evaporation pan measured potential ET and Priestley-Taylor calculated AET. In Figure 10 and Figure 12 potential ET always has a higher summer total to the Priestley-Taylor calculated actual ET. Yet with the use of the pan coefficient, evaporation pan measured potential evaporation can be reduced to the actual ET, resulting in a close relationship between measured pan evaporation and calculated Priestley-Taylor ET.

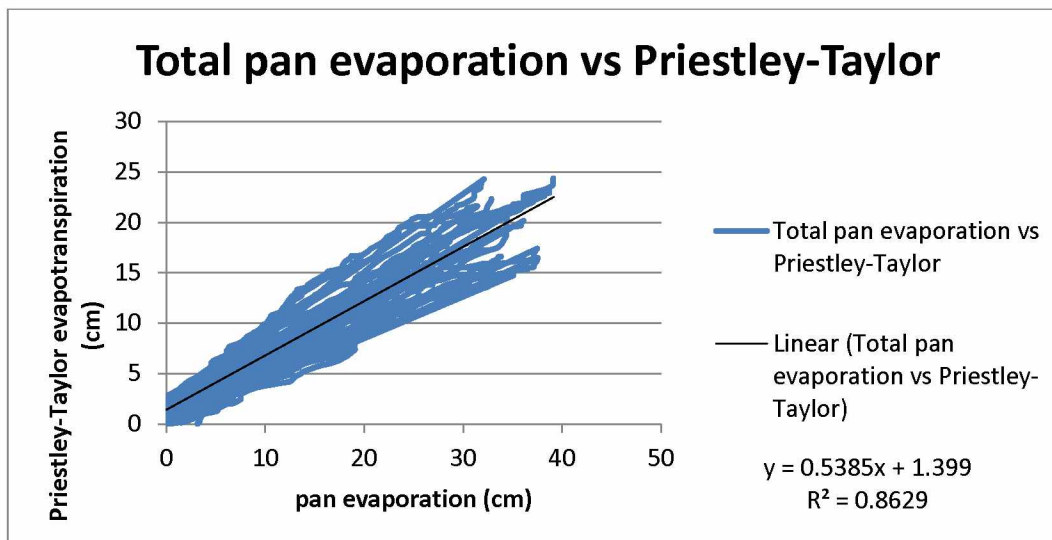


Figure 25- 22 years of summer cumulative pan ET vs. Priestley-Taylor calculated ET.

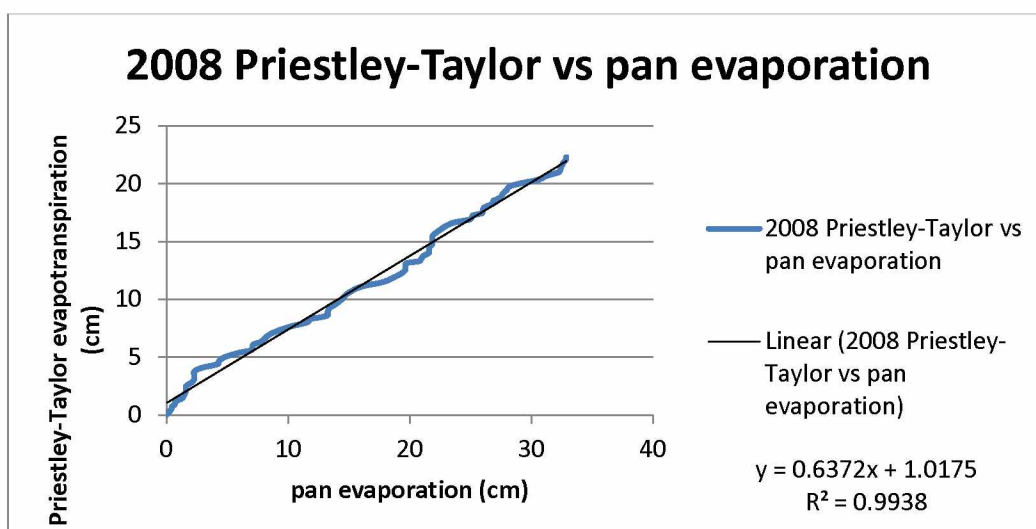


Figure 26- 2008 relationship between potential ET and actual ET.

Chapter 4-Analysis

4.1 Evaporation Pan

Pan evaporation was measured from break up, until the initiation of snowfall and temperatures dropped to freezing or below. Measurements typically started in May and concluded in September; however, there was never a full month of data in May or September. To make the yearly data sets uniform, comparisons were based on the period from June 1 to August 31. It did change warm season totals since the evaporation pan data presented here does not cover May or September, yet it was more consistent year to year when trying to compare all summer data to other variables for the period of June, July and August. June and July had the highest amounts of monthly evaporation. It varied over the 22 years which specific month had more evaporation, but overall June had the highest (Figure 9). This high June evaporation happens since a large amount of water is available from snowmelt, plus the high air temperatures and high solar radiation near solstice provide the energy necessary to drive evaporation (Rouse and Stewart, 1976). It is important to look at June as the month with the highest amounts of monthly evaporation and July a close second, due to the energy available to produce pan evaporation. Energy can come from many sources such as high air temperatures, sensible heat, and long and short wave radiation on the longer days. In early summer the air/surface temperatures increases to annual highs, and then starts to decrease through July and August. Radiation is at its highest near the June 21 solstice, the longest day of the year. Vapor pressure starts to decrease into June after the break-up driving a higher evaporation rate, August is on average the rainiest month on the North Slope of Alaska (Kane et al., 1990) followed closely by July where the evaporation rates are lower than June.

The summer cumulative pan evaporation totals for the maximum year is 34.9 cm, minimum year is 19.7 cm, and the average year cumulative total over the 22 years is 29.9 cm for the June through August period being studied here. As mentioned earlier I focused only on the complete months of June, July, and August in order to have data for the same time period each year (also allowing for a better chance of developing statistically significant relationships, and decreasing outliers). Although there is year-to-year variation, evaporation has slightly

increased over the last 22 years (Figure 10 and Table 4). This increase of evaporation from the pan is caused by an increase of available energy (higher air/surface temperatures and net radiation) since the pan doesn't lack water for evaporation. Figures 13 and 14 (net radiation and thawing degree days) show the increase during the summer months over the 22 year study (1986 thru 2008, missing 1989). Yet there are many other variables that could be causing this increase of evaporation such as an increase of the vapor pressure deficit (VPD).

4.2 Priestly-Taylor/Coefficient

Actual evapotranspiration (ET) was calculated from the data collected from the meteorological station next to the evaporation pan. The Priestley-Taylor equation was used to calculate the actual estimate of ET for the summer months (which should always be lower than the measured potential evaporation). If you take the actual ET/potential ET ratio you end up with an ET pan coefficient which is another simple way to estimate of actual ET (by multiplying the pan coefficient times the measured pan evaporation). The evaporation pan coefficient for the 22years of warm season evaporation average ended up being 0.58. This is a slight increase from the 2003 evaporation coefficient of 0.55 by Kane and Yang (2004); this can be due to not including the outliers from the months of May and September in the calculations here. Overall, the average pan coefficient reported here and the one by Kane and Yang (2004) are very close over the 22 year period.

4.3 Variable Comparison/Calculated Potential Evaporation

The evaporation pan data has a strong linear relationship with the three meteorological variables: thawing degree days, net radiation, and vapor pressure deficit. Thawing degree days (TDD) and net radiation (Rnet) are both good proxies for the surface energy balance (the warmer the atmosphere the more energy available for latent energy fluxes), therefore highly correlated with pan evaporation. Both had best fit equations where the measured TDD and Rnet data can be used to successfully calculate estimates of potential evaporation. The correlation between TDD and pan evaporation is extremely high with all 22 years summer total correlations being $r^2 > 0.91$ (see Figure 16 for an example, refer also to results in the appendices D thru H, and S). Equation 9 was produced from the 22 years of summer data, having a correlation of slightly less than 1.0 means there will be a small amount of variations between potential evaporation that is calculated through this equation (using TDD as x) and measured potential evaporation through pan evaporation.

Net radiation had the lowest linear relationship statistically between the three variables used to predict PET (which is measured pan evaporation). This is because of the amount of net radiation it takes to provide the energy for latent fluxes are not consistent with the amount of variations in net radiation due to cloud cover; while the air temperature and the PET rate increase while net radiation does not (Priestley and Taylor, 1972). Also, higher net radiation doesn't exactly result in more pan evaporation due to increases of both precipitation and water vapor in the atmosphere causing lower rates of evaporation. Net radiation and thawing degree days data were compiled through 22 years while vapor pressure deficit data was compiled only for two years since there were large amounts of missing data.

VPD also appears to be an excellent proxy for estimating potential pan evaporation and the higher the VPD the higher will be the ET. VPD is the difference between the saturated vapor pressure at the ground surface minus the vapor pressure in the atmosphere above the ground surface. The lower the moisture level in the atmosphere the greater the amount of potential evaporation. Pan evaporation has an extremely strong linear relationship with VPD of $r^2 > 0.95$ for only two years. There were only two summers (defined as June, July, and August) that had

complete summers of data for determining VPD without having large windows of missing data. Thus, this correlation has some uncertainty. Overall, the results of calculating potential evaporation using the variable VPD had the best correlation results to the measured pan evaporation (Figure 20), and therefore show potential use in estimating pan evaporation.

The results in Tables 8, 9, 10, and 11 cover the monthly (June, July, August) and entire warm season totals for the calculated potential evaporation using variables and the measured pan evaporation. Tables 8, 9, and 10 cover the monthly totals for June, July, and August and thawing degree days had the closest results with the measured pan evaporation. Net radiation underestimated the results with the measured pan evaporation with August being its poorest month. Vapor pressure deficit had close results with the measured pan evaporation over the three months for the two years. Table 11 shows the warm season totals for the calculated potential evaporation. Thawing degree days had the closest total warm season totals of the three variables while net radiation had the largest percent difference between calculated potential evaporation warm season totals (Table 7). Vapor pressure deficit has good potential with having a close total warm season totals of two years (2007 and 2008). Graphs of the entire warm season totals for the calculated potential evaporation using environmental variables and the measured pan evaporation are located in Appendix S.

Overall thawing degree days had the highest correlated relationship, causing it to produce the best percent difference between the measured pan evaporation and the calculated potential evaporation. Net radiation had the largest percent difference of the three environmental variables which was mostly caused by inconsistency of net radiation (being affected by cloud cover over the warm season). This was evident when air temperature and evaporation rates continued to increase while cumulative net radiation didn't. August being the lowest correlated month for net radiation could be due to the inconsistency of low cloud cover and the decreasing amount of net radiation caused by the low amount of time of sunlight.

Vapor pressure deficit, having two complete warm season years of data, only allowed me to investigate its potential for calculating potential evaporation. The two years of observation

produced good comparison between the measured pan evaporation and the calculated potential evaporation.

One thing that may increase the strength of the relationships between these variables and pan evaporation is to combine two or three different variables, and produce more complicated equations that would calculate more accurate potential evaporation. Most evapotranspiration equations require more than one variable to produce accurate estimates. Using two or more environmental variables could possibly result in a better fit equation also for the 22 year period, between predicted and measured pan evaporation. But this means the quality of the data needs to be preserved; this is not an easy thing to accomplish in these remote Arctic environments. It is also possible to break warm season totals down to monthly totals and setting up a monthly best fit equation for June, July, and August since the time of year affects the amount of sunlight, moisture availability, and air temperatures. Also trying a non-linear relationship equation to calculate the potential evaporation using the environmental variables could prevent the under and over calculating of potential evaporation. Overall it seemed that the measured pan evaporation difficulty with the relationships and equations was due to small human and nature errors caused by animals, wind, and missing data. These small errors could lower the predictability of the potential evaporation produced by the environmental variables.

Chapter 5-Discussion

The results of this study have many interesting comparisons with past studies. Over the 22 years of measurements made with the evaporation pan the best correlation was in June, and generally decreased over the summer months. This was demonstrated in past studies as in Kane and Yang (2004), Rovantsek et al. (1996), Kane et al. (1990), and Hinzman et al. (1996). They all noted that the highest evaporation occurs right after the snowmelt runoff which occurs in late May and early June in the Imnavait Creek Basin. Also with the high solar radiation in June, more energy is available to potentially cause higher evaporation rates. Ohmura (1982) observed that most of the daily evaporation occurred during the periods of higher solar elevation at mid-day. This is especially true around the June solstice.

The summer cumulative pan evaporation totals for the maximum year is 34.9 cm, minimum year is 19.7 cm, and the average year cumulative total over the 22 years is 29.9 cm for the June through August period being studied here. It was also mentioned by Weller and Holmgren (1974) that an energy balance method shouldn't be used during the snow melt period unless one accounts for the latent energy used for snow ablation. Also in May the start of spring break-up varies, and in September the beginning of winter varies when it begins; both not allowing for full month of pan evaporation data.

The daily average evaporation pan rate for June was 4 mm/d, in July the daily average was 3.6 mm/d and in August the daily average was 2.4 mm/d. The daily average for the 22 years of pan data was 3.3 mm/d. In past studies (Mendez et al., 1998) evaporation rates after the snowmelt averaged 3.11 mm/day using the water balance method near the coast. Also Kane and Carlson (1973) had an evaporation pan near the Putuligayuk River basin near Prudhoe Bay, Alaska; the pan evaporation rate in this area was 2.4 mm/d which is lower than what was measured at Imnavait Creek basin which is located south of Prudhoe Bay, Alaska at lower latitude, but higher elevation. Kane and Yang (2004) and Shutov et al. (2006) both observed that evapotranspiration decreases with higher latitudes, due to lack of energy and lack of moisture.

The net radiation and air temperature also have increased during the summer months over the 22 past years (Figures 13 and 14). Pan evaporation also has slightly increased over the last 22

years (Figure 10). This increase of evaporation from the pan is caused by an increase of energy (air/surface temperatures, sensible heat, net radiation) while the evaporation pan has unlimited water. It was noted by Shutov et al. (2006) that actual evapotranspiration is strongly controlled by soil moisture levels and incoming solar radiation. Incoming solar radiation is closely related to net radiation and air temperature. Increasing both of these environmental variables means this could increase evapotranspiration.

Using the Priestley-Taylor method to calculate actual evapotranspiration over the 22 years was pursued due to its simplicity (minimal amount of data required) and its consistent estimates for tundra uplands in the Arctic. Mendez et al. (1998) noted that Priestley-Taylor model is best used to estimate ET from wetland tundra, if you don't want to investigate different variables such as vapor pressure or wind speed. Kane et al. (1990) and Hinzman et al. (1996) observed that the Priestley-Taylor method with a constant α of 0.95 produced good estimates of evapotranspiration with small amounts of data. Also Rovanešek et al. (1996) noted that the α was consistent in the drier uplands using a constant of $\alpha = 0.95$.

The evaporation pan coefficient was the lowest when the Priestley-Taylor calculated ET was at its lowest. The ET pan coefficient average over 22 years is 0.58 (Table 6). Kane et al. (1990) and Hinzman et al. (1996) measured that the evaporation pan predicted sufficient total evapotranspiration amounts over the summer while using a pan coefficient of 0.49. Also Kane and Yang (2004) noted with additional data that the pan coefficient averaged out as 0.55. The increase was partially due to not including the outliers from the months of May and September in the calculations, but overall the two pan coefficients were very similar.

Three different variables (thawing degree days, net radiation, and VPD) had strong relationships with potential evaporation from the 22 years of evaporation pan data. Shutov et al. (2006) observed that evaporation is strongly controlled by incoming solar radiation which affects thawing degree days, and net radiation. Thawing degree days had the best percent difference between its calculated potential evaporation and the measured pan evaporation, while net radiation had the lowest percent difference of the three variables. It seemed that the evaporation was strongly controlled by the incoming solar radiation for the air temperatures

but the limited measured net radiation due to cloud cover could have caused for the lower comparison. Pan evaporation had a strong linear relationship with VPD of $r^2 > 0.95$ for the two years of vapor pressure deficit data. It also had a close percent difference between the vapor pressure deficit warm season totals and the measured pan evaporation warm season totals for those two years (2007 and 2008). This showed good potential as a proxy for future studies. Lafleur and Rouse (1988) observed that evapotranspiration increased during the higher canopy resistance due to the large vapor pressure deficit. Though near the northern Alaska coast, Liljedahl et al. (2011) observed over a multi-year study using eddy covariance method that variations in the near-surface soil moisture and atmospheric vapor pressure deficit were found to have nonlinear effects on evapotranspiration rates. Also they observed that dry soils increased surface resistance, while wet soils favored ground heat flux which limited the available energy (latent and sensible heat flux) for evaporation. It might be very possible that the drier environment and the inland climate at Imnavait Creek basin might have allowed for such a close relationship between VPD and pan evaporation. It may also explain why July was its best calculated month of the three month with the lowest amount of moisture available of the three months.

Air temperature is measured at lots of places around the Arctic. Therefore, there are more opportunity to determine thawing degree days, and a less likelihood of measuring net radiation and vapor pressure deficit at the remote meteorological stations. This could allow for further look at stations in other basins such as the Upper Kuparuk, and using the air temperature measured in the basin could allow for a good estimate of potential evaporation for the Upper Kuparuk basin.

Chapter 6-Conclusions

An evaporation pan that was in place over a 22 year span, located on the North Slope of Alaska at Imnavait Creek Basin, was used to measure summer potential evaporation. The warm season evaporation pan coefficient for the North Slope in a foothills tundra environment was 0.58; this is slightly higher than the 2003 coefficient of 0.55 found by Kane et al (2004). This is partially due to 2007 and 2008 experiencing high pan coefficients and also only including June, July, and August data in this analysis. Yet overall, they are very similar and show the consistence of the 22 years of data. The summer cumulative maximum, average, minimum and standard deviation of potential evaporation from the pan are 34.9 cm, 29.9 cm, 19.7 cm and 9.3 cm respectively. The strongest relationships found between meteorological variables and pan evaporation over the 22 years was thawing degree days (TDD) $r^2 > 0.91$ and net radiation (Rnet) $r^2 > 0.90$. Vapor pressure deficit is also a good proxy with a strong relationship (VPD) $r^2 > 0.95$ for two years (2007 and 2008). Through analysis, it is possible to get quality estimates of potential ET using an evaporation pan to gain a general idea of the range of possible amounts of ET over the summer months and what environmental variables affect the rate of ET.

The measured environmental variables that have strong relationships with the evaporation pan can be used to estimate potential evaporation accurately at other locations where the environmental variables are measured (thus not requiring an evaporation pan). All three variables can be used to estimate potential evaporation by using the linear relationship between the variable and pan evaporation. Thus, one can generate highly correlated estimates of potential evaporation using measured environmental variables. Yet, to increase the accuracy of the predicted potential ET estimates additional steps could be taken. This could require more data collection. Also using a combination of using two to three different environmental variables to produce more complicated equations might produce better estimates of potential evaporation. The use of non-linear equations could possibly also increase the accuracy of the calculated potential evaporation.

Potential evaporation can be measured by the evaporation pan which has a strong relationship with environmental variables that can be measured with satellites, such as land surface

temperature. The variables can be measured by satellites yet not enough images were processed in this study to fully find out at how accurate and how well the potential evaporation can be estimated at the watershed scale. This needs further research to reach better conclusions. Once the ability to measure more high resolution images using land surface temperature data and meteorological variables such as VPD and Rnet data are just around the corner, and we should be able to measure potential evaporation at watershed scale using remote imagery. In the future, the usage of meteorological stations at locations that don't have an evaporation pan or the usage of satellites to collect data for measuring the variables that have a strong linear relationship with evaporation pan measurements will produce large scale estimates of the variability of potential evaporation on the North Slope of Alaska. For this to happen, there will need to be an increase in ground collected data from meteorological stations or in basins of interest, and an increase of summer imagery using Landsat imagery and higher resolution satellites.

REFERENCES

- Bindschadler, R. (2003), Landsat coverage of the earth at high latitudes. *Photogrammetric Engineering and Remote Sensing*, 69(12): 1333-1339.
- Black, R.F. (1969), Geology, especially geomorphology, of northern Alaska. *Arctic*, 22(3): 283-295.
- Chehbouni, A., Watts, C., Lagouarde, J.P., Kerr, Y.H., Rodriguez, J.C., Bonnefond, J.M., Santiago, F., Dedieu, G., Goodrich, D.C., Unkrich, C. (2000), Estimation of heat and momentum fluxes over complex terrain using a large aperture scintillometer. *Agricultural and Forest Meteorology*, 105(1-3): 215-226.
- Chen, D., Gao, G., Xu, C.Y., Guo, J., Ren, G. (2005), Comparison of the thornthwaite method and pan data with the standard penman-monteith estimates of reference evapotranspiration in China. *Climate Research*, 28: 123-132.
- Clebsch, E.E.D., Shanks, R.E. (1968), Summer climatic gradients and vegetation near Barrow, Alaska. *Arctic*, 21(3): 161-171.
- Cristobal, J., Jimenez-Munoz, J.C., Sobrino, J.A., Ninyerola, M., Pons, X. (2009), Improvements in land surface temperature retrieval from the landsat series thermal band using water vapor and air temperature. *Journal of Geophysical Research-Atmospheres*, 114: 16.
- Eaton, A.K., Rouse, W.R., Lafleur, P.M., Marsh, P., Blanken, P.D. (2000), Surface energy balance of the western and central Canadian subarctic: variations in the energy balance among five major terrain types. *Journal of Climate*, 14: 3692-3703.
- Gundalia, M.J., Dholakia, M.B. (2013), Dependence of evaporation on meteorological variables at daily time-scale and estimation of pan evaporation in Junagadh region. *American Journal of Engineering Research*, 2(10): 354-362.
- Hartogensis, O.K., Watts, C.J., Rodriguez, J.C., De Bruin, H.A.R. (2003), Derivation of an effective height for scintillometers: La Poza experiment in northwest Mexico. *Journal of Hydrometeorology*, 4: 915-928.
- Hickox, G.H. (1944), Evaporation from a free water surface. *Trans. American Society of Civil Engineers*, 70(8): 1297-1327.
- Hinzman, L.D., Kane, D.L. (1991), Snow hydrology of a headwater Arctic basin: 2. conceptual analysis and computer modeling. *Water Resources Research*, 27(6): 1111-1121.

- Hinzman, L.D., Kane, D.L., Gieck, R.E., Everett, K.R. (1991), Hydrologic and thermal-properties of the active layer in the Alaskan arctic. *Cold Regions Science and Technology*, 19(2): 95-110.
- Hinzman, L.D., Kane, D.L., Benson, C.S., Everett, K.R. (1996), Energy balance and hydrological processes in an arctic watershed. In: Reynolds J. F., Tenhunen, J. D., editors. *Ecological studies; landscape function and disturbance in arctic tundra*. 120 ed. New York (NY): Springer-Verlag. p. 131-154.
- Kane, D.L., Carlson, R.F. (1973), Hydrology of the central arctic river basins of Alaska. In: *Institute of Water Resources Report*. IWR-41. Fairbanks (AK): University of Alaska. p. 51.
- Kane, D.L., Hinzman, L.D., Benson, C.S., Everett, K.R. (1989), Hydrology of Imnavait Creek, an arctic watershed. *Holarctic Ecology*, 12: 262-271.
- Kane, D.L., Gieck, R.E., Hinzman, L.D. (1990), Evapotranspiration from a small Alaskan arctic watershed. *Nordic Hydrology*, 21: 253-272.
- Kane, D.L., Hinzman, L.D., Benson, C.S., Liston, G.E. (1991), Snow hydrology of a headwater Arctic basin: 1. Physical measurements and process studies. *Water Resources Research*, 27(6): 1099-1109.
- Kane, D.L., McNamara, J.P., Yang, D., Olsson, P.Q., Gieck, R.E. (2003), An extreme rainfall/runoff event in arctic Alaska. *Journal of Hydrometeorology*, 4(6): 1220-1228.
- Kane, D.L., Gieck, R.E., Kitover, D.C., Hinzman, L.D., McNamara, J.P., Yang, D. (2004), Hydrological cycle on the north slope of Alaska. In: Kane, D.L., Yang, D., editors. *Northern Research Basins Water Balance*. 290 ed. Wallingford (UK): IAHS Press. p. 224-236.
- Kane, D.L. and Yang, D. (2004), Overview of water balance determinations for high latitude watersheds. *Northern Research Basins Water Balance*. 290 ed. Wallingford (UK): IAHS Press. p. 1-12.
- Kane, D.L., Hinzman, L.D., Gieck, R.E., McNamara, J.P., Youcha, E.K., Oatley, J.A. (2008), Contrasting extreme runoff events in areas of continuous permafrost, Arctic Alaska. *Hydrology Research*, 39(4): 287-298.
- Lafleur, P.M., Rouse, W.R. (1988), The influence of surface cover and climate on energy partitioning and evaporation in a subarctic wetland. *Boundary-Layer Meteorology*, 44: 327-347.

- Liljedahl, A.K., Hinzman, L.D., Harazono, Y., Zona, D., Tweedie, C.E., Hollister, R.D., Engstrom, R., Oechel, W.C. (2011), Nonlinear controls on evapotranspiration in arctic coastal wetlands. *Biogeosciences*, 8: 3375-3389.
- Liu, C.F., Zhang, Z.Q., Sun, G., Zha, T.G., Zhu, J.Z., Shen, L.H., Chen, J., Fang, X.R., Chen, J.Q. (2009), Quantifying evapotranspiration and biophysical regulations of a poplar plantation assessed by eddy covariance and sap-flow methods. *Chinese Journal of Plant Ecology*, 33(4): 706-718.
- Marsh, P., Bigras, S.C. (1988), Evaporation from Mackenzie Delta Lakes, N.W.T., Canada. *Arctic and Alpine Research*, 20(2): 220-229.
- Mather, J.R., Thornthwaite, C.W. (1958), Microclimatic investigations at Point Barrow, Alaska, 1957-1958. *Climatology*, 11(2): 176.
- McNamara, J.P., Kane, D.L., Hinzman, L.D. (1997), Hydrograph separations in an arctic watershed using mixing model and graphical techniques. *Water Resources Research*, 33(7): 1707-1719.
- McNamara, J.P., Kane, D.L., Hinzman, L.D. (1998), An analysis of streamflow hydrology in the Kuparuk river basin, arctic Alaska: a nested watershed approach. *Journal of Hydrology*, 206(1-2): 39-57.
- McNamara, J.P., Kane, D.L., Hinzman, L.D. (1999), An analysis of an arctic channel network using a digital elevation model. *Geomorphology*, 29: 339-353.
- Mendez, J., Hinzman, L.D., Kane, D.L. (1998), Evapotranspiration from a wetland complex on the arctic coastal plain of Alaska. *Nordic Hydrology*, 29(4/5): 303-330.
- Ohmura, A. (1982), Evaporation from the surface of the arctic tundra on Axel Heiberg Island. *Water Resources Research*, 18(2): 291-300.
- Osterkamp, T.E., Payne, M.W. (1981), Estimates of permafrost thickness from well logs in northern Alaska. *Cold Regions Science and Technology*, 5(1): 13-27.
- Perlman, H. (2015), What is hydrology and what do hydrologists do?. *U.S. Geological Survey*. accessed 2015 October 17. <http://water.usgs.gov/edu/hydrology.html>.
- Persson, P.O.G., Fairall, C.W., Andreas, E.L., Guest, P.S., Perovich, D.K. (2002), Measurements near the atmospheric surface flux group tower at SHEBA: near-surface conditions and surface energy budget. *Journal of Geophysical Research-Oceans*, 107(C10): 35.

- Priestley, C.H.B., Taylor, R.J. (1972), On the assessment of surface heat flux and evaporation using large scale parameters. *Monthly Weather Review*, 100(2): 81-92.
- Reid, B., Faria, D. (2004), Evaporation studies in small NWT watersheds. In: Kane, D.L., Yang, D., editors. *Northern Research Basins Water Balance*. 290 ed. Wallingford (UK): IAHS Press. p. 178-185.
- Rouse, W.R., Stewart, R.B. (1976), Simple models for calculating evaporation from dry and wet tundra surfaces. *Arctic and Alpine Research*, 8(3): 263-274.
- Rouse, W.R. (1982a), The water balance of upland tundra in the Hudson Bay lowlands-measured and modeled. *Le Naturaliste Canadien*, 109: 457-467.
- Rouse, W.R. (1982b), Microclimate of low arctic tundra and forest at Churchill, Manitoba. In: French, H.M., editor. *The Roger J.E. Brown memorial volume: proceedings of the Fourth Canadian Permafrost Conference, Calgary, Alberta, March 2-6, 1981*. Ottawa (Canada): National Research Council of Canada. p. 68-80.
- Rovansek, R.J., Hinzman, L.D., Kane, D.L. (1996), Hydrology of a tundra wetland complex on the Alaskan Arctic Coastal Plain, U.S.A. *Arctic and Alpine Research*, 28(3): 311-317.
- Shutov, V., Gieck, R.E., Hinzman, L.D., Kane, D.L. (2006), Evaporation from land surface in high latitude areas: a review of methods and study results. *Nordic Hydrology*, 37(4-5): 393-411.
- Trochim, E.D. (2009), Modeling discharge in Imnavait Basin, north slope, Alaska. MS-Thesis. Fairbanks (AK): University of Alaska-Fairbanks.
- Walker, M.D., Walker, D.A., Everett, K.R. (1989), Wetland soils and vegetation, arctic foothills, Alaska. *U.S. Fish and Wildlife Service*, p. 89.
- Walker, M.D., Walker, D.A., Auerbach, N.A. (1994), Plant communities of a tussock tundra landscape in the Brooks Range foothills, Alaska. *Journal of Vegetation Science*, 5: 843-866.
- Waner, S. (c2000-2008), Finite mathematics on-line topic: linear and exponential regression. updated 2008; accessed 2015 October 25.
<http://www.zweigmedia.com/RealWorld/calctopic1/regression.html>.
- Weller, G., Holmgren, B. (1974), The microclimates of the arctic tundra. *Journal of Applied Meteorology*, 13(8): 854-862.
- Wright, R.K. (1981), The water balance of a lichen tundra underlain by permafrost. *McGill SubArctic Research Papers, no 33; Climatological Research Series*. 11 ed. Montreal (Quebec): Centre of Northern Studies and Research, McGill University. p. 110.

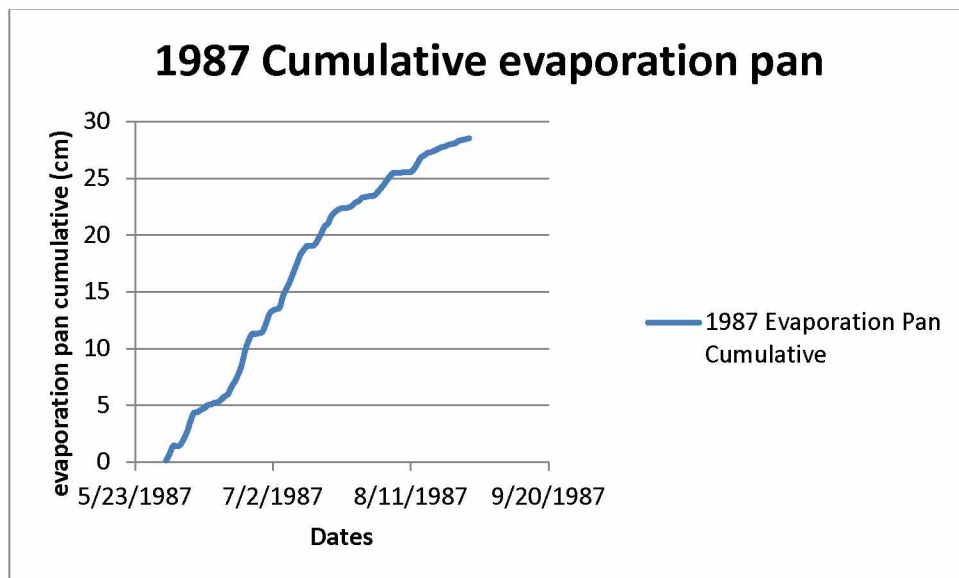
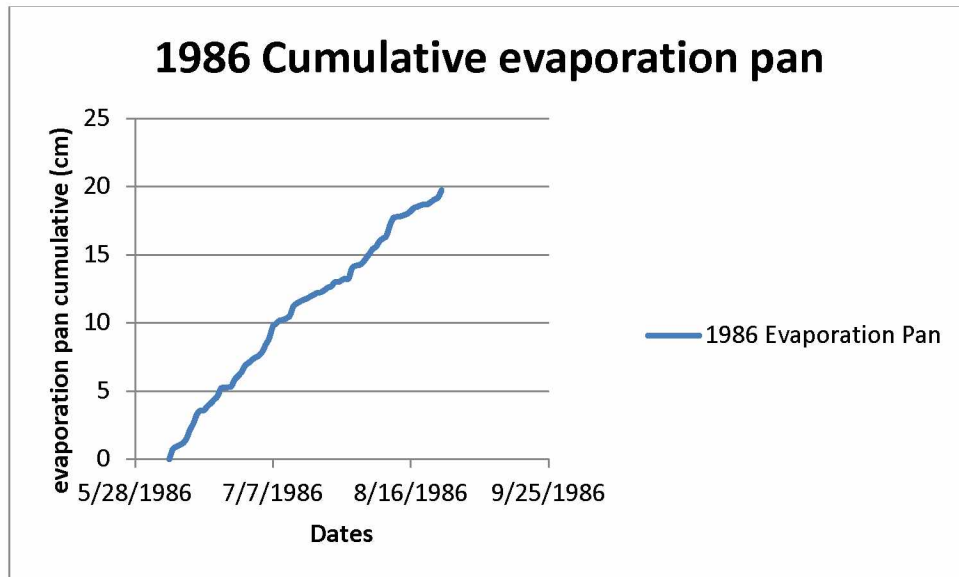
Xu, C.Y., Singh, V.P. (1998), Dependence of evaporation on meteorological variables at different time-scales and intercomparison of estimation methods. *Hydrological Processes*, 12: 429-442.

Young, K.L., Woo, M.K., Edlund, S.A. (1997), Influence of local topography, soils, and vegetation on microclimate and hydrology at a high arctic site, Ellesmere Island, Canada. *Arctic and Alpine Research* 29(3): 270-284.

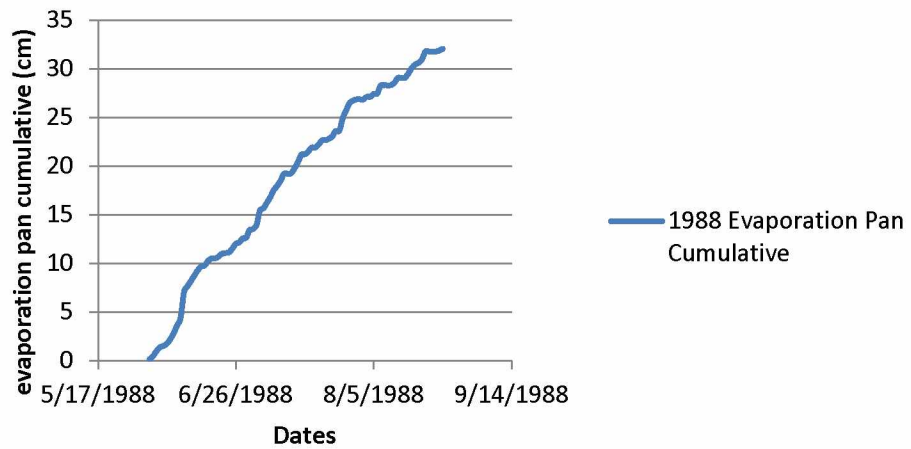
Zhang, K., Kimball, J.S., Mu, Q.Z., Jones, L.A., Goetz, S.J., Running, S.W. (2009), Satellite based analysis of northern evapotranspiration trends and associated changes in the regional water balance from 1983 to 2005. *Journal of Hydrology*, 379(1-2): 92-110.

APPENDICES

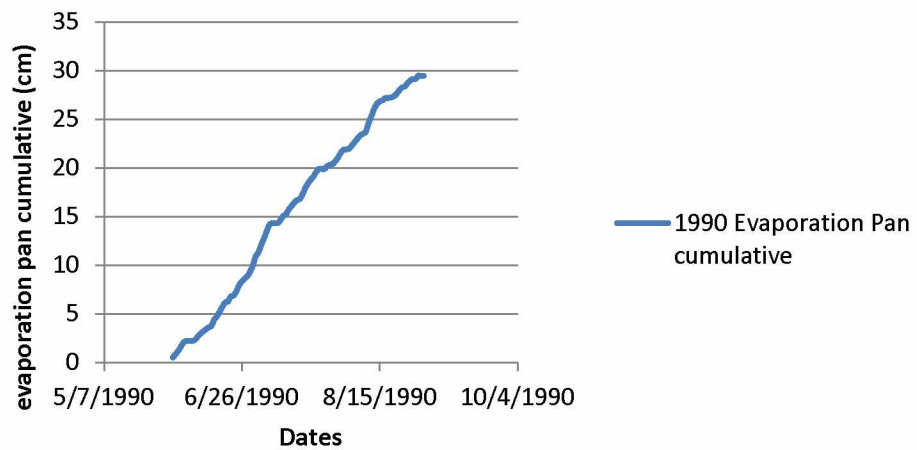
Appendix A: Warm Season Cumulative pan evaporation 1986-2008.



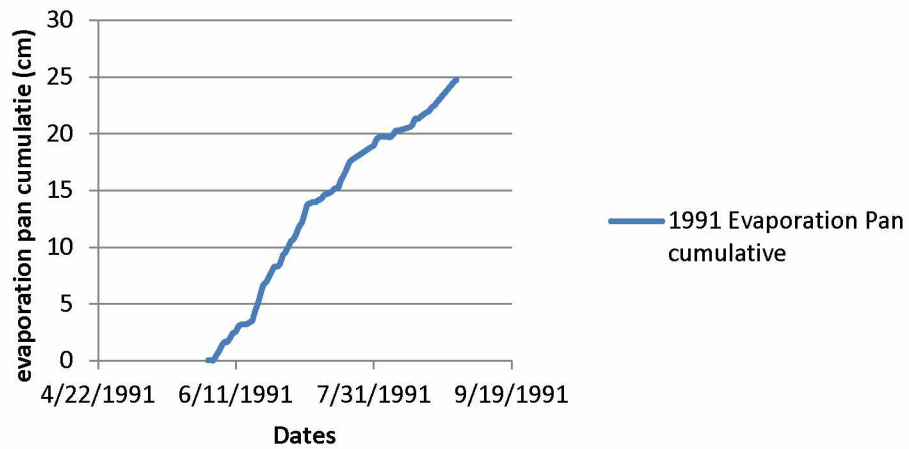
1988 Cumulative evaporation pan



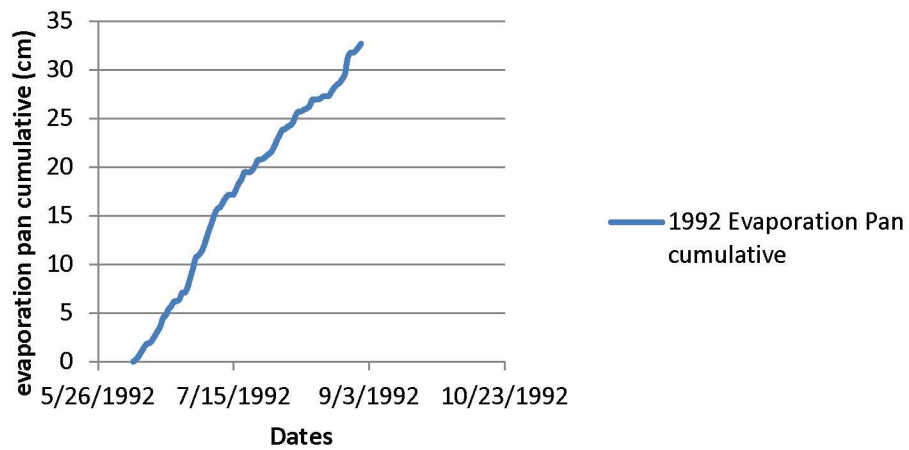
1990 Cumulative evaporation pan



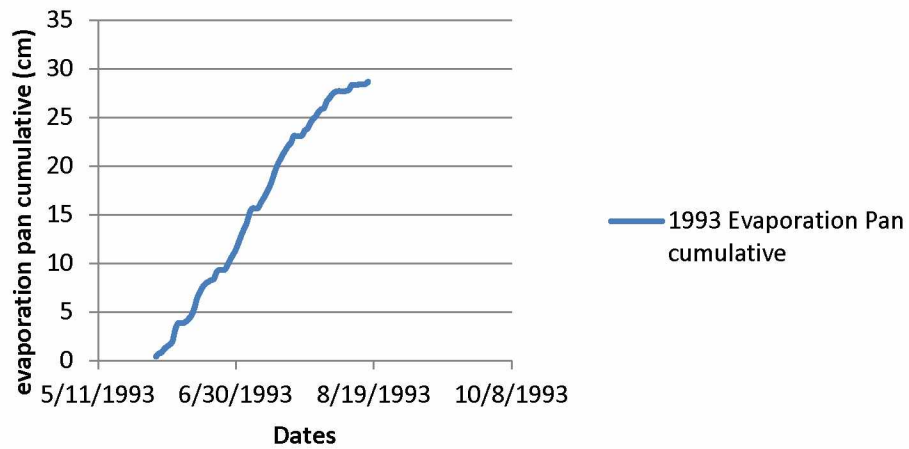
1991 Cumulative evaporation pan



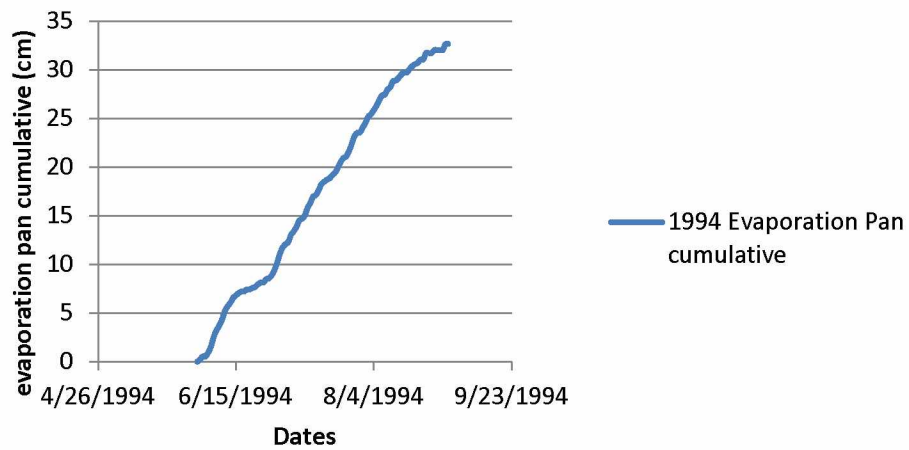
1992 Cumulative evaporation pan



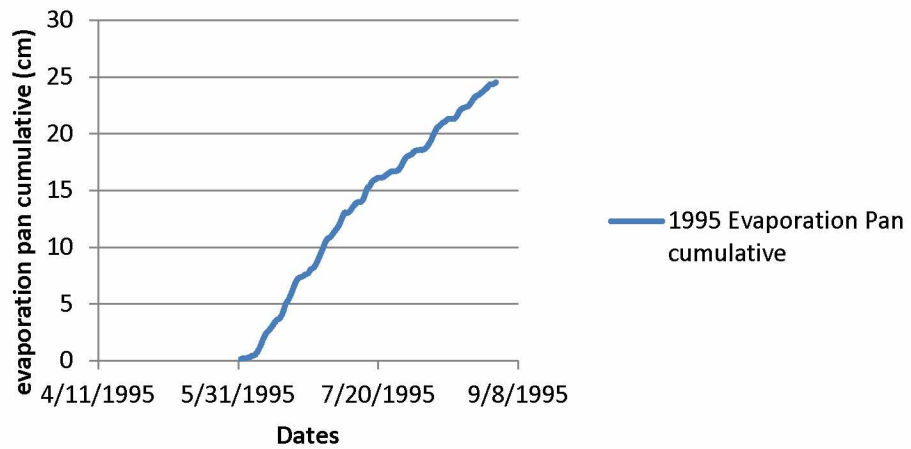
1993 Cumulative evaporation pan



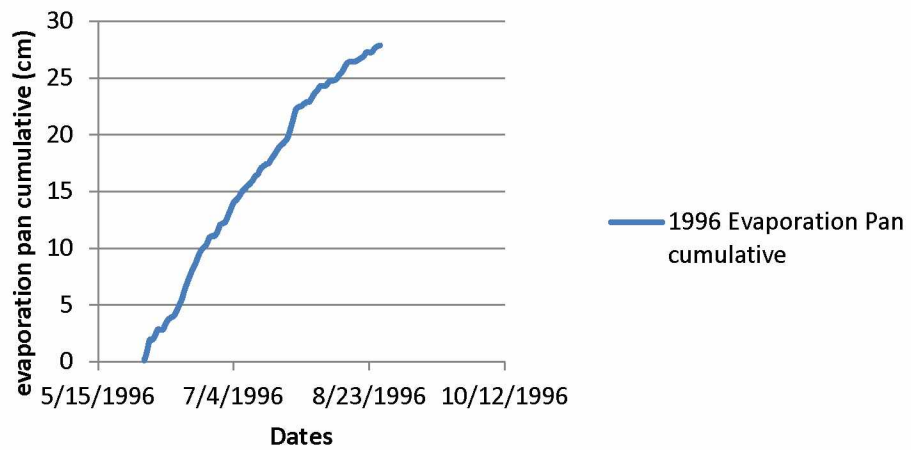
1994 Cumulative evaporation pan



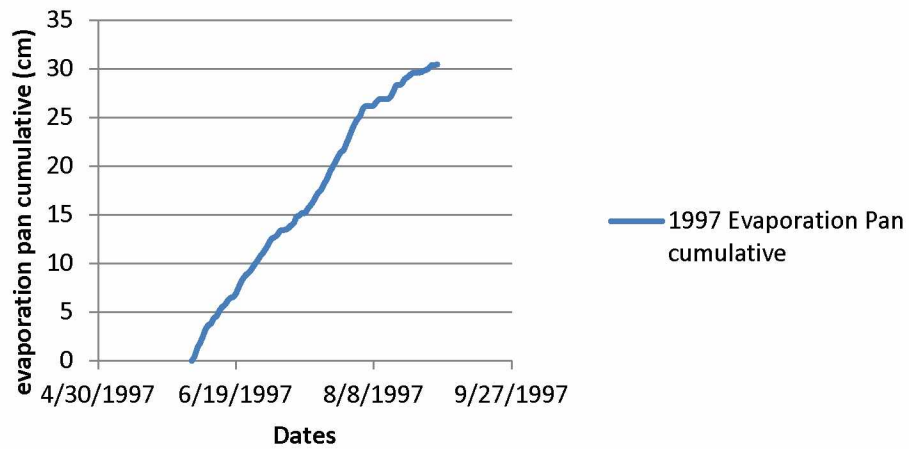
1995 Cumulative evaporation pan



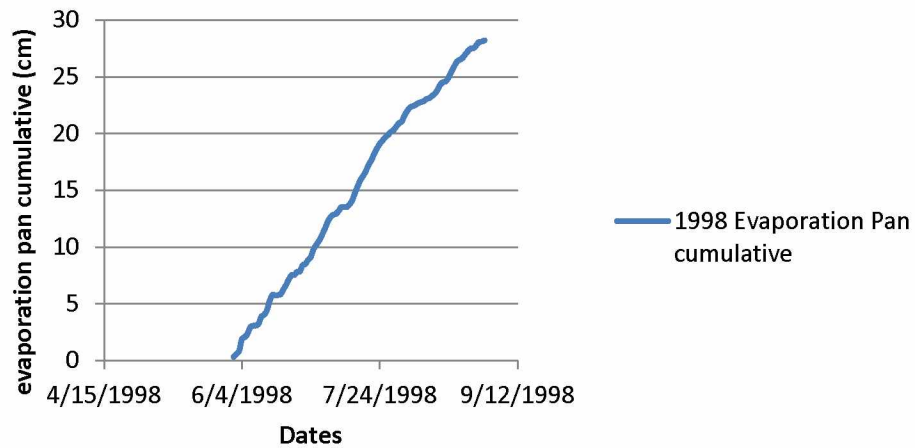
1996 Cumulative evaporation pan



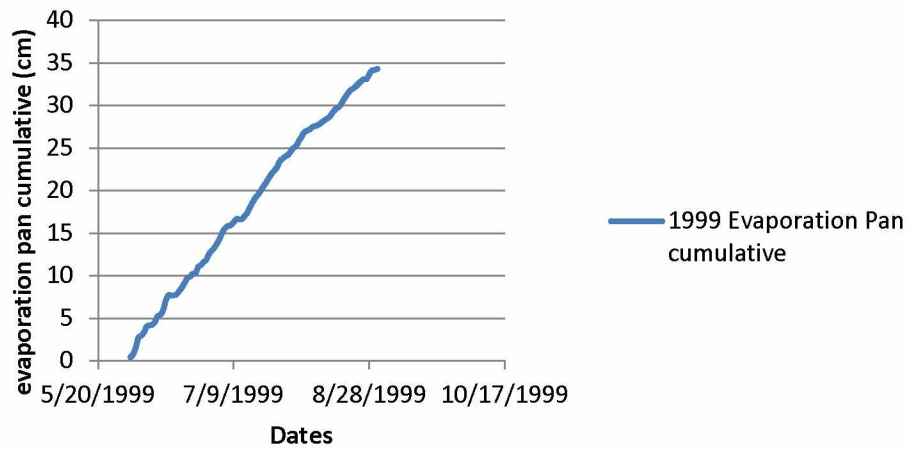
1997 Cumulative evaporation pan



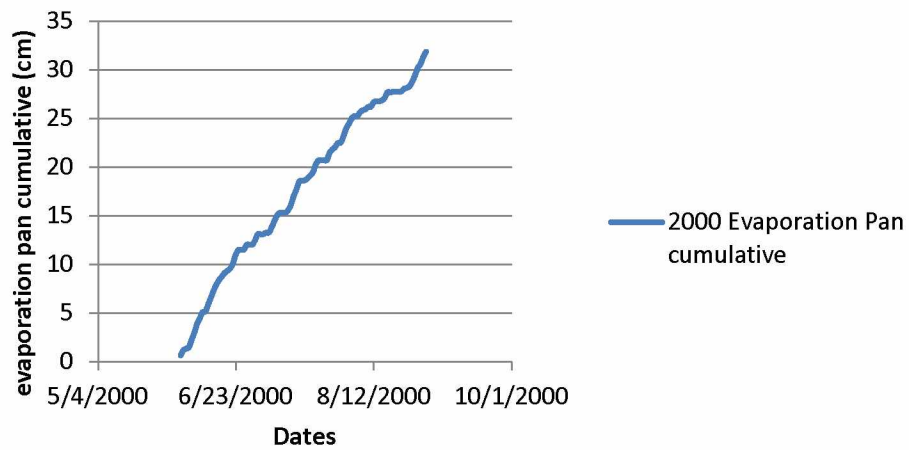
1998 Cumulative evaporation pan



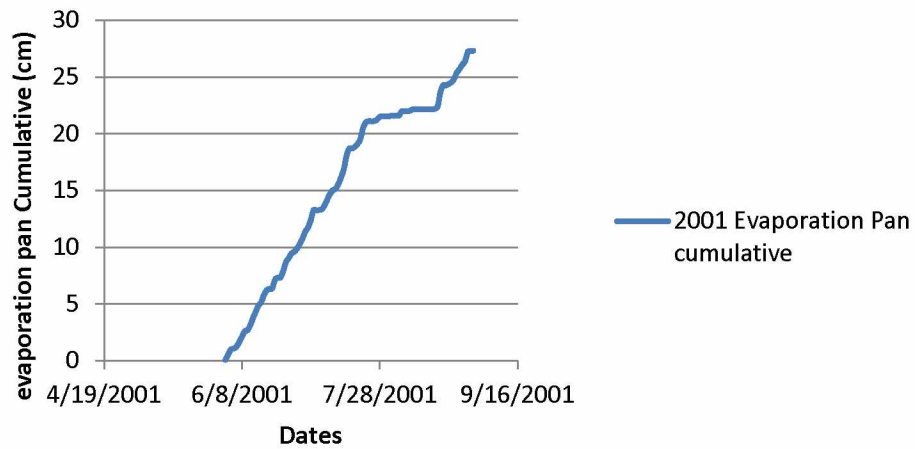
1999 Cumulative evaporation pan



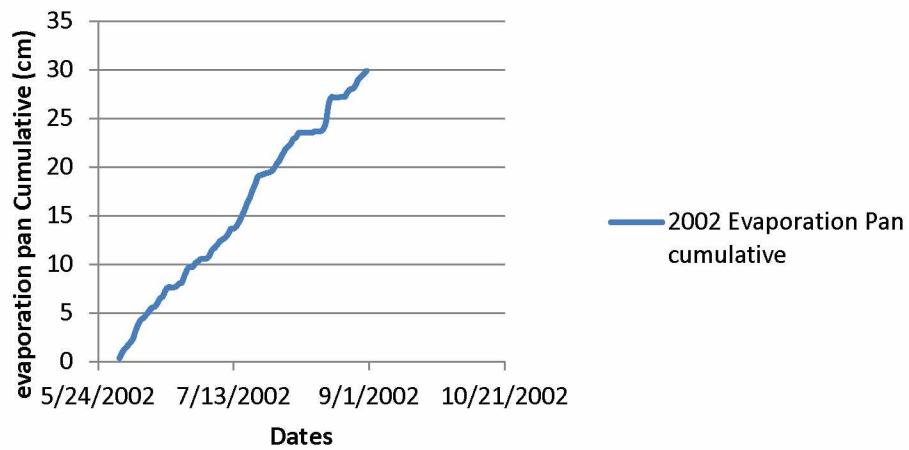
2000 Cumulative evaporation pan



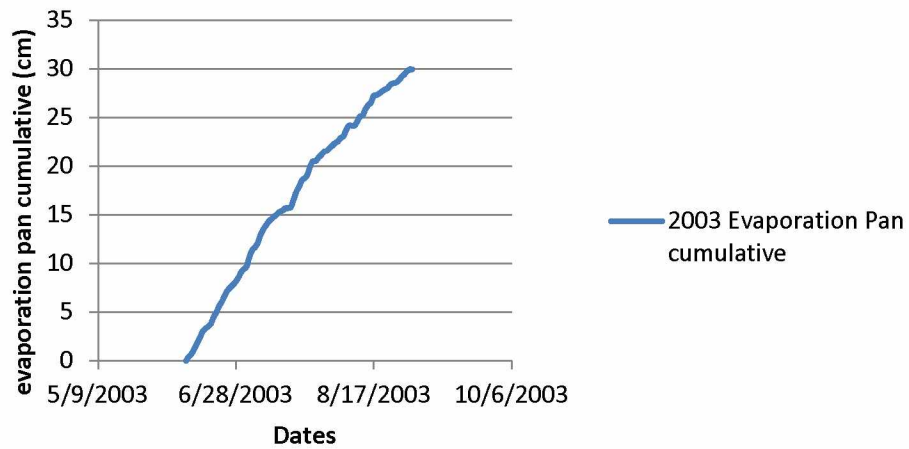
2001 Cumulative evaporation pan



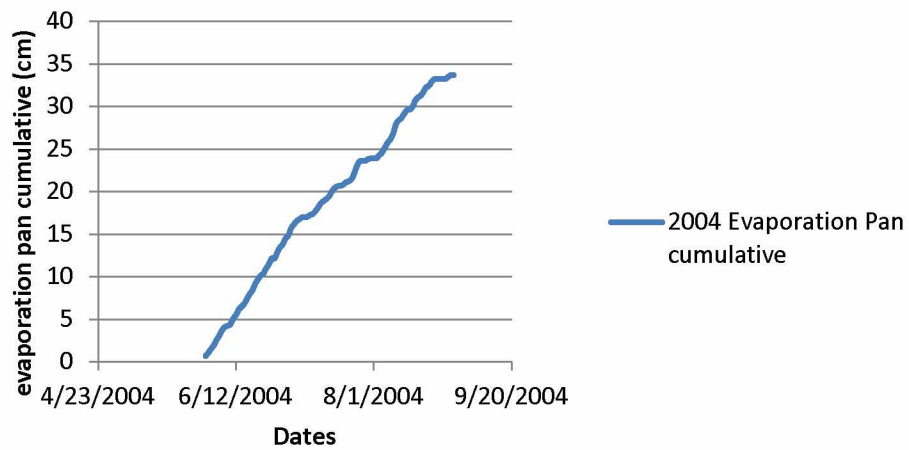
2002 Cumulative evaporation pan



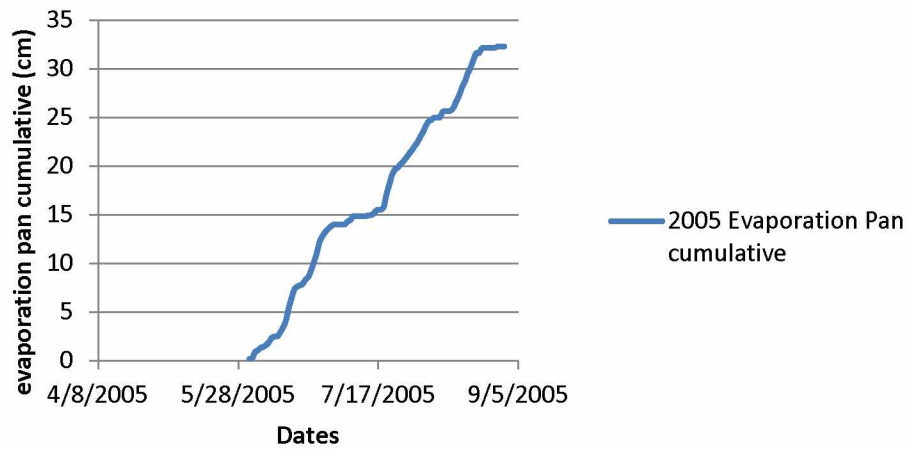
2003 Cumulative evaporation pan



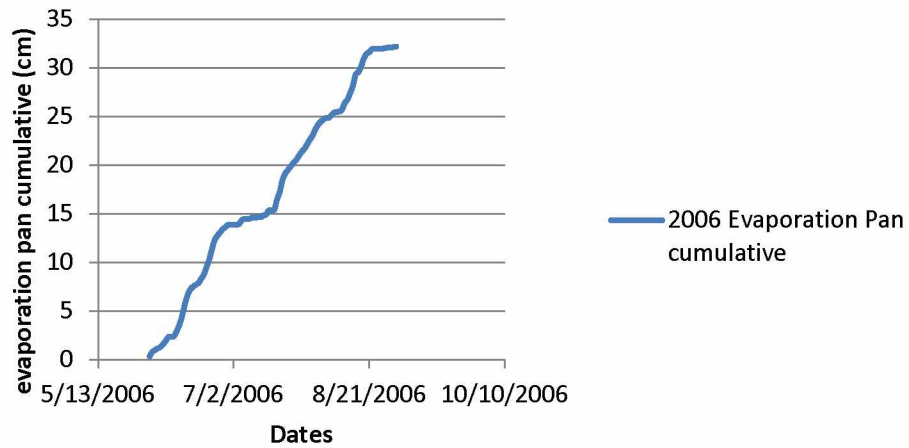
2004 Cumulative evaporation pan



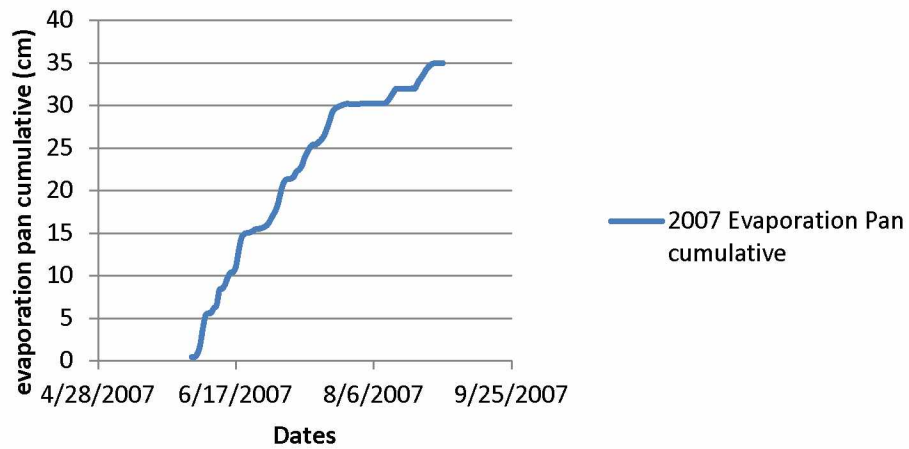
2005 Cumulative evaporation pan



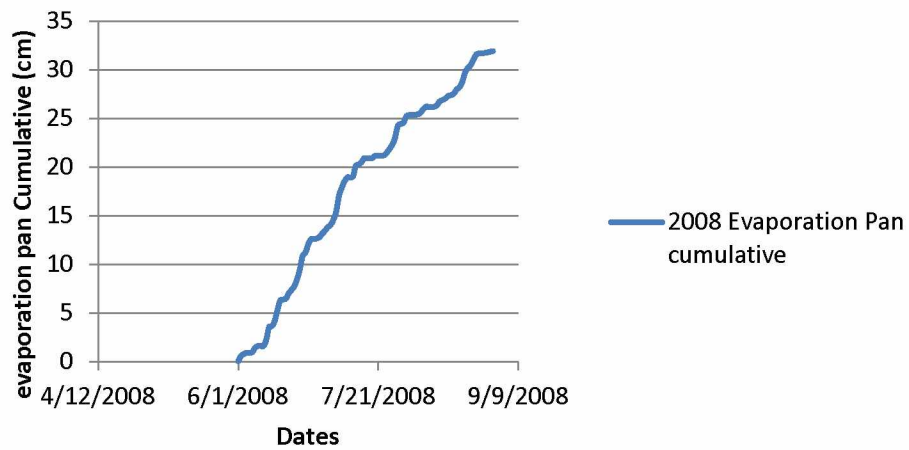
2006 Cumulative evaporation pan



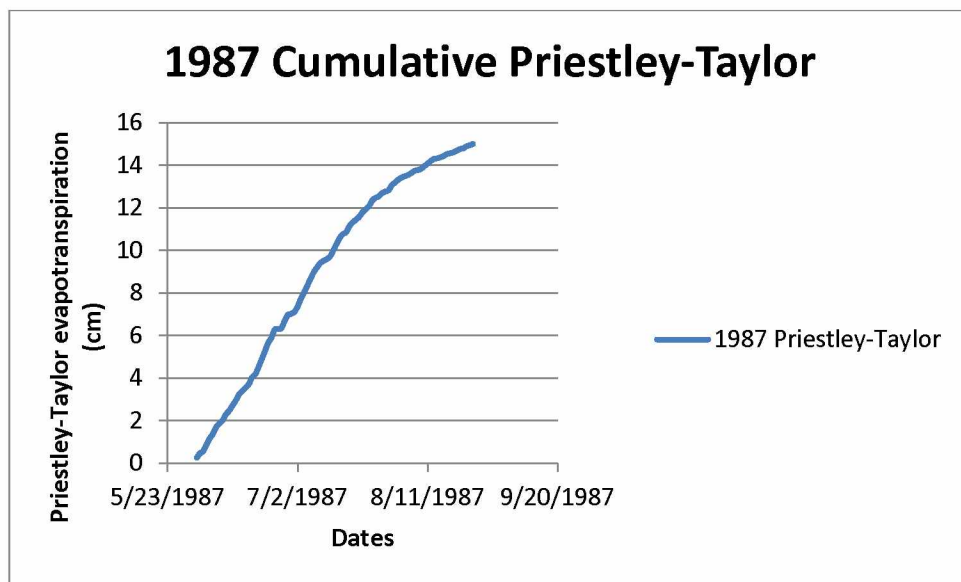
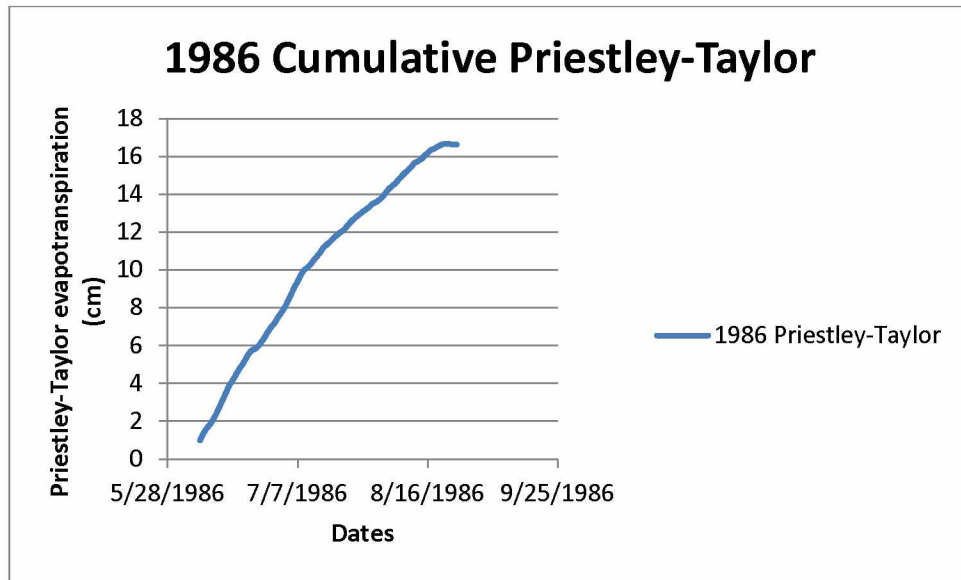
2007 Cumulative evaporation pan



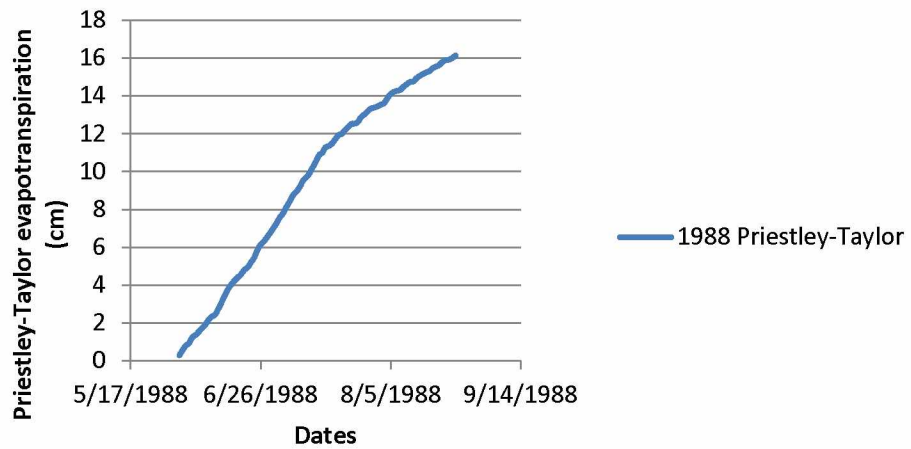
2008 Cumulative evaporation pan



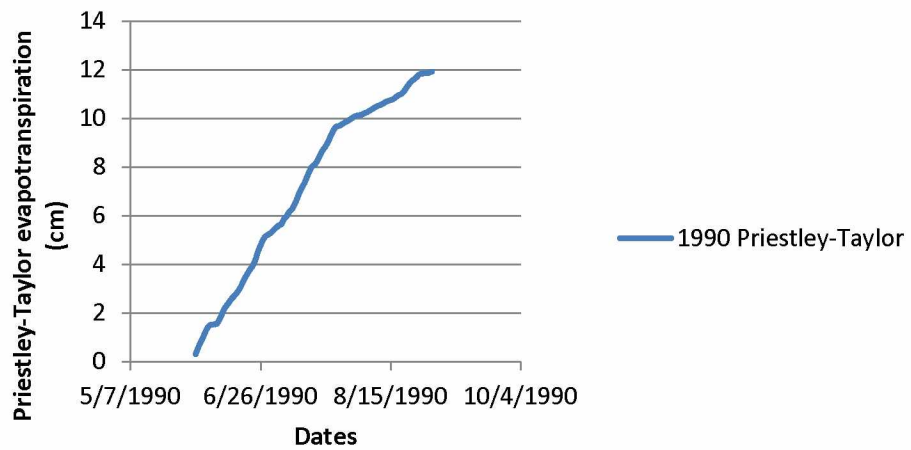
Appendix B: Warm Season Cumulative Priestley-Taylor calculated evapotranspiration 1986-2008.



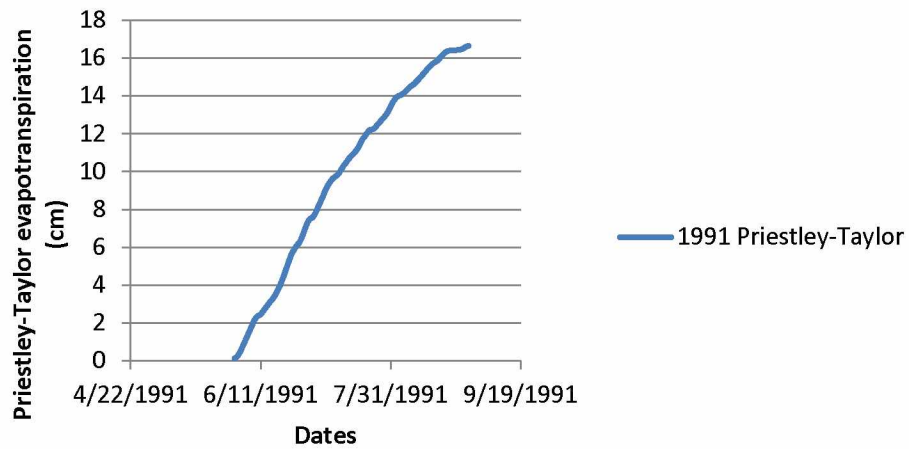
1988 Cumulative Priestley-Taylor



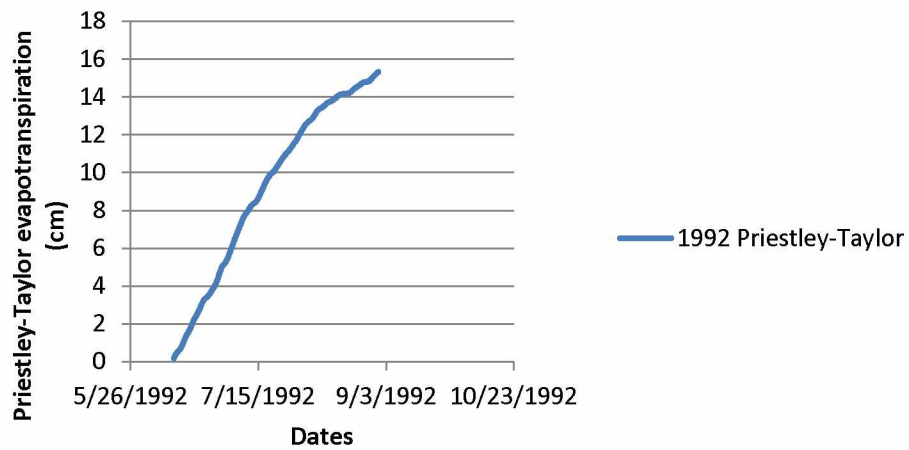
1990 Cumulative Priestley-Taylor



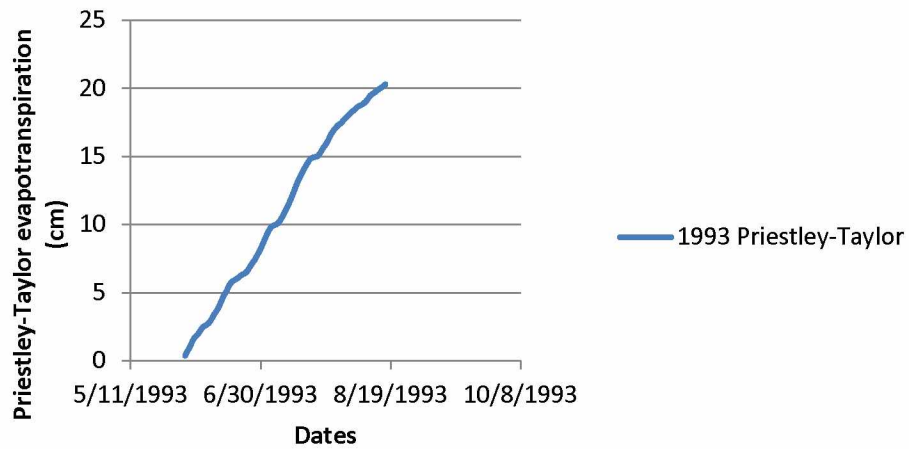
1991 Cumulative Priestley-Taylor



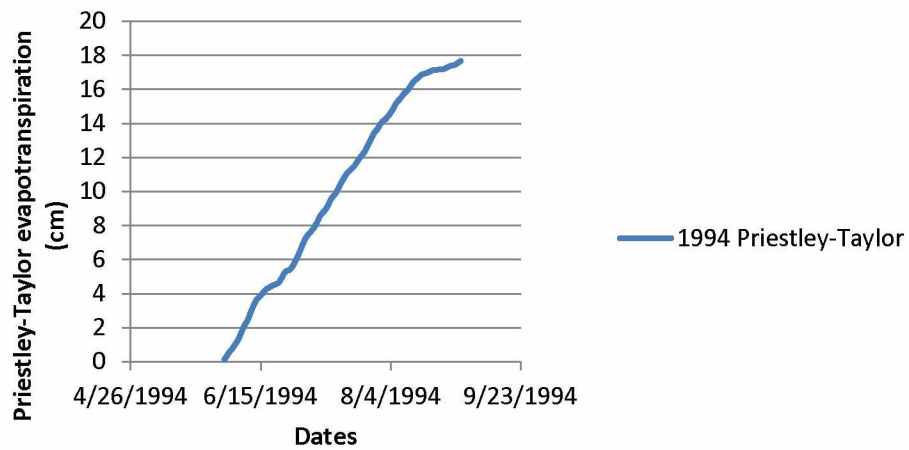
1992 Cumulative Priestley-Taylor



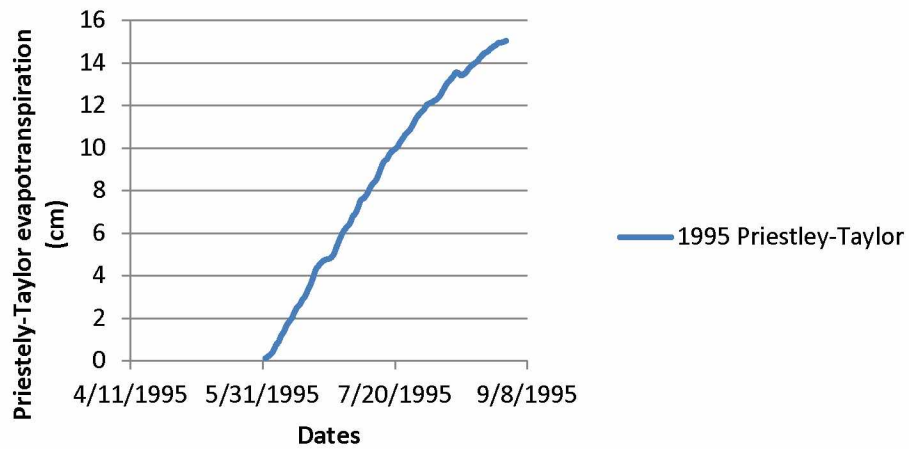
1993 Cumulative Priestley-Taylor



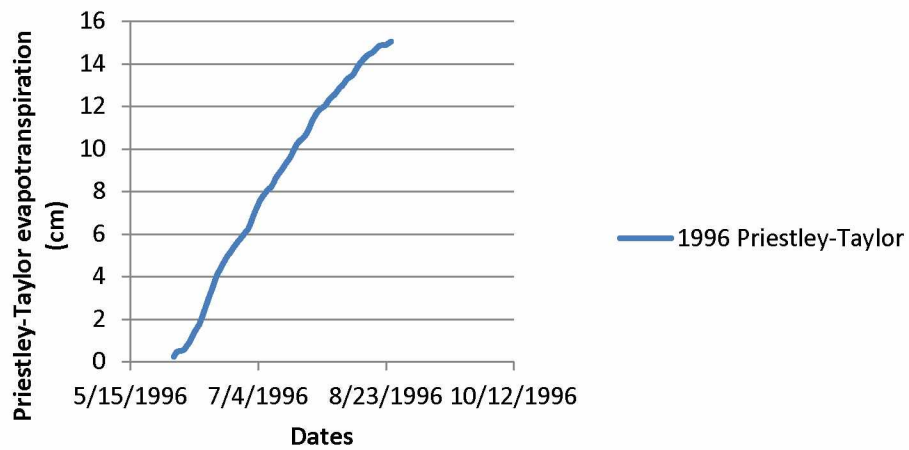
1994 Cumulative Priestley-Taylor



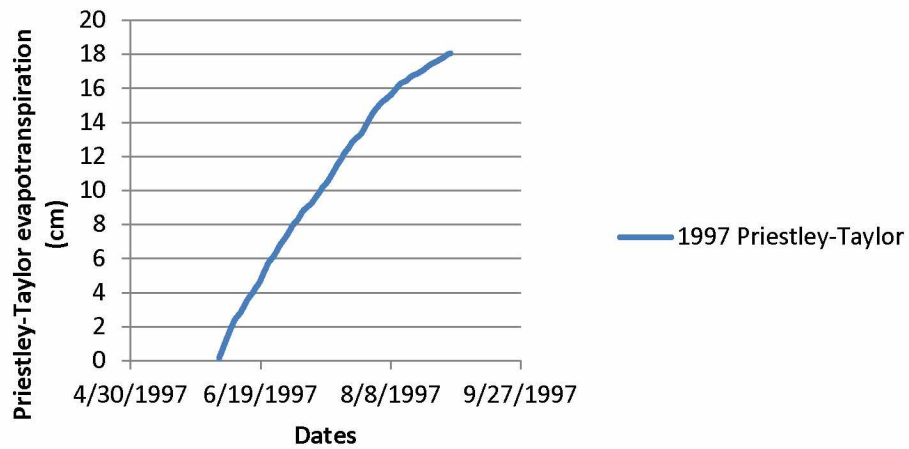
1995 Cumulative Priestley-Taylor



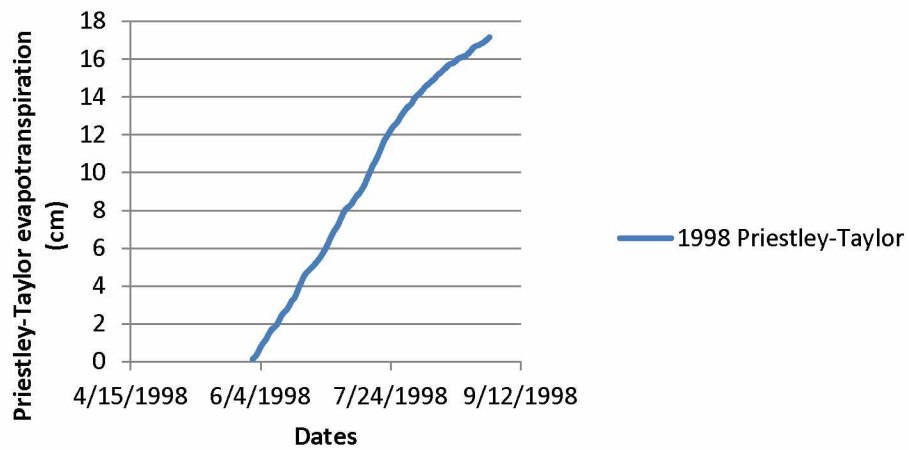
1996 Cumulative Priestley-Taylor



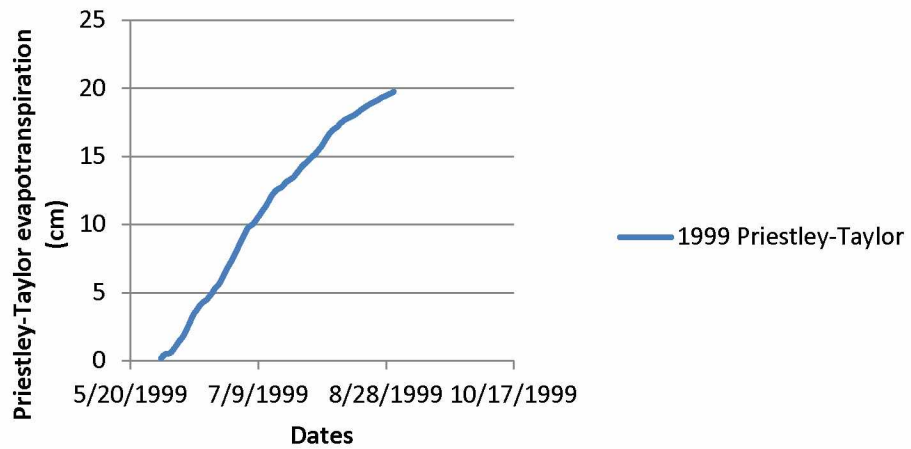
1997 Cumulative Priestley-Taylor



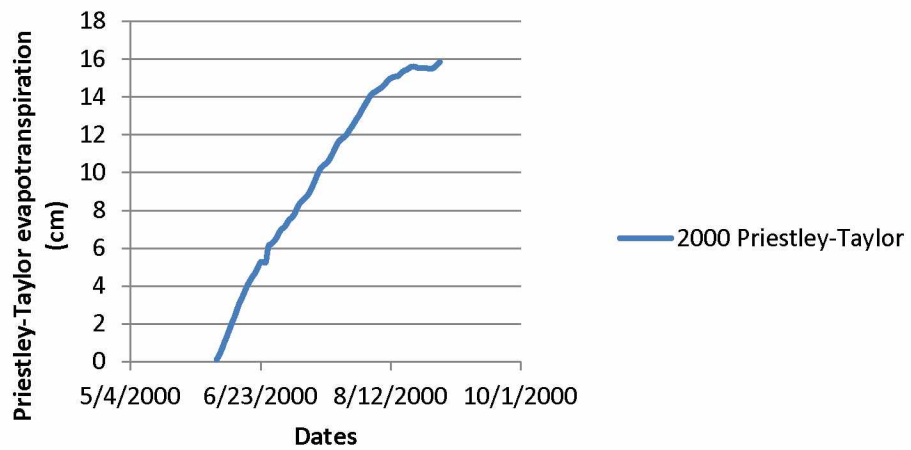
1998 Cumulative Priestley-Taylor



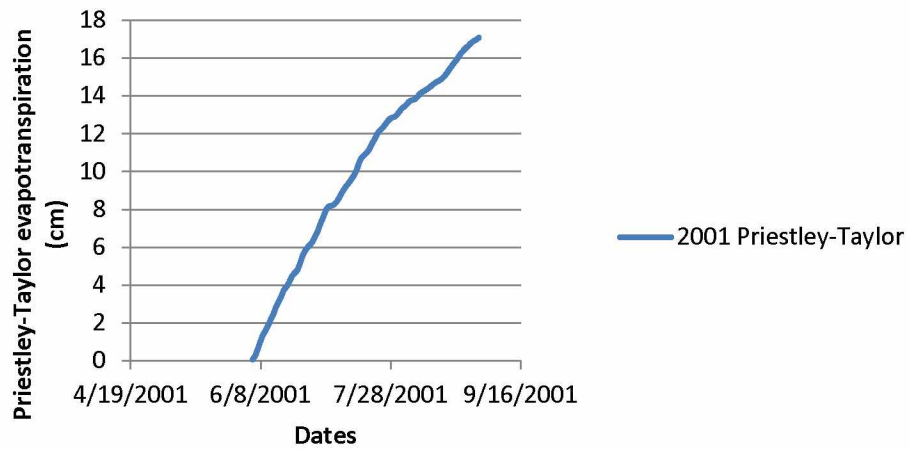
1999 Cumulative Priestley-Taylor



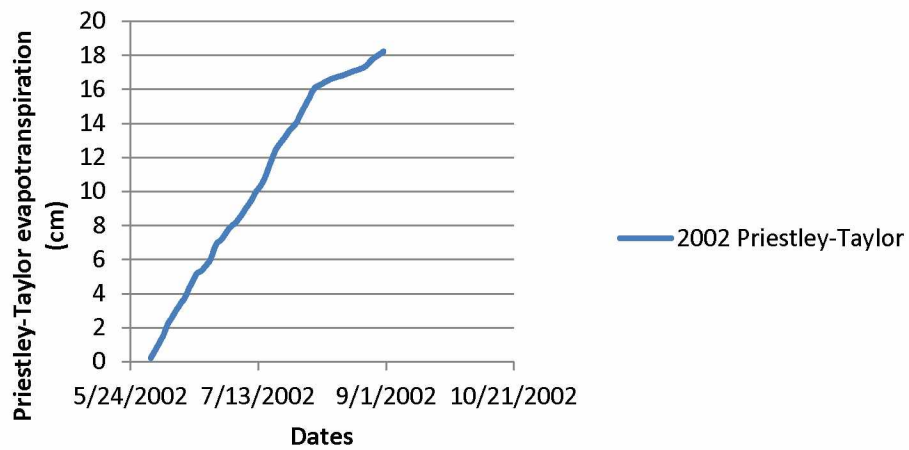
2000 Cumulative Priestley-Taylor



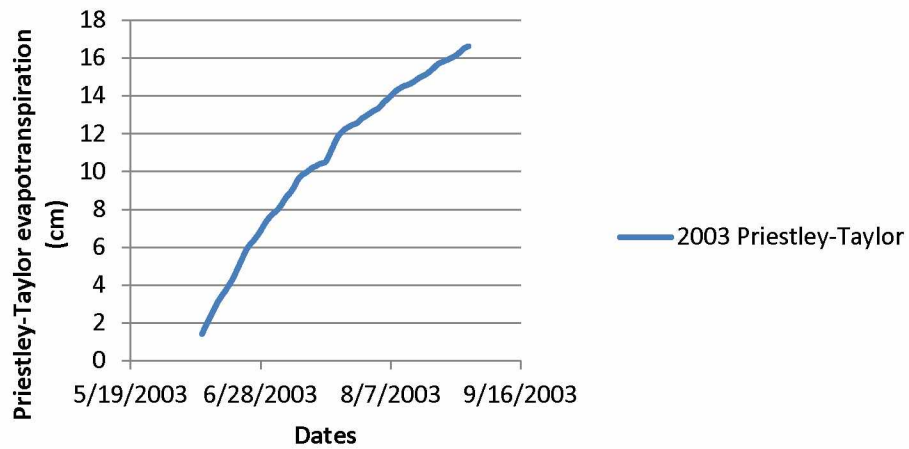
2001 Cumulative Priestley-Taylor



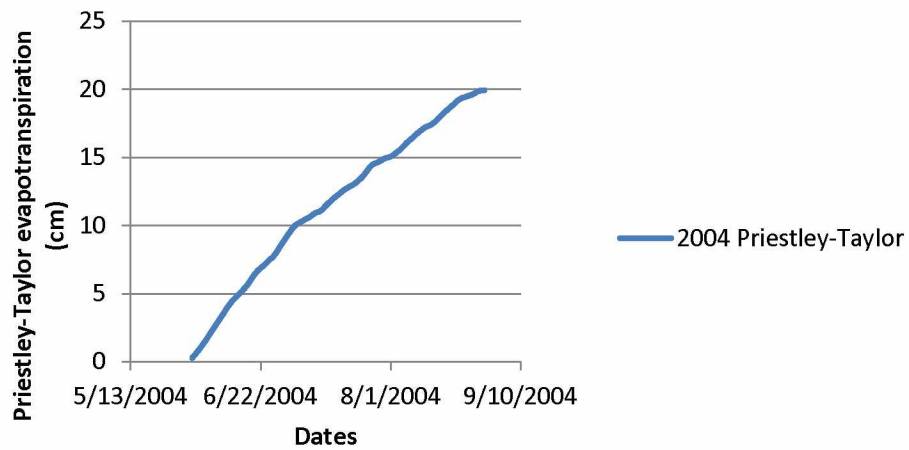
2002 Cumulative Priestley-Taylor



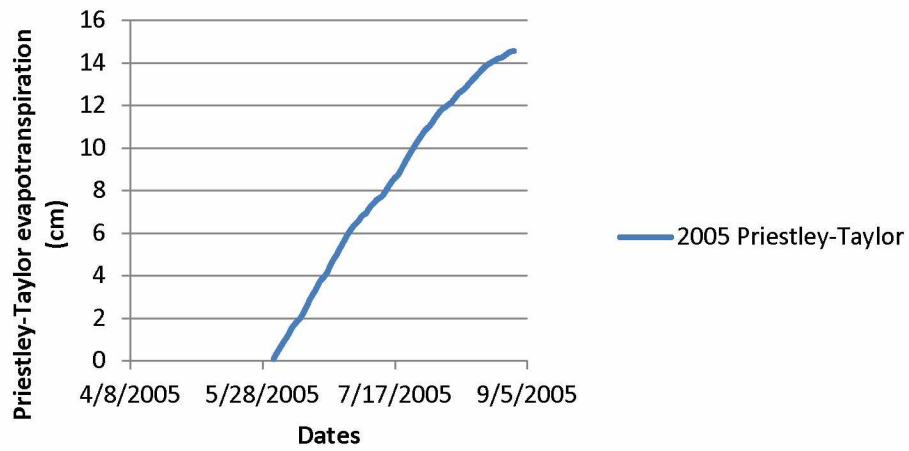
2003 Cumulative Priestley-Taylor



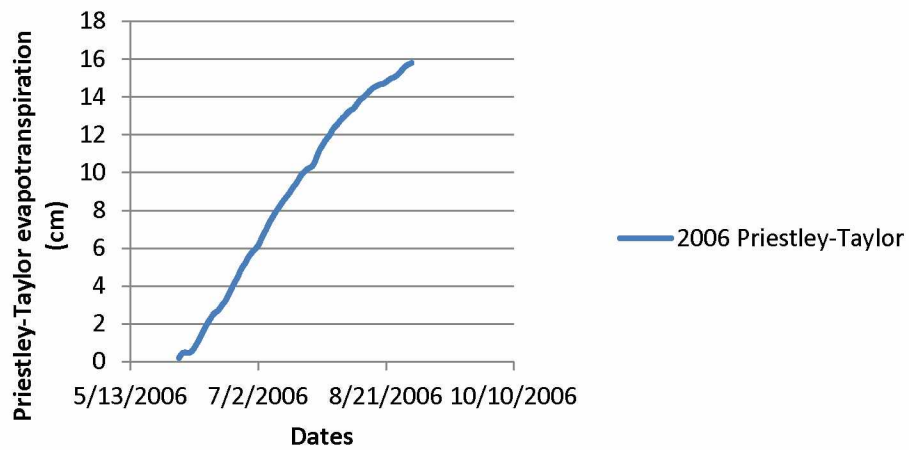
2004 Cumulative Priestley-Taylor



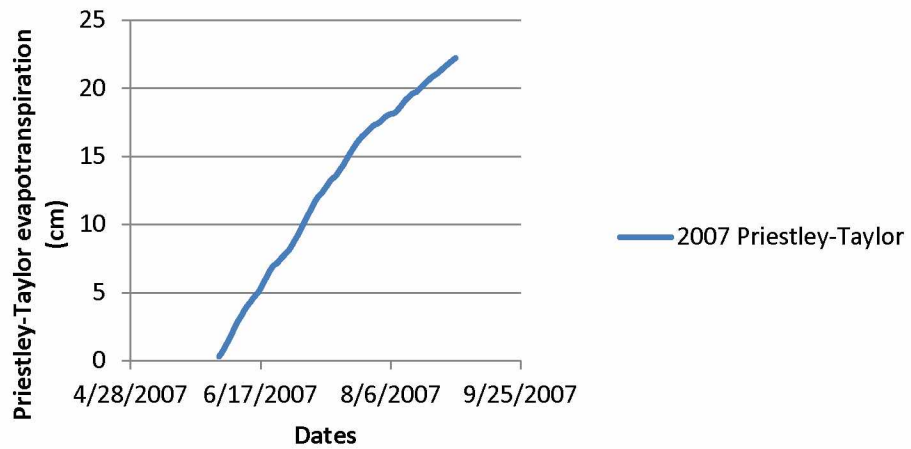
2005 Cumulative Priestley-Taylor



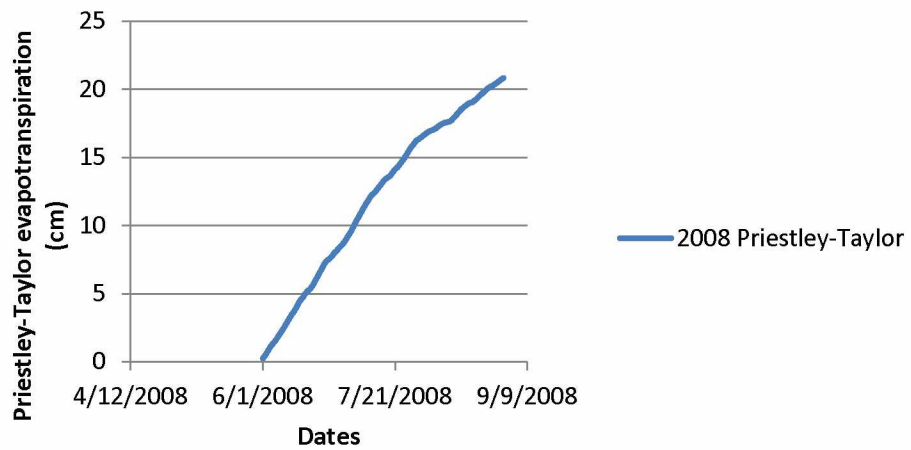
2006 Cumulative Priestley-Taylor



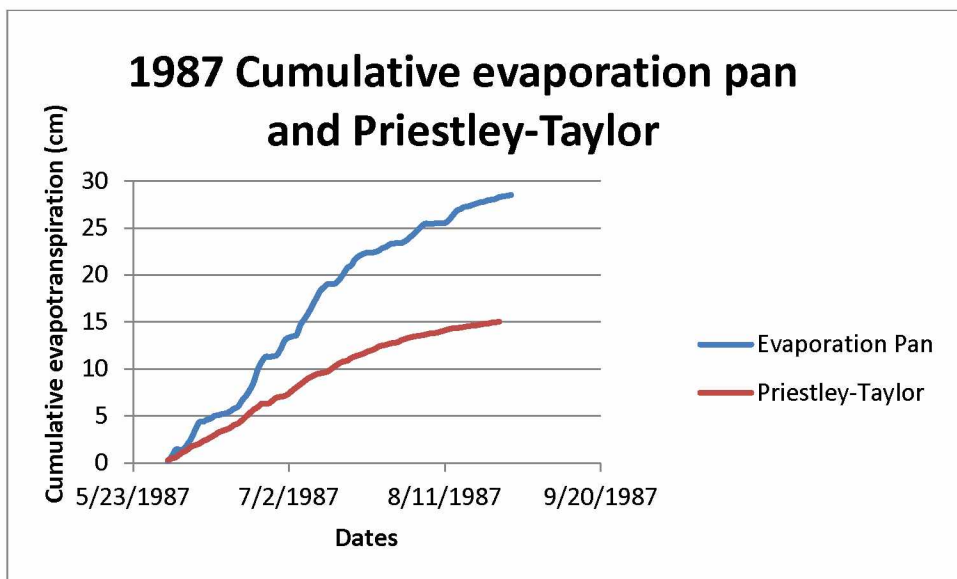
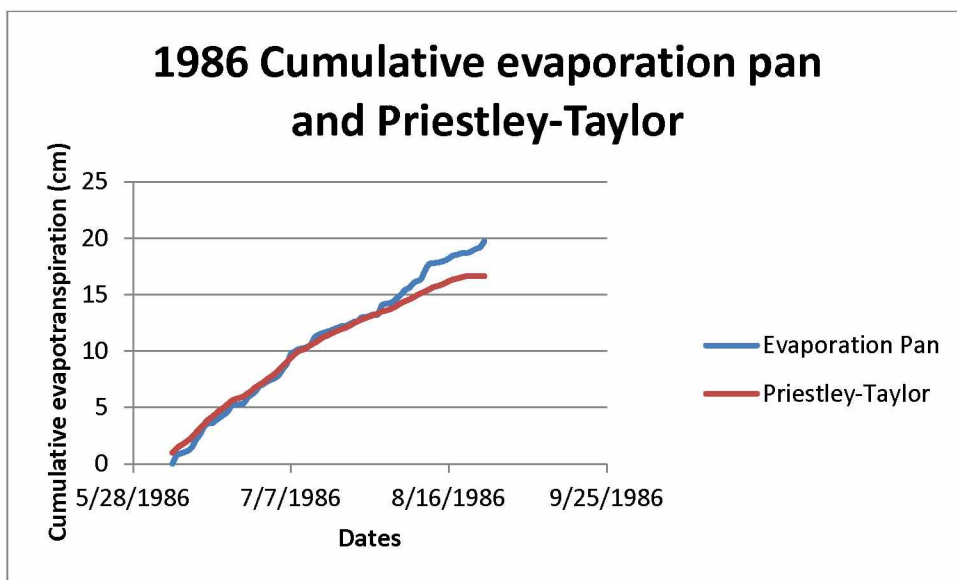
2007 Cumulative Priestley-Taylor



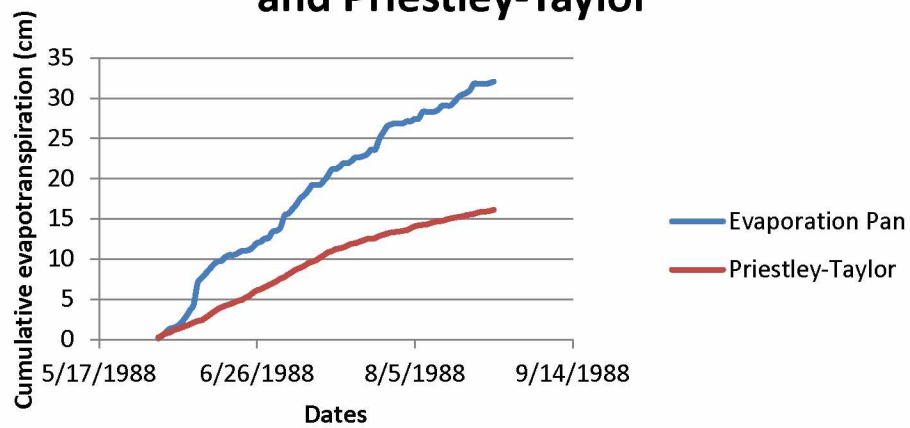
2008 Cumulative Priestley-Taylor



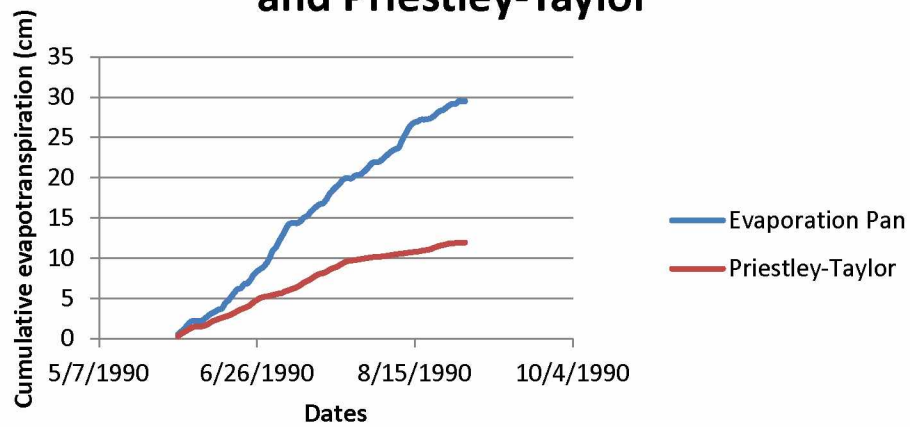
Appendix C: Warm Season Cumulative pan evaporation and Priestley-Taylor evapotranspiration 1986-2008.



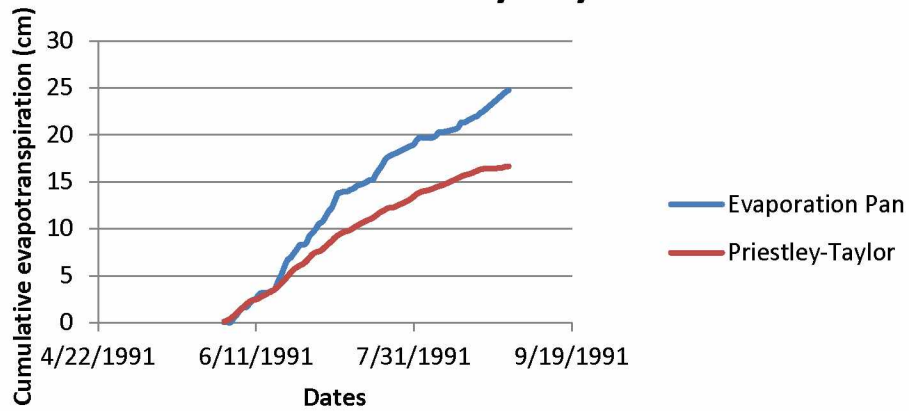
1988 Cumulative evaporation pan and Priestley-Taylor



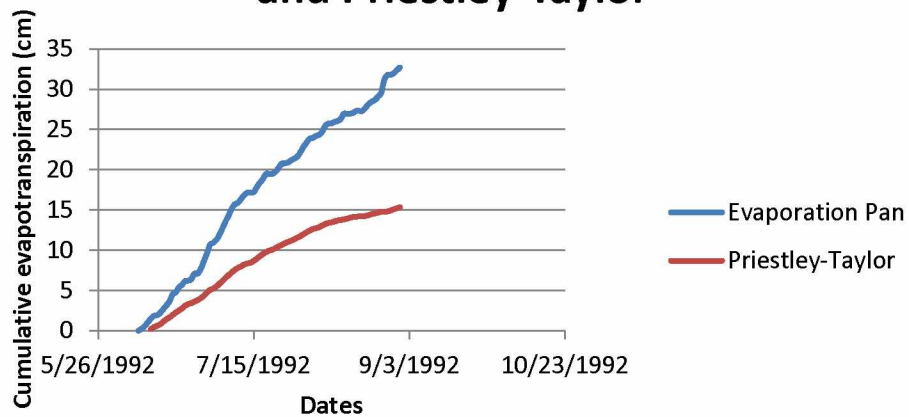
1990 Cumulative evaporation pan and Priestley-Taylor



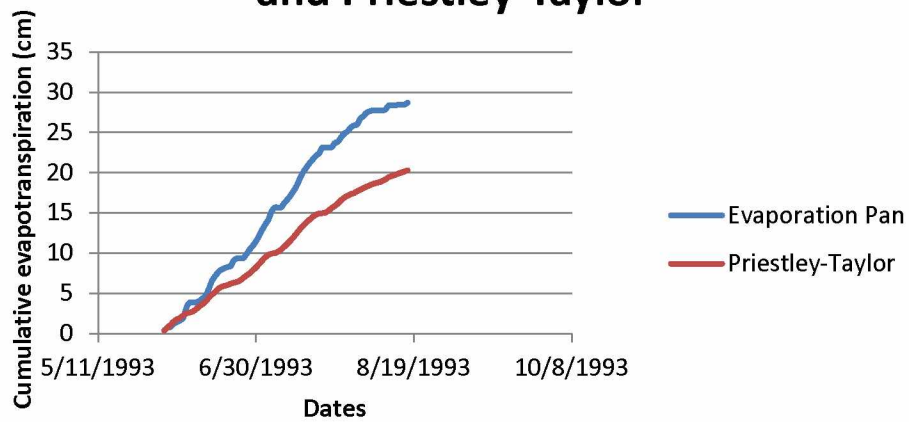
1991 Cumulative evaporation pan and Priestley-Taylor



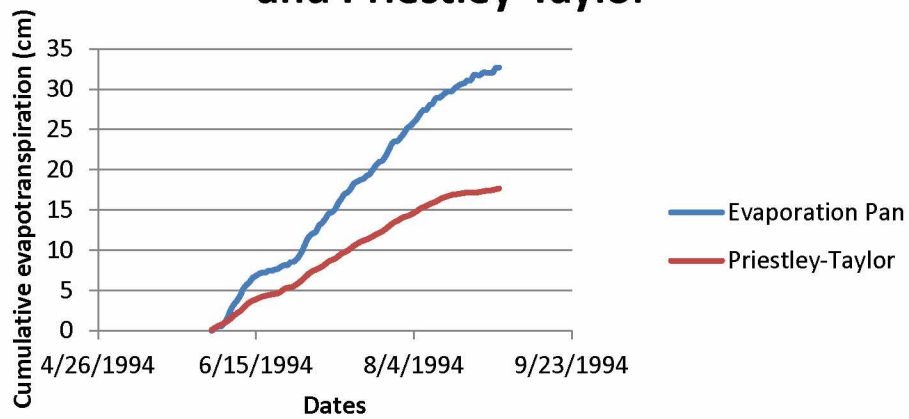
1992 Cumulative evaporation pan and Priestley-Taylor



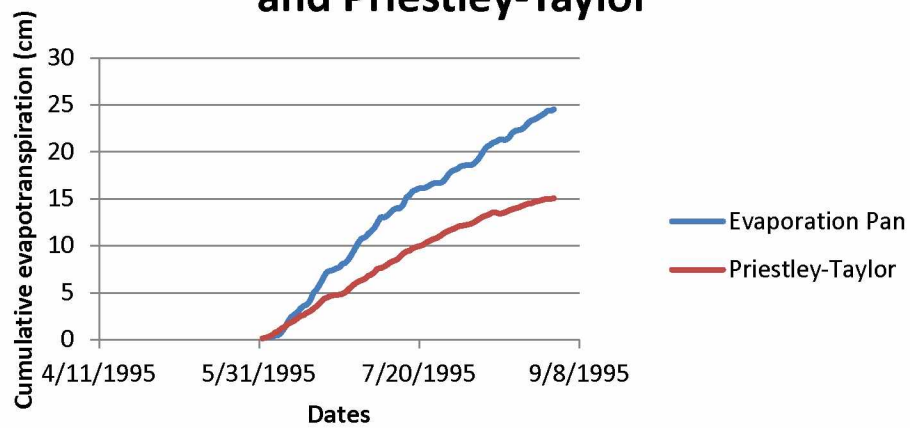
1993 Cumulative evaporation pan and Priestley-Taylor



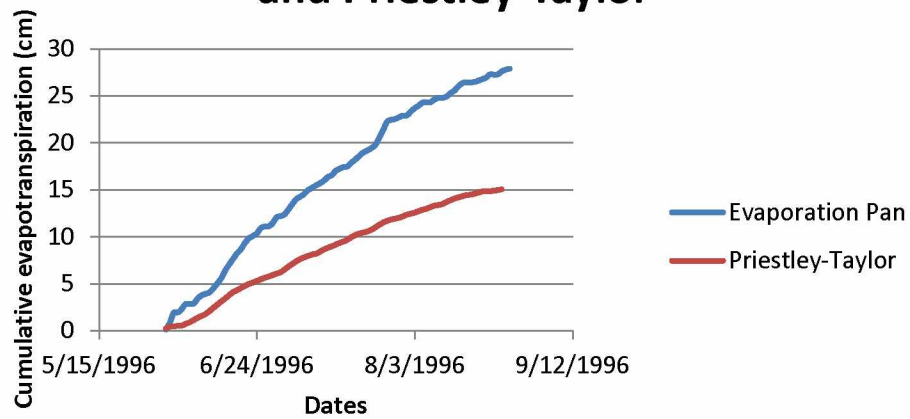
1994 Cumulative evaporation pan and Priestley-Taylor



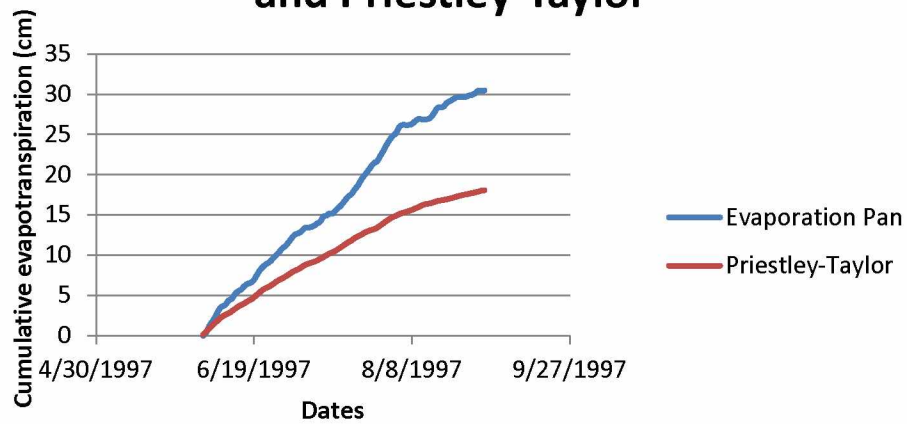
1995 Cumulative evaporation pan and Priestley-Taylor



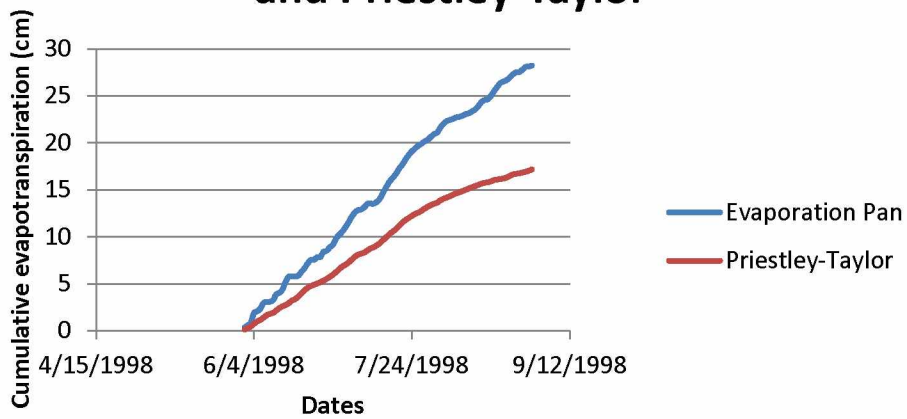
1996 Cumulative evaporation pan and Priestley-Taylor



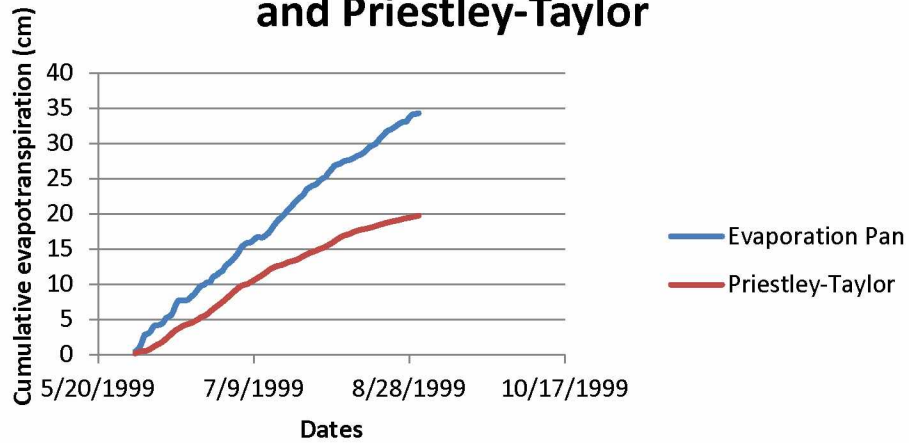
1997 Cumulative evaporation pan and Priestley-Taylor



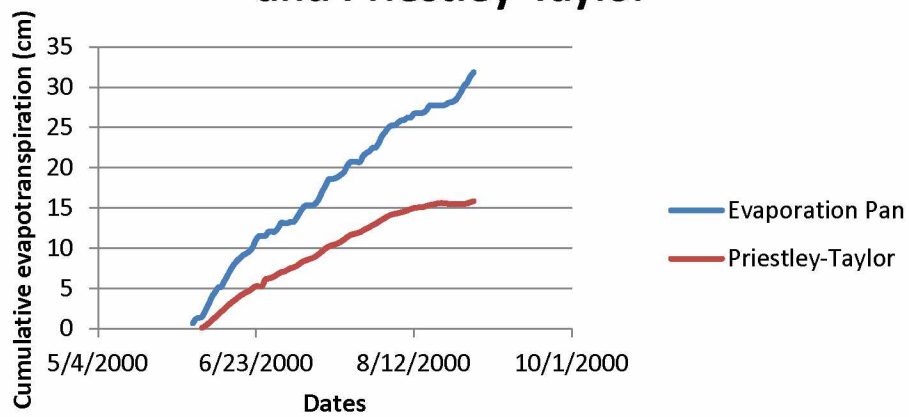
1998 Cumulative evaporation pan and Priestley-Taylor



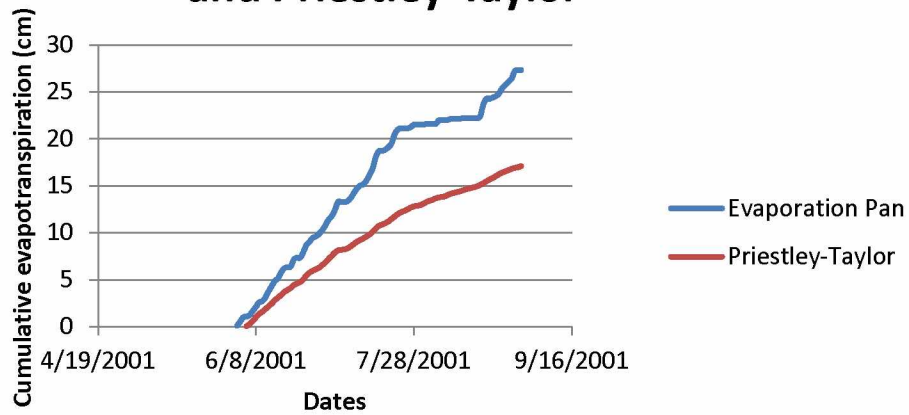
1999 Cumulative evaporation pan and Priestley-Taylor



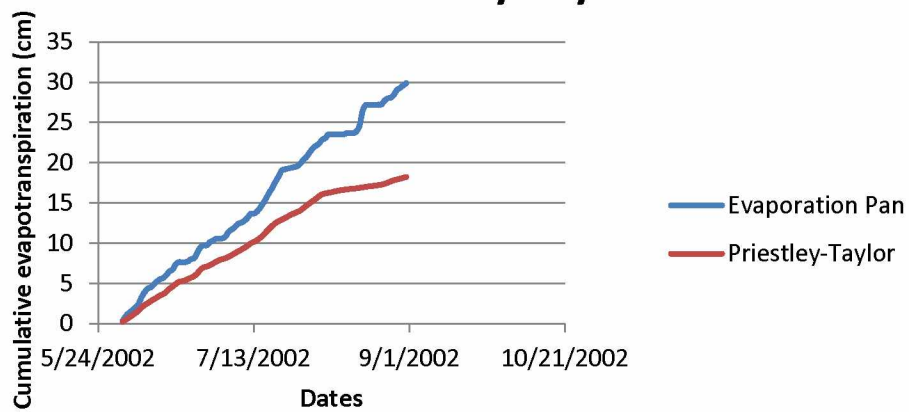
2000 Cumulative evaporation pan and Priestley-Taylor



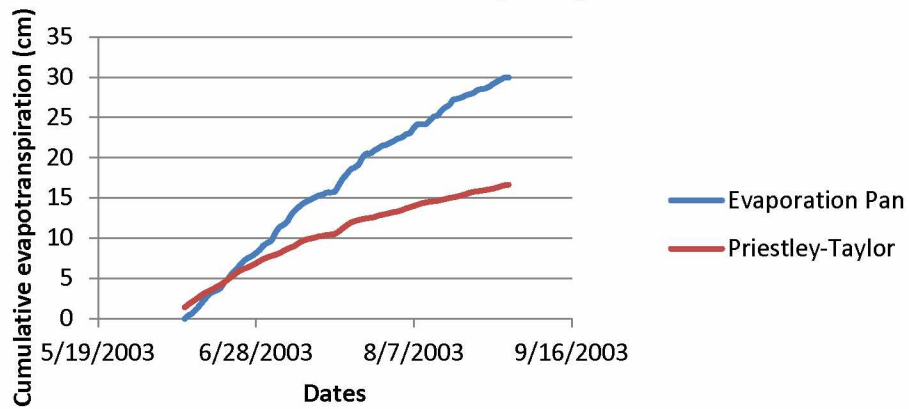
2001 Cumulative evaporation pan and Priestley-Taylor



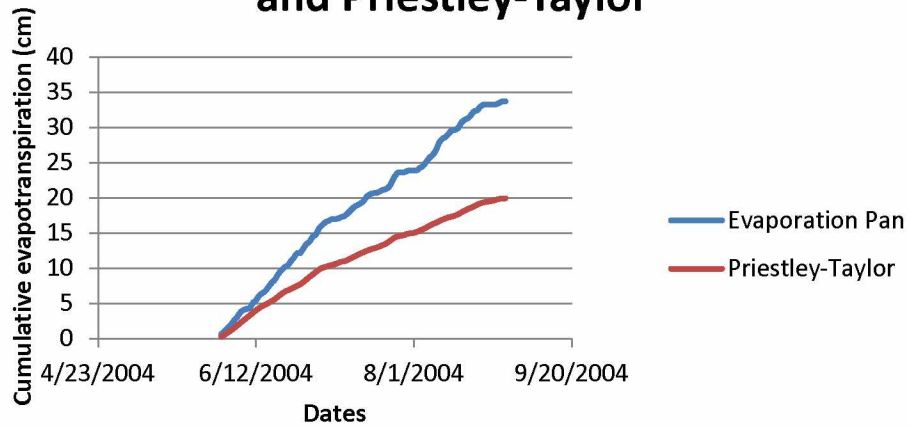
2002 Cumulative evaporation pan and Priestley-Taylor



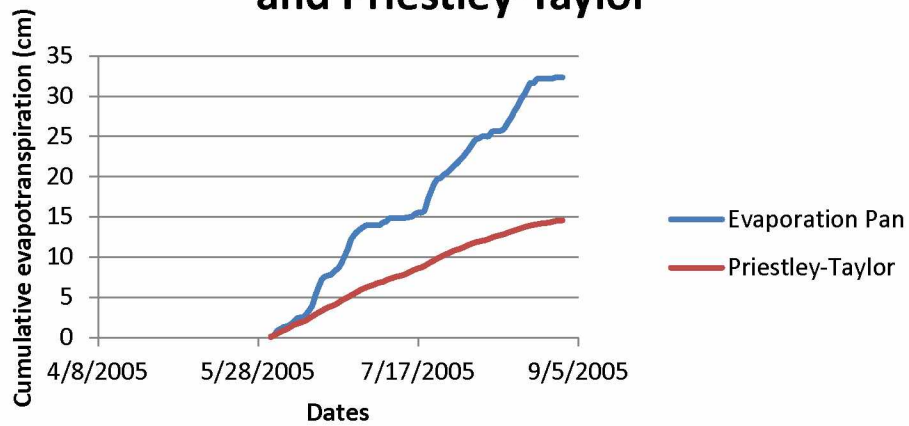
2003 Cumulative evaporation pan and Priestley-Taylor



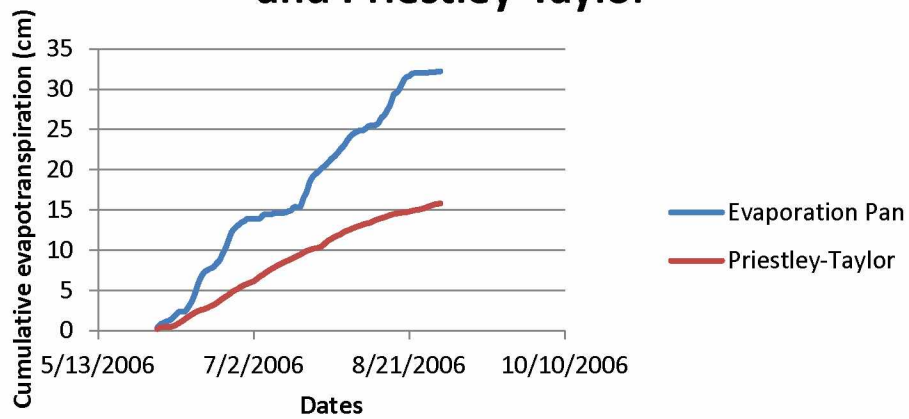
2004 Cumulative evaporation pan and Priestley-Taylor



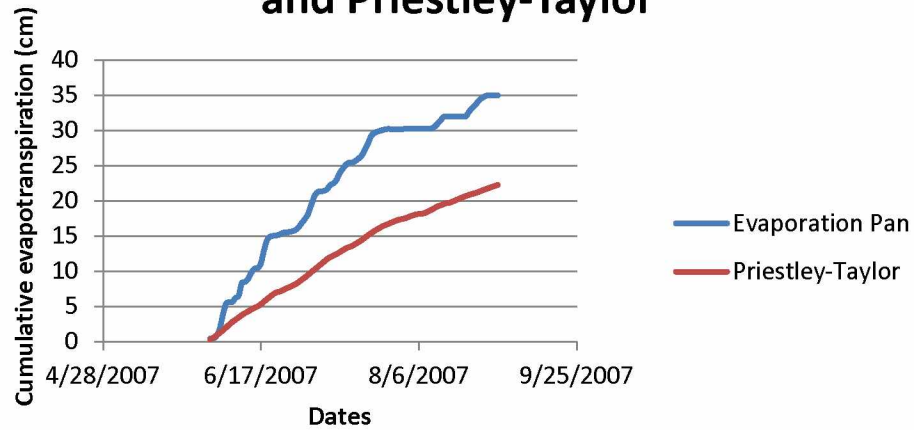
2005 Cumulative evaporation pan and Priestley-Taylor



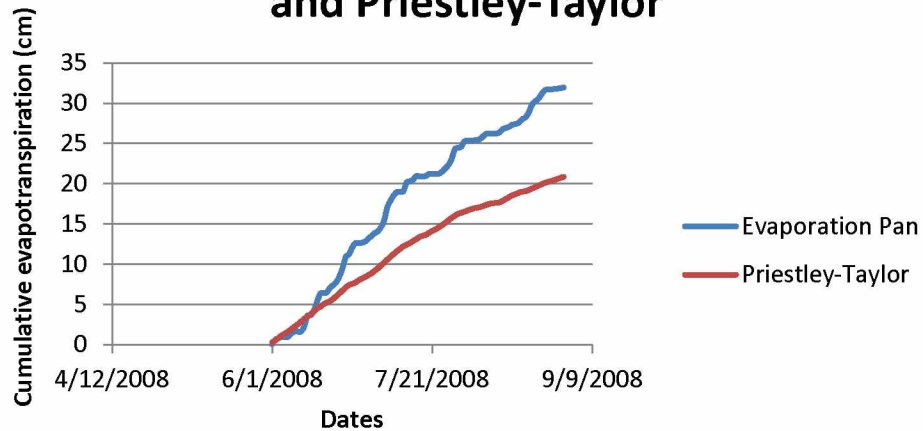
2006 Cumulative evaporation pan and Priestley-Taylor



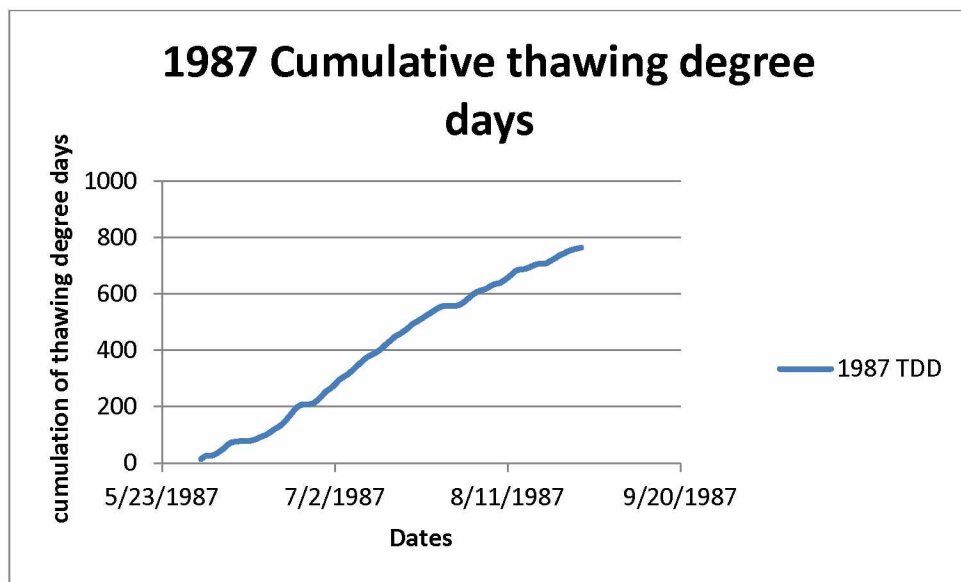
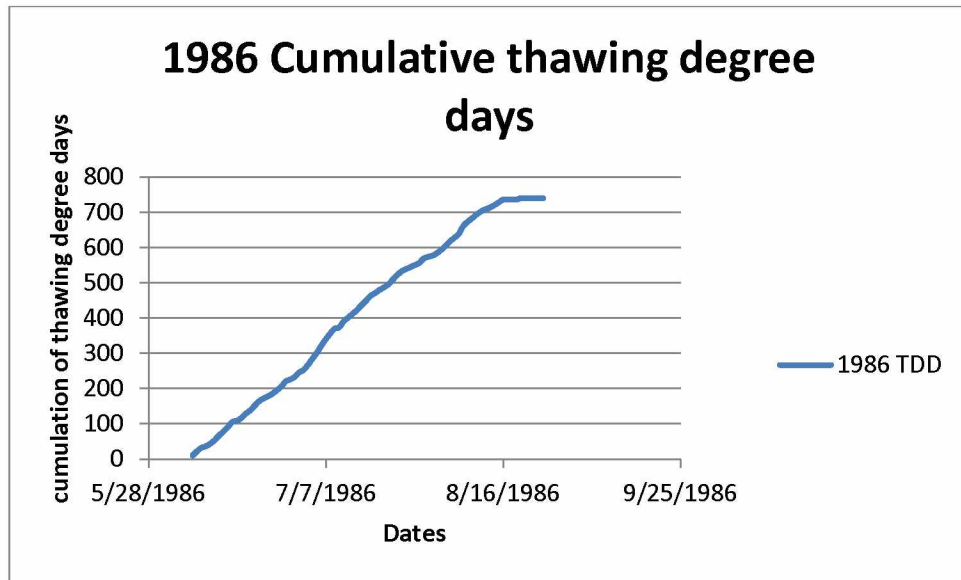
2007 Cumulative evaporation pan and Priestley-Taylor



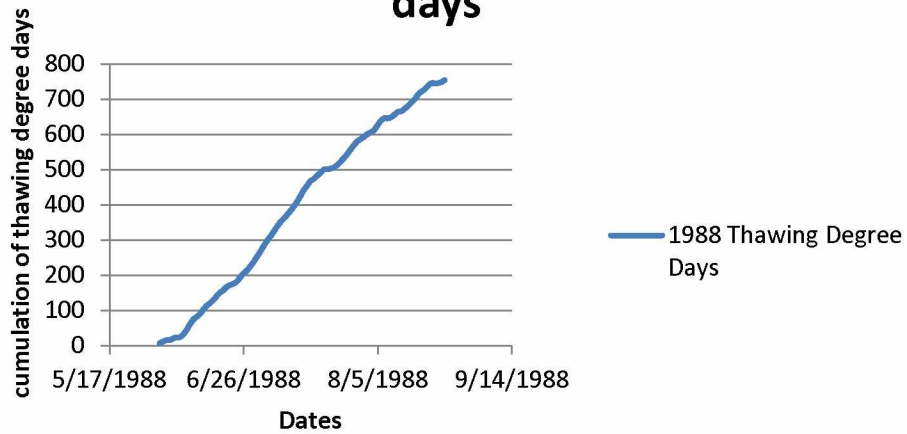
2008 Cumulative evaporation pan and Priestley-Taylor



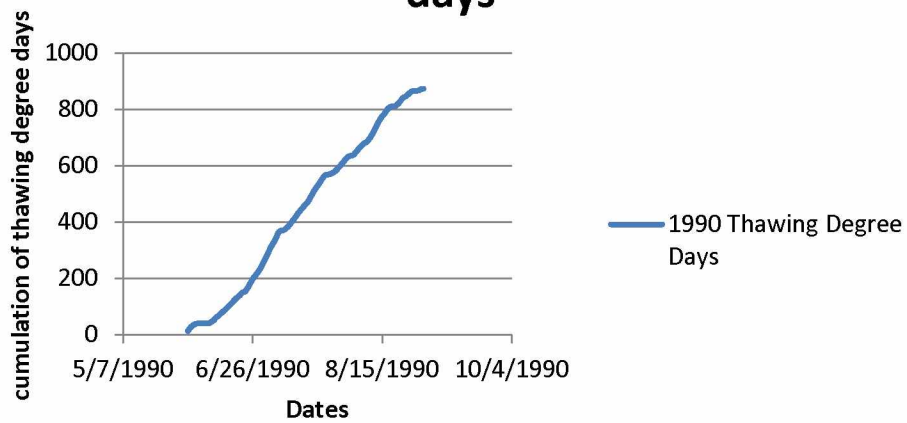
Appendix D: Warm Season thawing degree days versus times, 1986-2008.



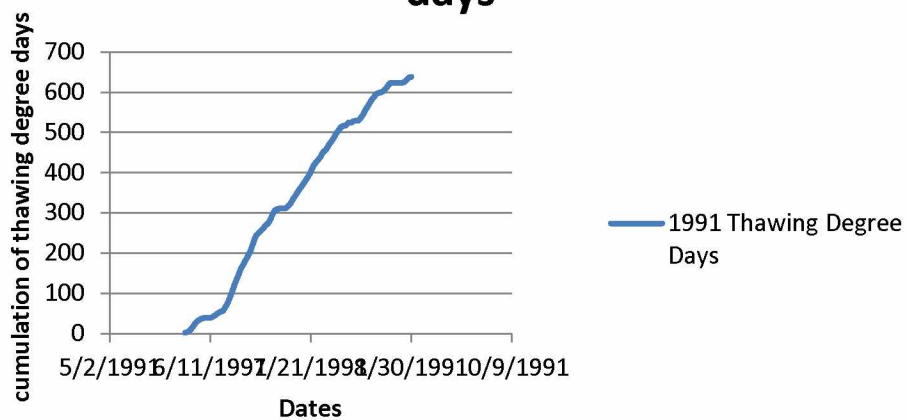
1988 Cumulative thawing degree days



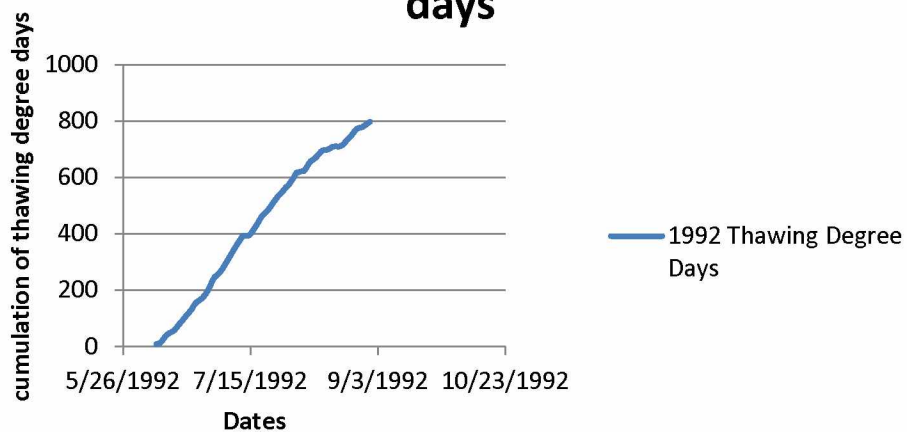
1990 Cumulative thawing degree days



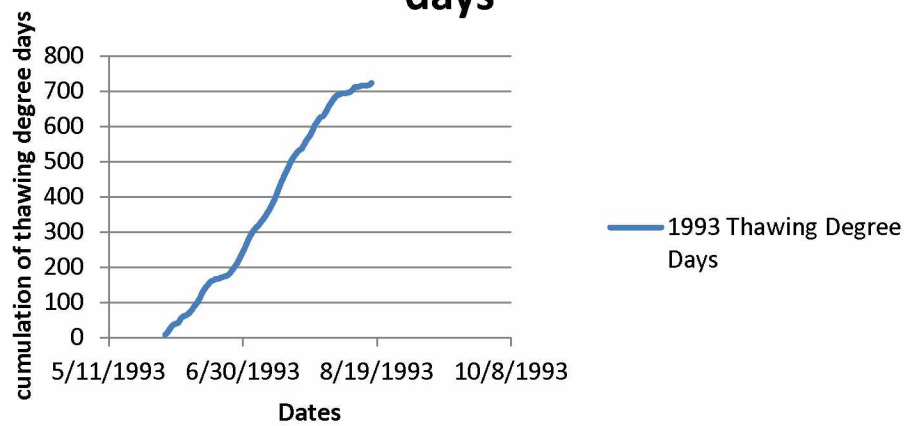
1991 Cumulative thawing degree days



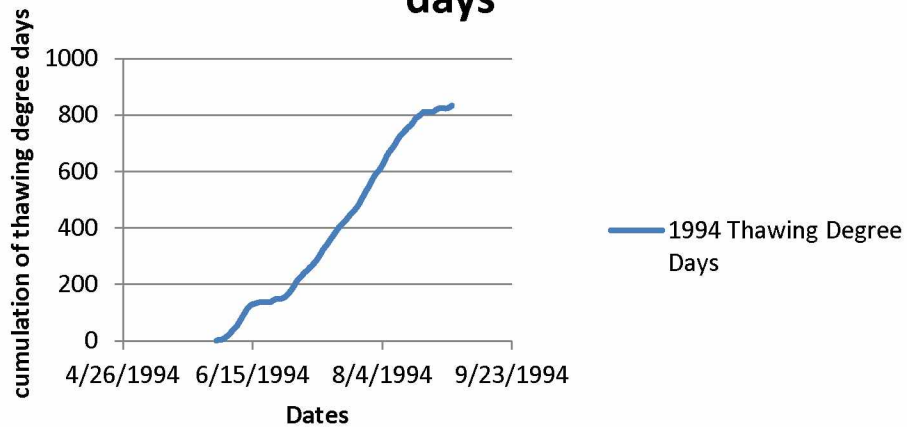
1992 Cumulative thawing degree days



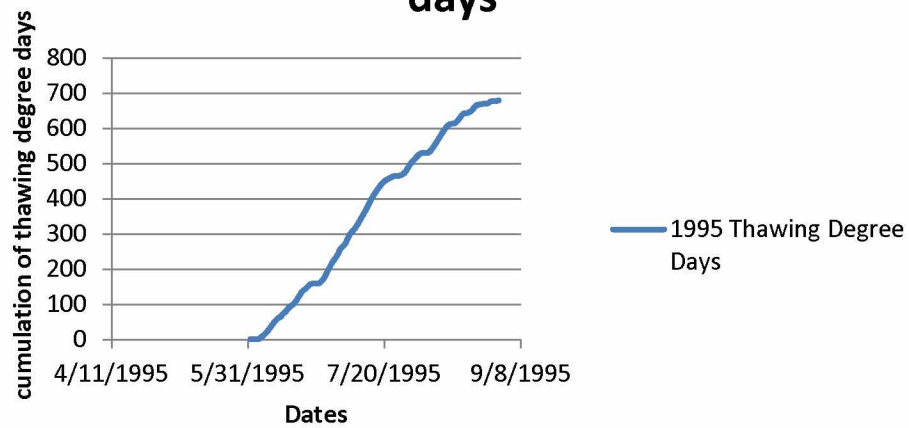
1993 Cumulative thawing degree days



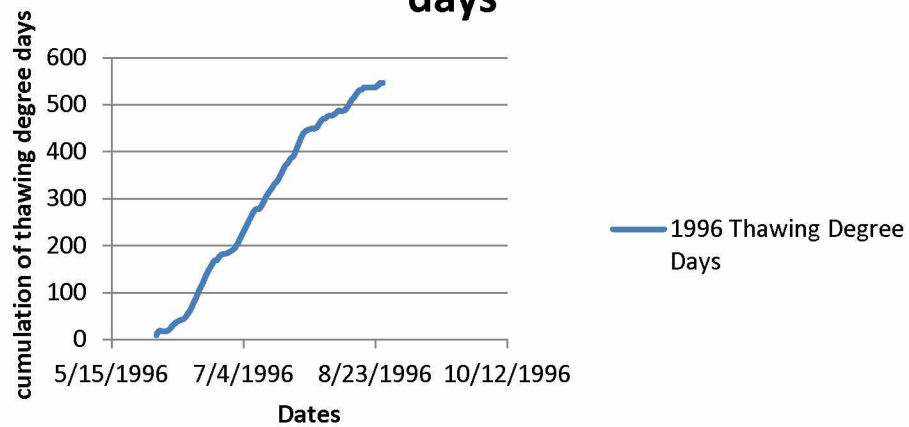
1994 Cumulative thawing degree days



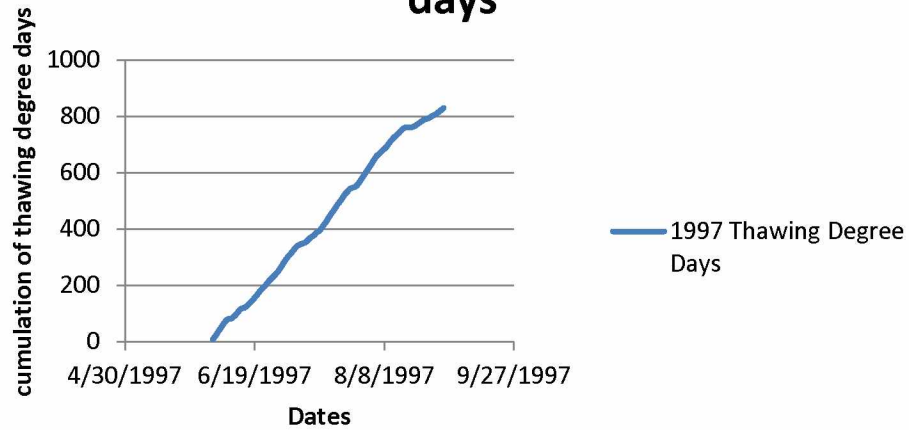
1995 Cumulative thawing degree days



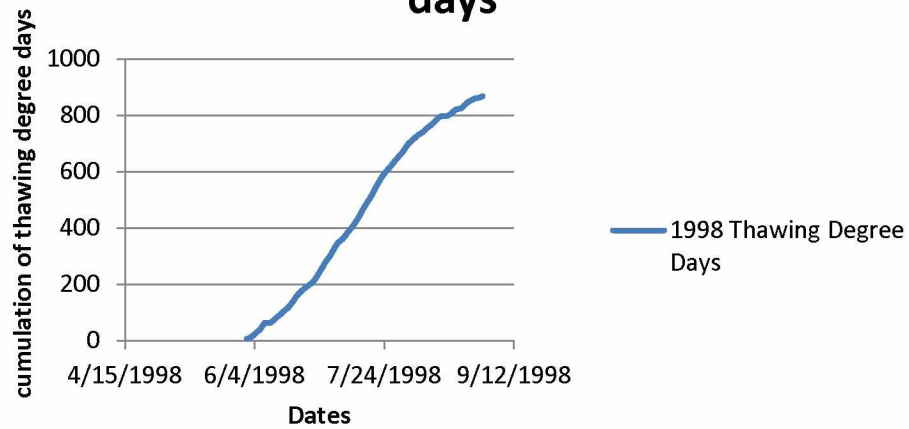
1996 Cumulative thawing degree days



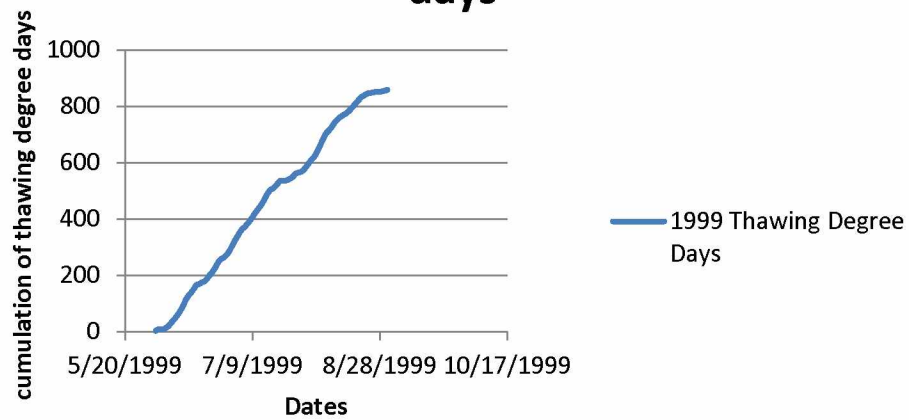
1997 Cumulative thawing degree days



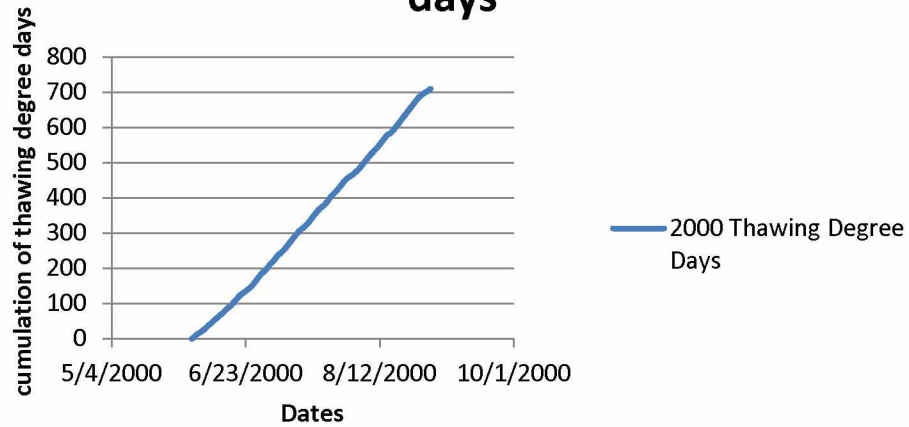
1998 Cumulative thawing degree days



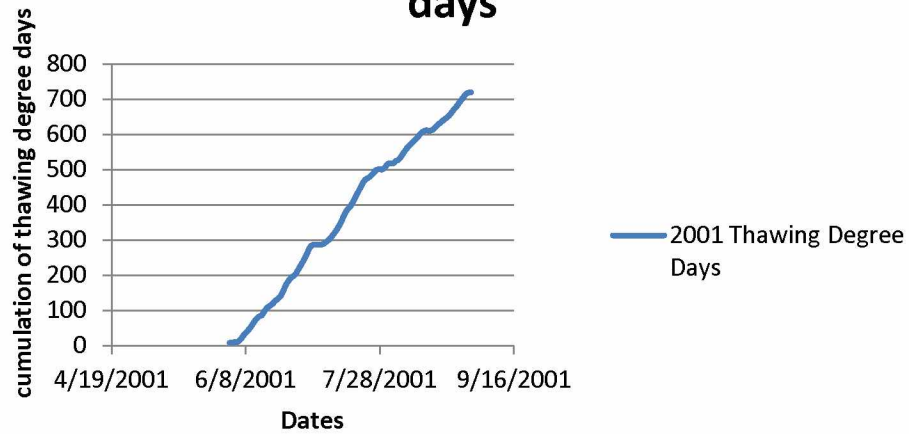
1999 Cumulative thawing degree days



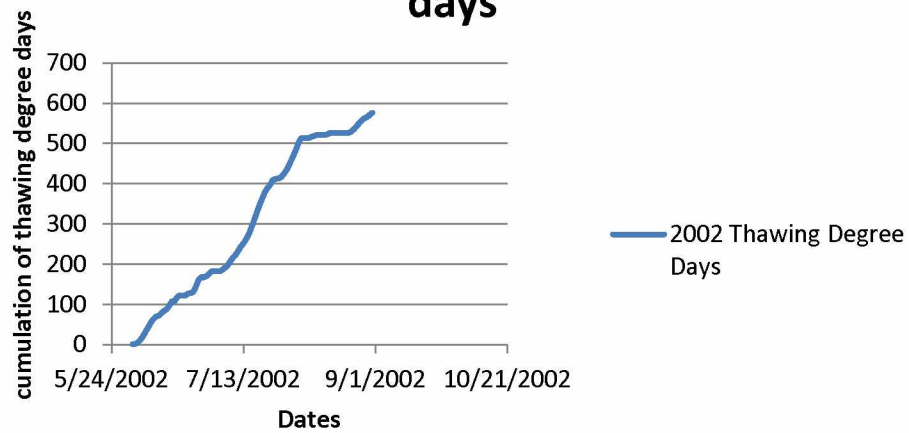
2000 Cumulative thawing degree days



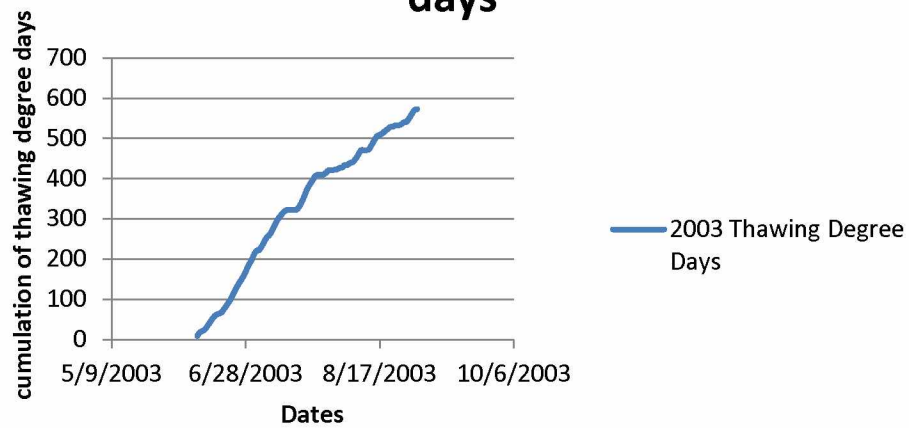
2001 Cumulative thawing degree days



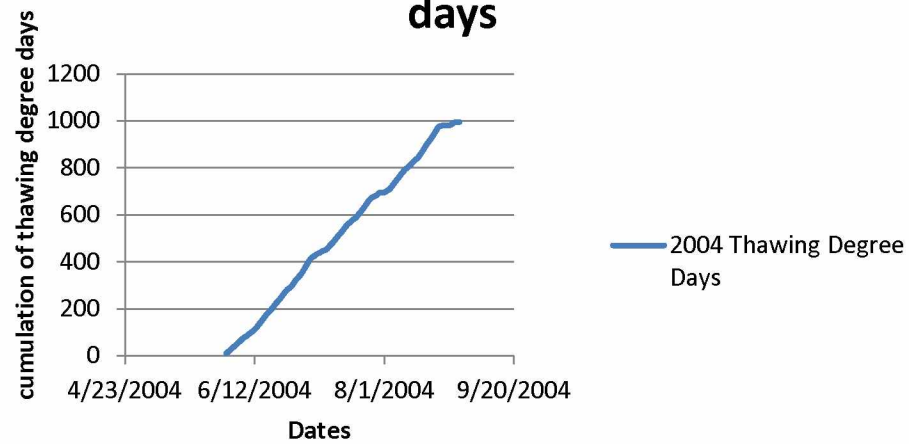
2002 Cumulative thawing degree days



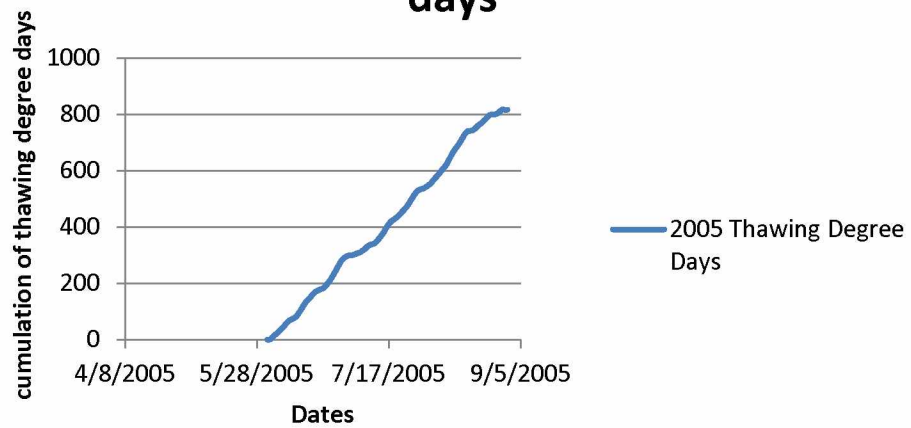
2003 Cumulative thawing degree days



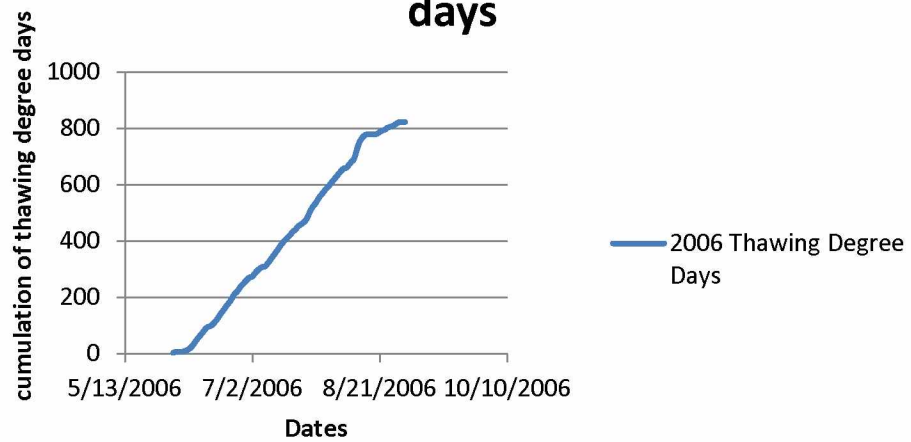
2004 Cumulative thawing degree days



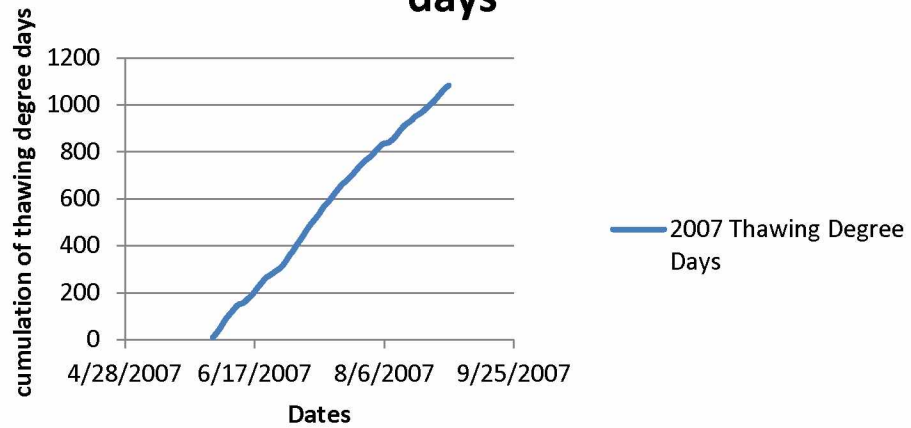
2005 Cumulative thawing degree days



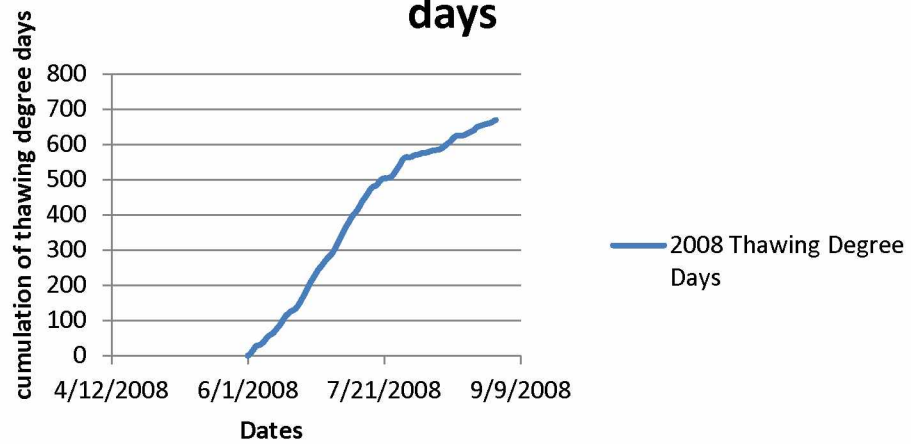
2006 Cumulative thawing degree days



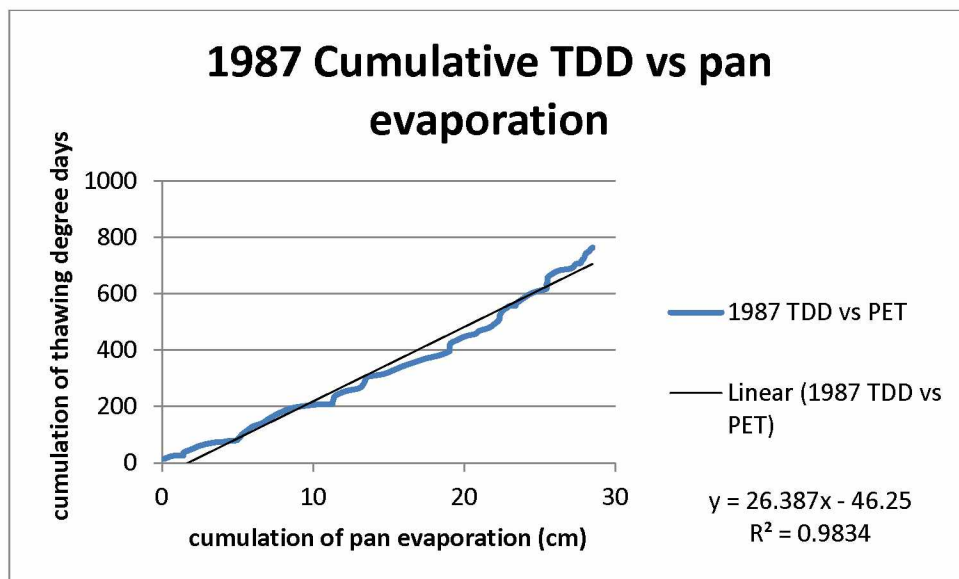
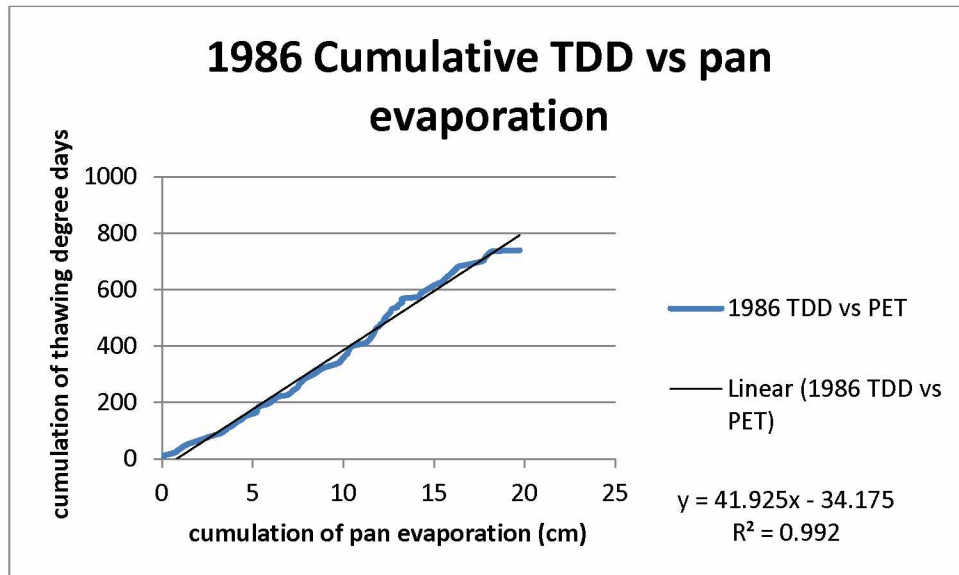
2007 Cumulative thawing degree days



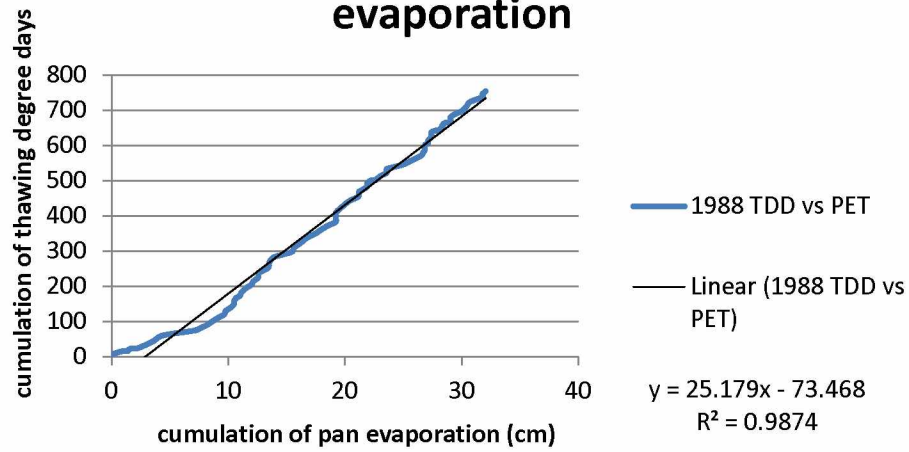
2008 Cumulative thawing degree days



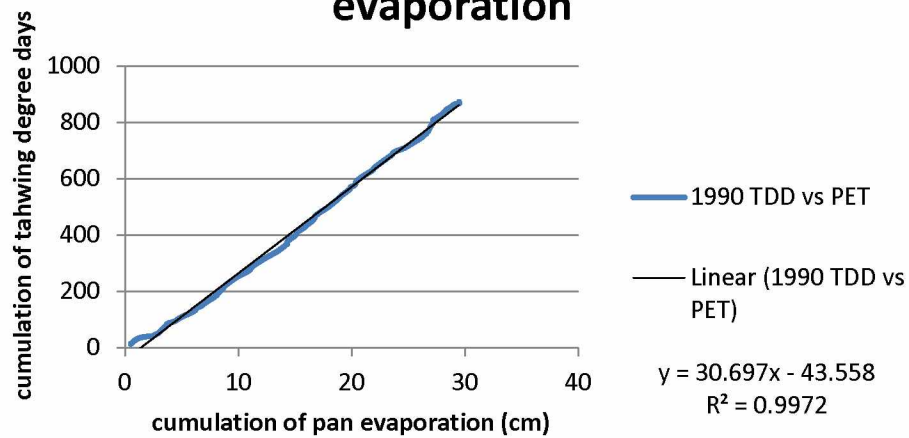
Appendix E: Warm Season Comparison (relationship) between thawing degree days and pan evaporation (potential evaporation) 1986-2008.



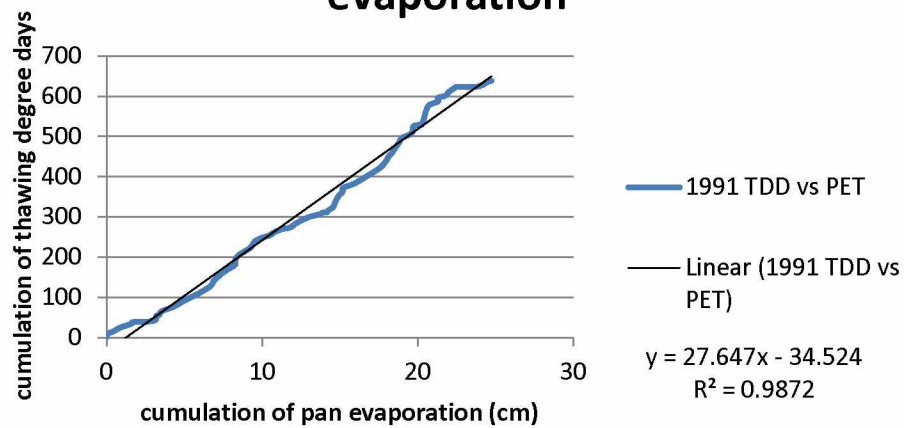
1988 Cumulative TDD vs pan evaporation



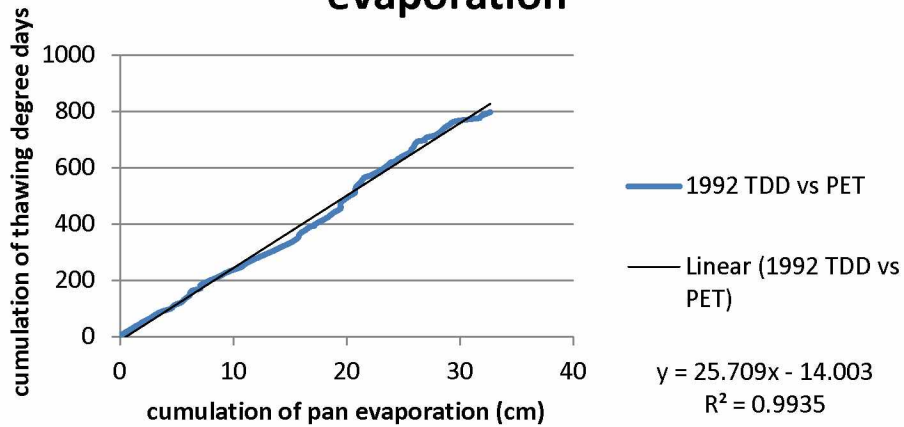
1990 Cumulative TDD vs pan evaporation



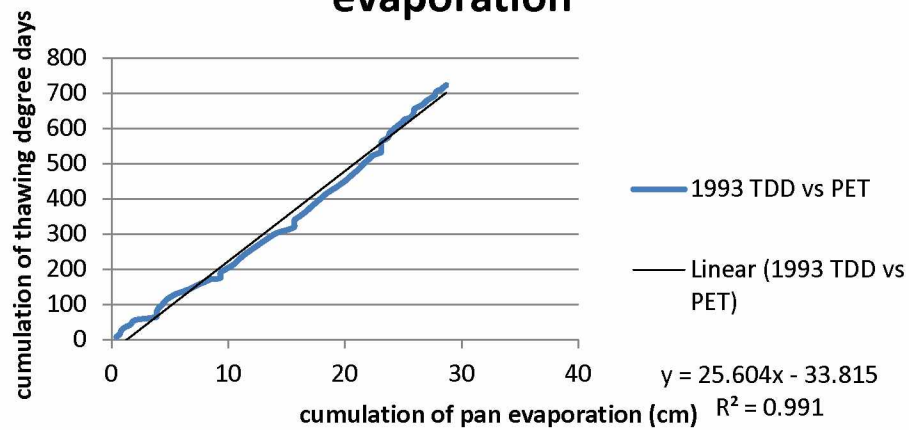
1991 Cumulative TDD vs pan evaporation



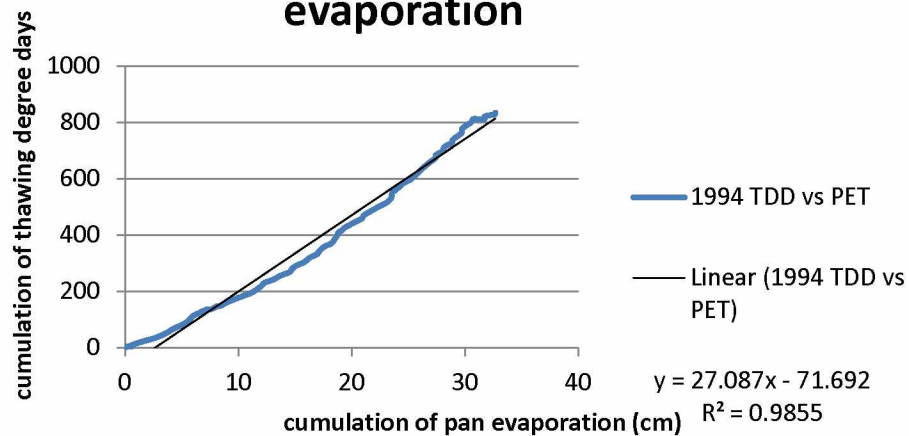
1992 Cumulative TDD vs pan evaporation



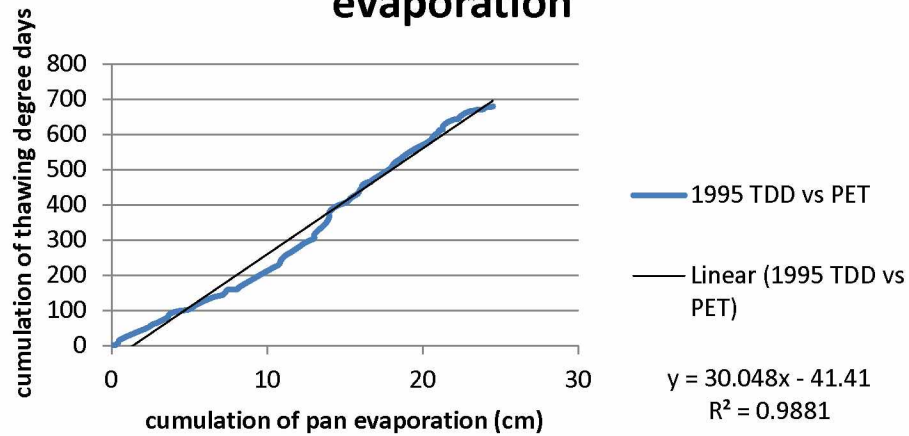
1993 Cumulative TDD vs pan evaporation



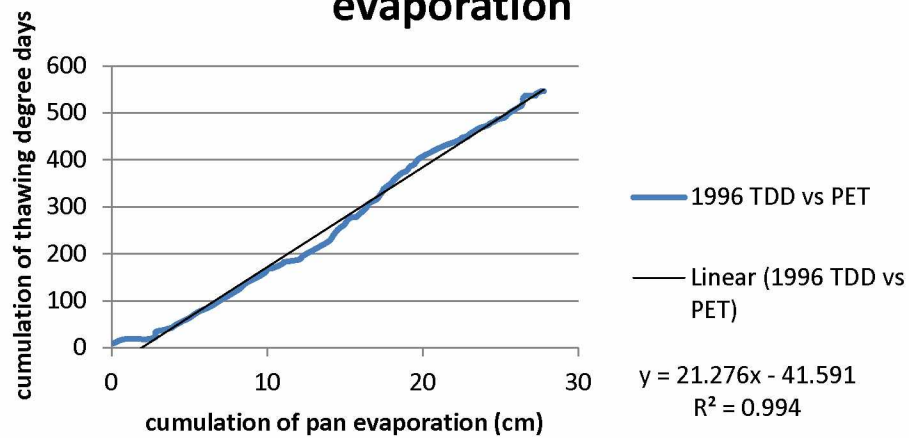
1994 Cumulative TDD vs pan evaporation



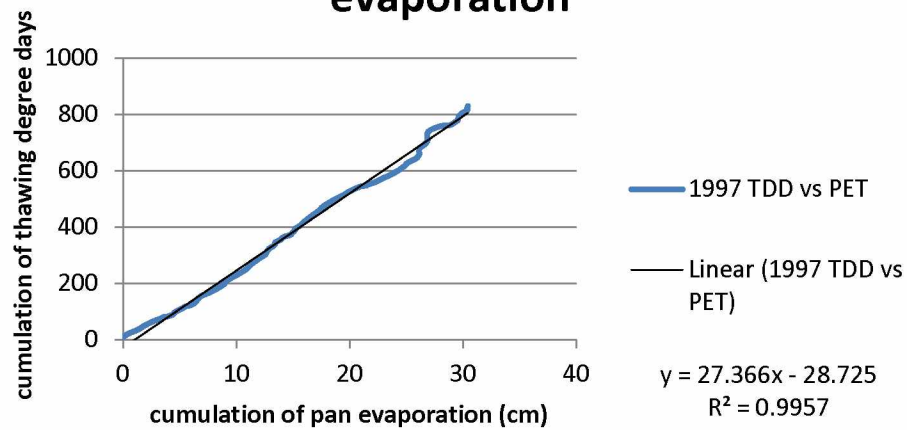
1995 Cumulative TDD vs pan evaporation



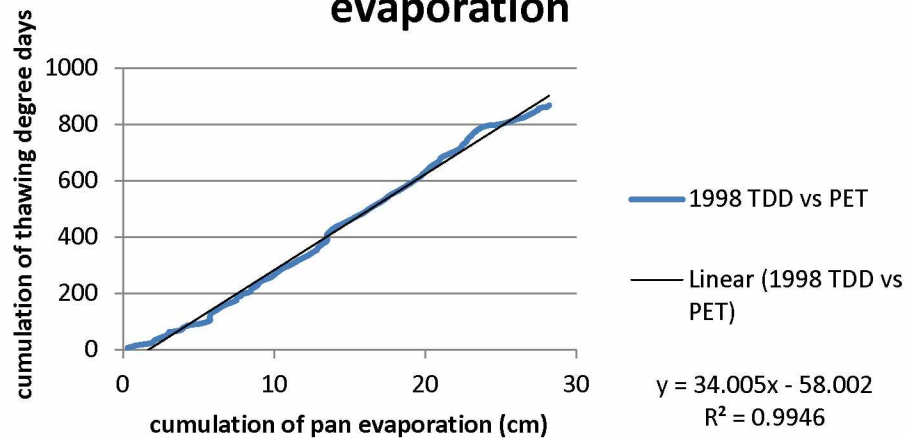
1996 Cumulative TDD vs pan evaporation



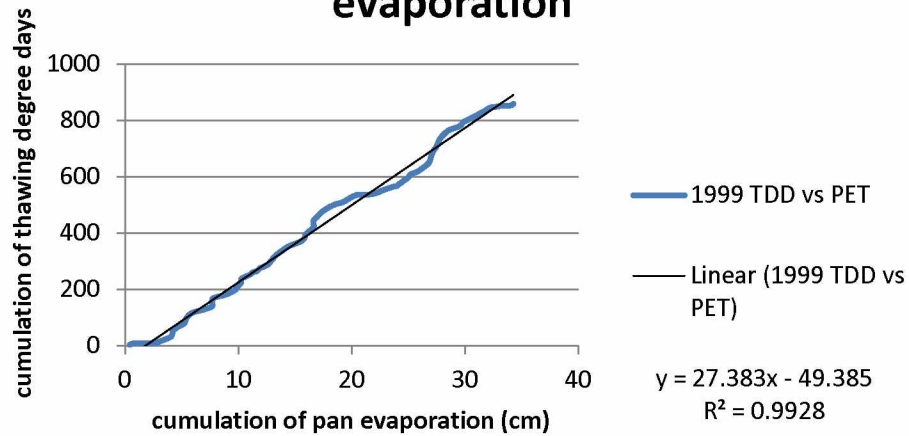
1997 Cumulative TDD vs pan evaporation



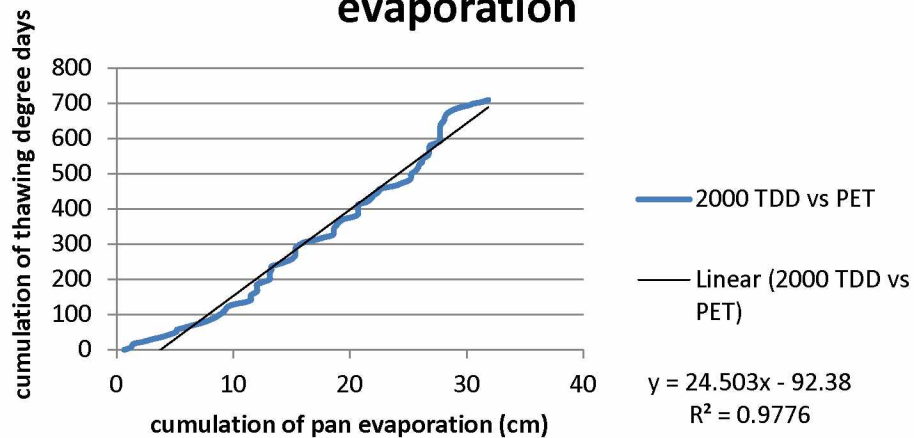
1998 Cumulative TDD vs pan evaporation



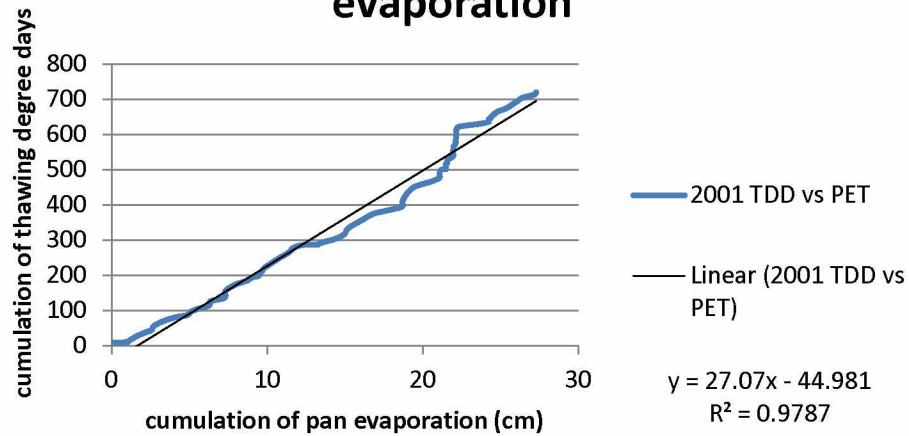
1999 Cumulative TDD vs pan evaporation



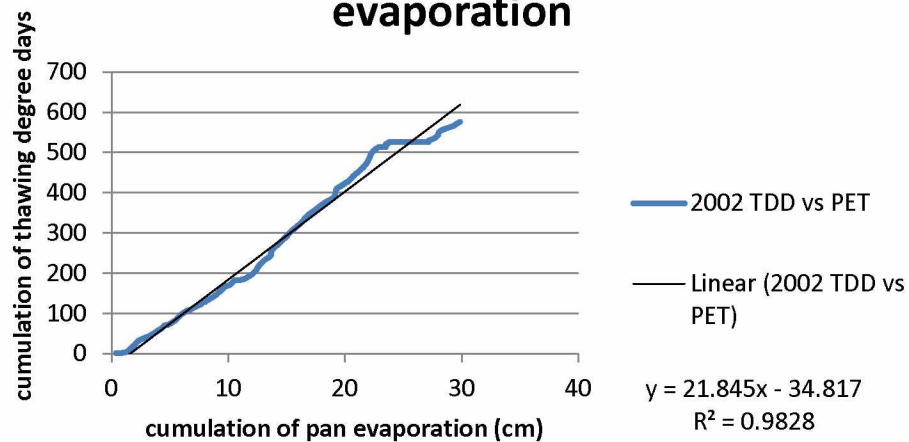
2000 Cumulative TDD vs pan evaporation



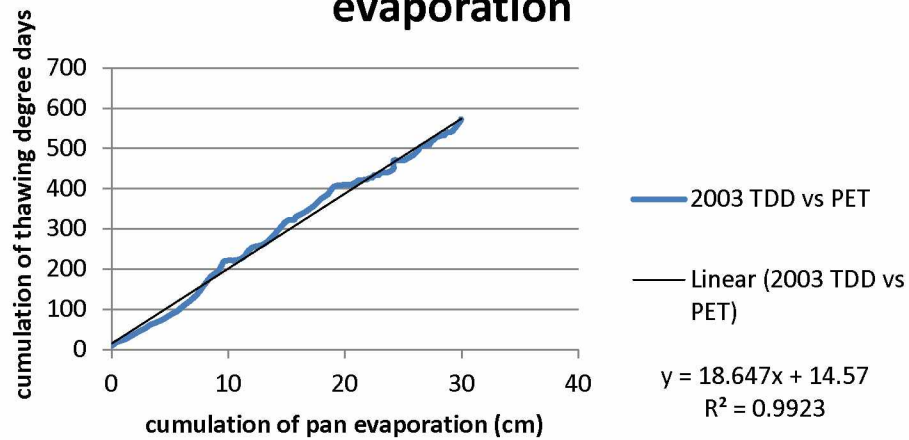
2001 Cumulative TDD vs pan evaporation



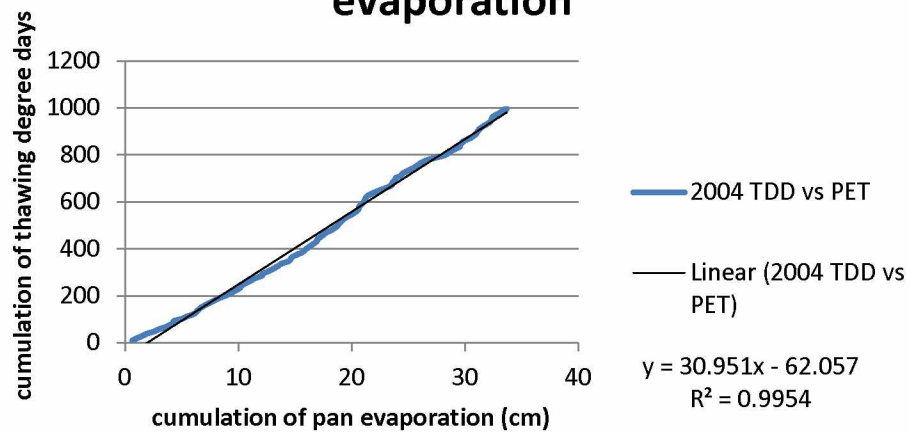
2002 Cumulative TDD vs pan evaporation



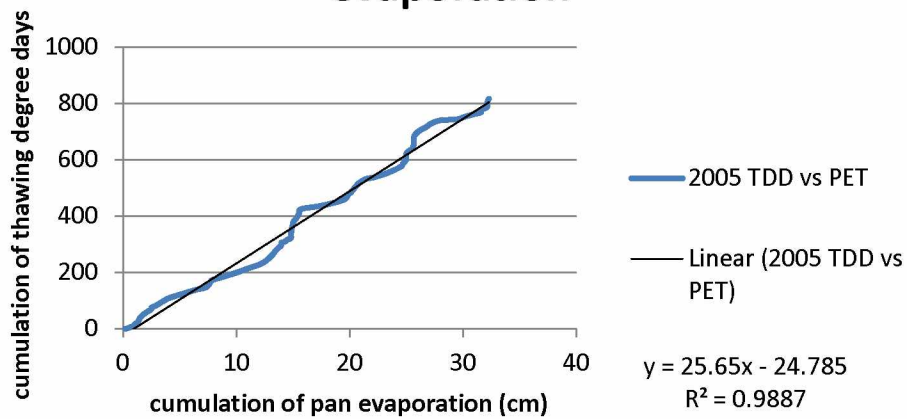
2003 Cumulative TDD vs pan evaporation



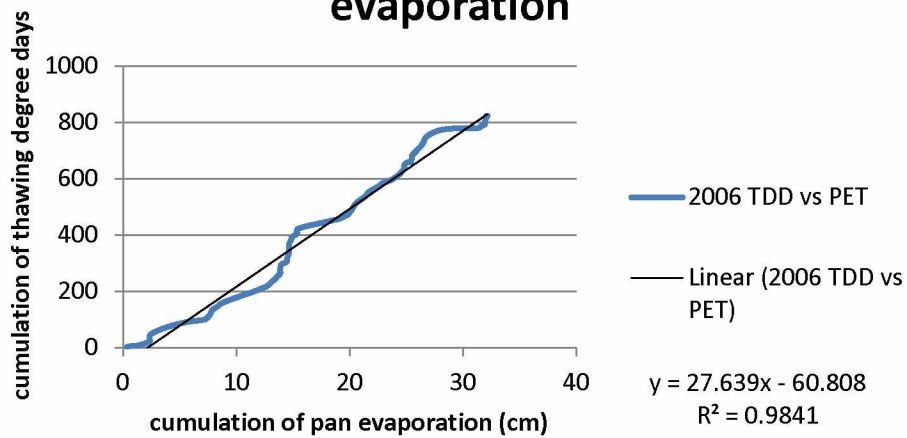
2004 Cumulative TDD vs pan evaporation



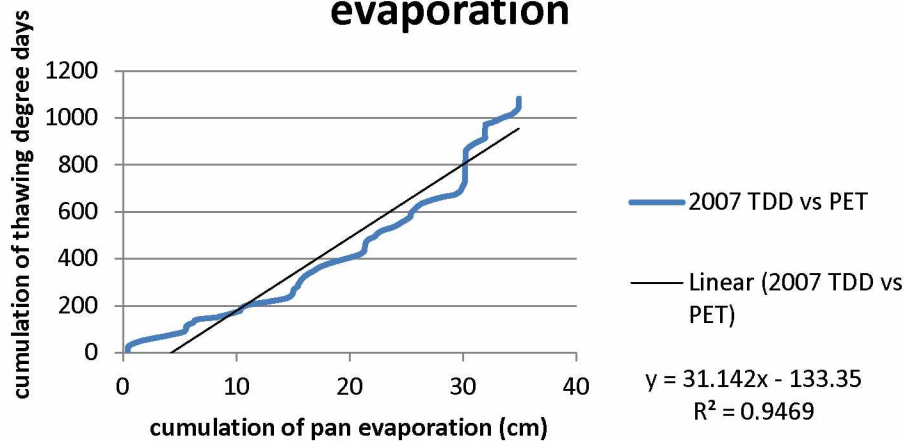
2005 Cumulative TDD vs pan evaporation



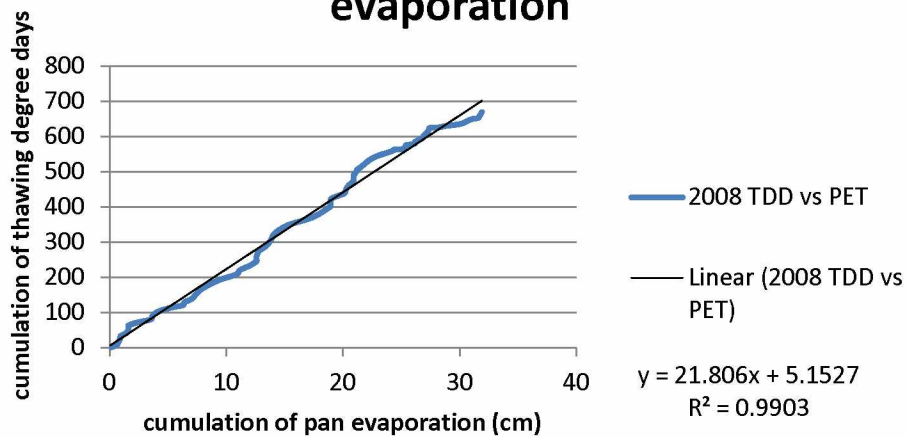
2006 Cumulative TDD vs pan evaporation



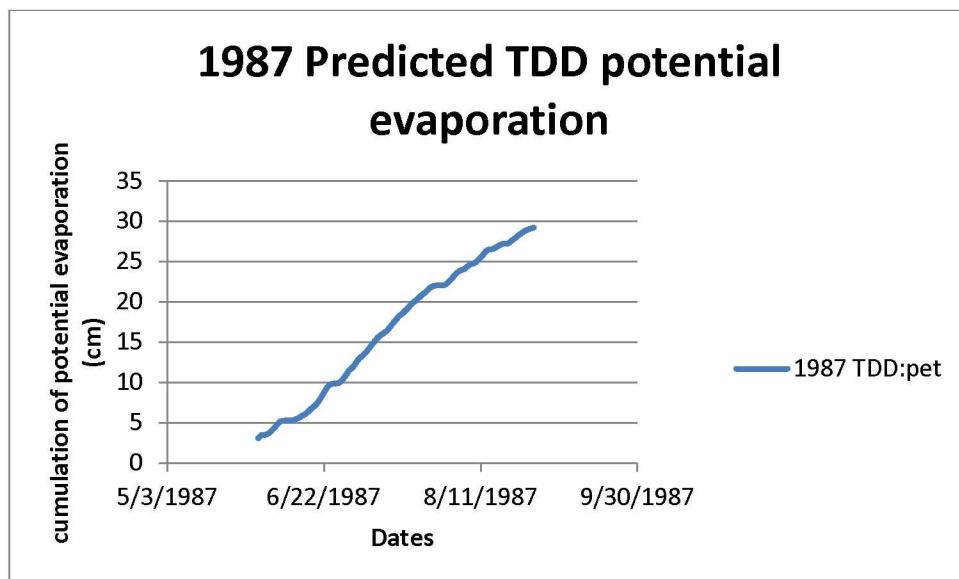
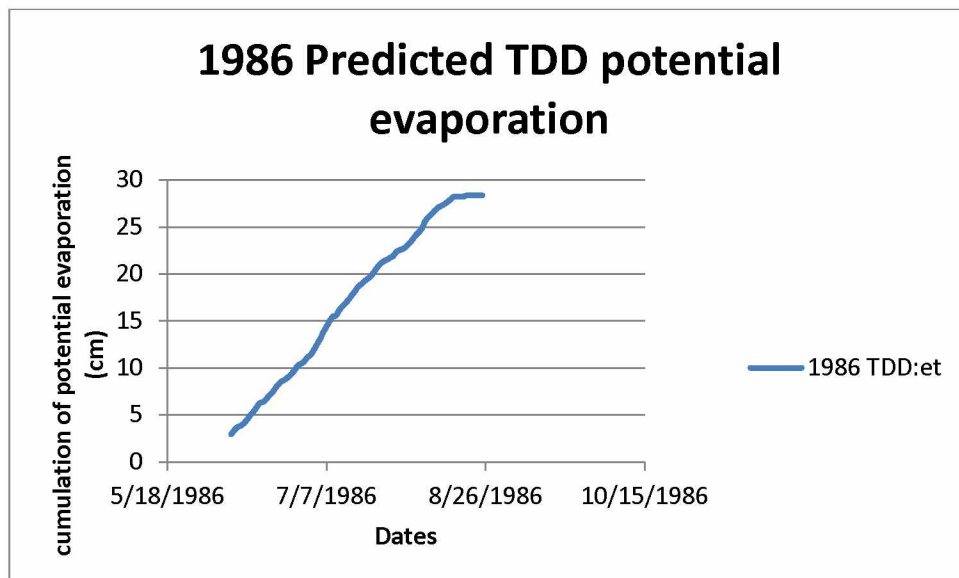
2007 Cumulative TDD vs pan evaporation



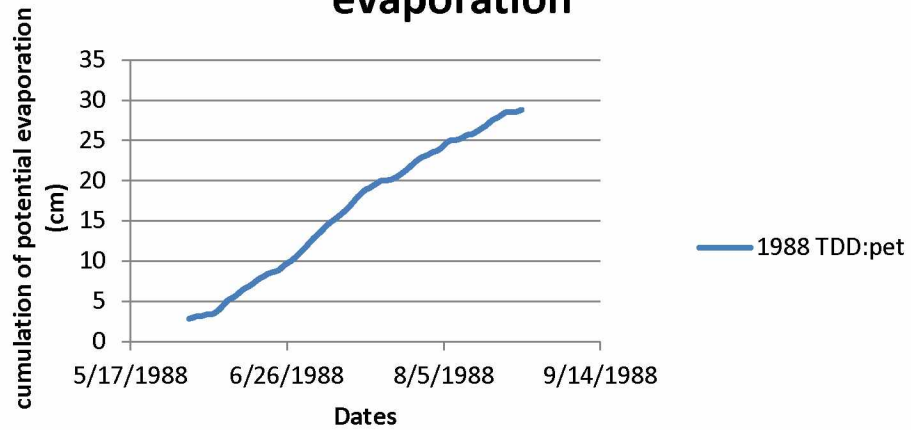
2008 Cumulative TDD vs pan evaporation



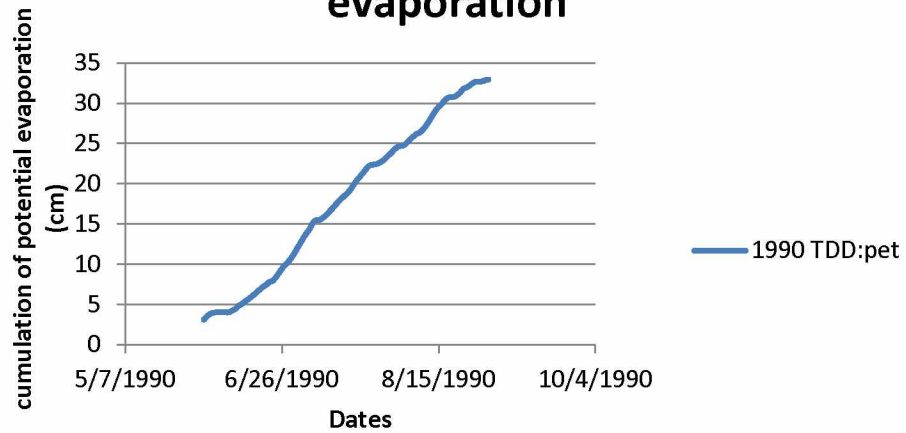
Appendix F: Warm Season Cumulative Calculated potential evaporation using thawing degree days measurements 1986-2008.



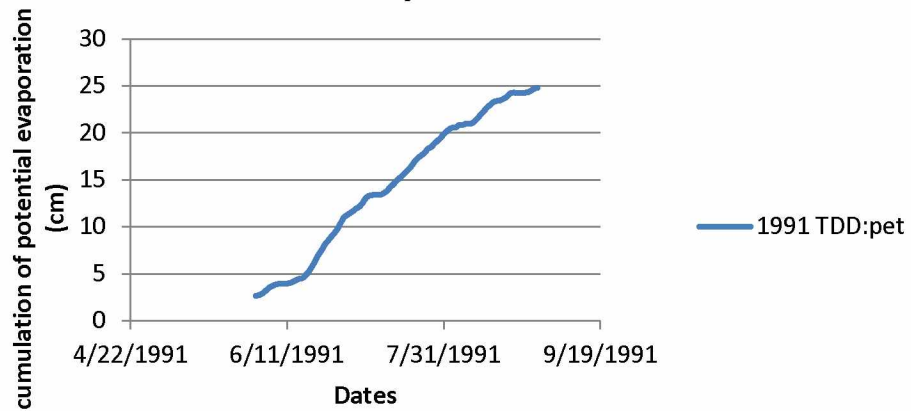
1988 Predicted TDD potential evaporation



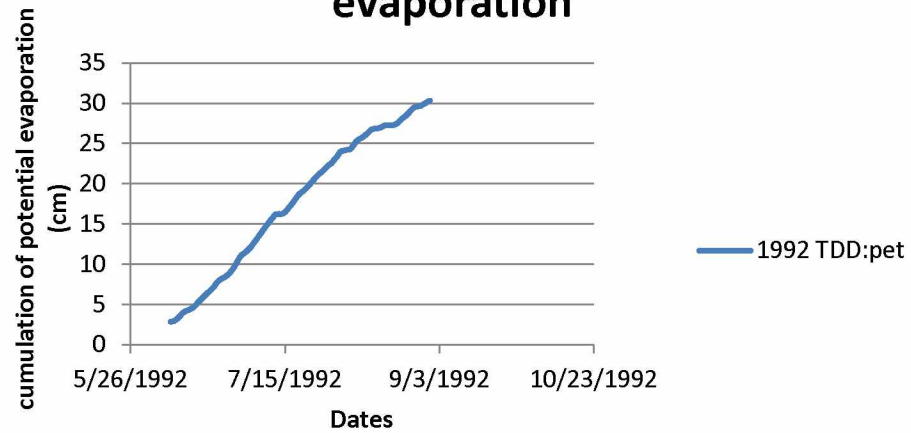
1990 Predicted TDD potential evaporation



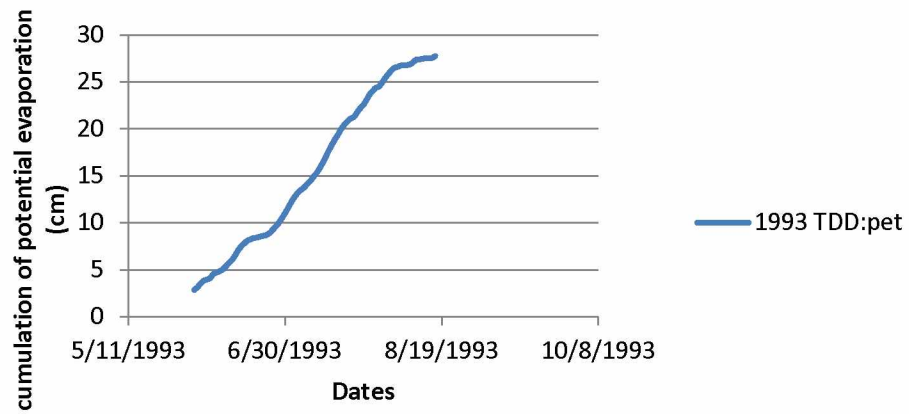
1991 Predicted TDD potential evaporation



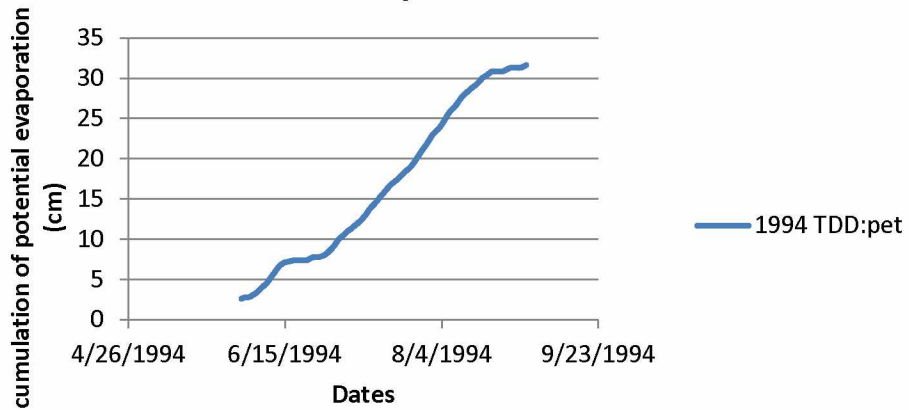
1992 Predicted TDD potential evaporation



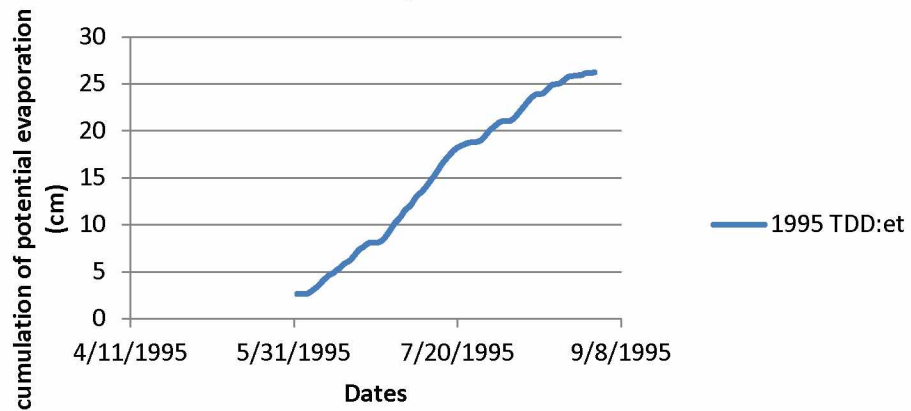
1993 Predicted TDD potential evaporation



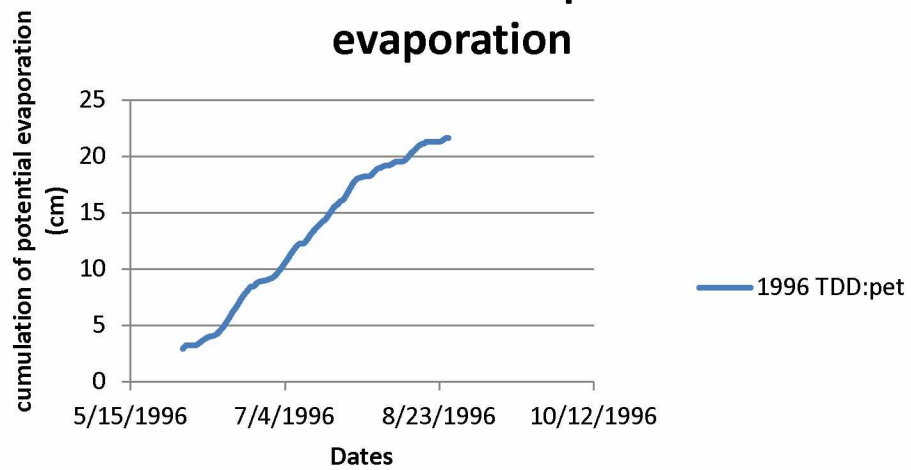
1994 Predicted TDD potential evaporation



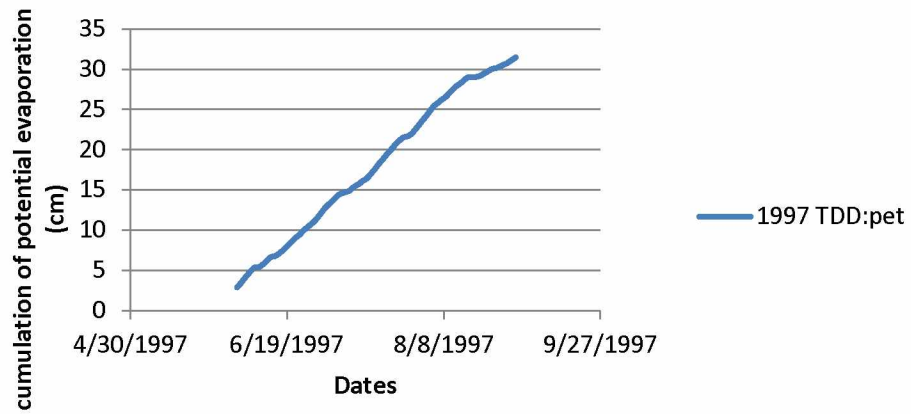
1995 Predicted TDD potential evaporation



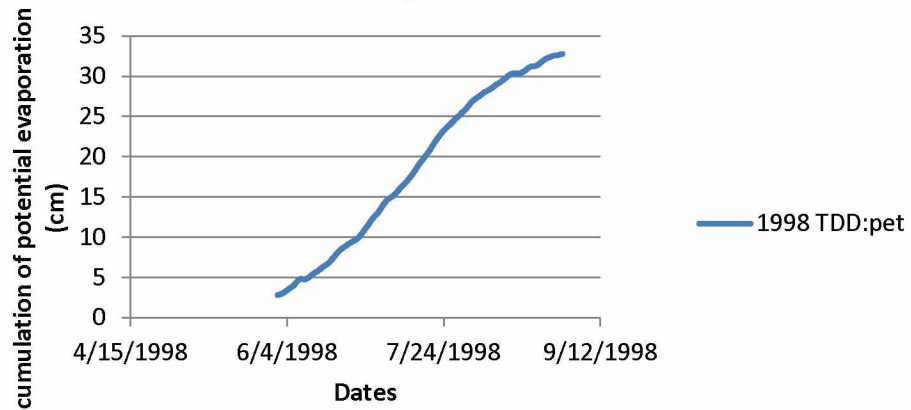
1996 Predicted TDD potential evaporation



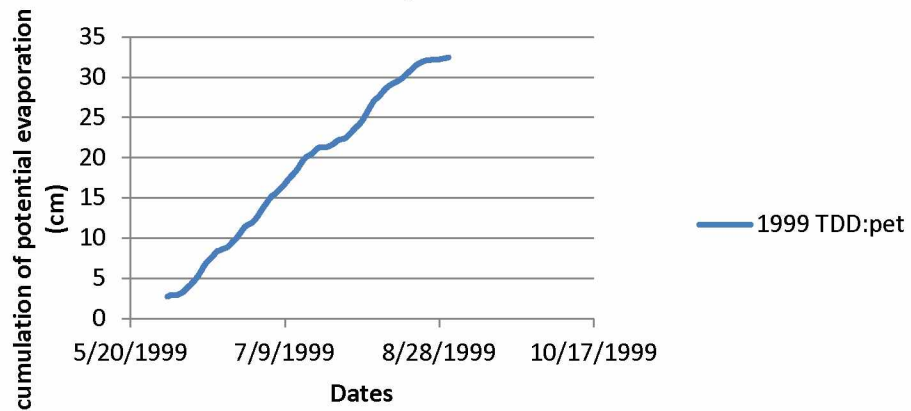
1997 Predicted TDD potential evaporation



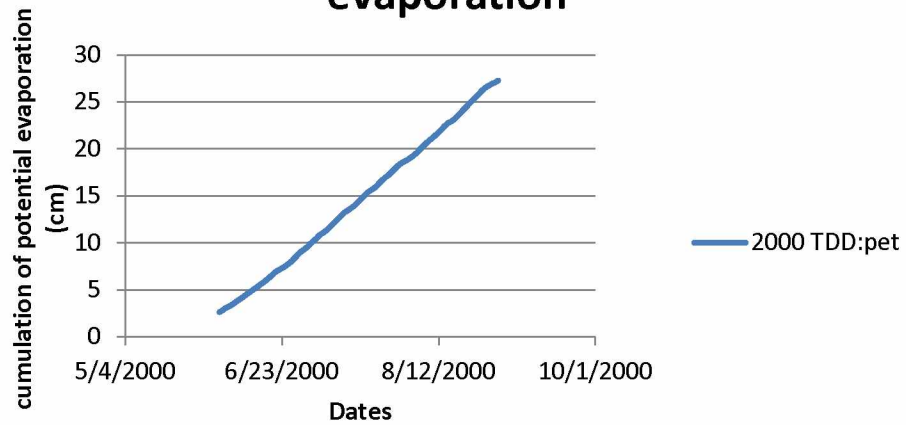
1998 Predicted TDD potential evaporation



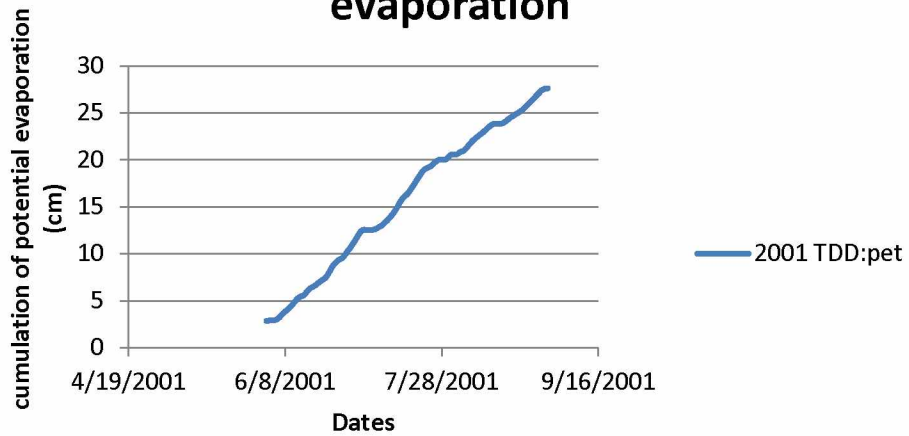
1999 Predicted TDD potential evaporation



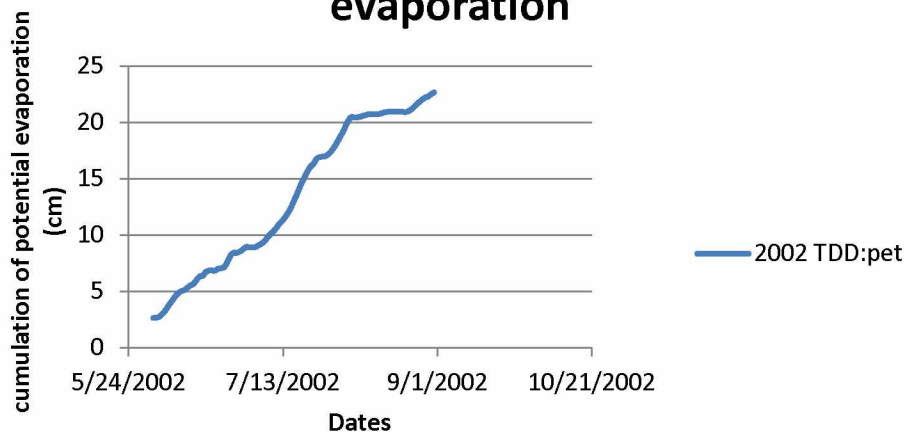
2000 Predicted TDD potential evaporation



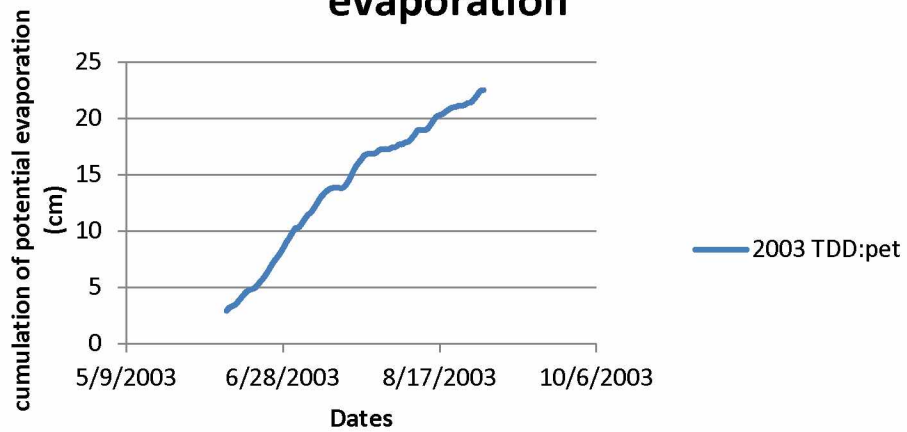
2001 Predicted TDD potential evaporation



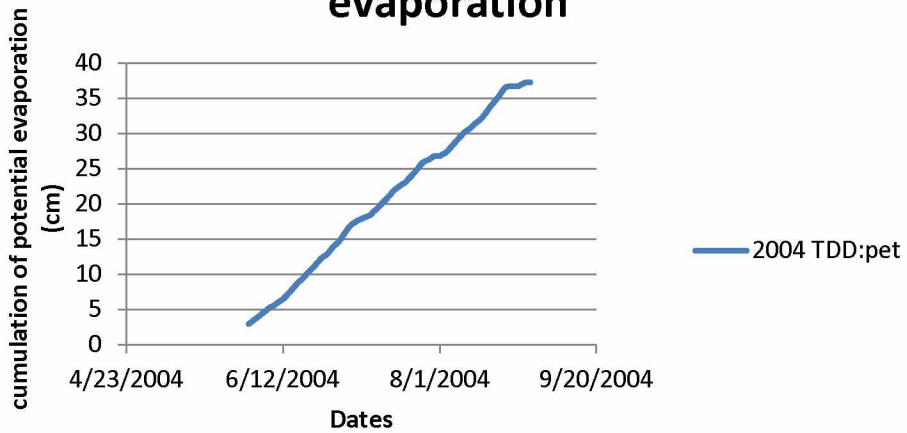
2002 Predicted TDD potential evaporation



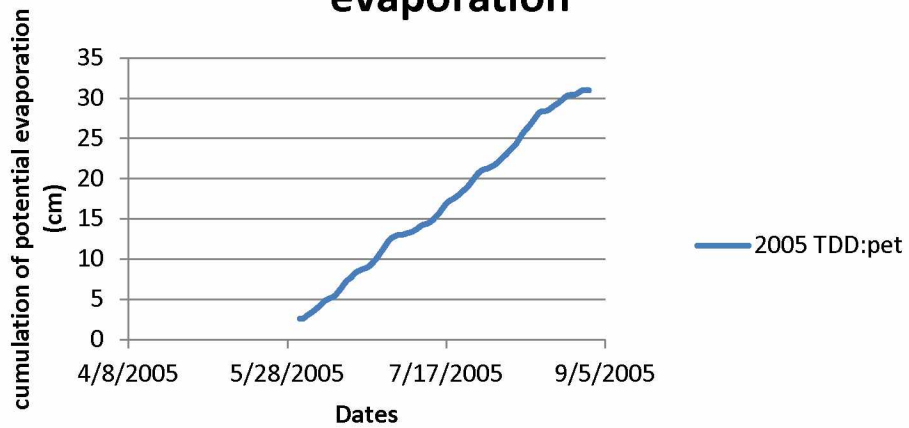
2003 Predicted TDD potential evaporation



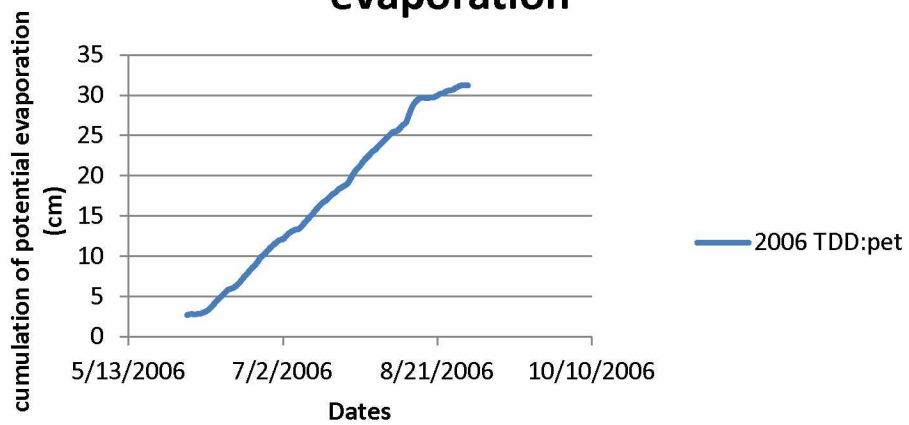
2004 Predicted TDD potential evaporation



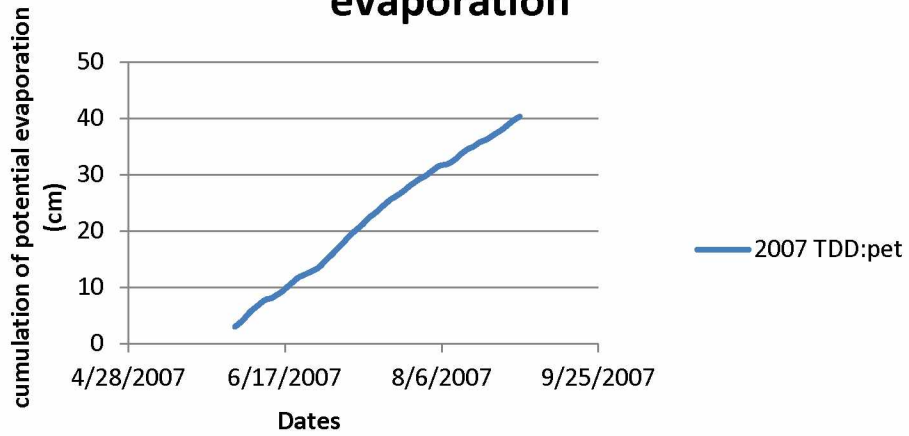
2005 Predicted TDD potential evaporation



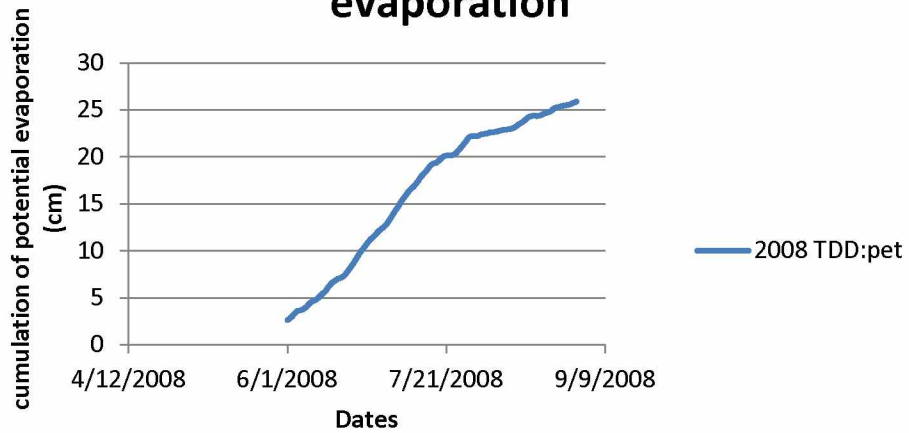
2006 Predicted TDD potential evaporation



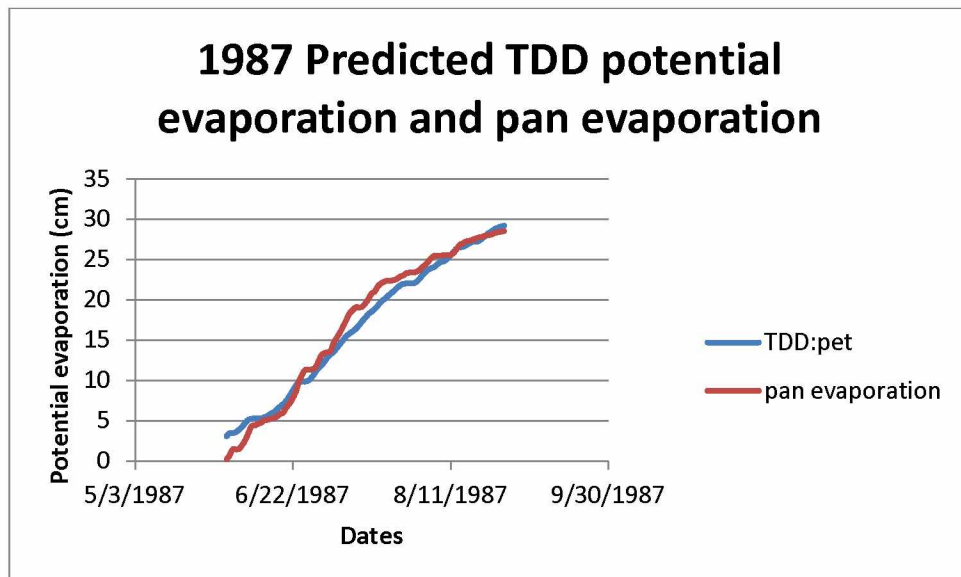
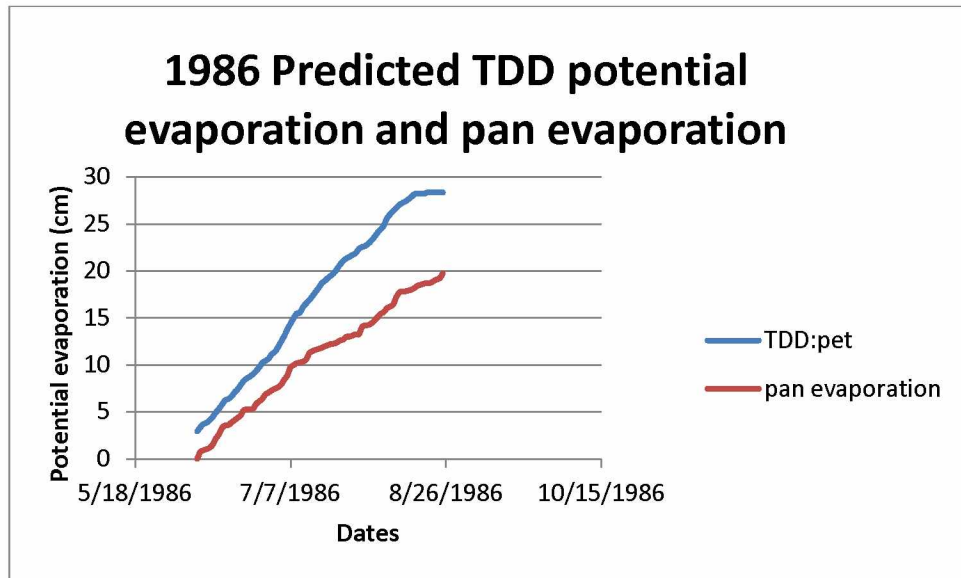
2007 Predicted TDD potential evaporation



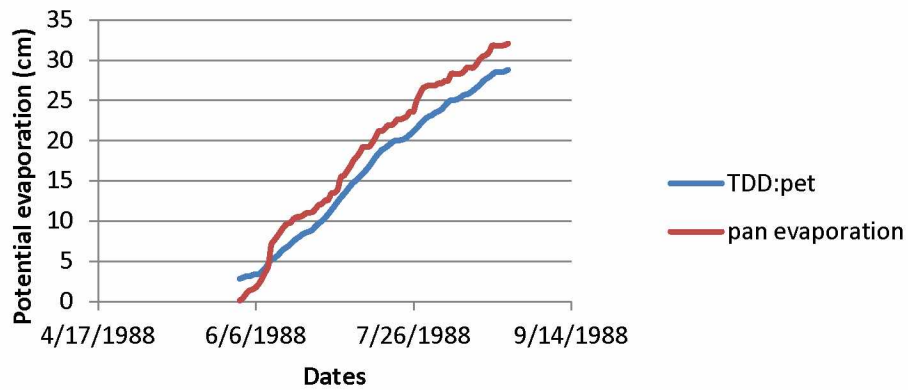
2008 Predicted TDD potential evaporation



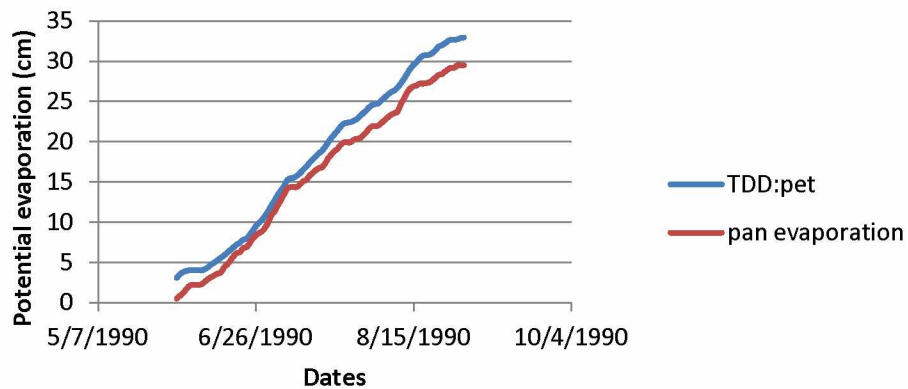
Appendix G: Warm Season Cumulative measured pan evaporation (potential evaporation) and Calculated potential evaporation using thawing degree days 1986-2008.



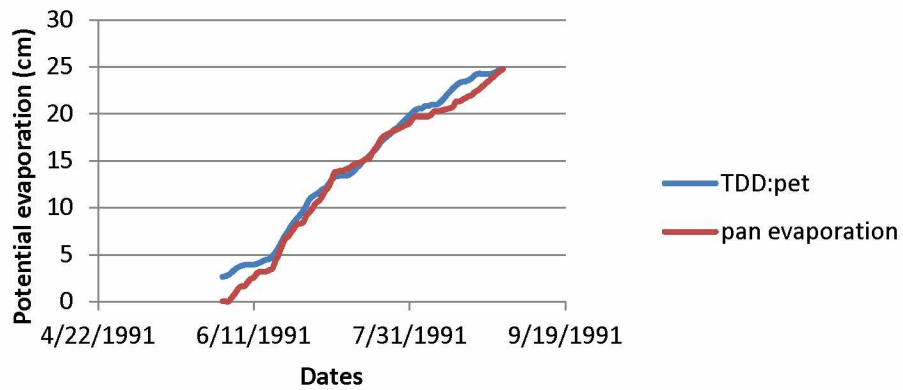
1988 Predicted TDD potential evaporation and pan evaporation



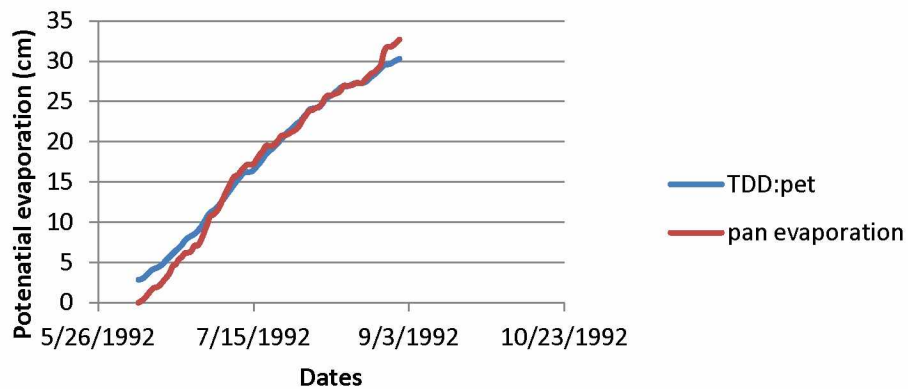
1990 Predicted TDD potential evaporation and pan evaporation



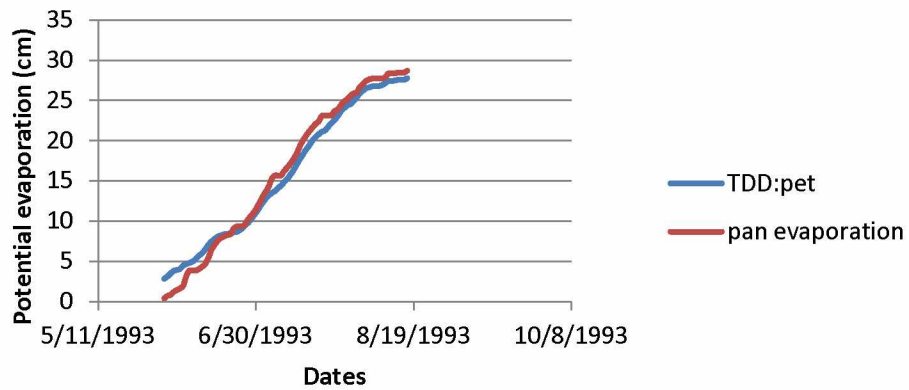
1991 Predicted TDD potential evaporation and pan evaporation



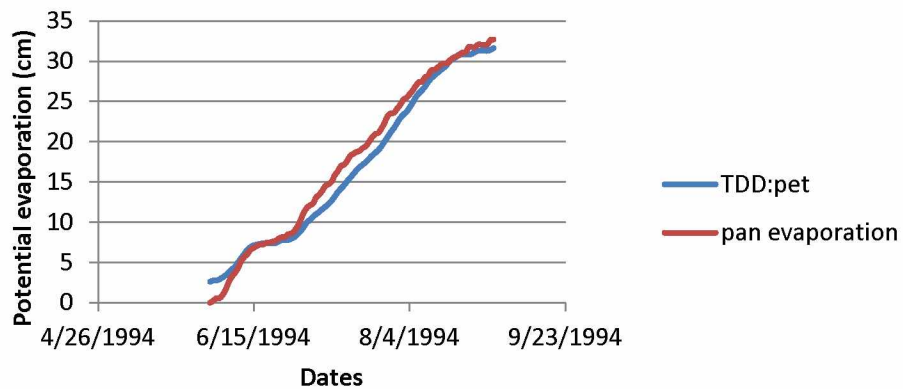
1992 Predicted TDD potential evaporation and pan evaporation



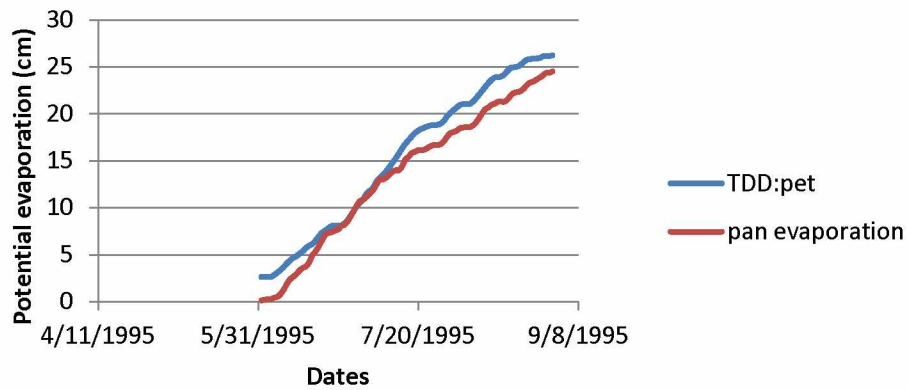
1993 Predicted TDD potential evaporation and pan evaporation



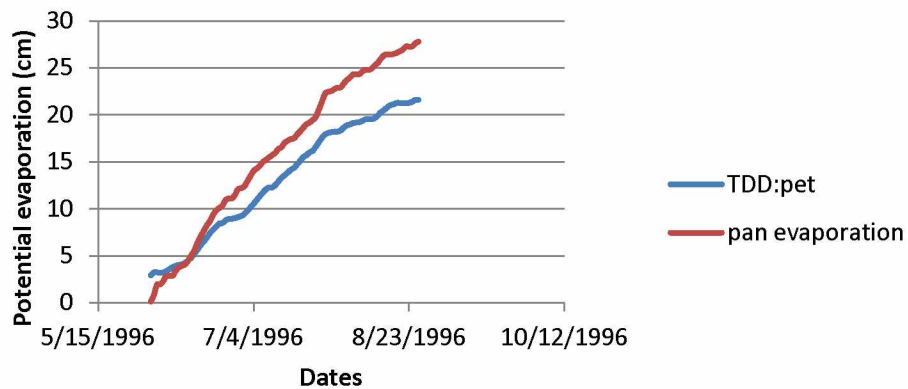
1994 Predicted TDD potential evaporation and pan evaporation



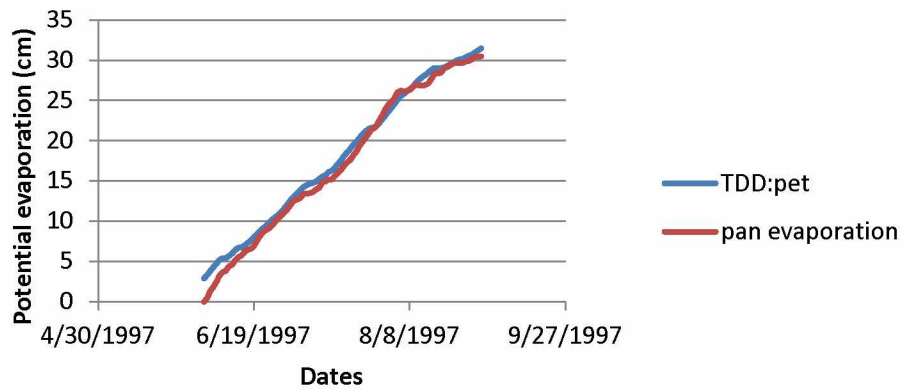
1995 Predicted TDD potential evaporation and pan evaporation



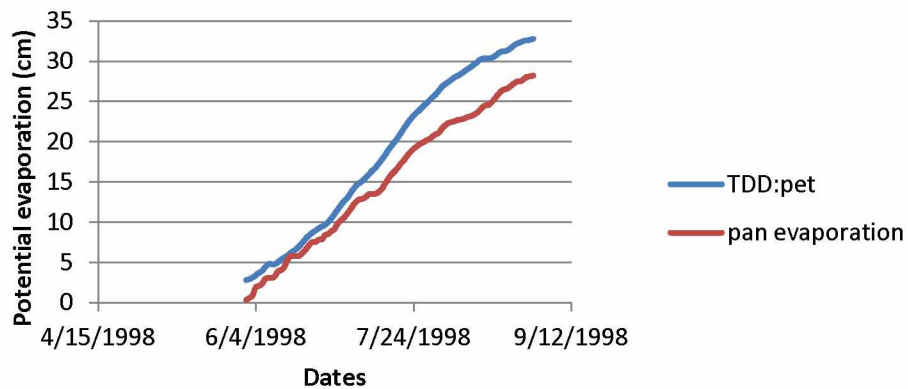
1996 Predicted TDD potential evaporation and pan evaporation



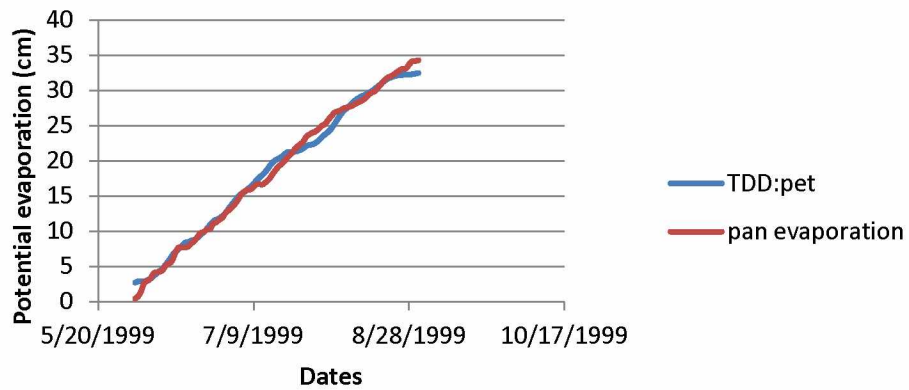
1997 Predicted TDD potential evaporation and pan evaporation



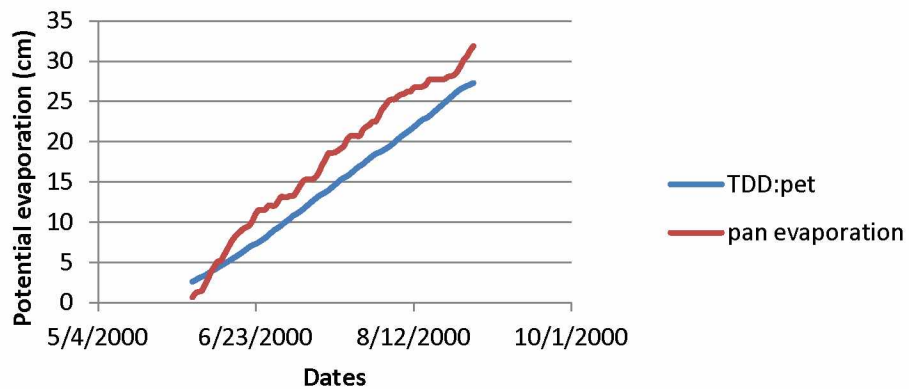
1998 Predicted TDD potential evaporation and pan evaporation



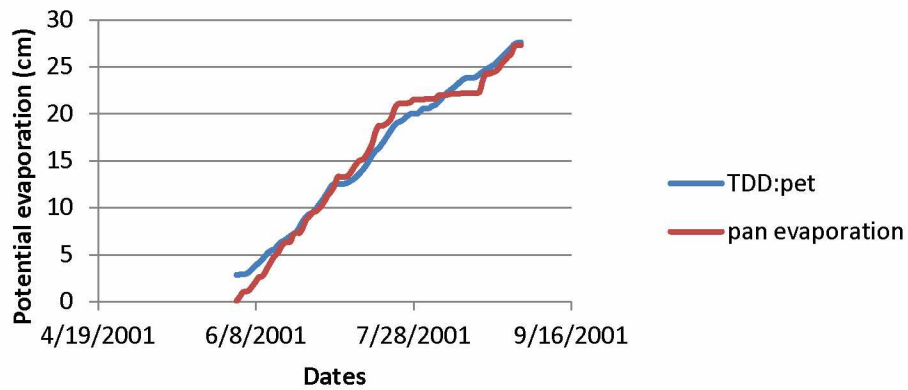
1999 Predicted TDD potential evaporation and pan evaporation



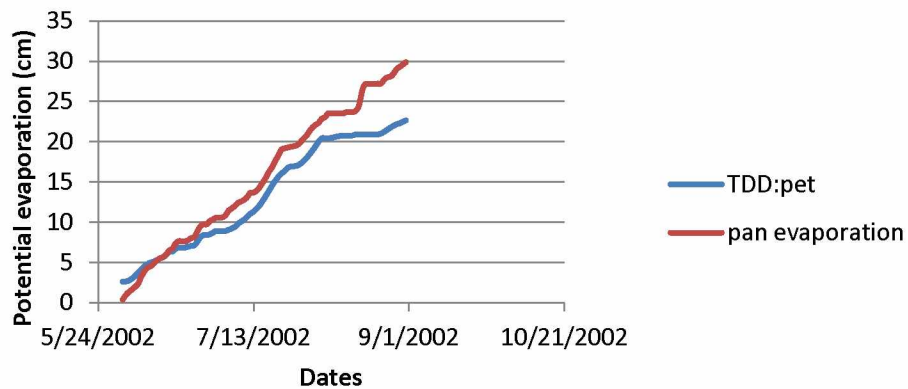
2000 Predicted TDD potential evaporation and pan evaporation



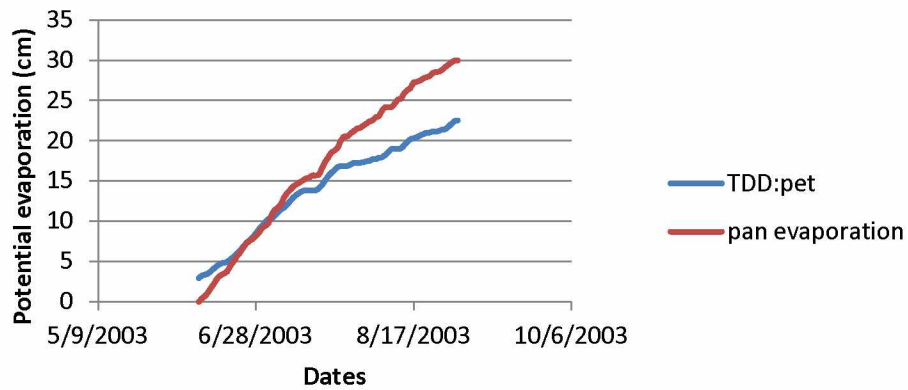
2001 Predicted TDD potential evaporation and pan evaporation



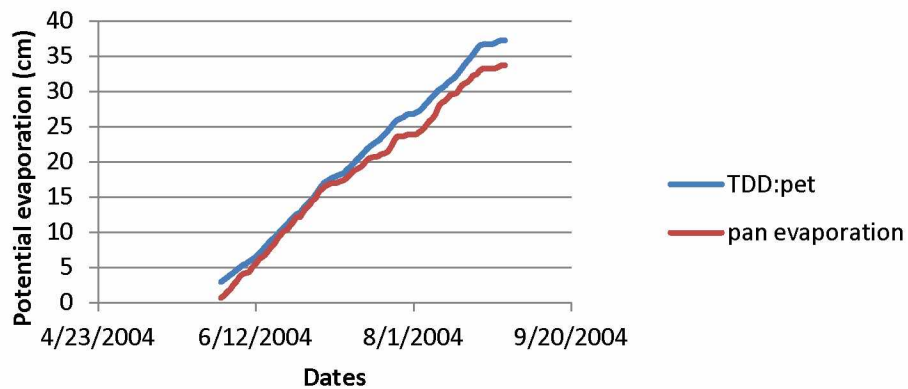
2002 Predicted TDD potential evaporation and pan evaporation



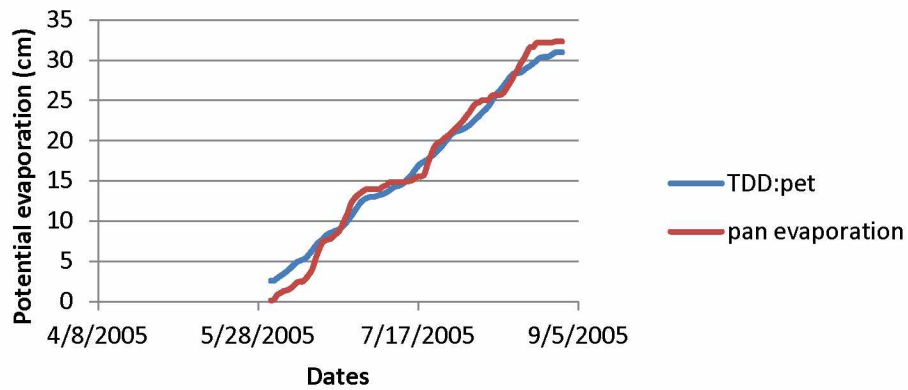
2003 Predicted TDD potential evaporation and pan evaporation



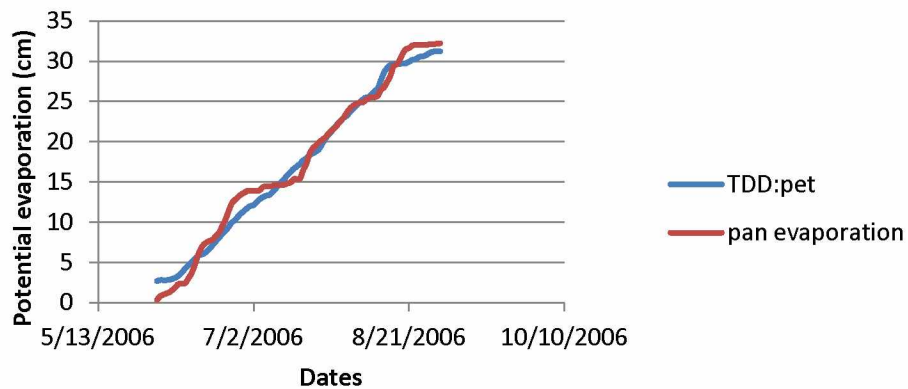
2004 Predicted TDD potential evaporation and pan evaporation



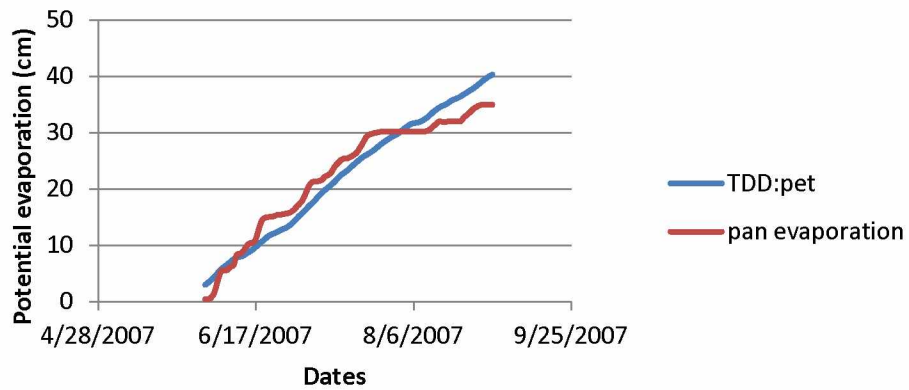
2005 Predicted TDD potential evaporation and pan evaporation



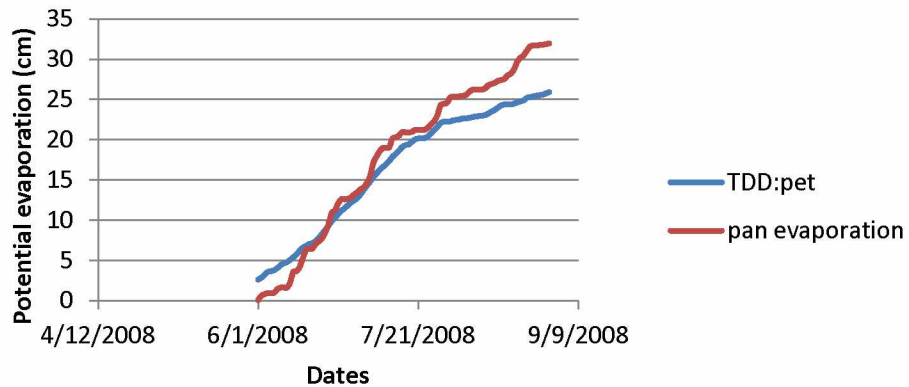
2006 Predicted TDD potential evaporation and pan evaporation



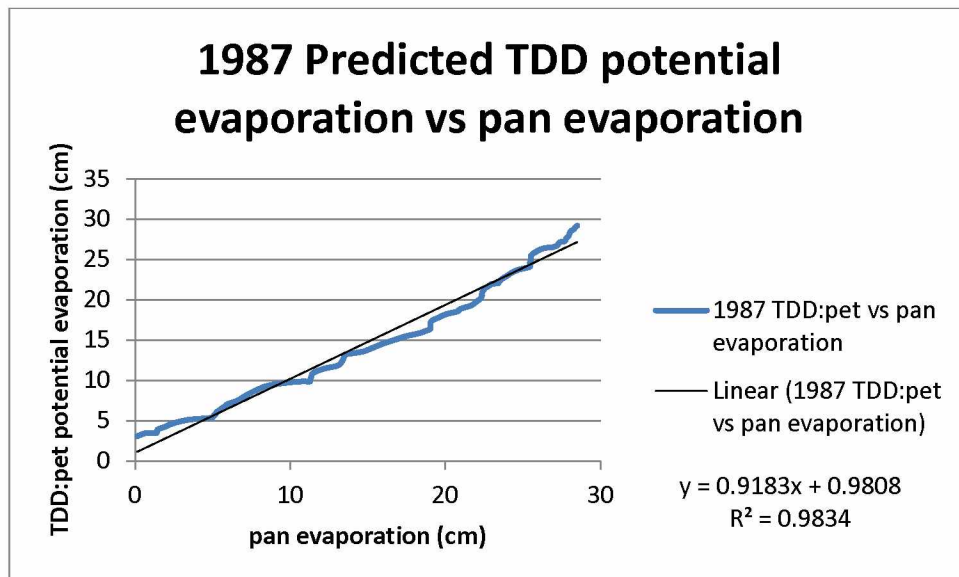
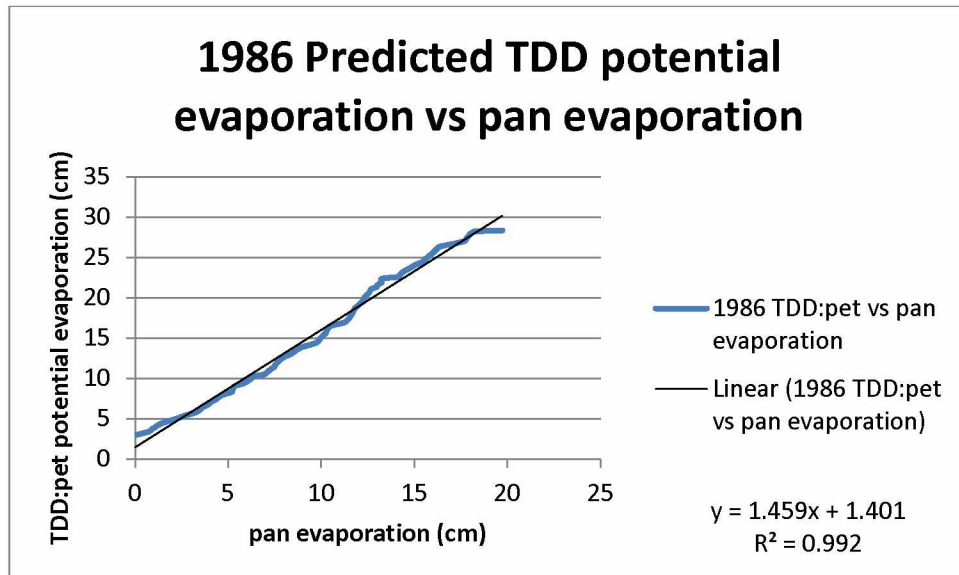
2007 Predicted TDD potential evaporation and pan evaporation



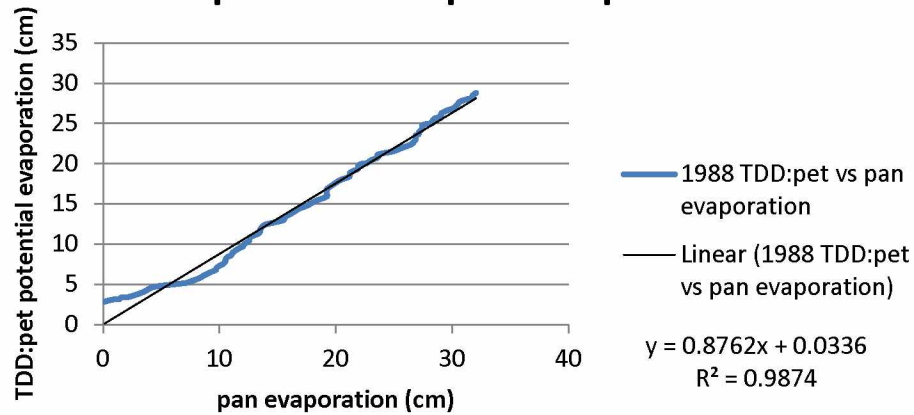
2008 Predicted TDD potential evaporation and pan evaporation



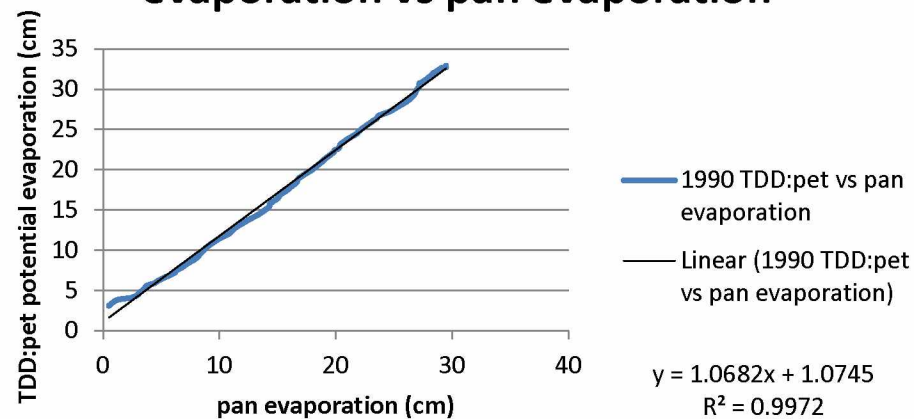
Appendix H: Warm Season Comparison between measured and calculated potential evaporation using thawing degree days and pan evaporation 1986-2008.



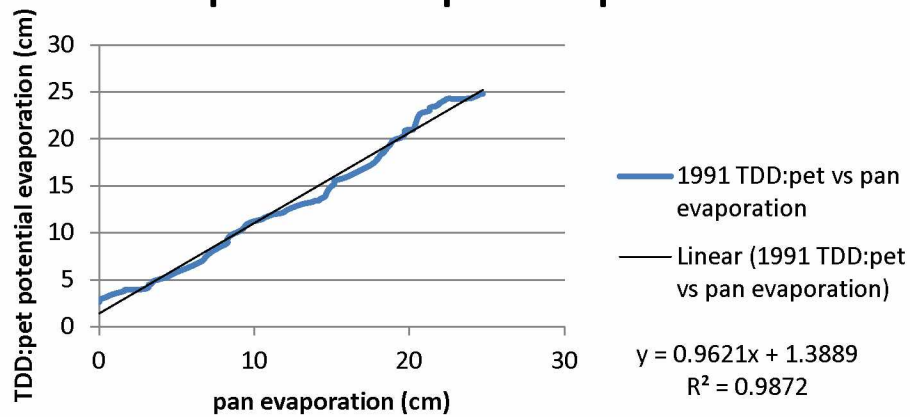
1988 Predicted TDD potential evaporation vs pan evaporation



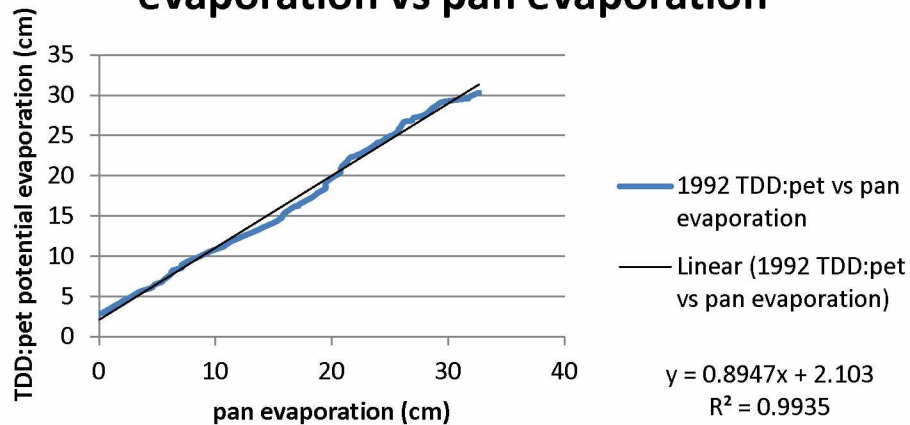
1990 Predicted TDD potential evaporation vs pan evaporation



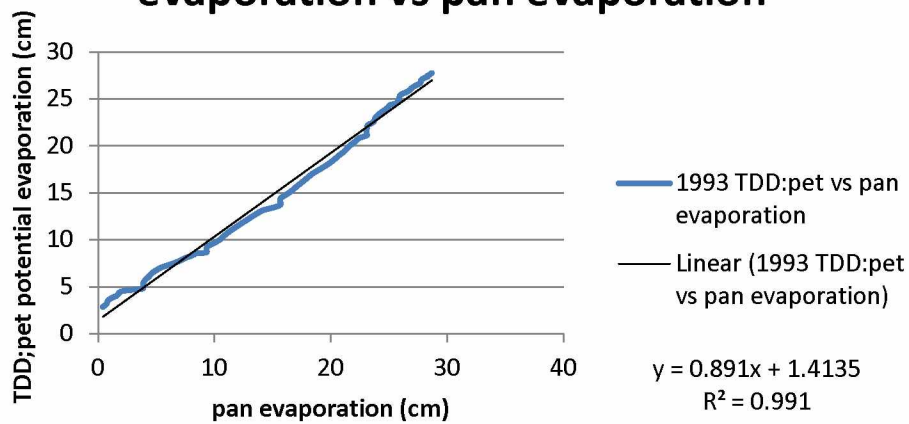
1991 Predicted TDD potential evaporation vs pan evaporation



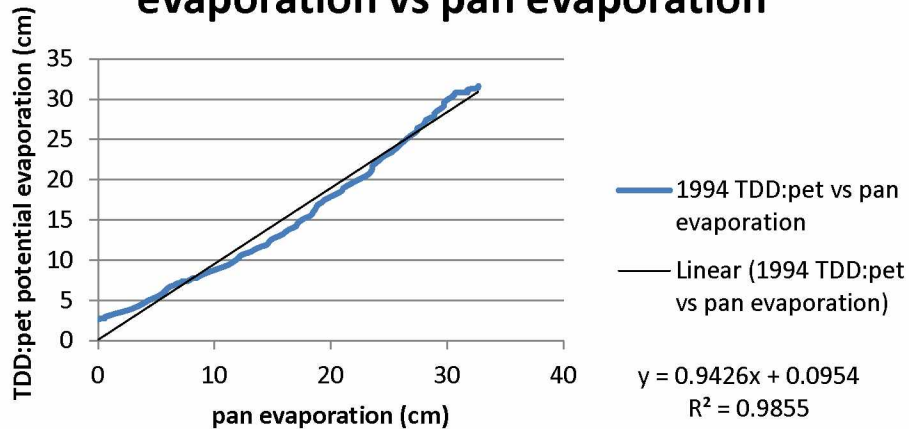
1992 Predicted TDD potential evaporation vs pan evaporation



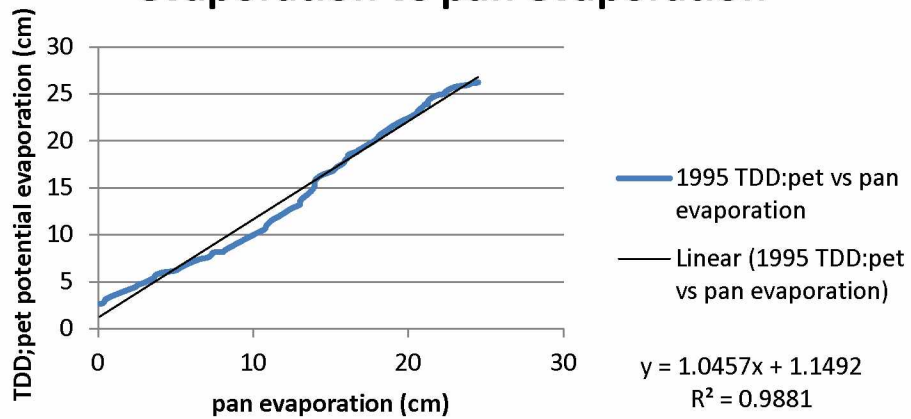
1993 Predicted TDD potential evaporation vs pan evaporation



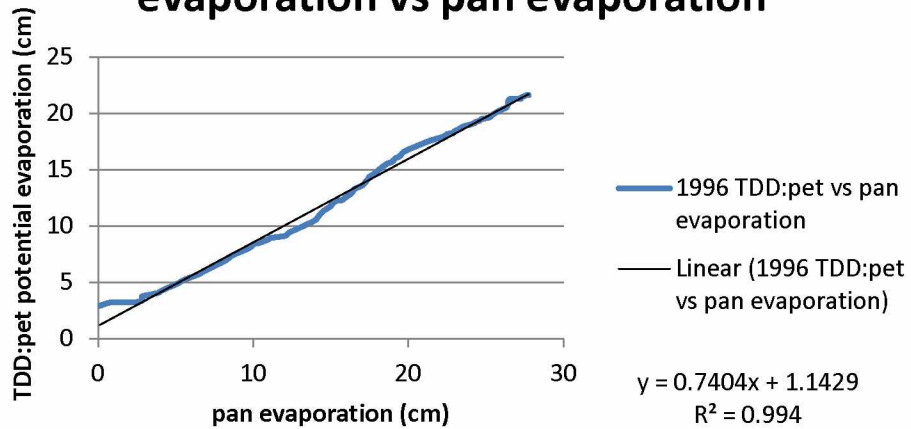
1994 Predicted TDD potential evaporation vs pan evaporation



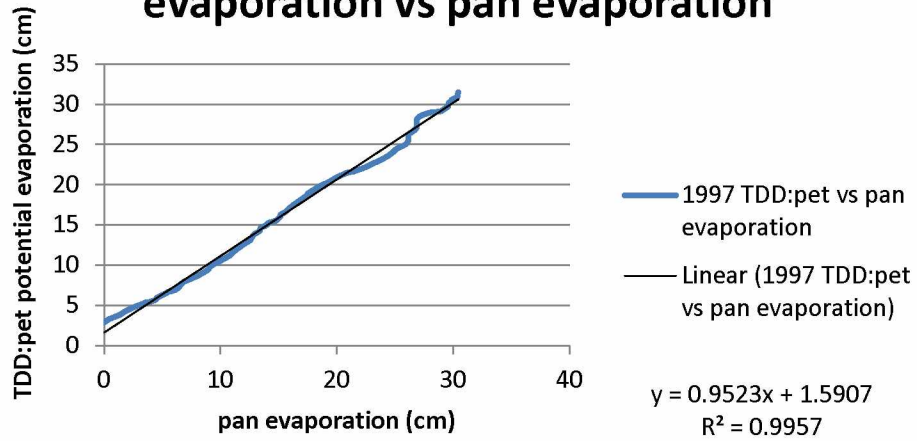
1995 Predicted TDD potential evaporation vs pan evaporation



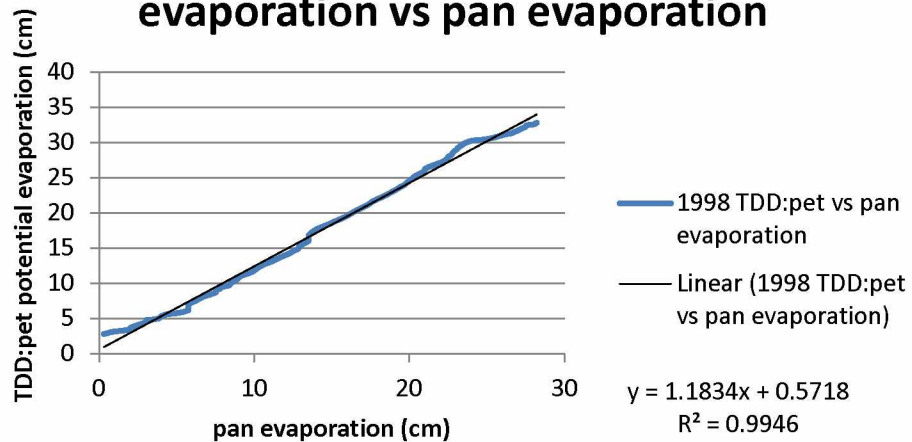
1996 Predicted TDD potential evaporation vs pan evaporation



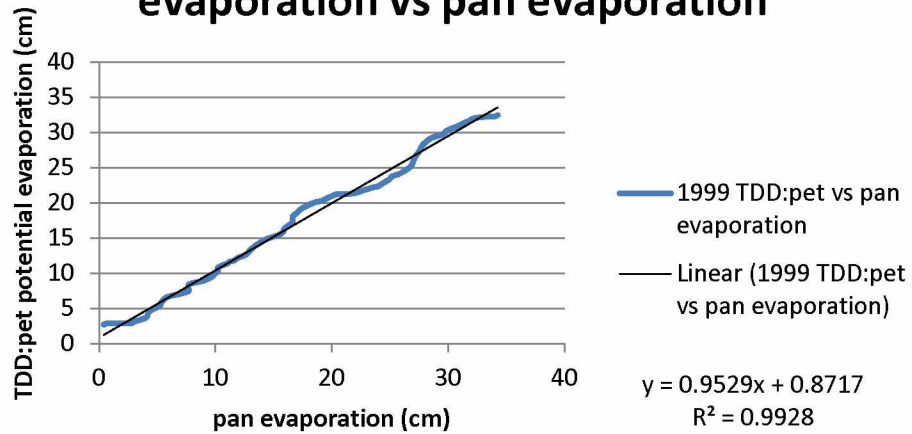
1997 Predicted TDD potential evaporation vs pan evaporation



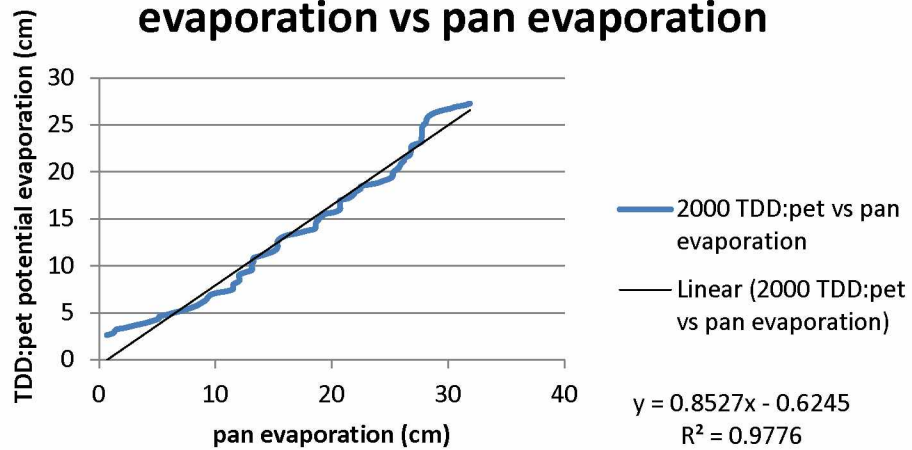
1998 Predicted TDD potential evaporation vs pan evaporation



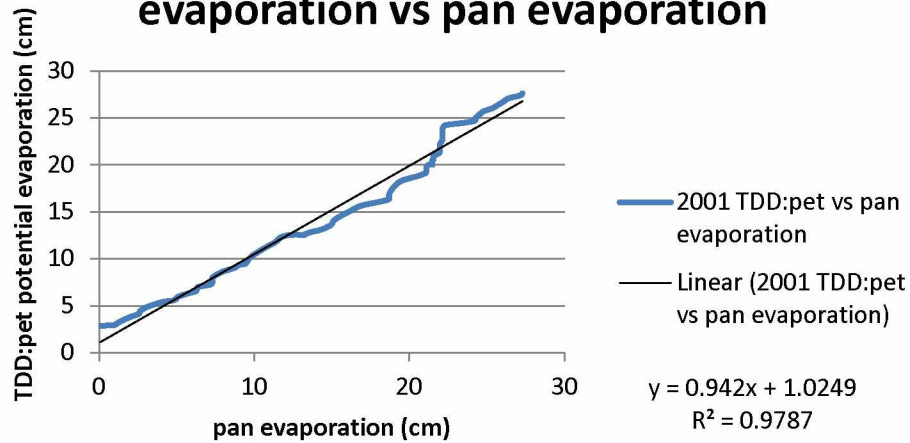
1999 Predicted TDD potential evaporation vs pan evaporation



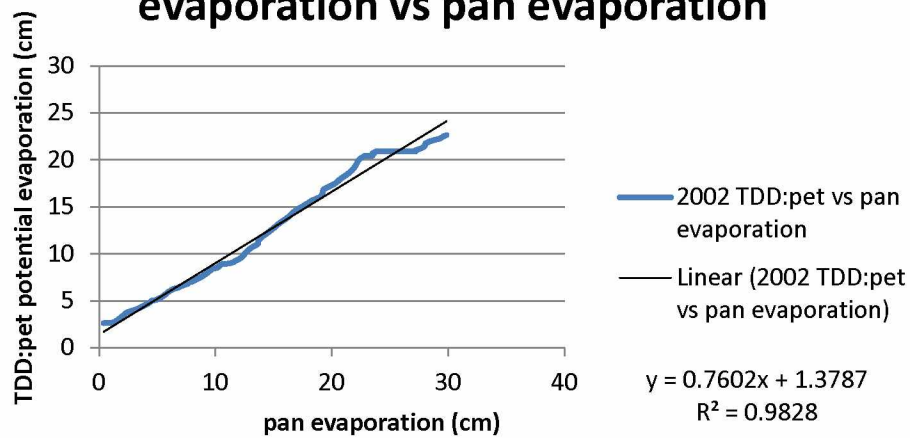
2000 Predicted TDD potential evaporation vs pan evaporation



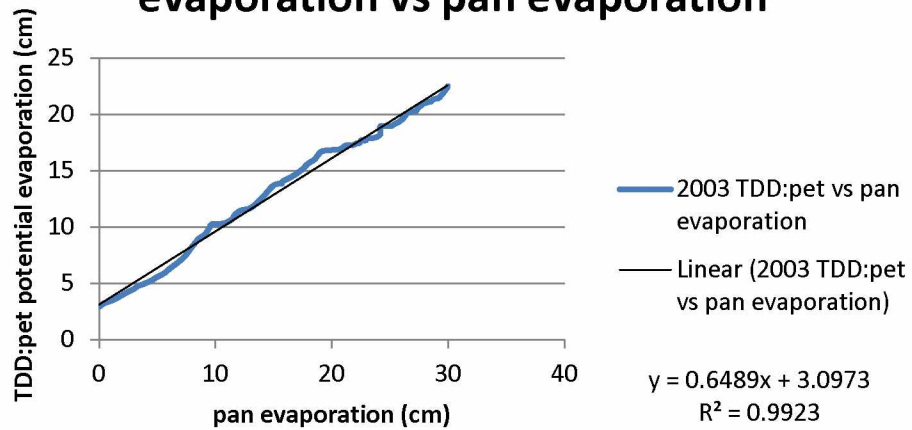
2001 Predicted TDD potential evaporation vs pan evaporation



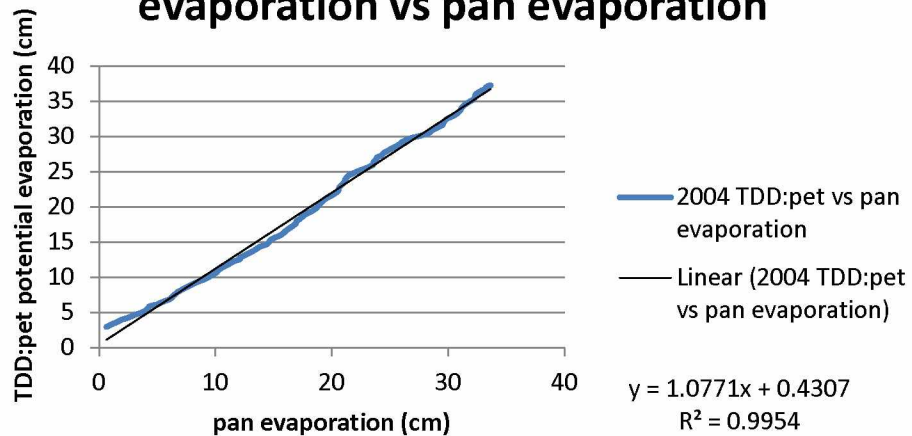
2002 Predicted TDD potential evaporation vs pan evaporation



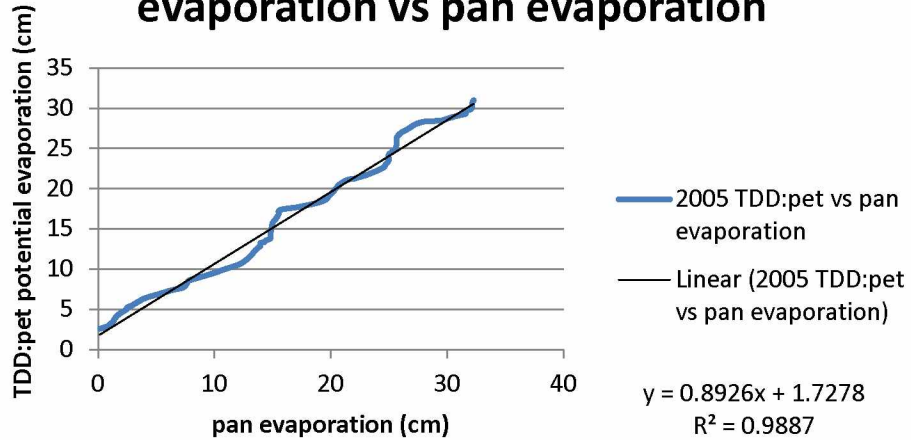
2003 Predicted TDD potential evaporation vs pan evaporation



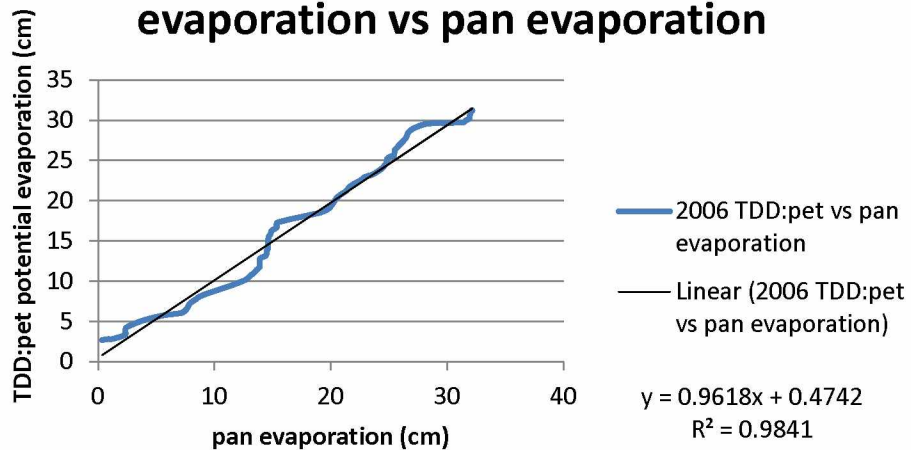
2004 Predicted TDD potential evaporation vs pan evaporation

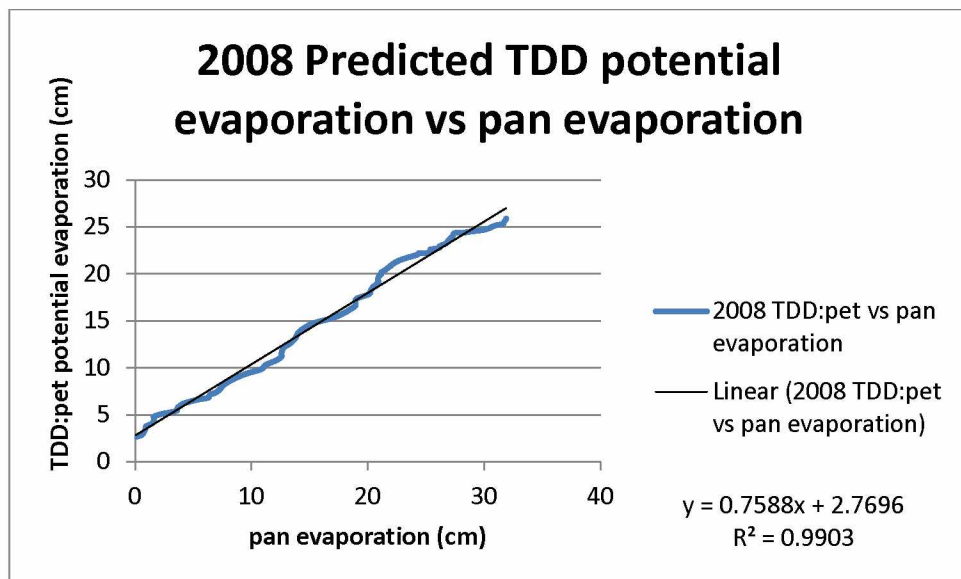
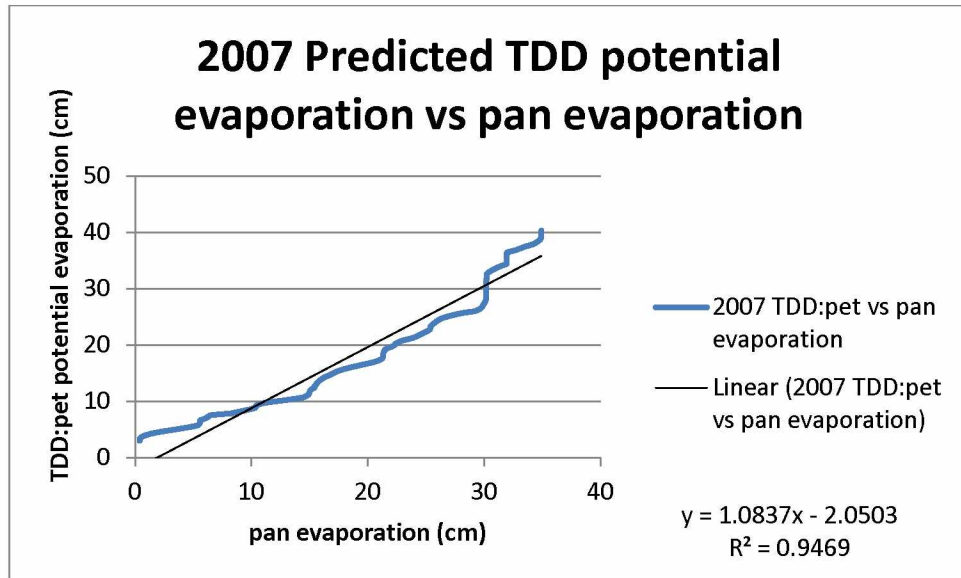


2005 Predicted TDD potential evaporation vs pan evaporation

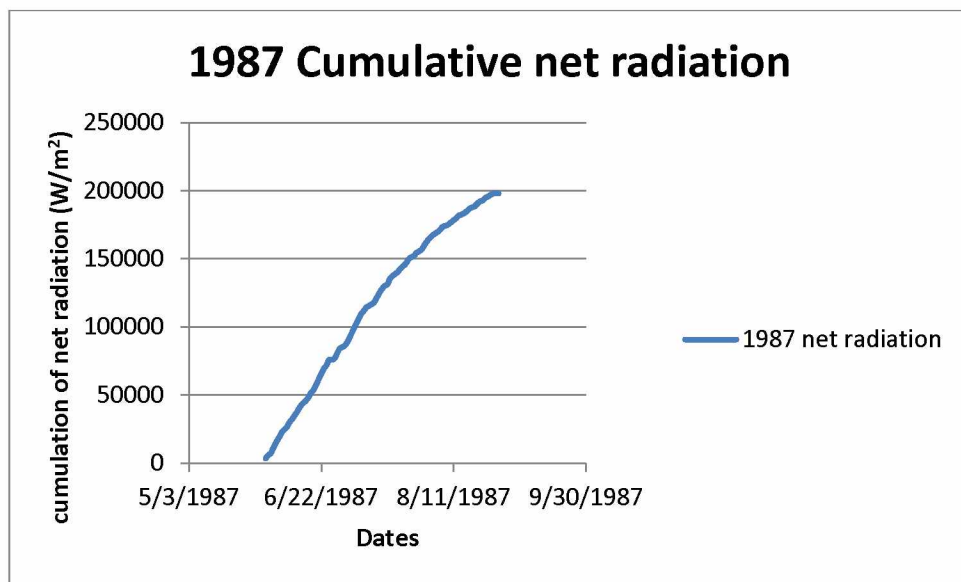
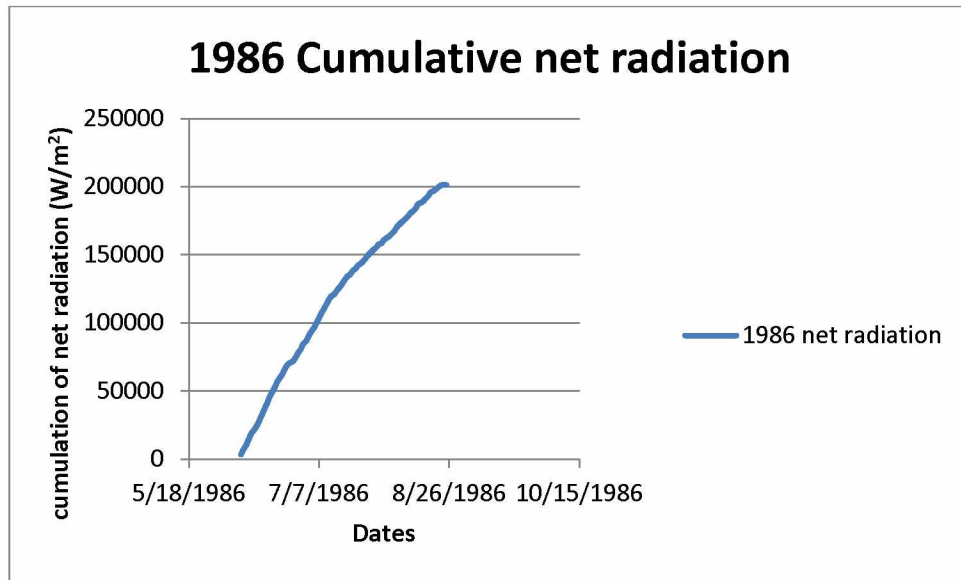


2006 Predicted TDD potential evaporation vs pan evaporation

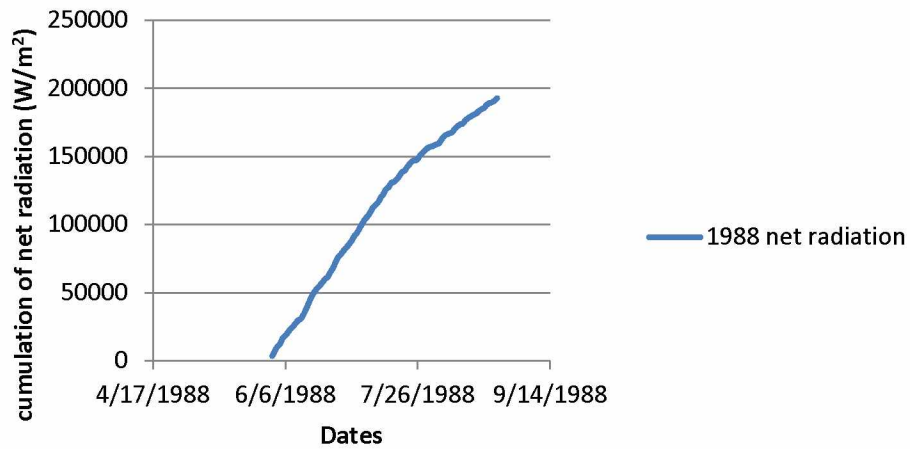




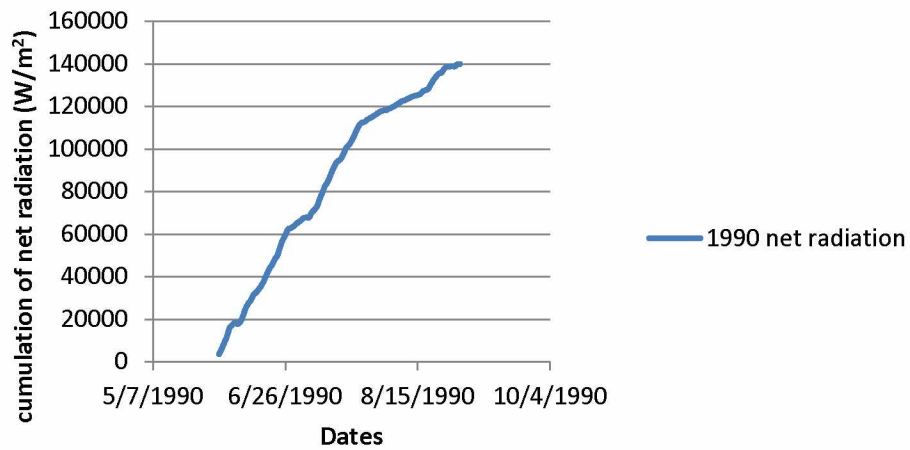
Appendix I: Warm Season Cumulative net radiation 1986-2008.



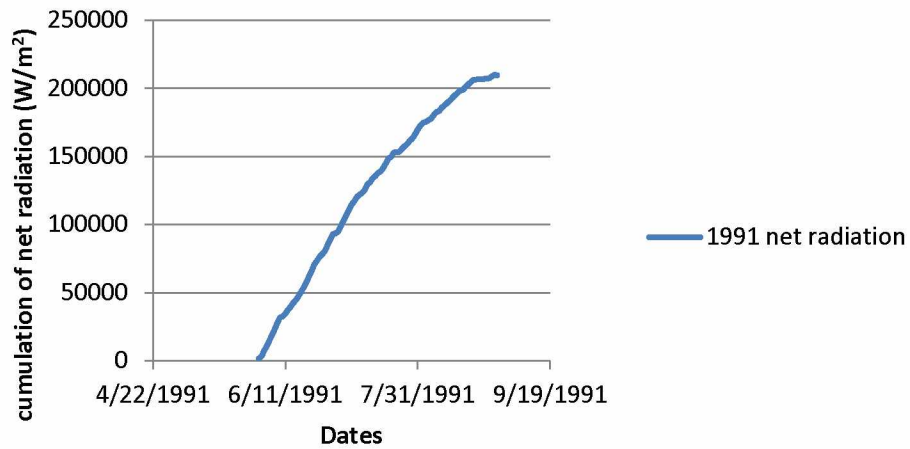
1988 Cumulative net radiation



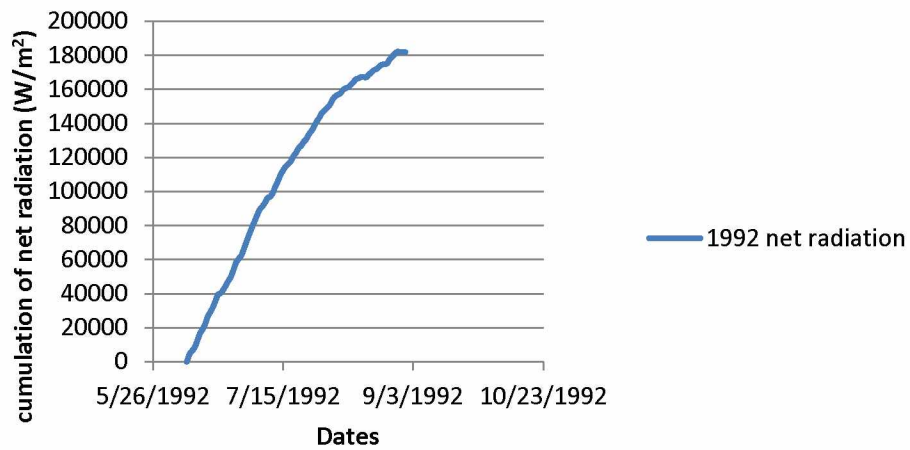
1990 Cumulative net radiation



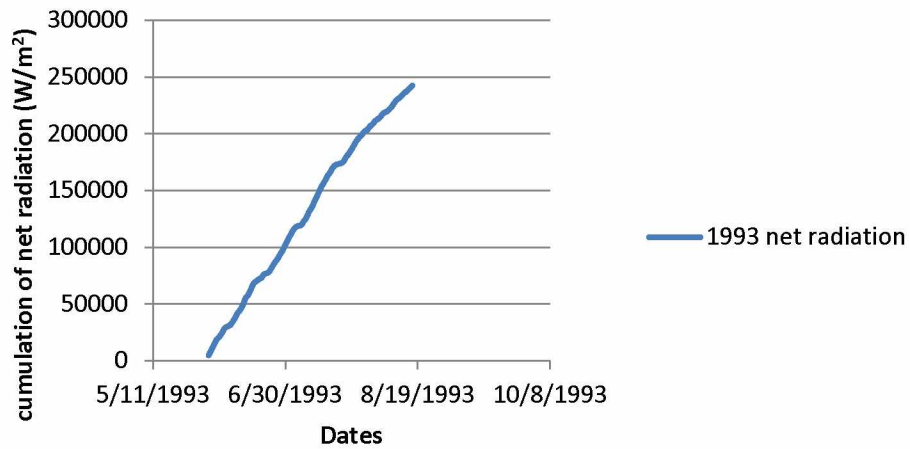
1991 Cumulative net radiation



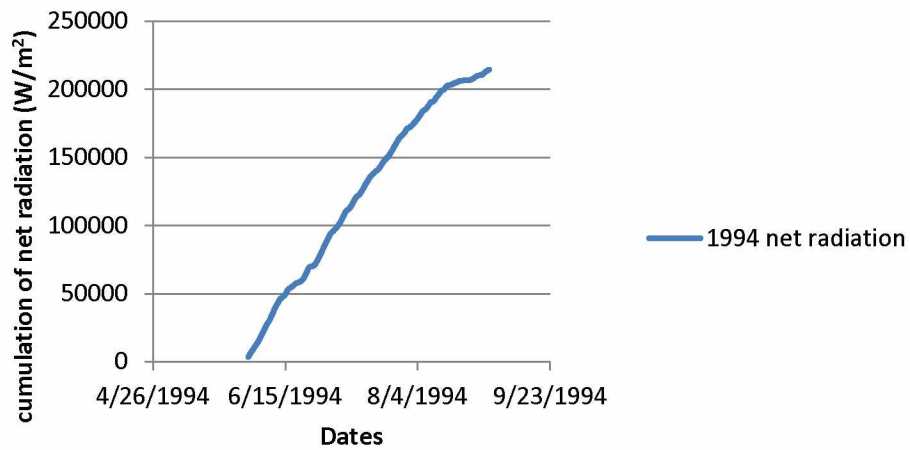
1992 Cumulative net radiation



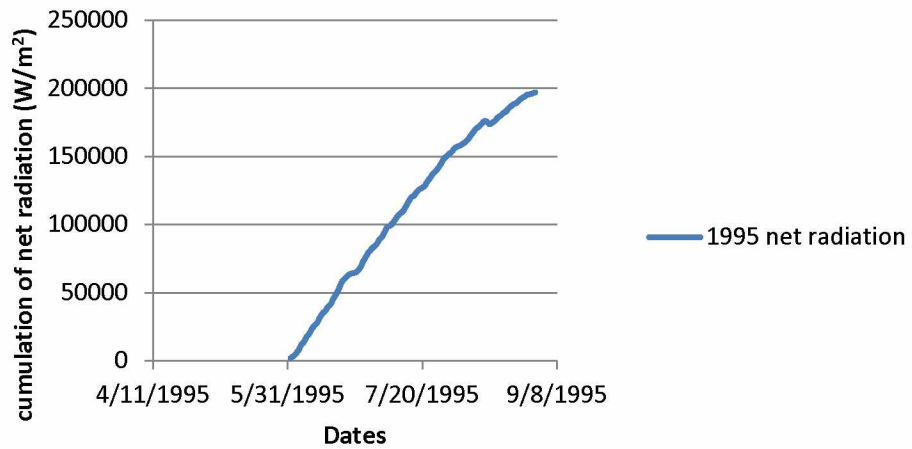
1993 Cumulative net radiation



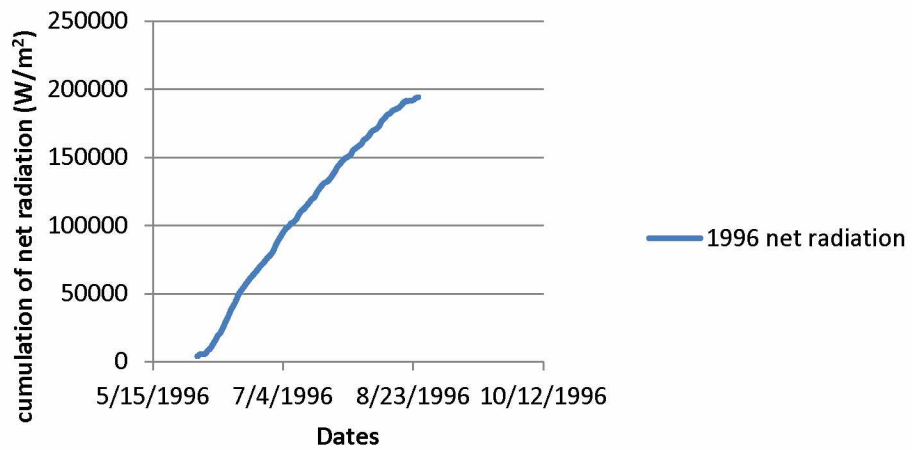
1994 Cumulative net radiation



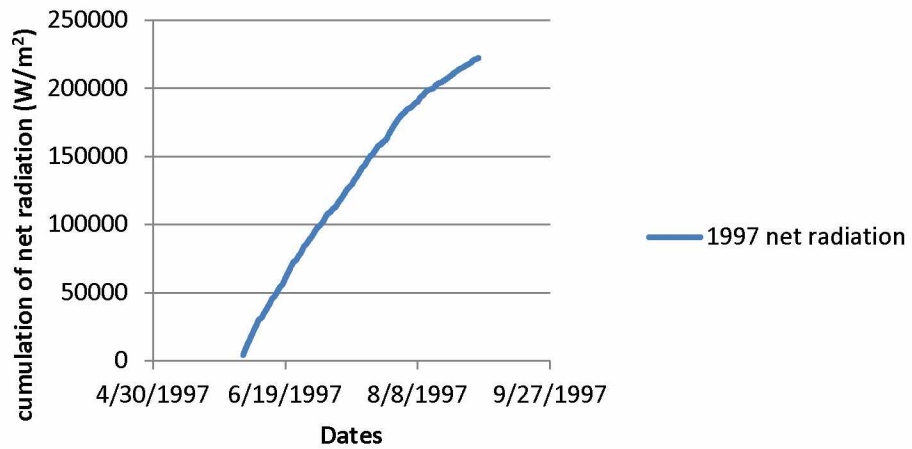
1995 Cumulative net radiation



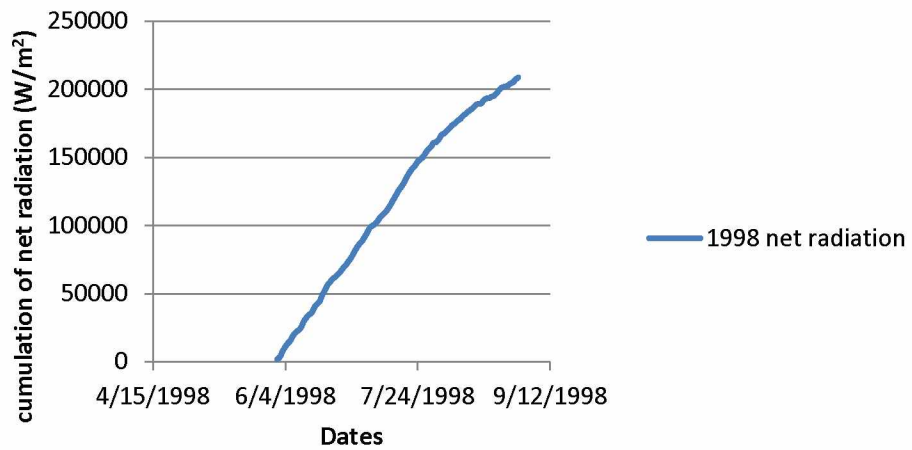
1996 Cumulative net radiation



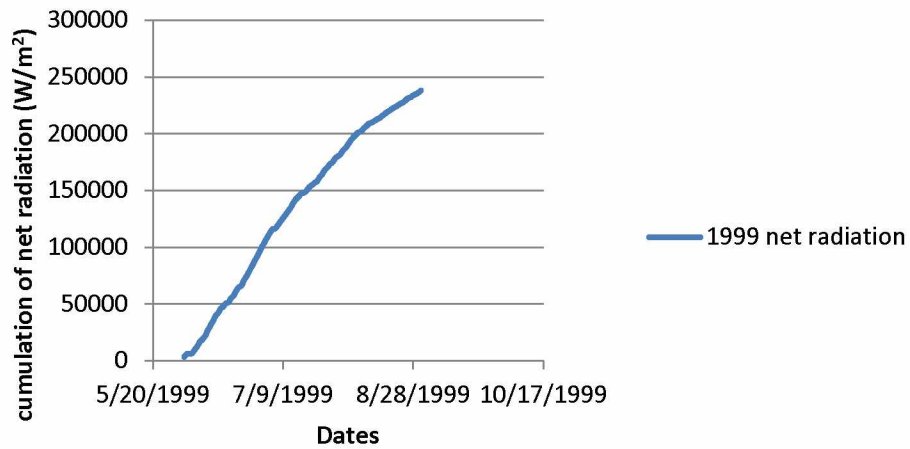
1997 Cumulative net radiation



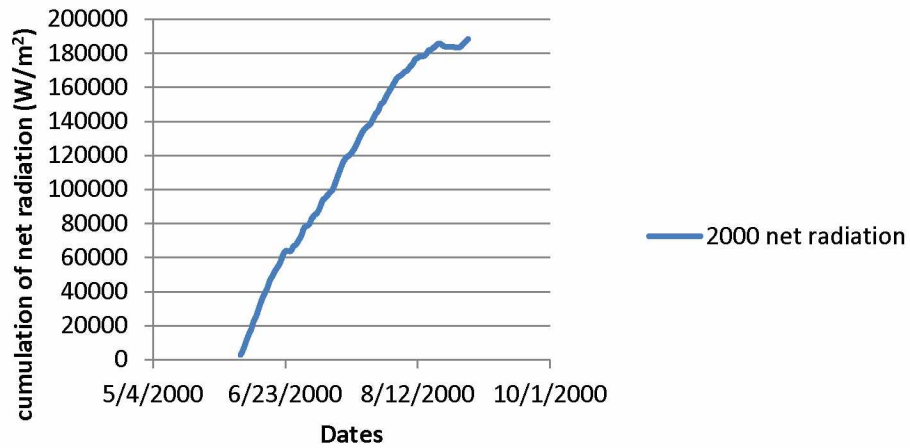
1998 Cumulative net radiation



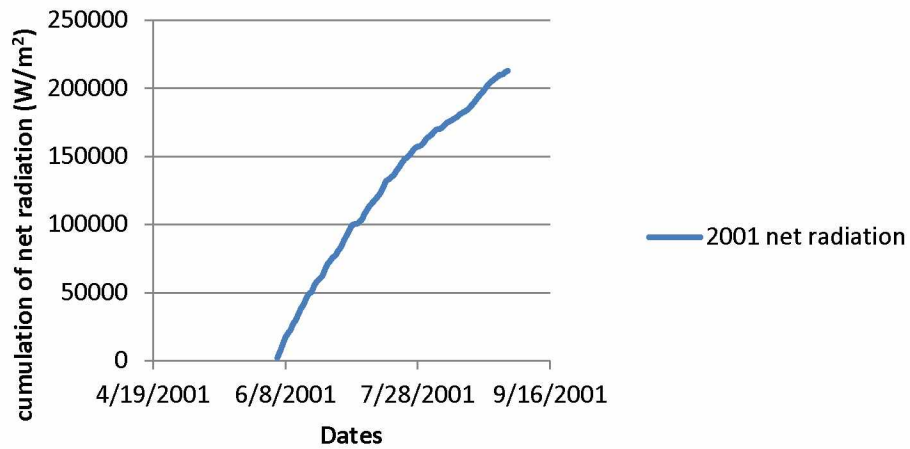
1999 Cumulative net radiation



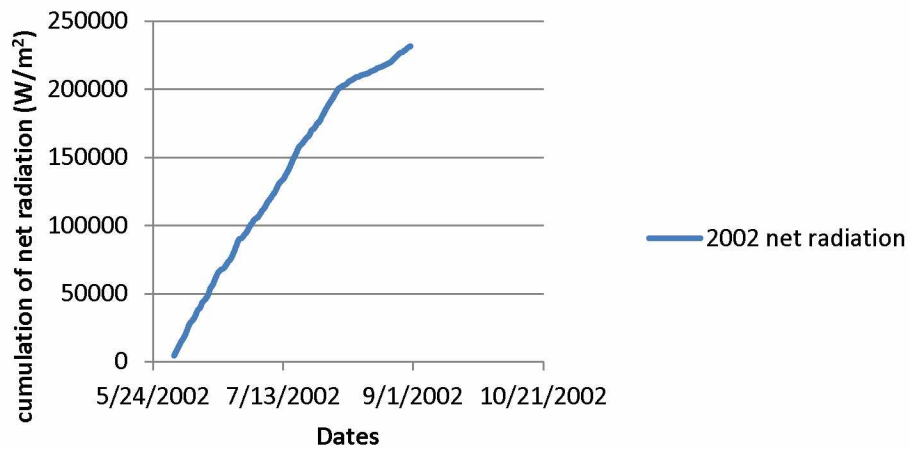
2000 Cumulative net radiation



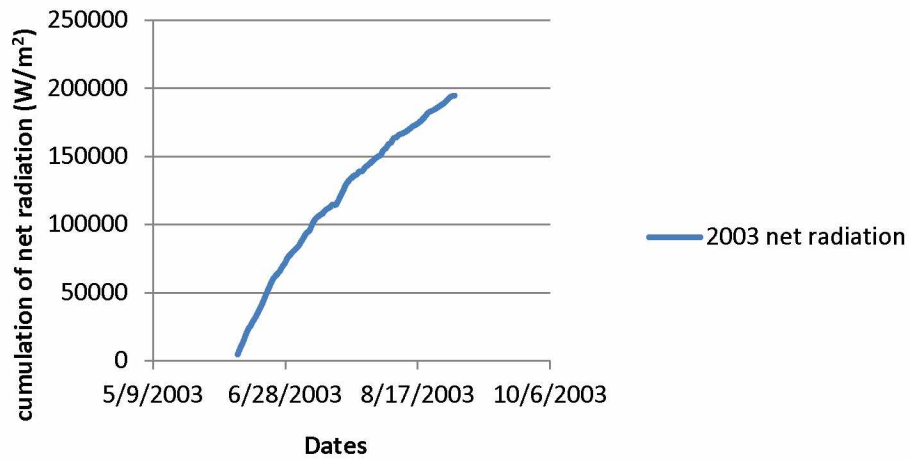
2001 Cumulative net radiation



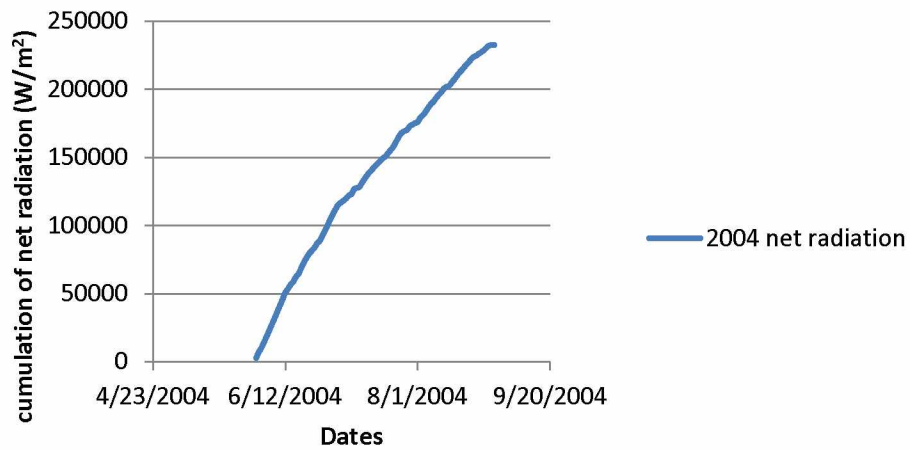
2002 Cumulative net radiation



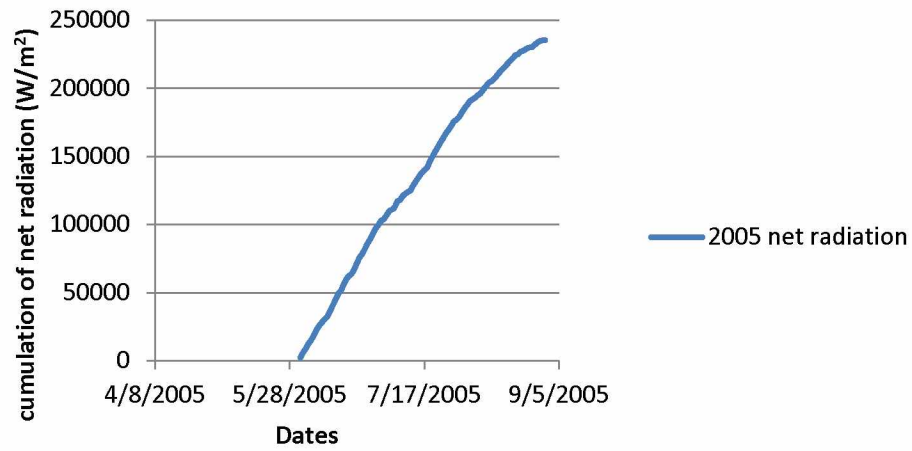
2003 Cumulative net radiation



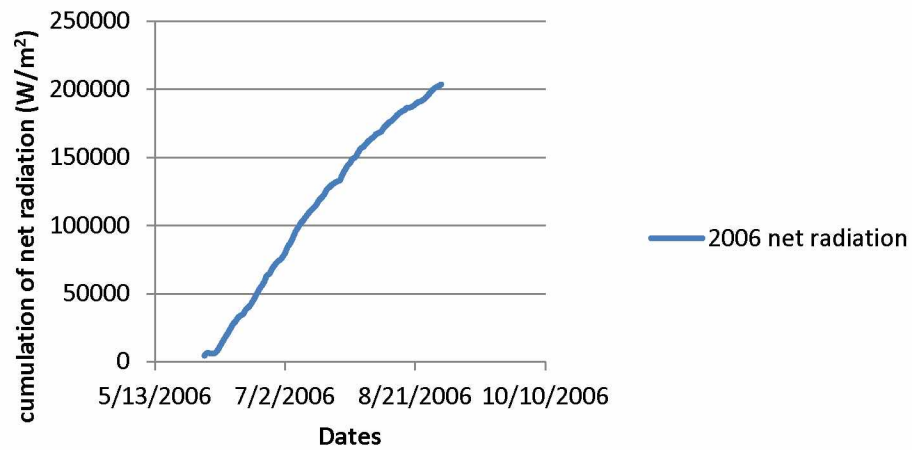
2004 Cumulative net radiation



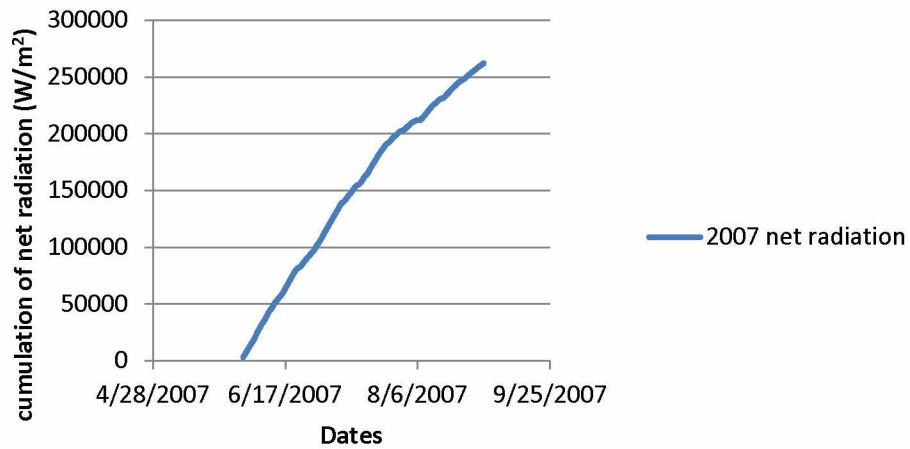
2005 Cumulative net radiation



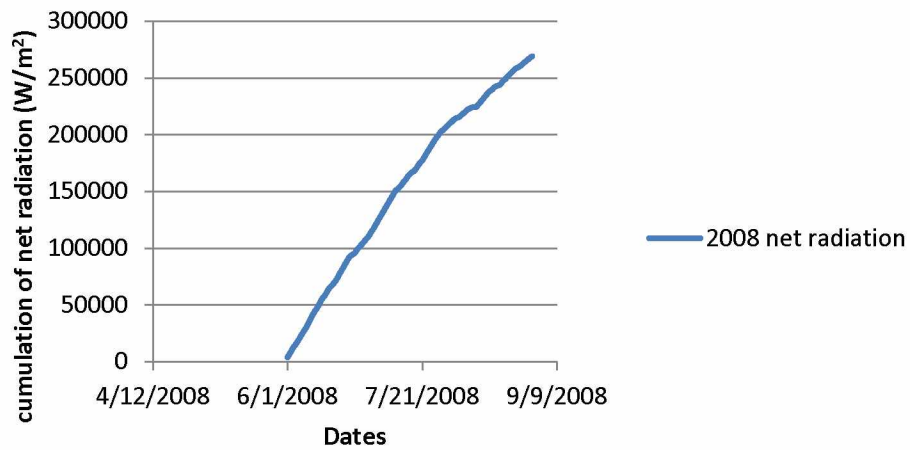
2006 Cumulative net radiation



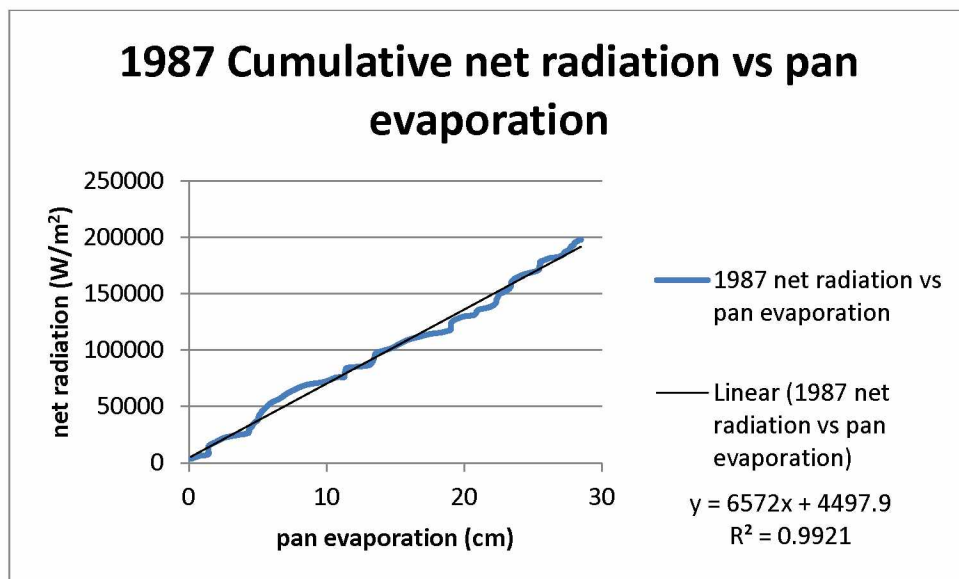
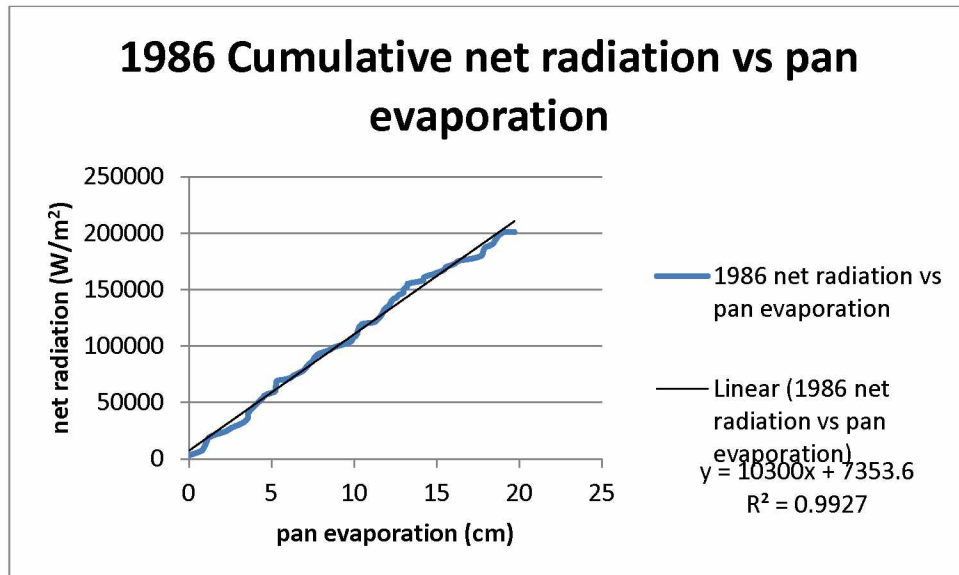
2007 Cumulative net radiation



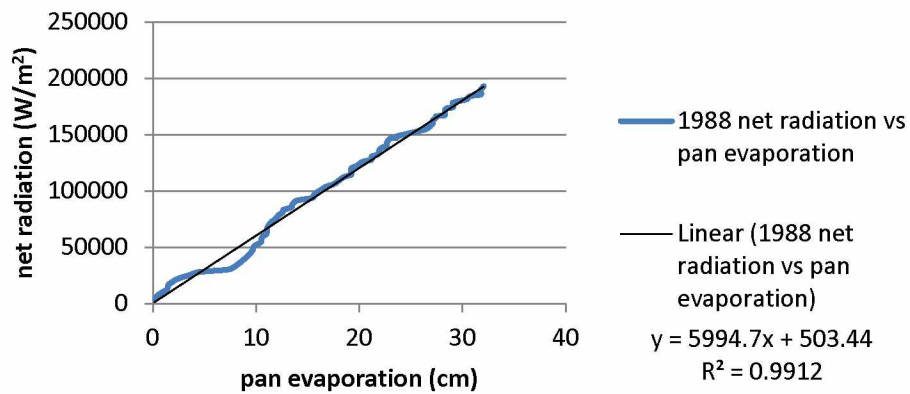
2008 Cumulative net radiation



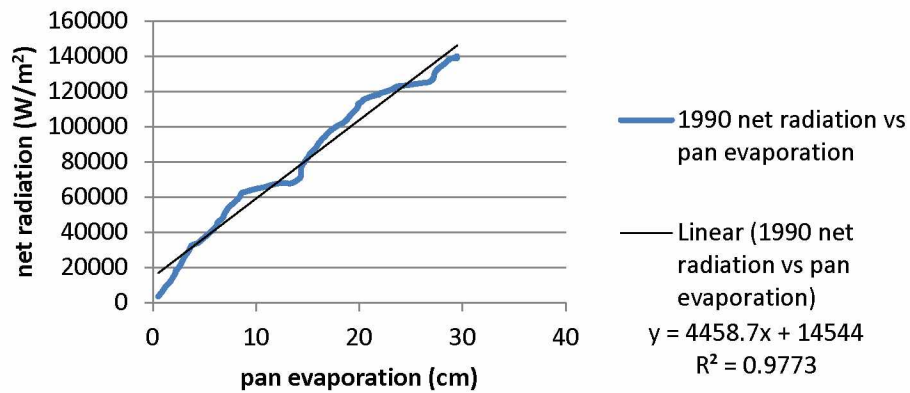
Appendix J: Warm Season Comparison (relationship) between net radiation and pan evaporation (potential evaporation) 1986-2008.



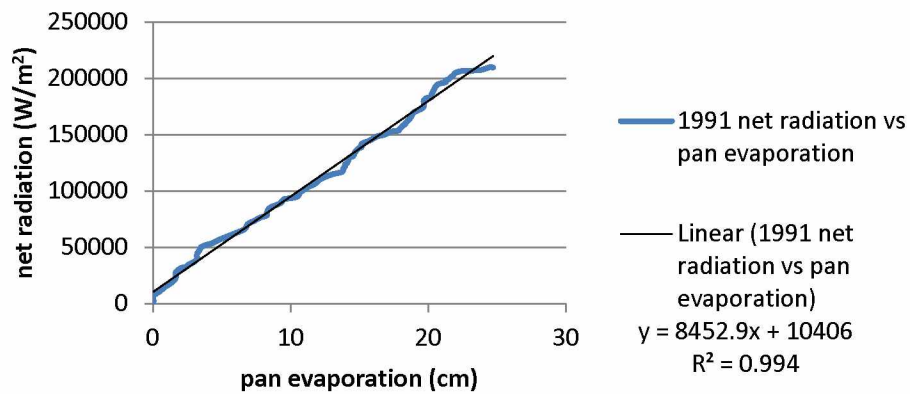
1988 Cumulative net radiation vs pan evaporation



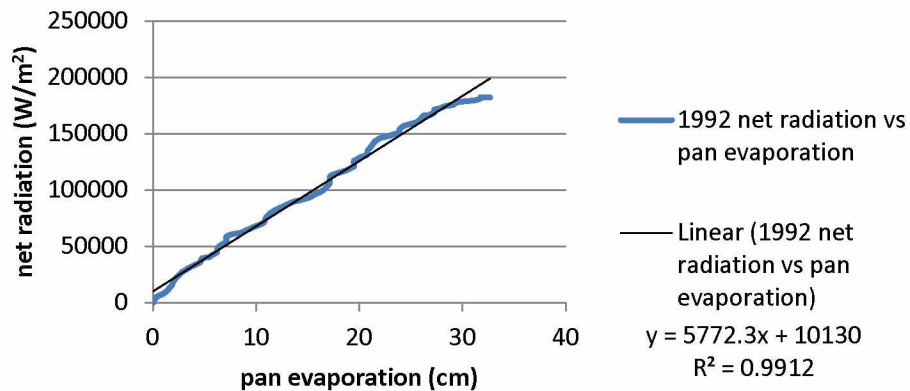
1990 Cumulative net radiation vs pan evaporation



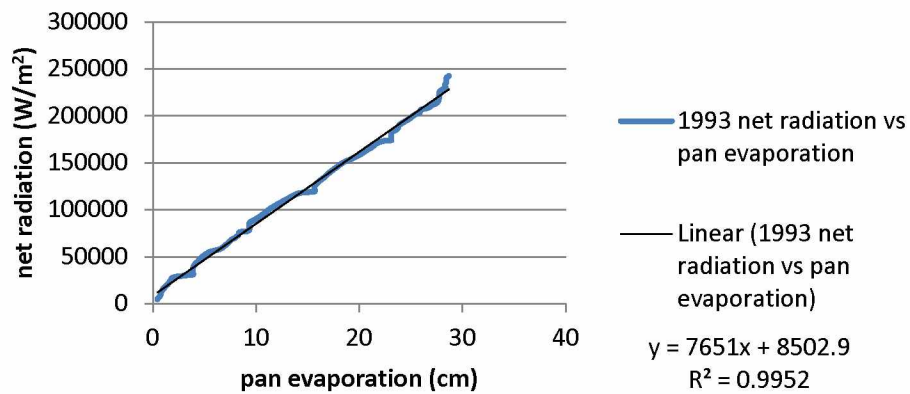
1991 Cumulative net radiation vs pan evaporation



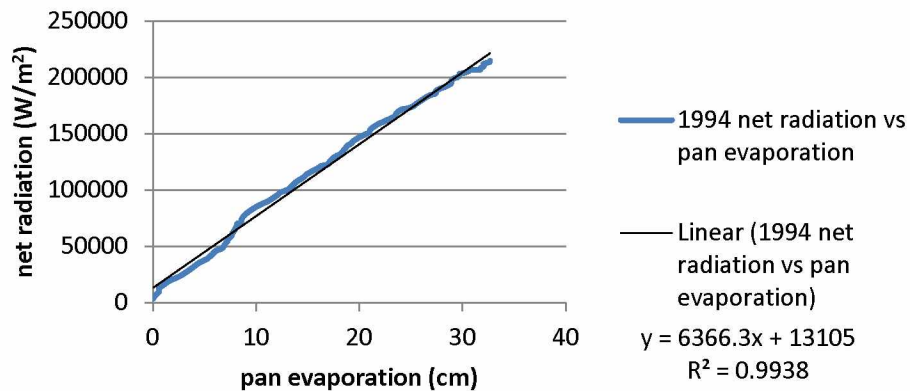
1992 Cumulative net radiation vs pan evaporation



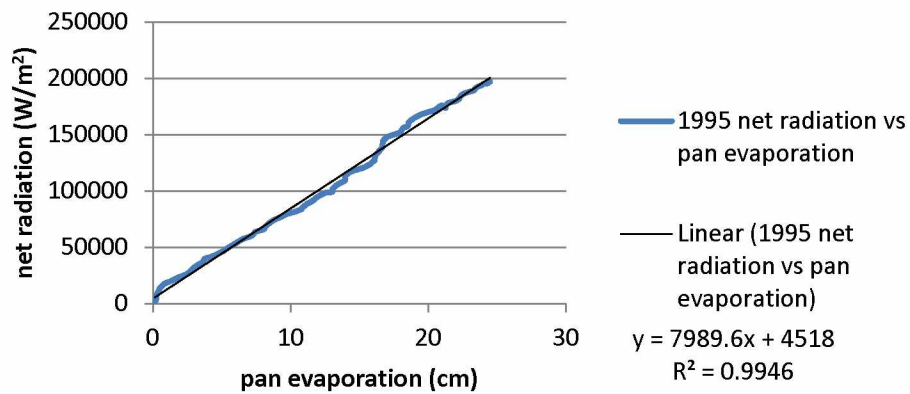
1993 Cumulative net radiation vs pan evaporation



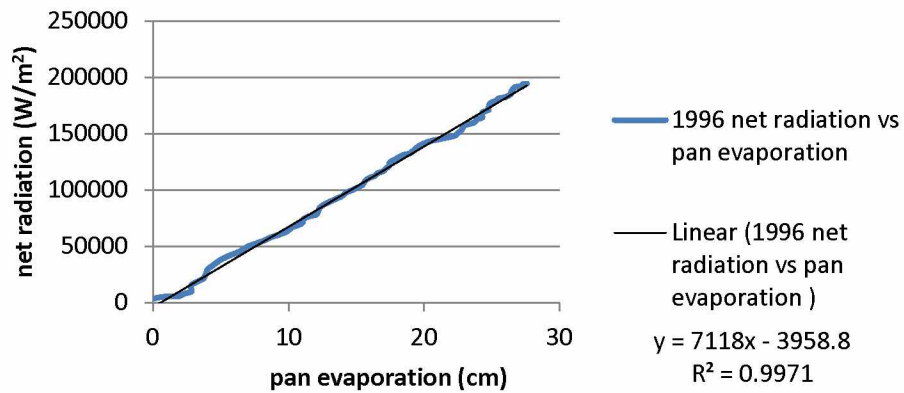
1994 Cumulative net radiation vs pan evaporation



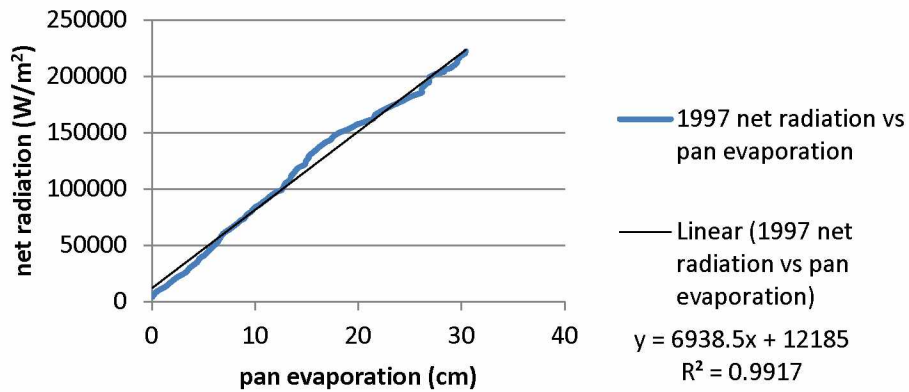
1995 Cumulative net radiation vs pan evaporation



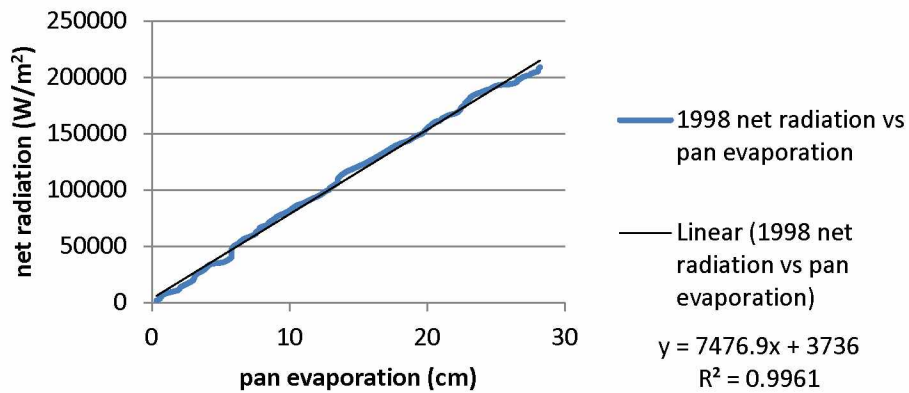
1996 Cumulative net radiation vs pan evaporation



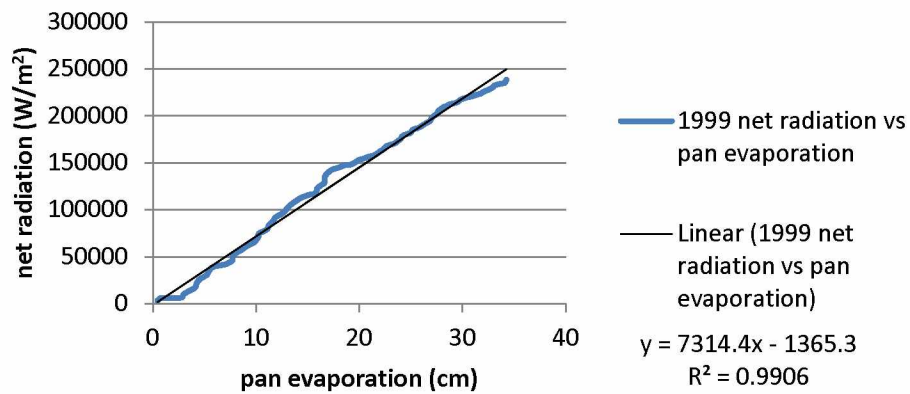
1997 Cumulative net radiation vs pan evaporation



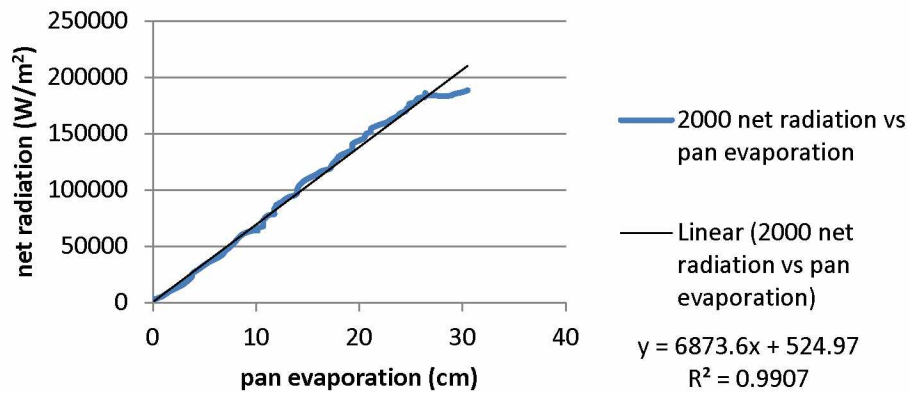
1998 Cumulative net radiation vs pan evaporation



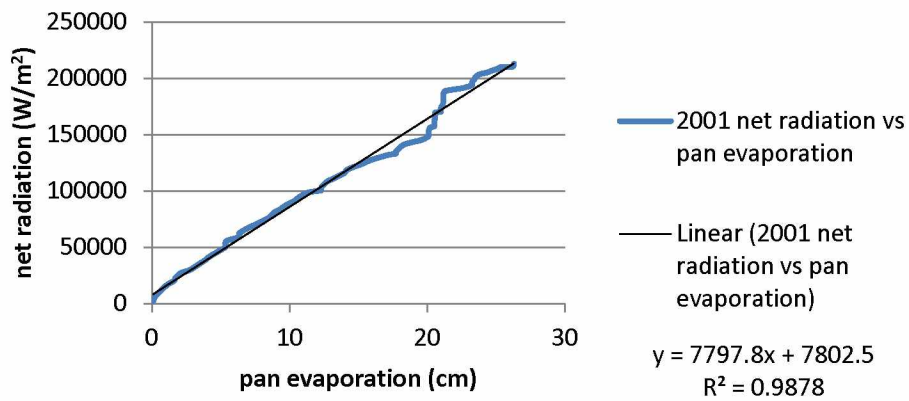
1999 Cumulative net radiation vs pan evaporation



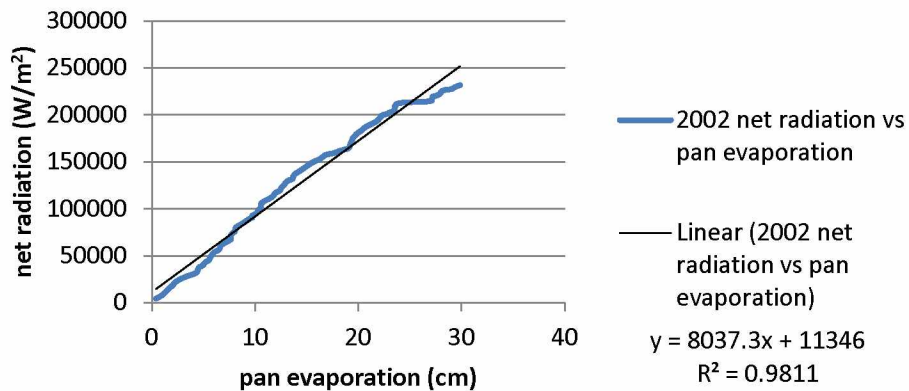
2000 Cumulative net radiation vs pan evaporation



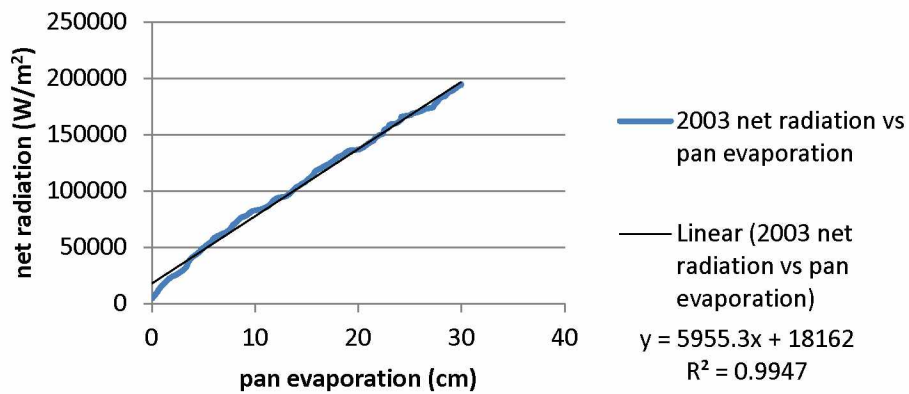
2001 Cumulative net radiation vs pan evaporation



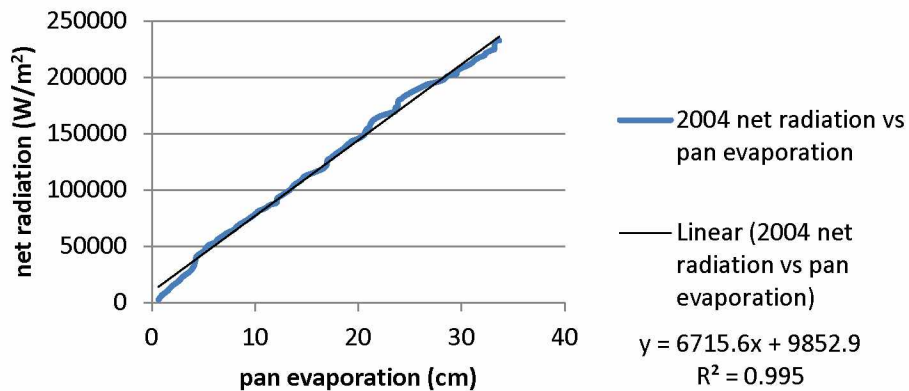
2002 Cumulative net radiation vs pan evaporation



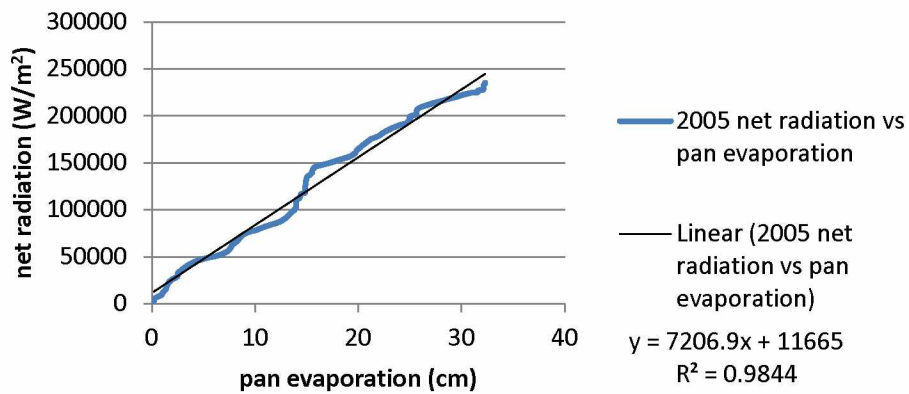
2003 Cumulative net radiation vs pan evaporation



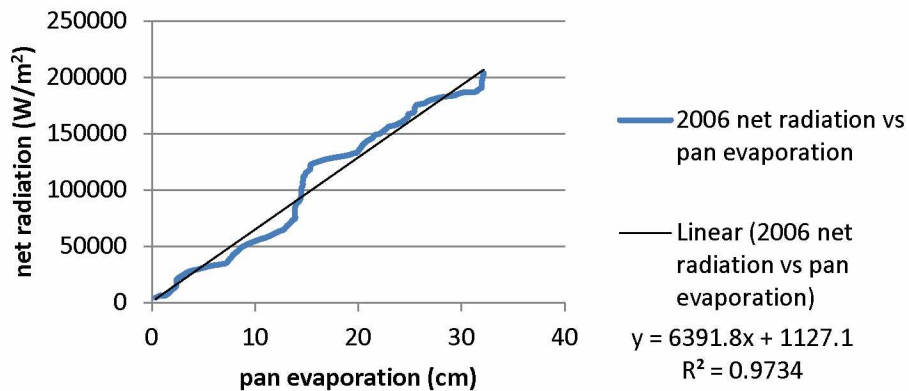
2004 Cumulative net radiation vs pan evaporation



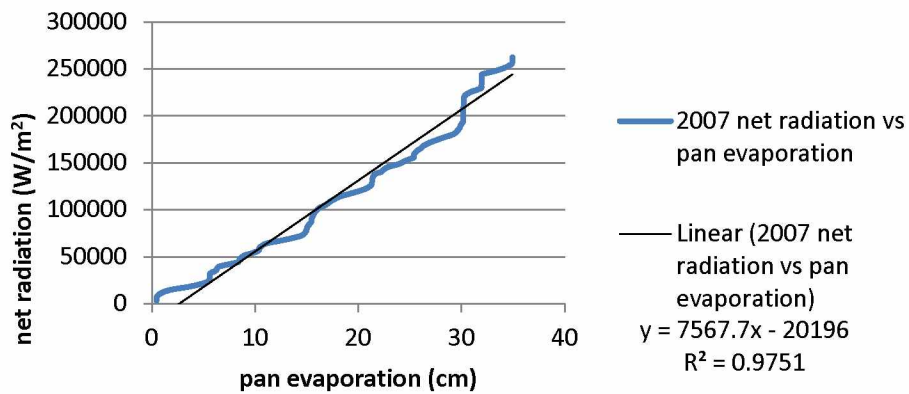
2005 Cumulative net radiation vs pan evaporation



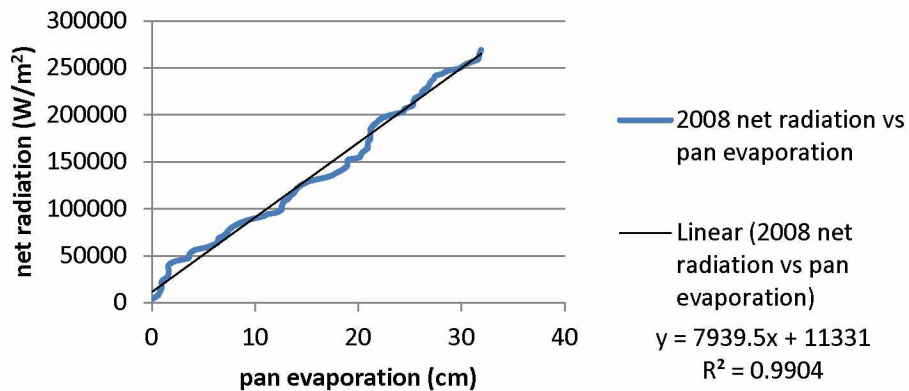
2006 Cumulative net radiation vs pan evaporation



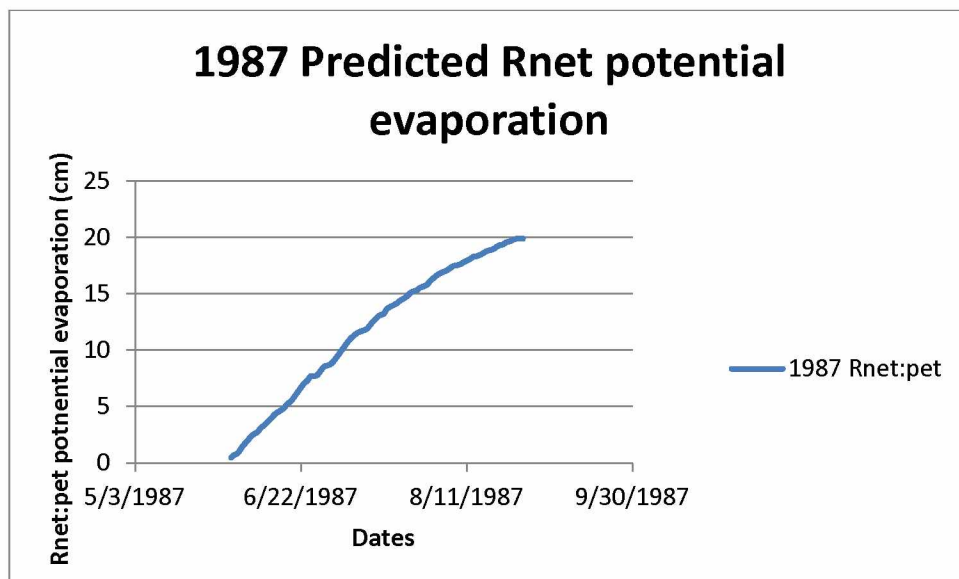
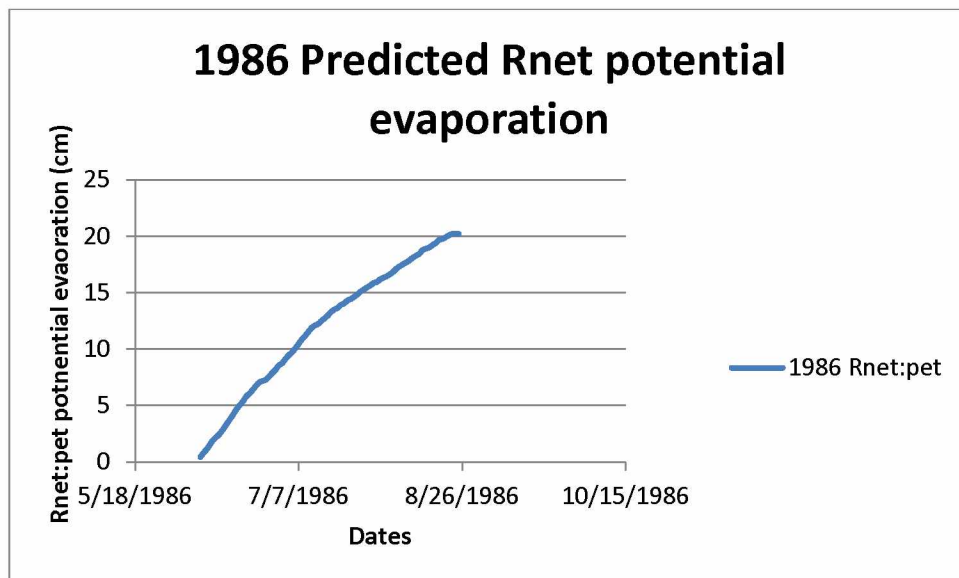
2007 Cumulative net radiation vs pan evaporation



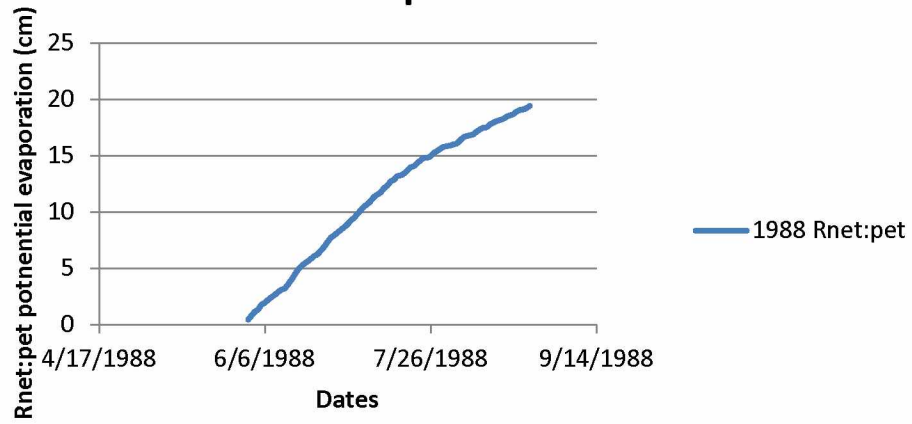
2008 Cumulative net radiation vs pan evaporation



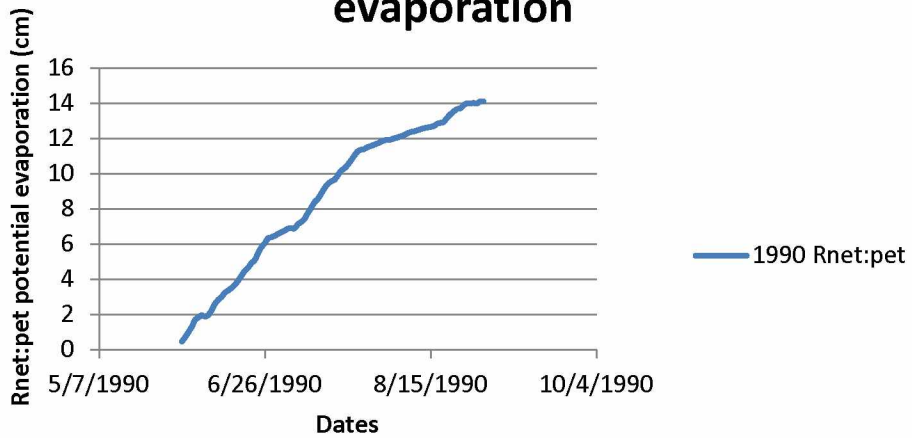
Appendix K: Warm Season Cumulative Calculated potential evaporation using net radiation measurements 1986-2008.



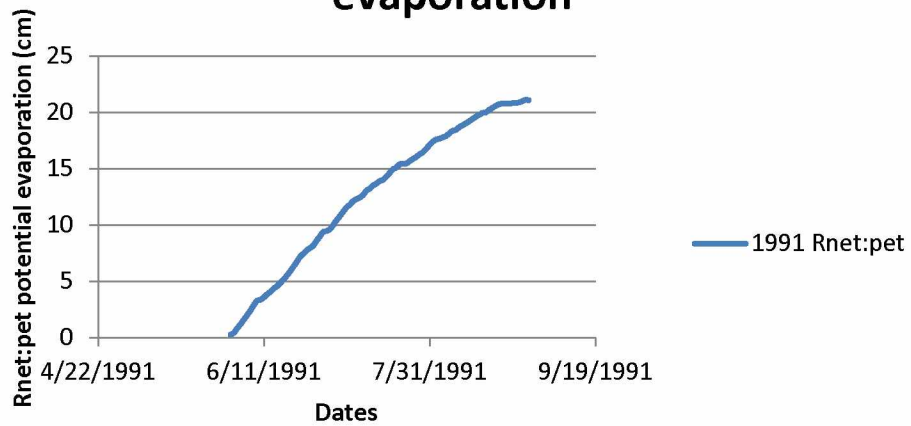
1988 Predicted Rnet potential evaporation



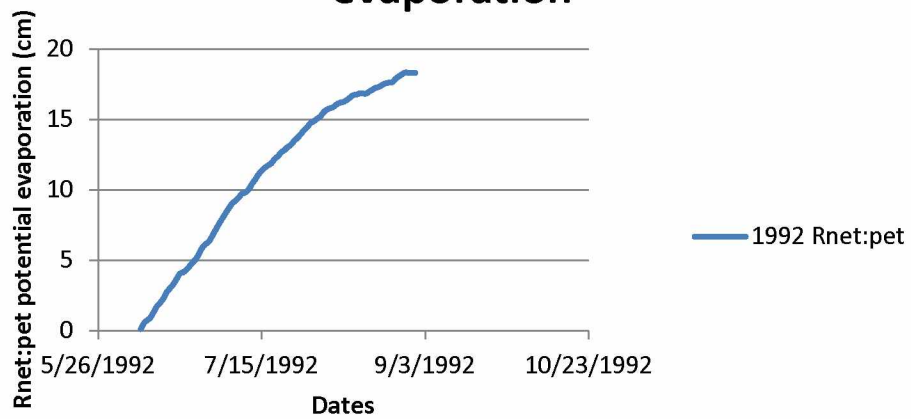
1990 Predicted Rnet potential evaporation



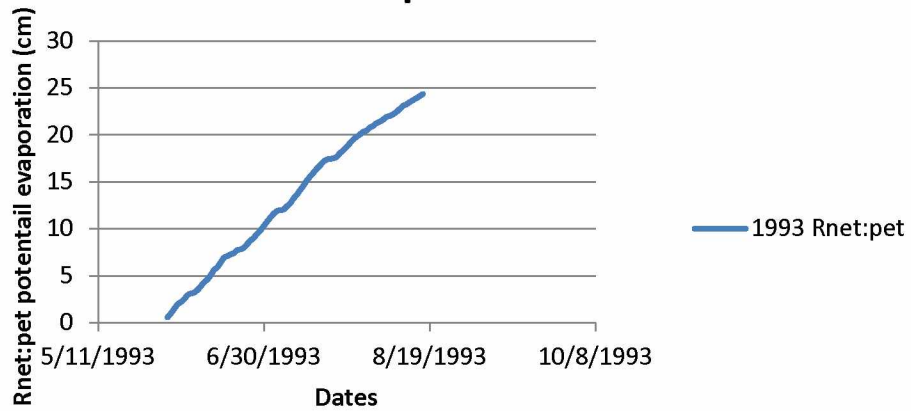
1991 Predicted Rnet potential evaporation



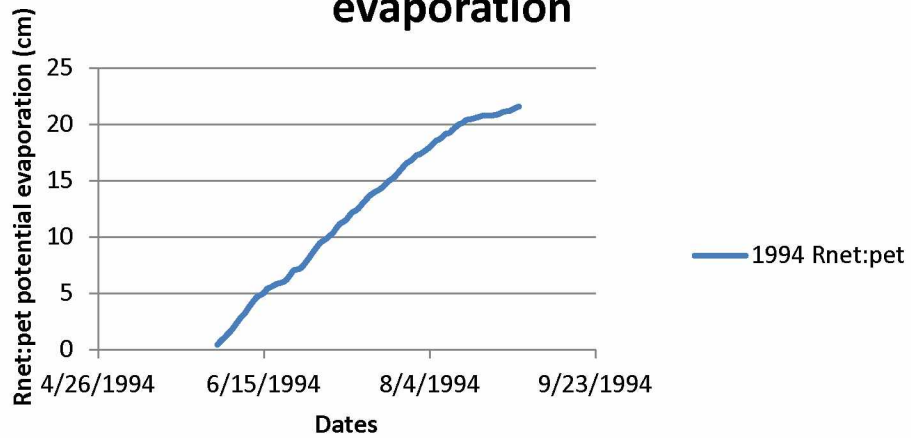
1992 Predicted Rnet potential evaporation



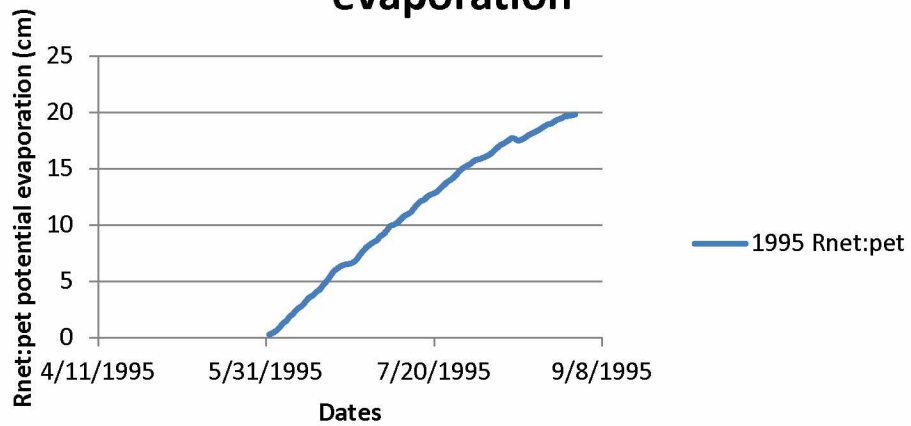
1993 Predicted Rnet potential evaporation



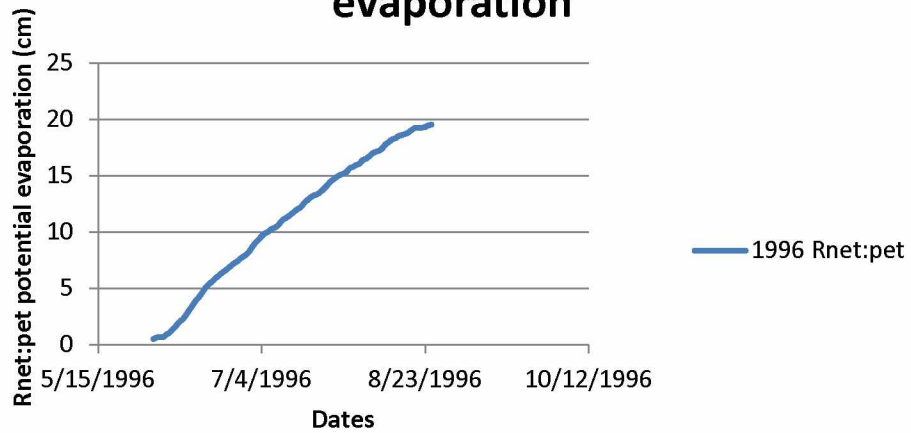
1994 Predicted Rnet potential evaporation



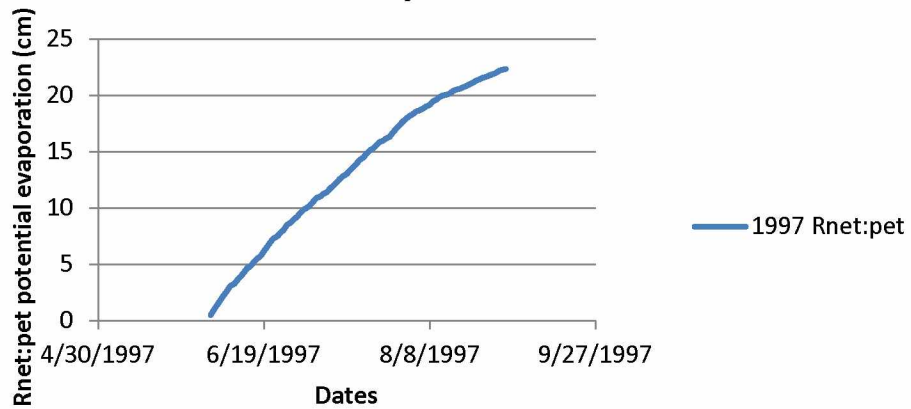
1995 Predicted Rnet potential evaporation



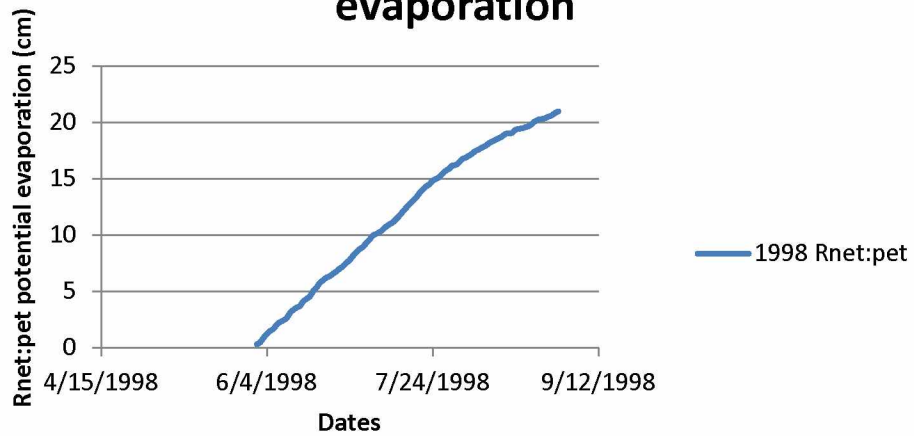
1996 Predicted Rnet potential evaporation



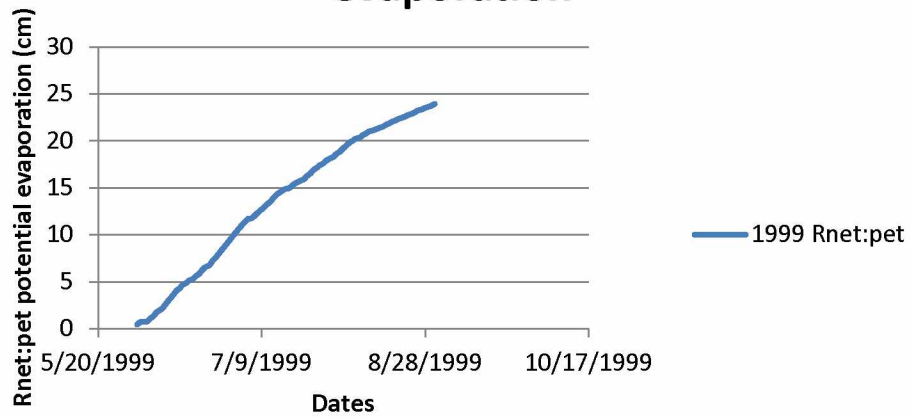
1997 Predicted Rnet potential evaporation



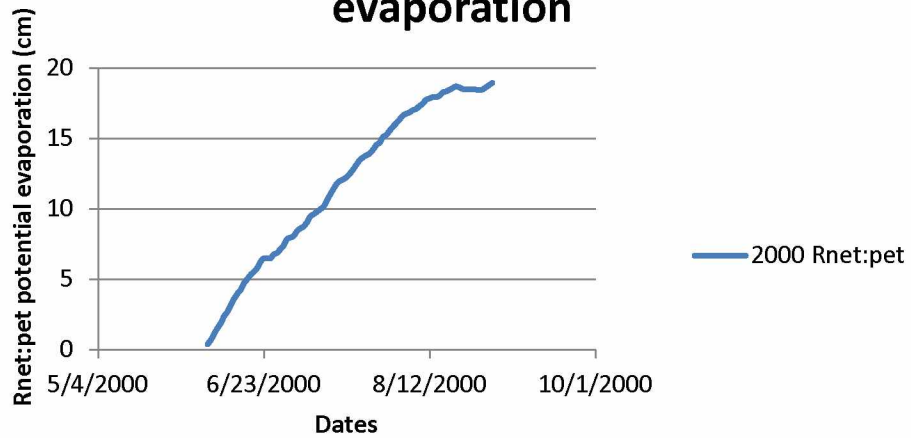
1998 Predicted Rnet potential evaporation



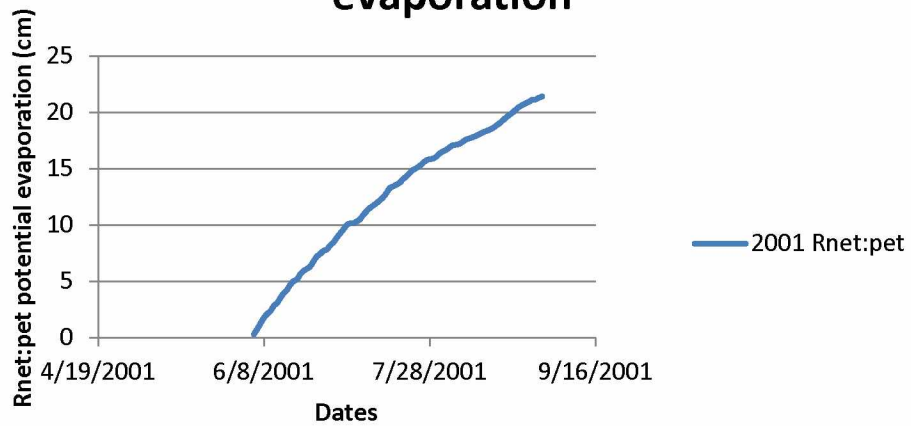
1999 Predicted Rnet potential evaporation



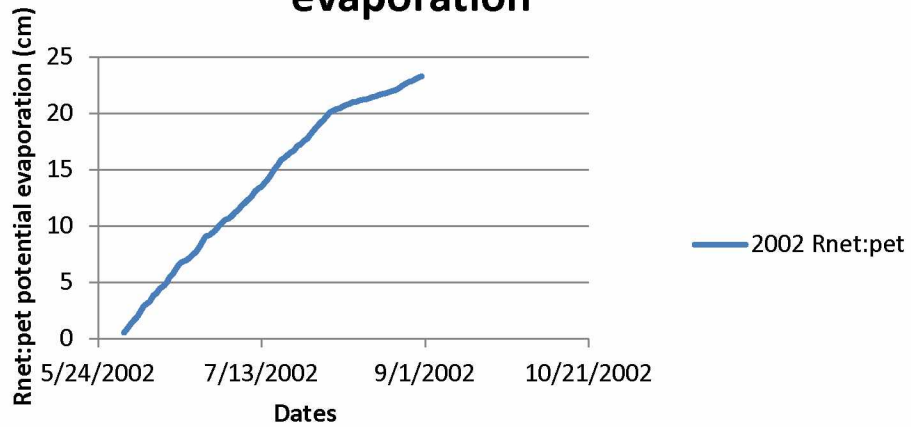
2000 Predicted Rnet potential evaporation



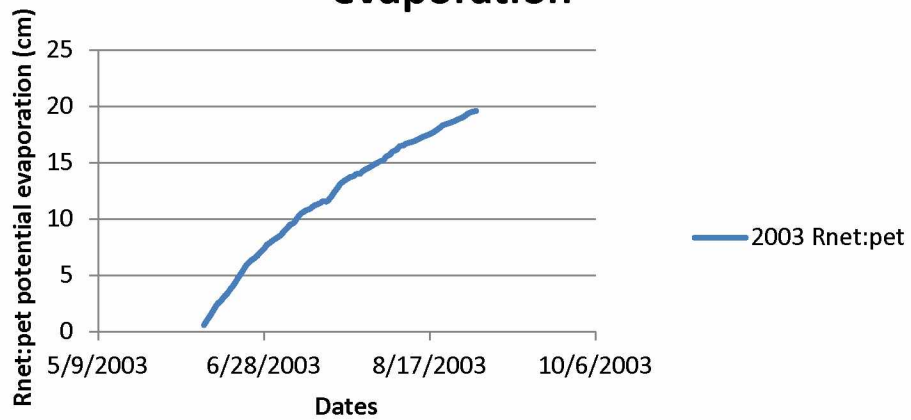
2001 Predicted Rnet potential evaporation



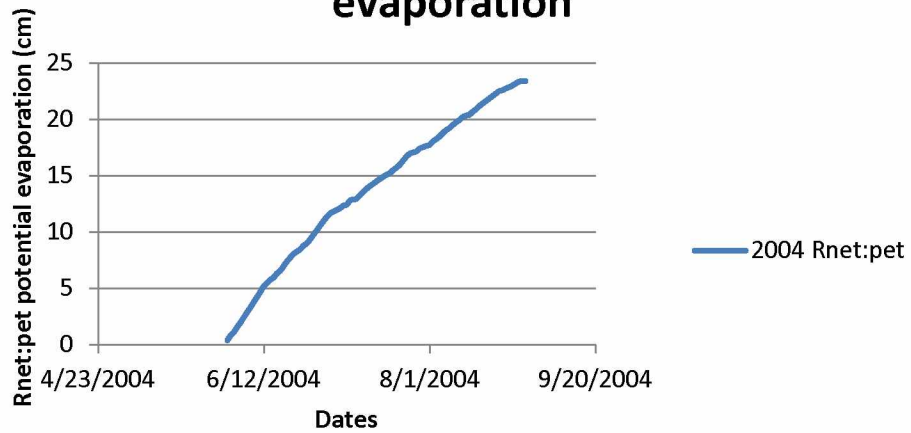
2002 Predicted Rnet potential evaporation



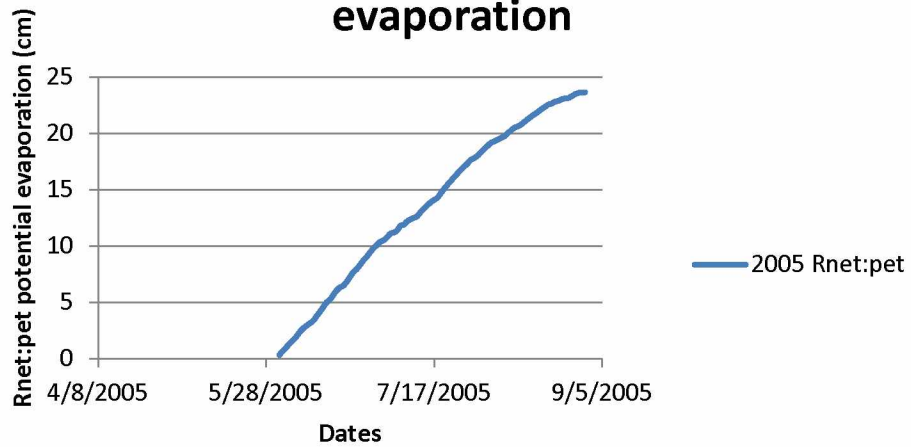
2003 Predicted Rnet potential evaporation



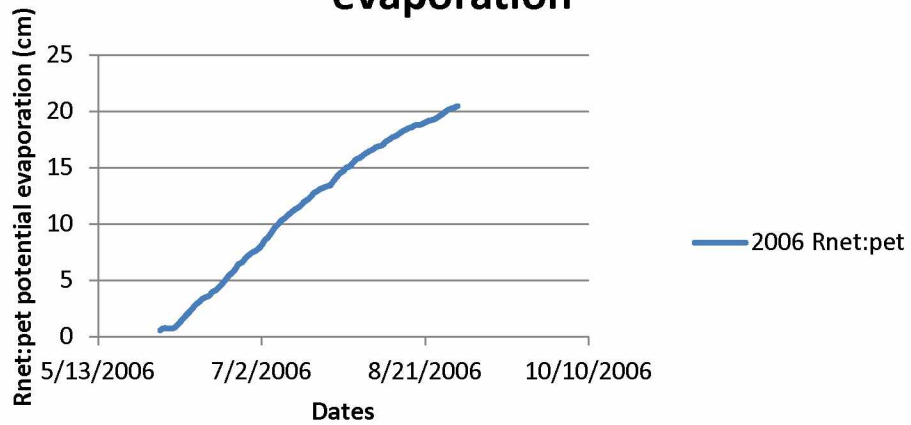
2004 Predicted Rnet potential evaporation



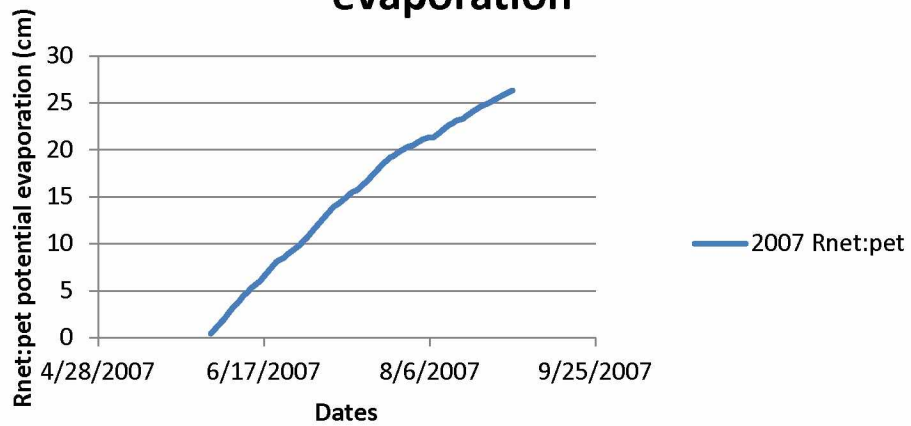
2005 Predicted Rnet potential evaporation



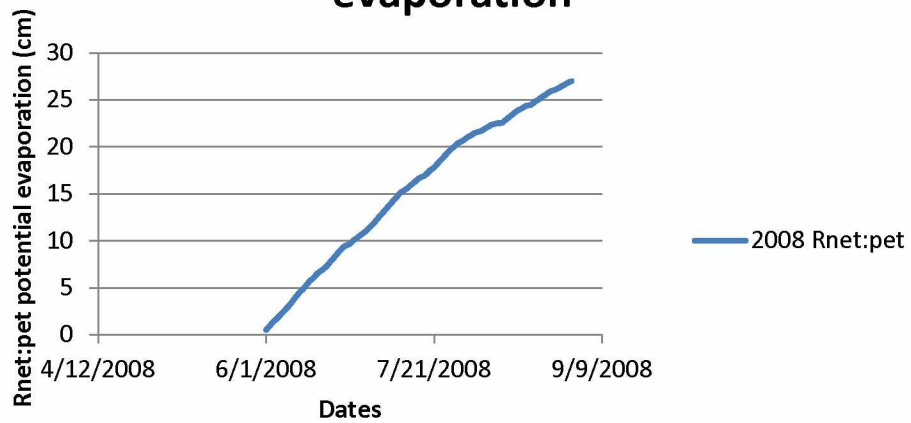
2006 Predicted Rnet potential evaporation



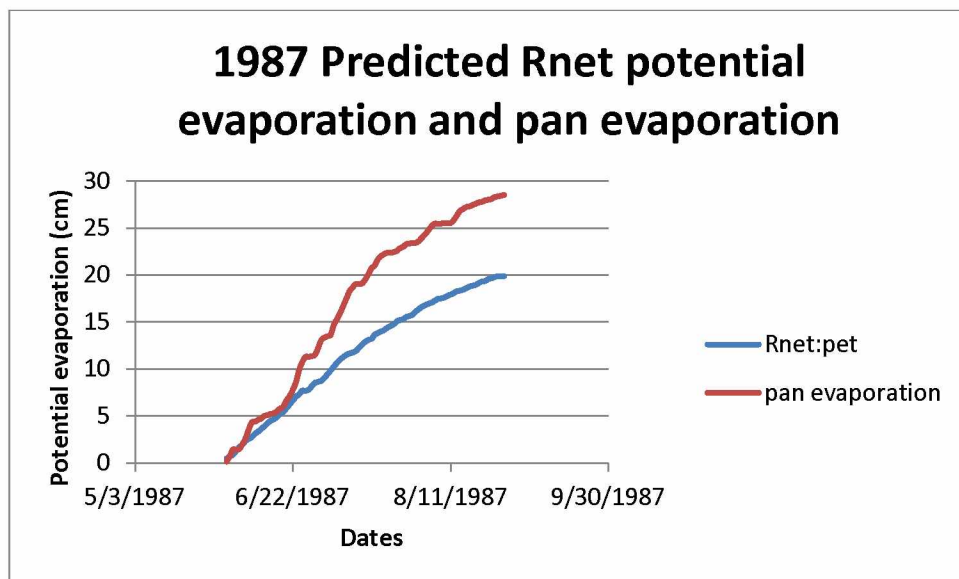
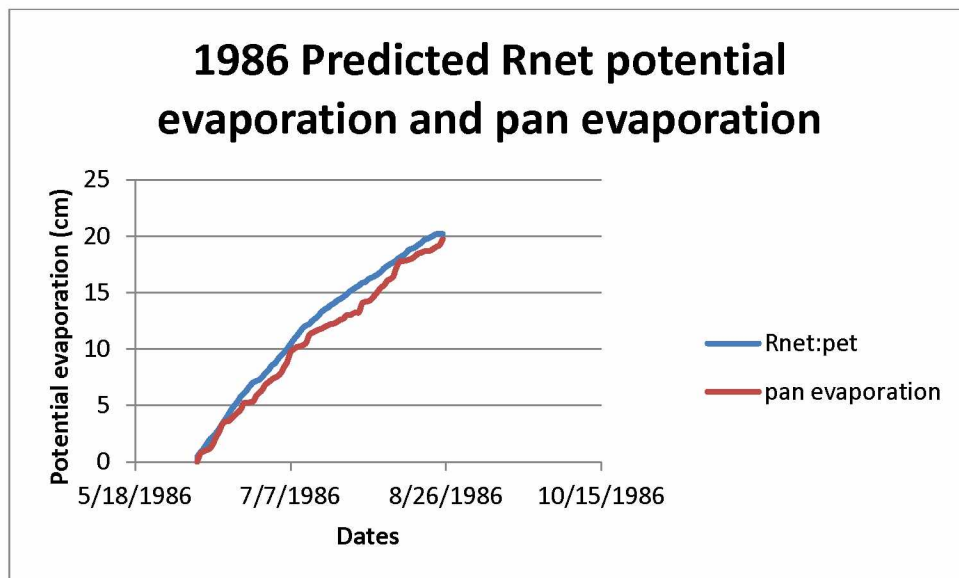
2007 Predicted Rnet potential evaporation



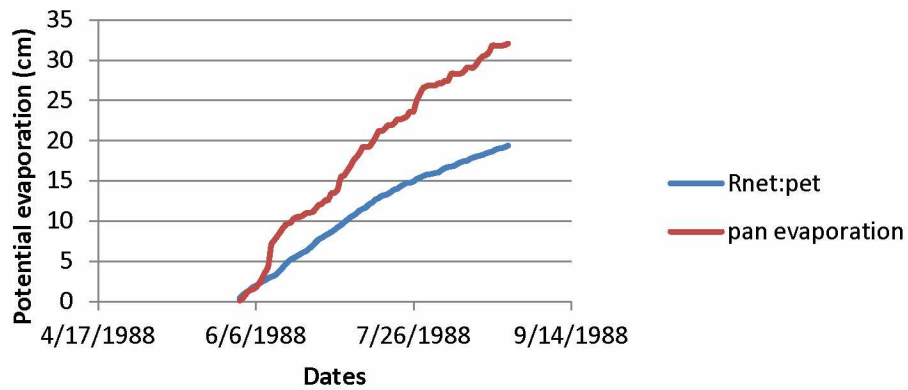
2008 Predicted Rnet potential evaporation



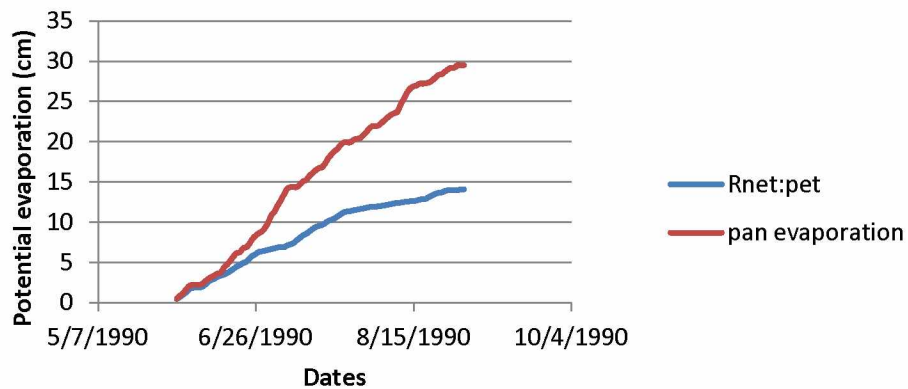
Appendix L: Warm Season Cumulative measured pan evaporation (potential evaporation) and Calculated potential evaporation using net radiation 1986-2008.



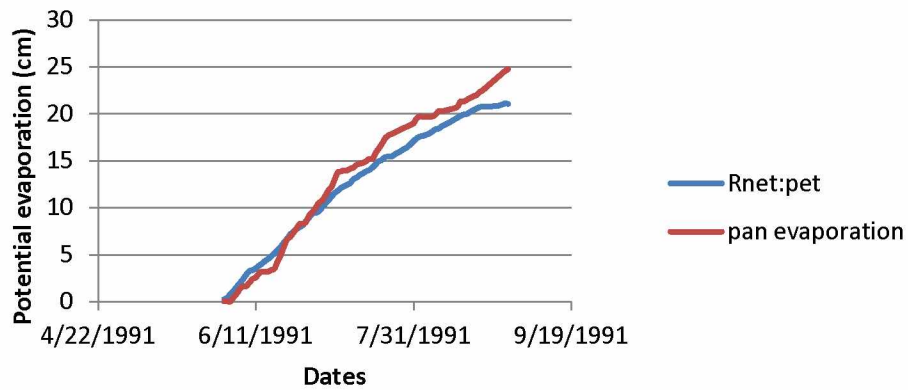
1988 Predicted Rnet potential evaporation and pan evaporation



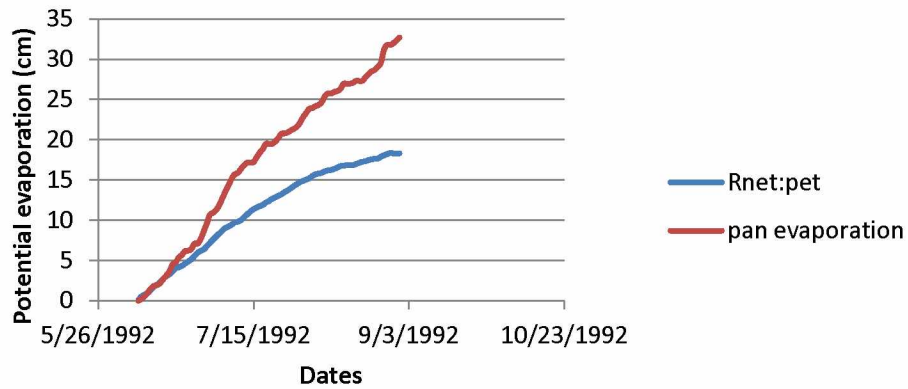
1990 Predicted Rnet potential evaporation and pan evaporation



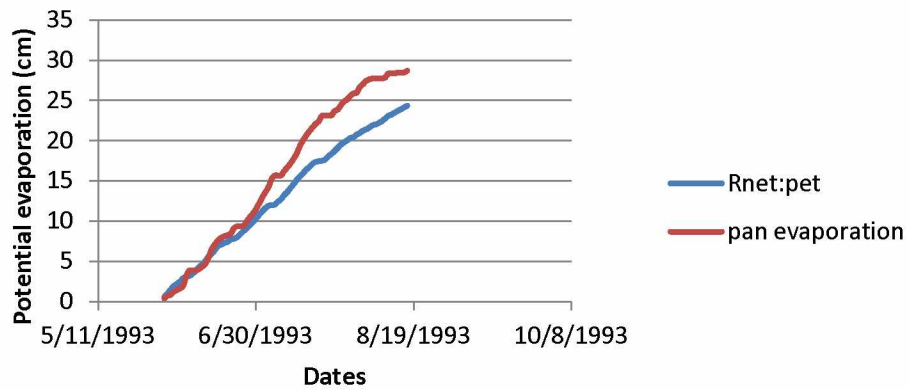
1991 Predicted Rnet potential evaporation and pan evaporation



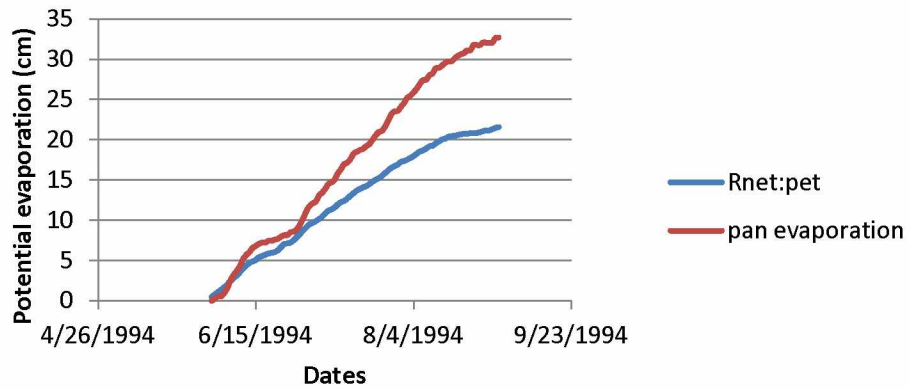
1992 Predicted Rnet potential evaporation and pan evaporation



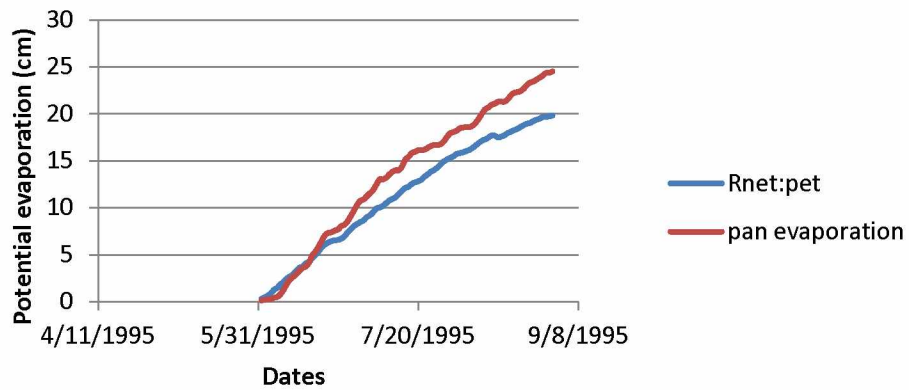
1993 Predicted Rnet potential evaporation and pan evaporation



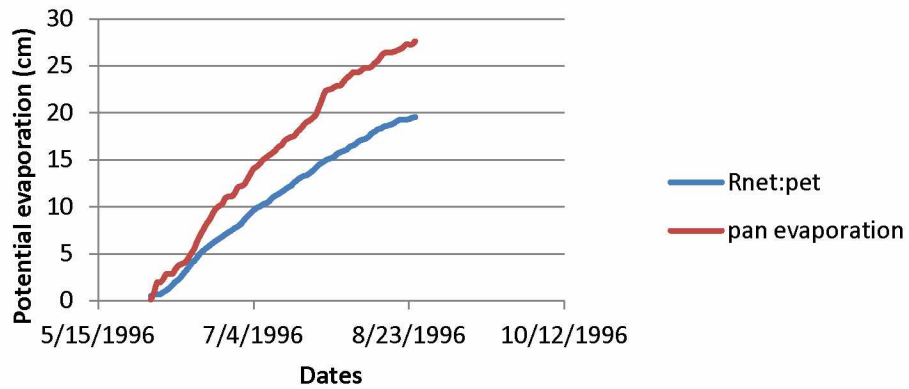
1994 Predicted Rnet potential evaporation and pan evaporation



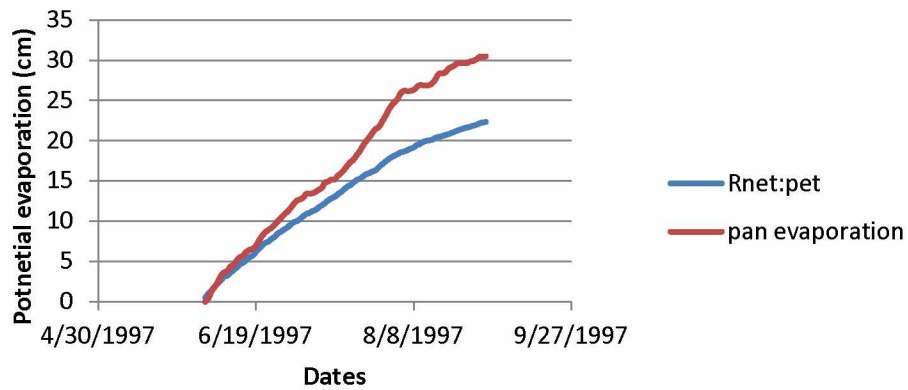
1995 Predicted Rnet potential evaporation and pan evaporation



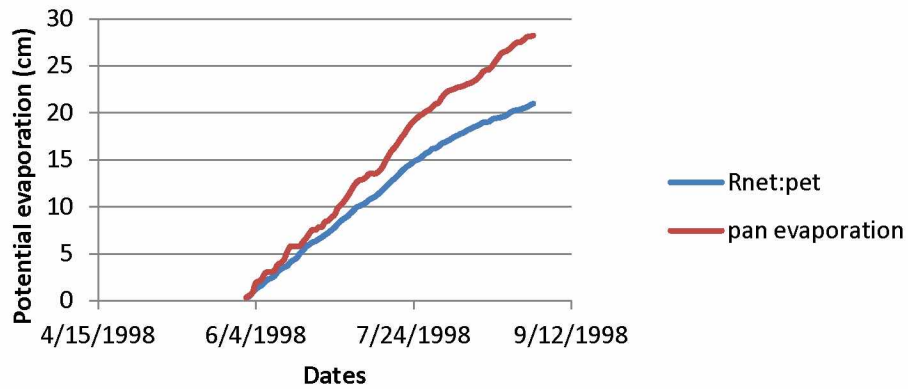
1996 Predicted Rnet potential evaporation and pan evaporation



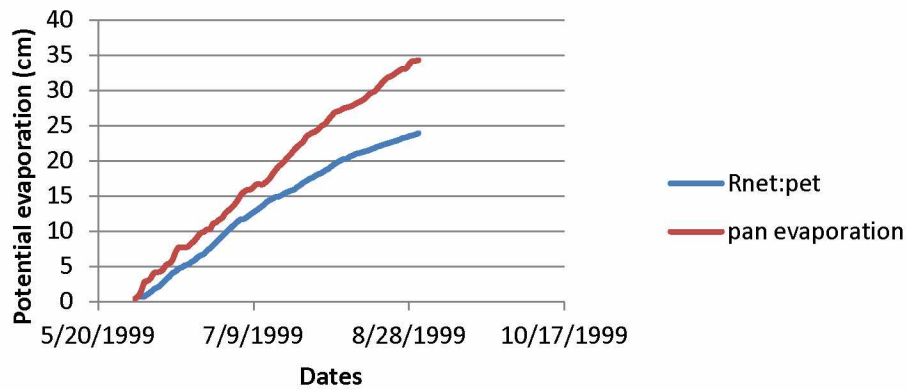
1997 Predicted Rnet potential evaporation and pan evaporation



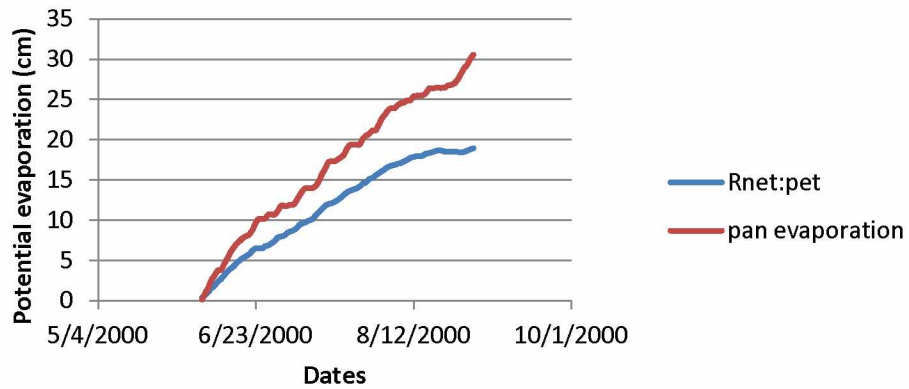
1998 Predicted Rnet potential evaporation and pan evaporation



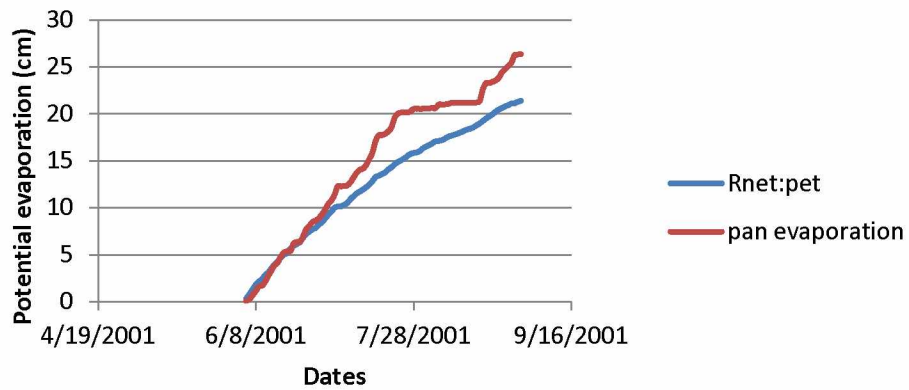
1999 Predicted Rnet potential evaporation and pan evaporation



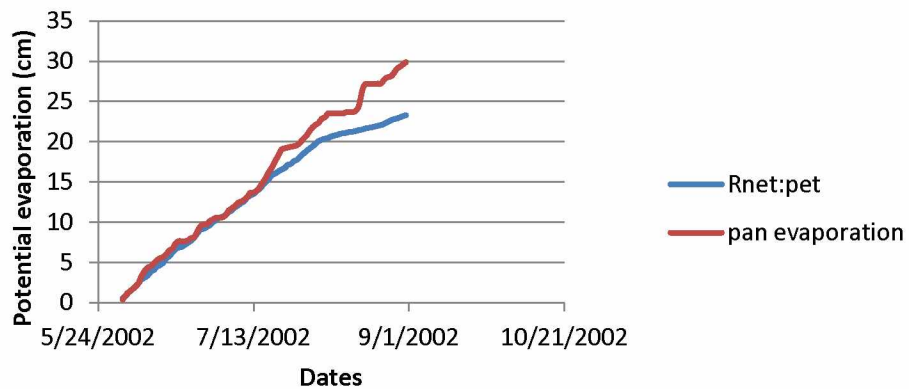
2000 Predicted Rnet potential evaporation and pan evaporation



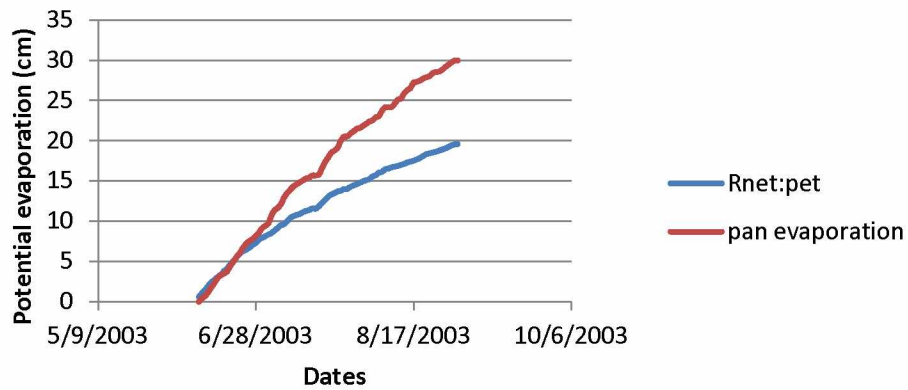
2001 Predicted Rnet potential evaporation and pan evaporation



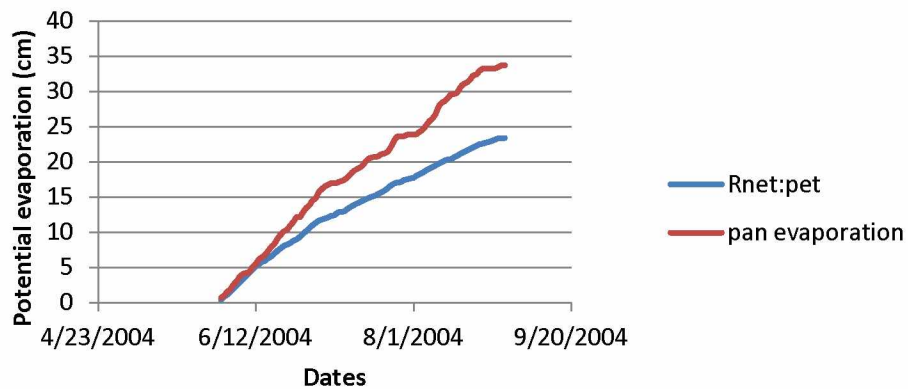
2002 Predicted Rnet potential evaporation and pan evaporation



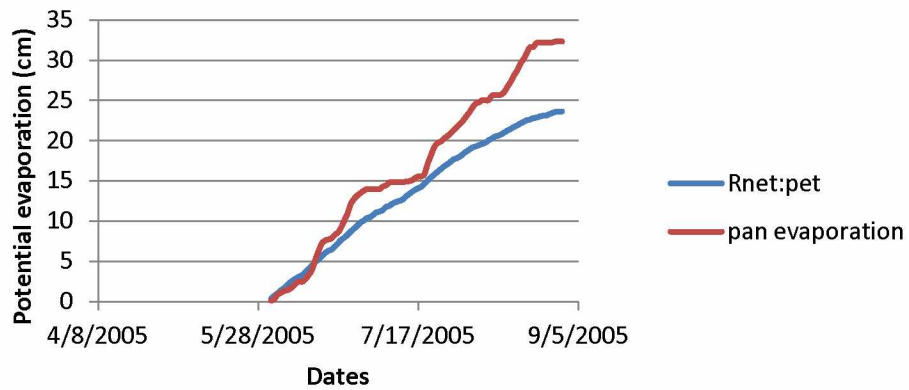
2003 Predicted Rnet potential evaporation and pan evaporation



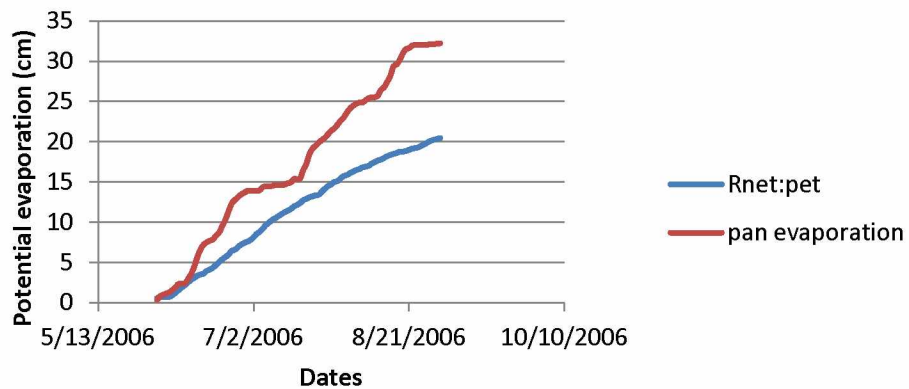
2004 Predicted Rnet potential evaporation and pan evaporation



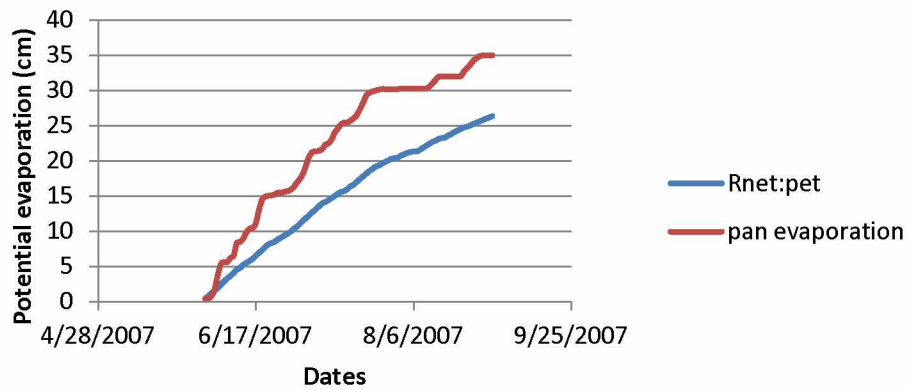
2005 Predicted Rnet potential evaporation and pan evaporation



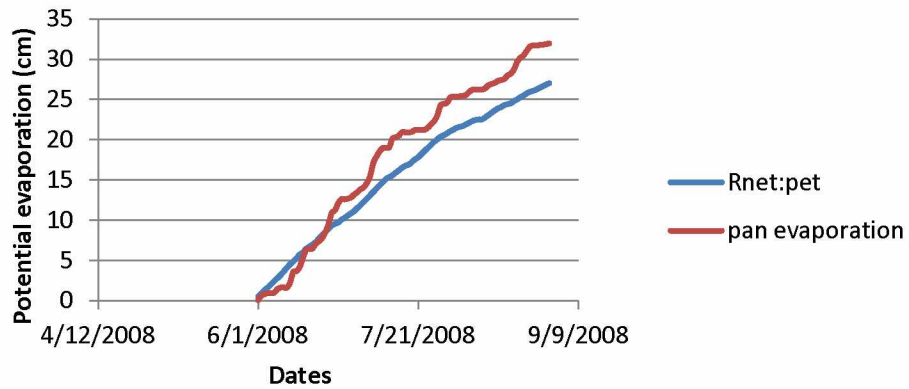
2006 Predicted Rnet potential evaporation and pan evaporation



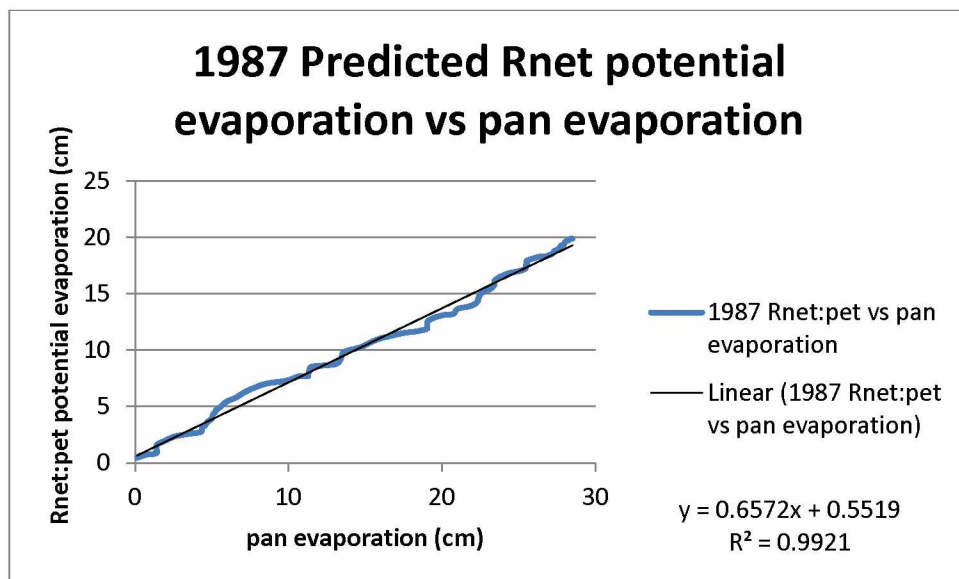
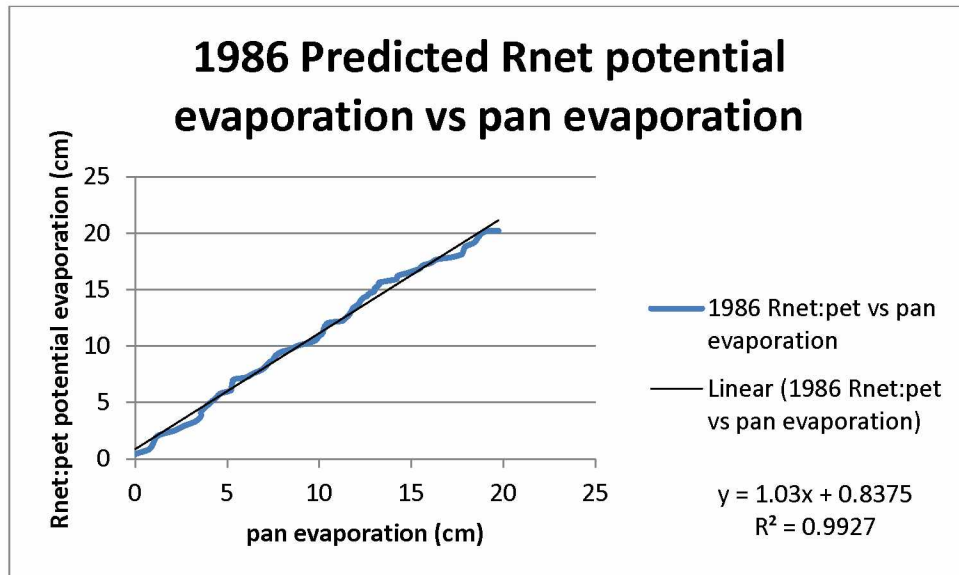
2007 Predicted Rnet potential evaporation and pan evaporation



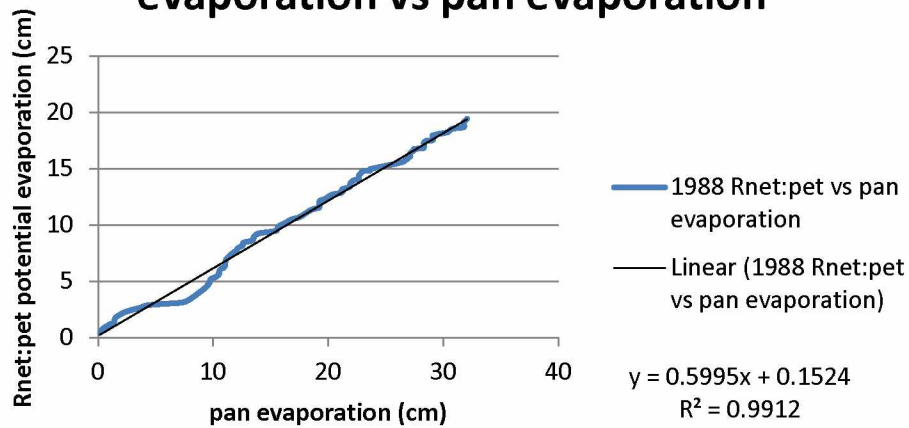
2008 Predicted Rnet potential evaporation and pan evaporation



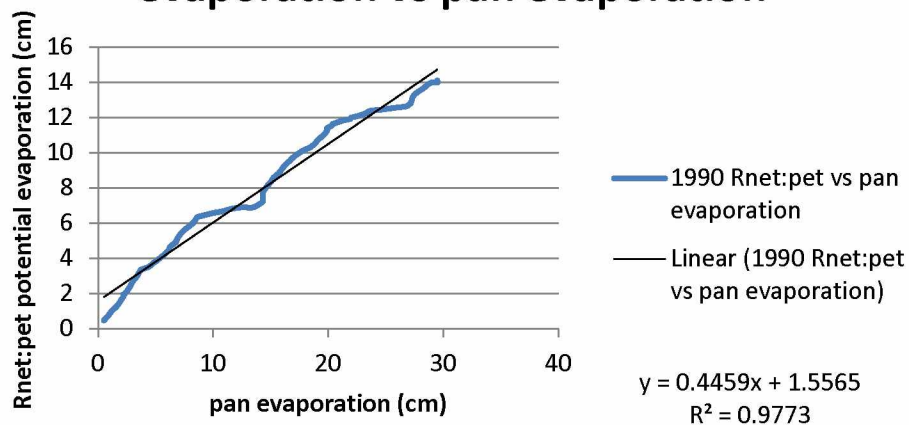
Appendix M: Warm Season Comparison between measured and calculated potential evaporation using net radiation and pan evaporation 1986-2008.



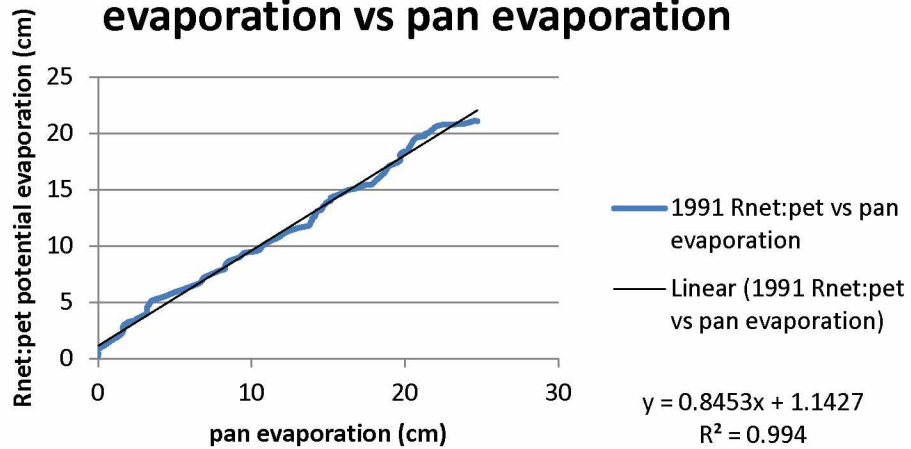
1988 Predicted Rnet potential evaporation vs pan evaporation



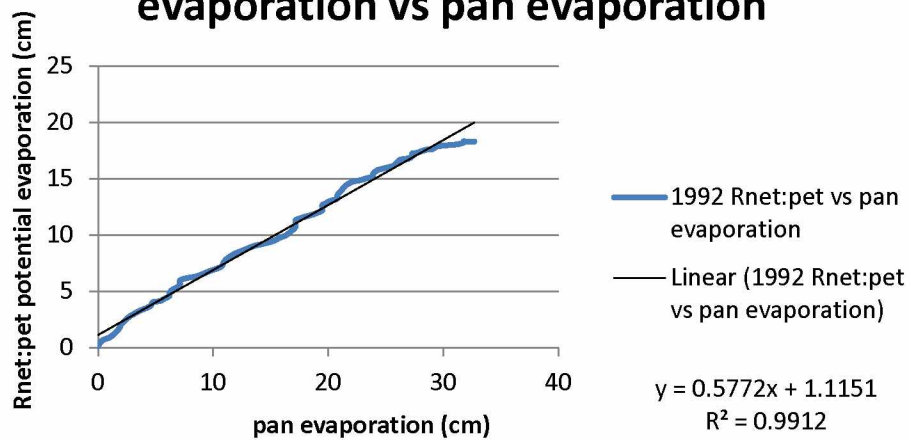
1990 Predicted Rnet potential evaporation vs pan evaporation



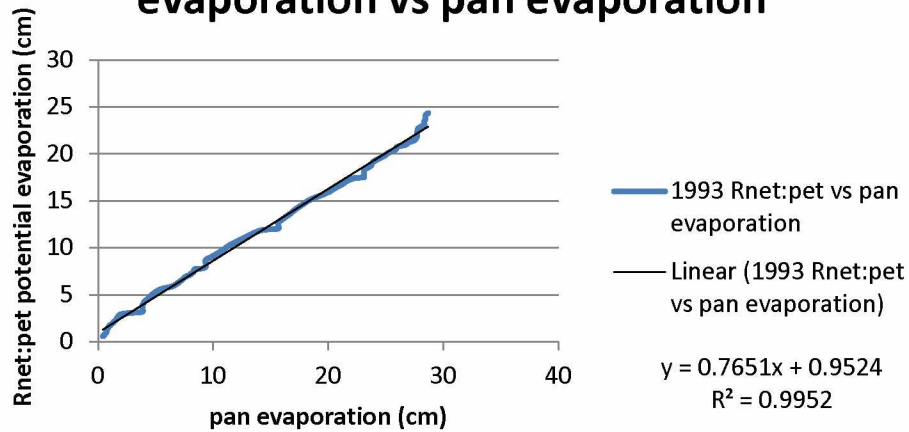
1991 Predicted Rnet potential evaporation vs pan evaporation



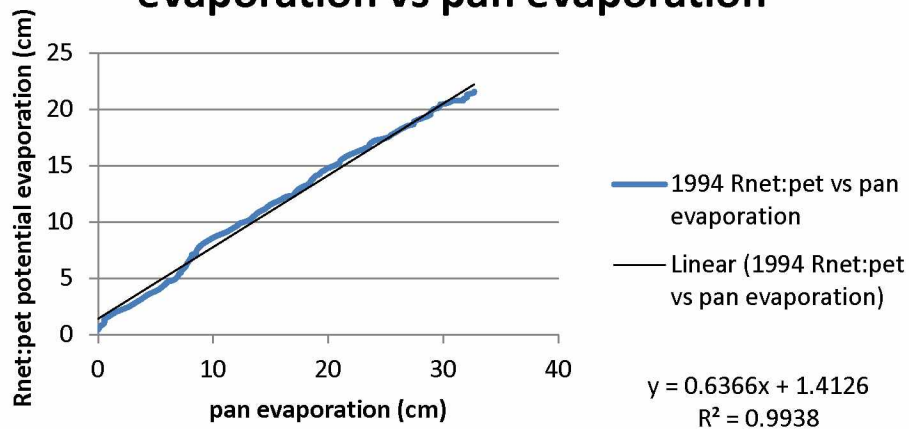
1992 Predicted Rnet potential evaporation vs pan evaporation



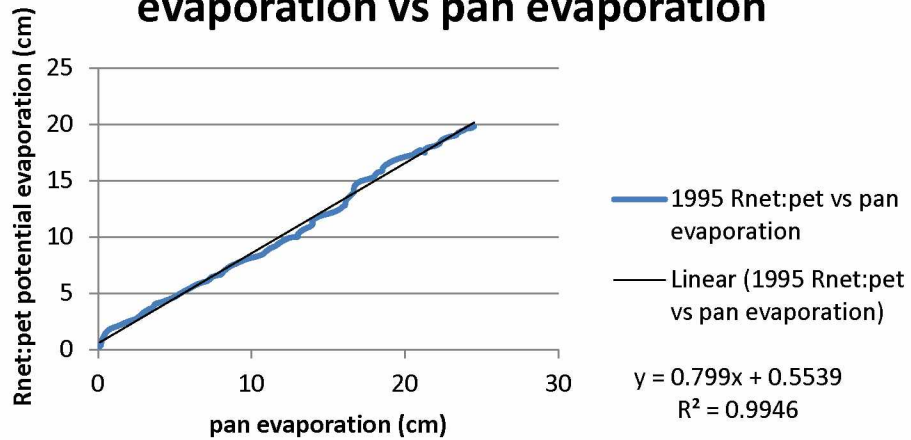
1993 Predicted Rnet potential evaporation vs pan evaporation



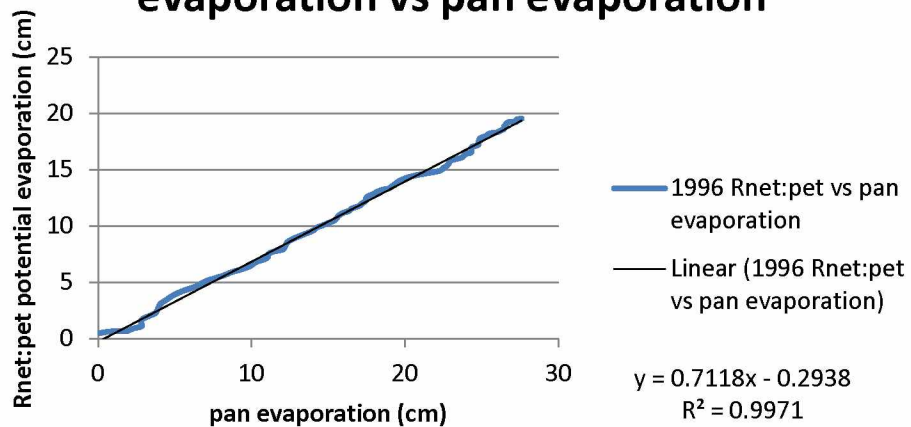
1994 Predicted Rnet potential evaporation vs pan evaporation



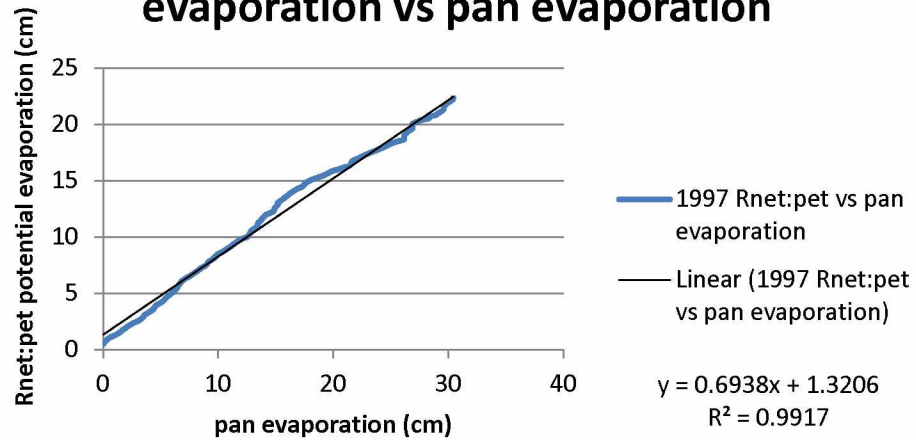
1995 Predicted Rnet potential evaporation vs pan evaporation



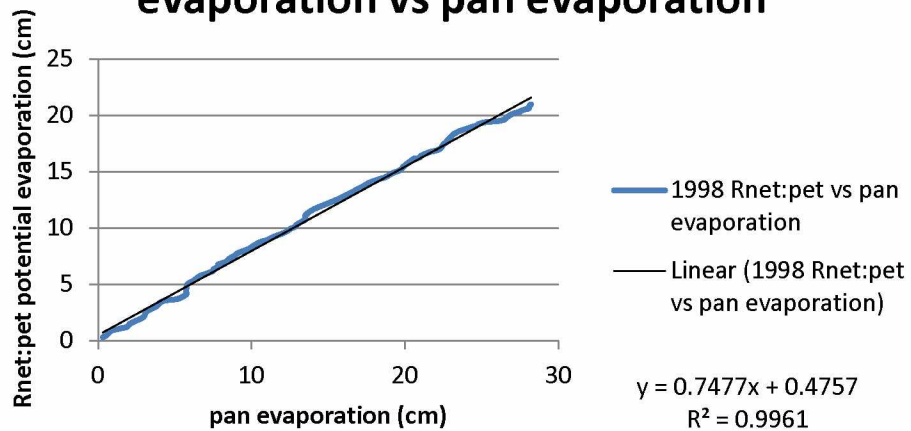
1996 Predicted Rnet potential evaporation vs pan evaporation



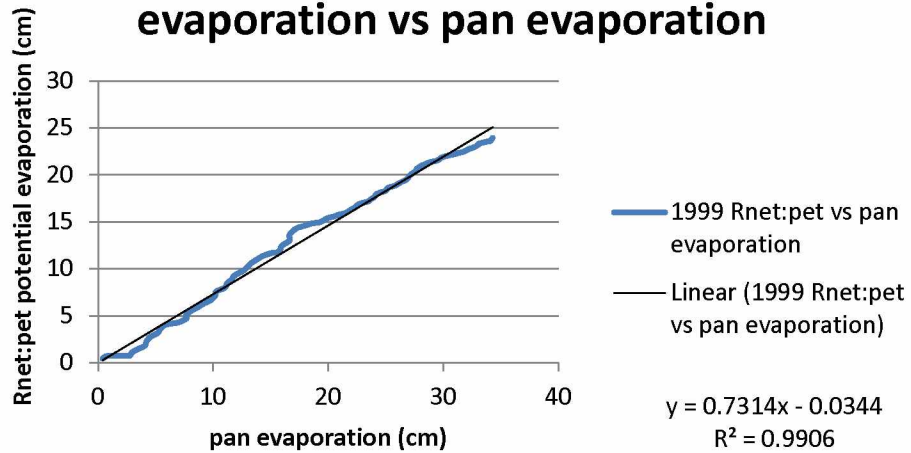
1997 Predicted Rnet potential evaporation vs pan evaporation



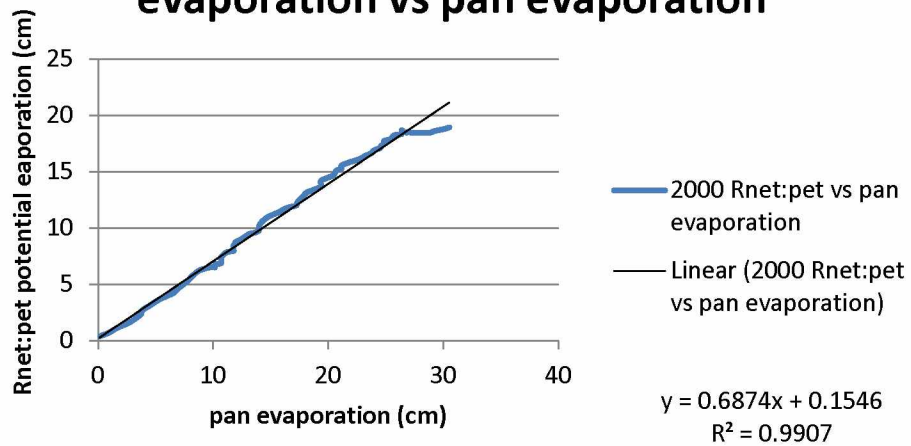
1998 Predicted Rnet potential evaporation vs pan evaporation



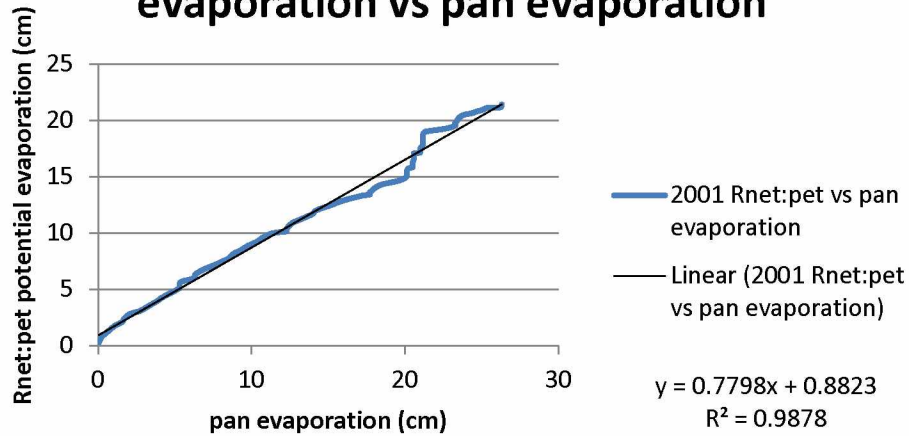
1999 Predicted Rnet potential evaporation vs pan evaporation



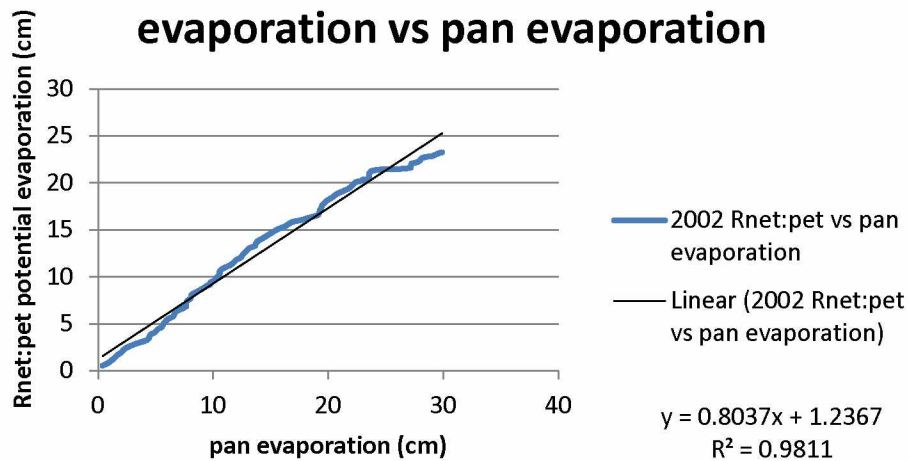
2000 Predicted Rnet potential evaporation vs pan evaporation



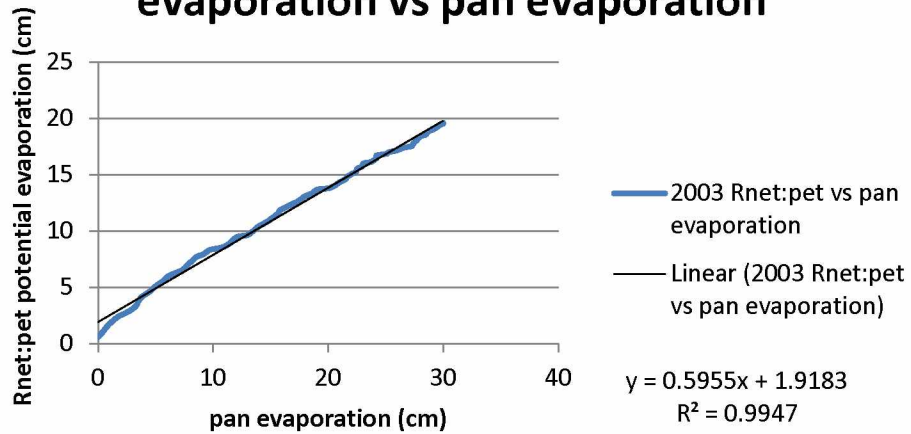
2001 Predicted Rnet potential evaporation vs pan evaporation



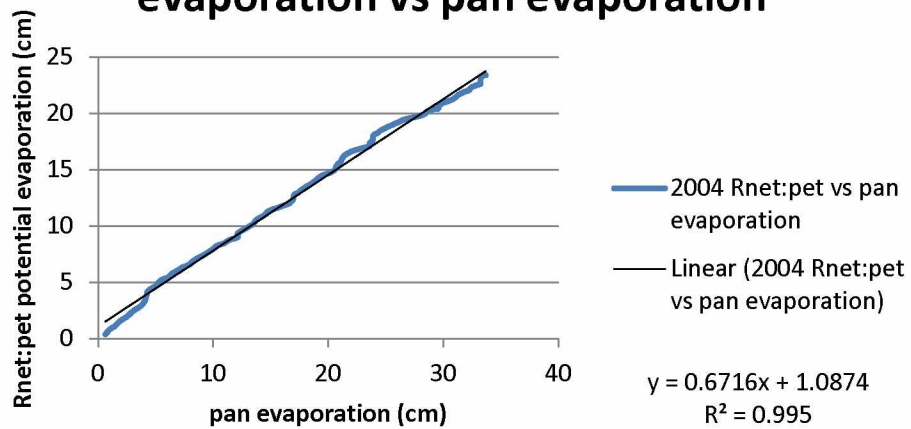
2002 Predicted Rnet potential evaporation vs pan evaporation



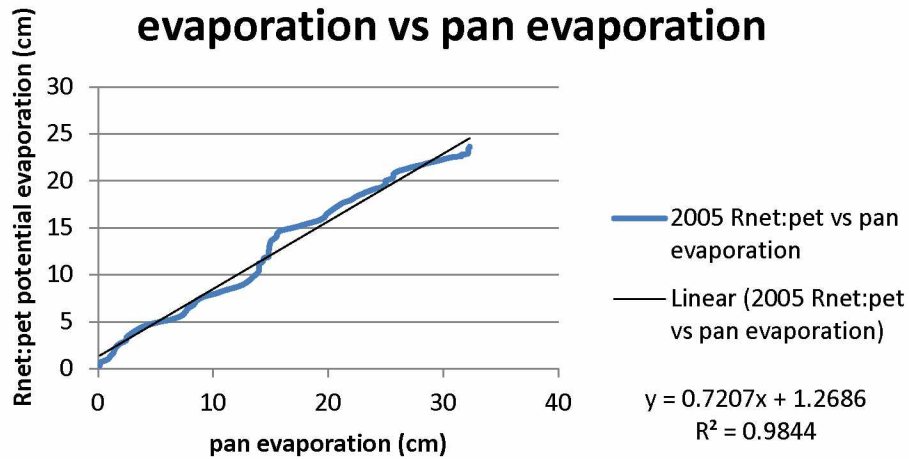
2003 Predicted Rnet potential evaporation vs pan evaporation



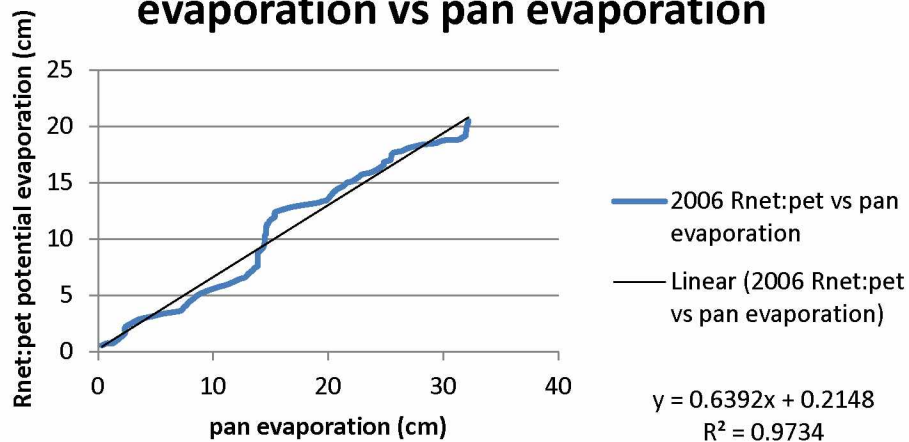
2004 Predicted Rnet potential evaporation vs pan evaporation



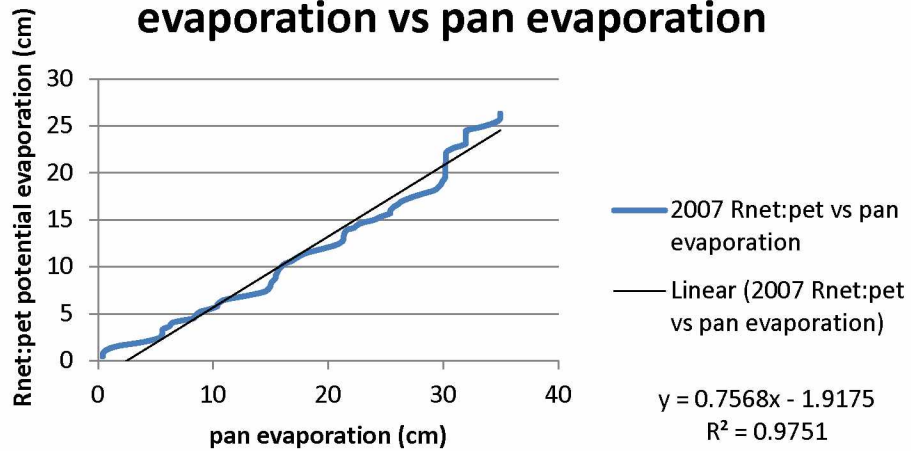
2005 Predicted Rnet potential evaporation vs pan evaporation



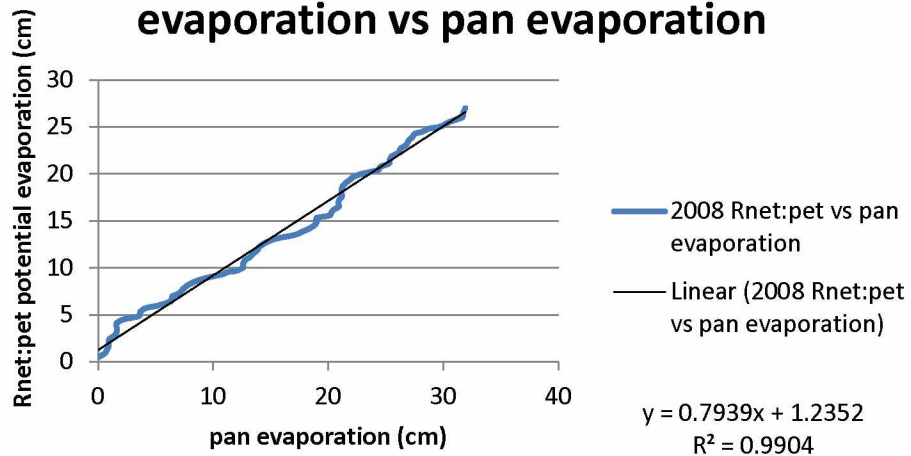
2006 Predicted Rnet potential evaporation vs pan evaporation



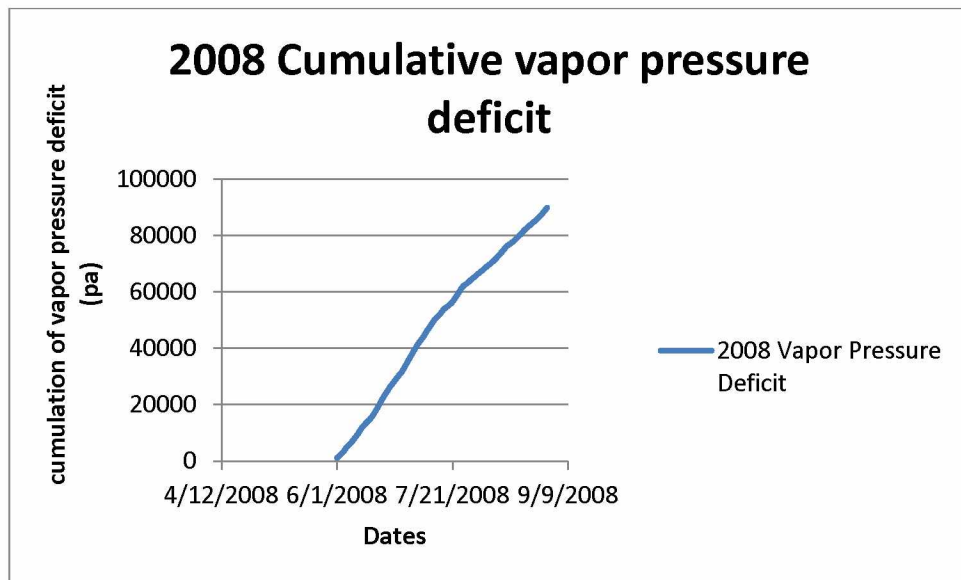
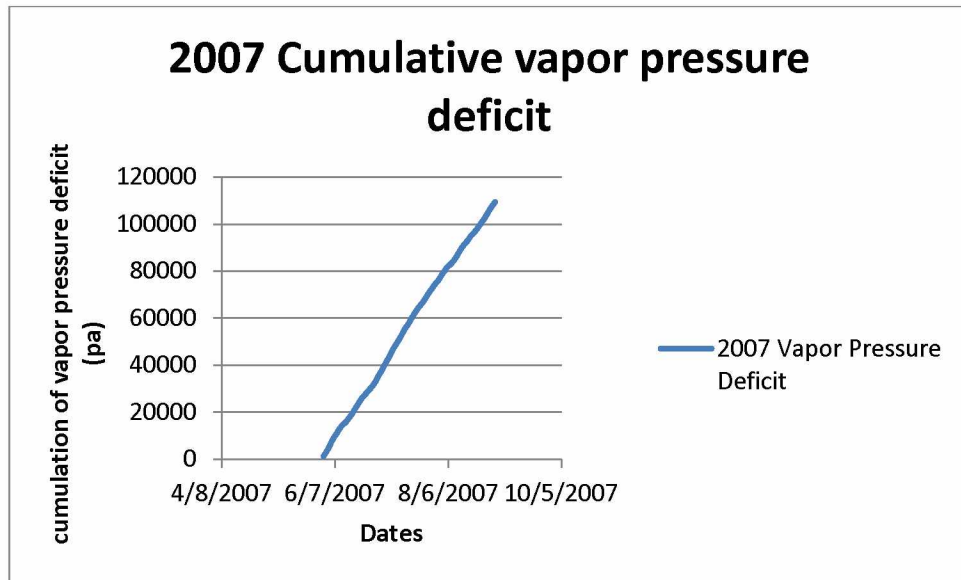
2007 Predicted Rnet potential evaporation vs pan evaporation



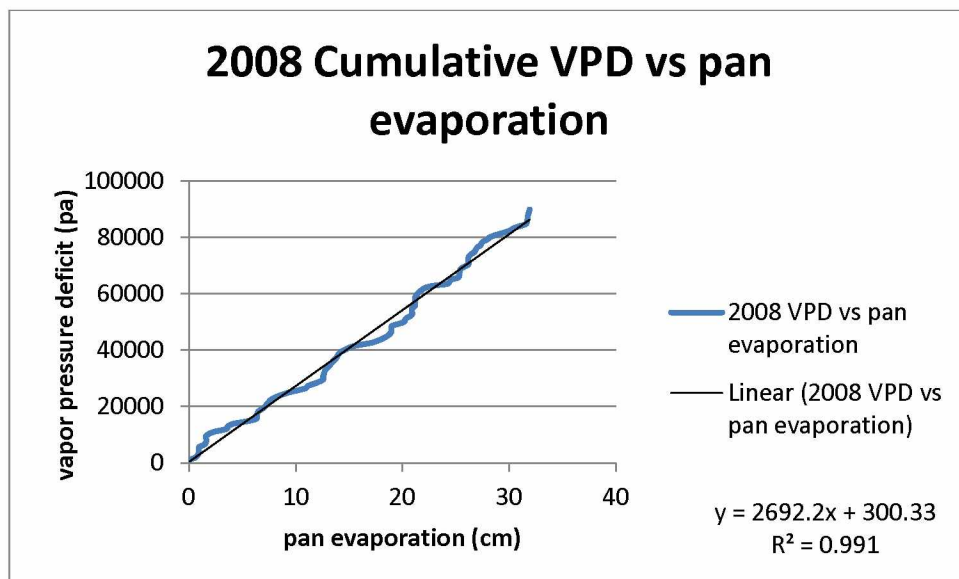
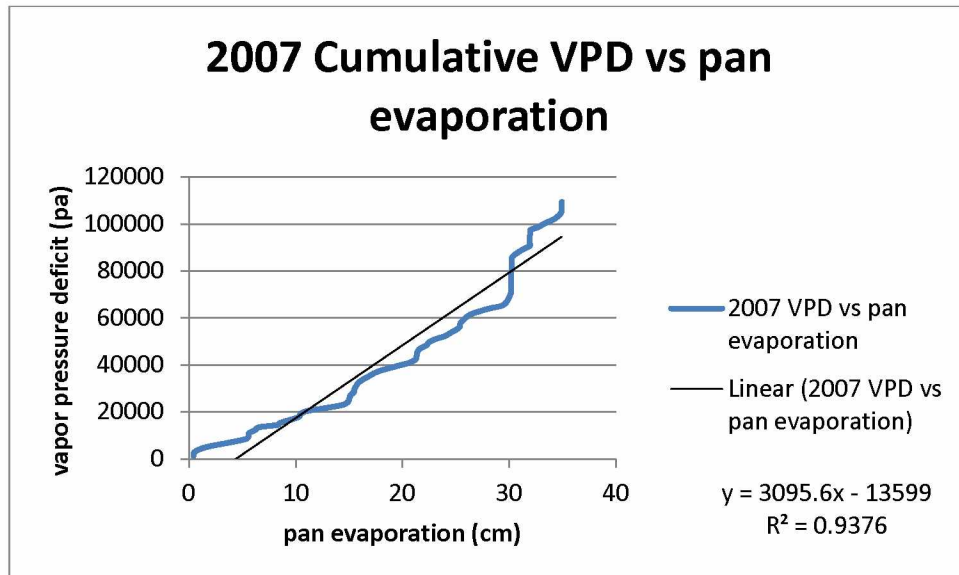
2008 Predicted Rnet potential evaporation vs pan evaporation



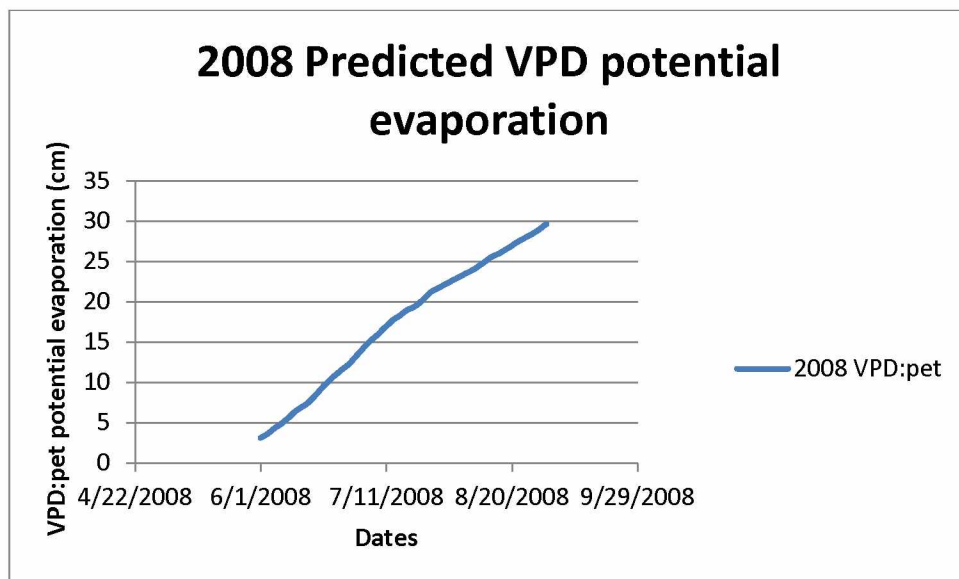
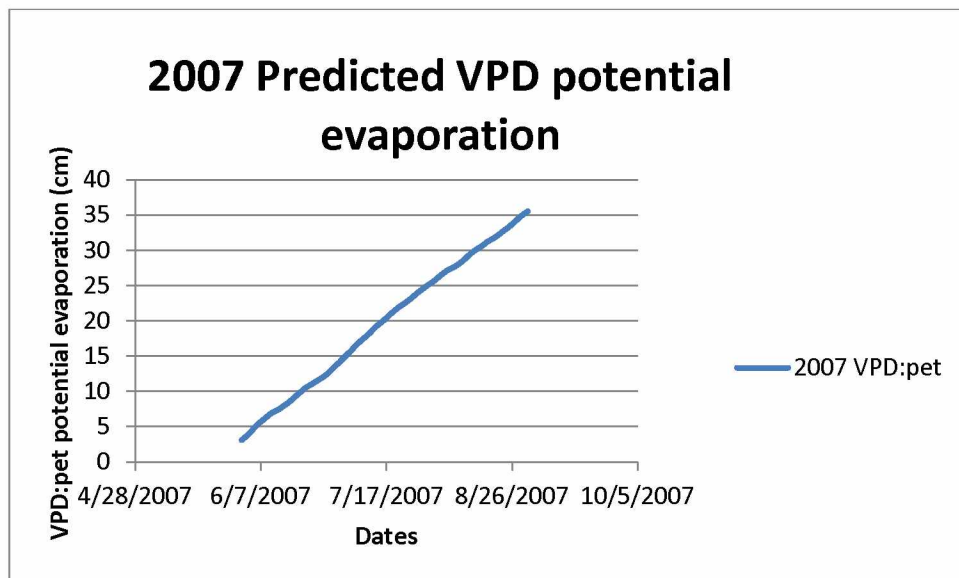
Appendix N: Warm Season Cumulative vapor pressure deficit 2007-2008.



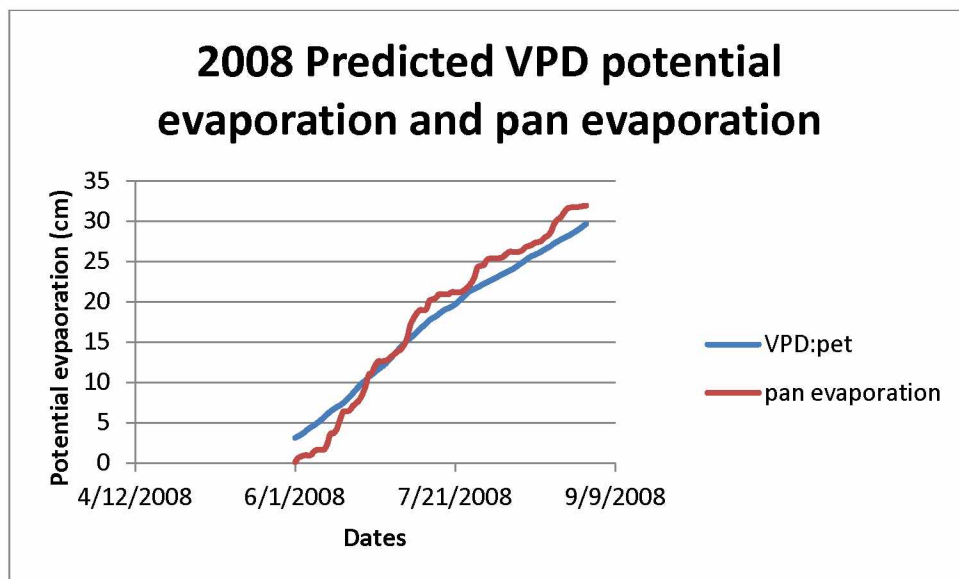
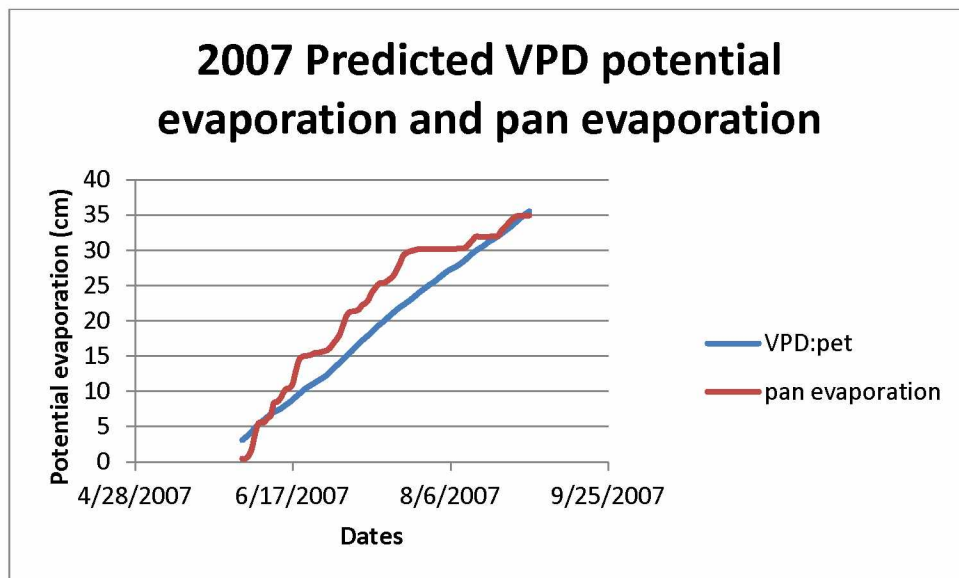
Appendix O: Warm Season Comparison (relationship) between vapor pressure deficit and pan evaporation (potential evaporation) 2007-2008.



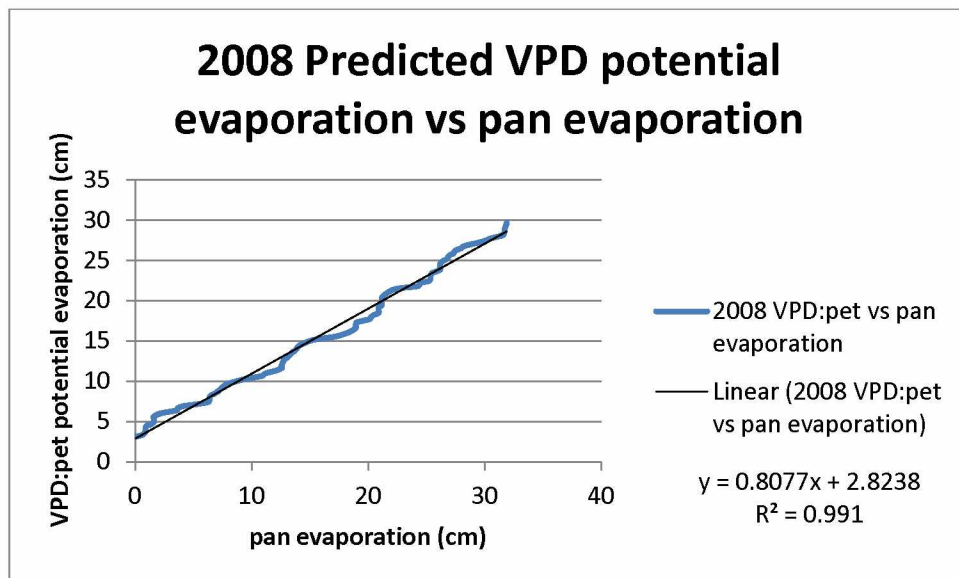
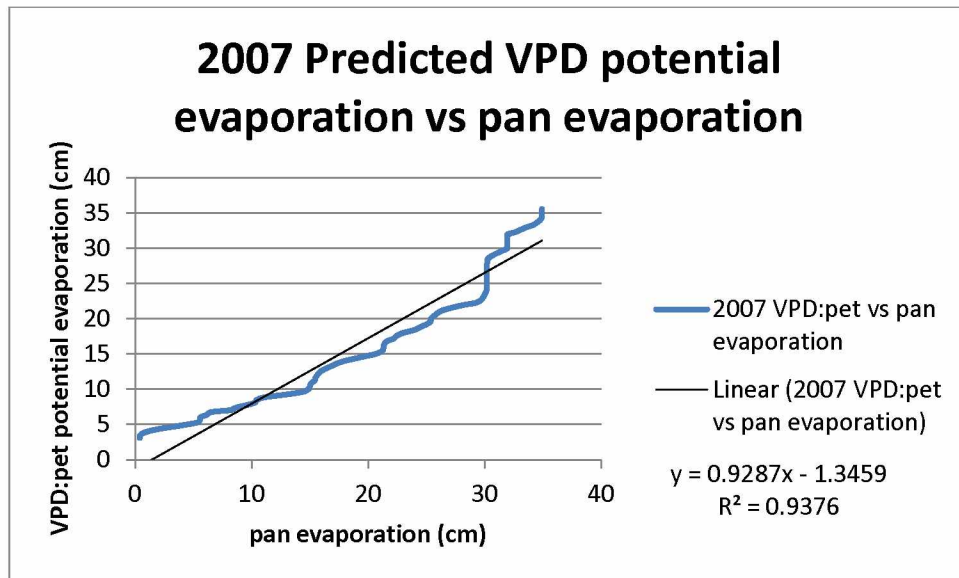
Appendix P: Warm Season Cumulative Calculated potential evaporation using vapor pressure deficit measurements 2007-2008.



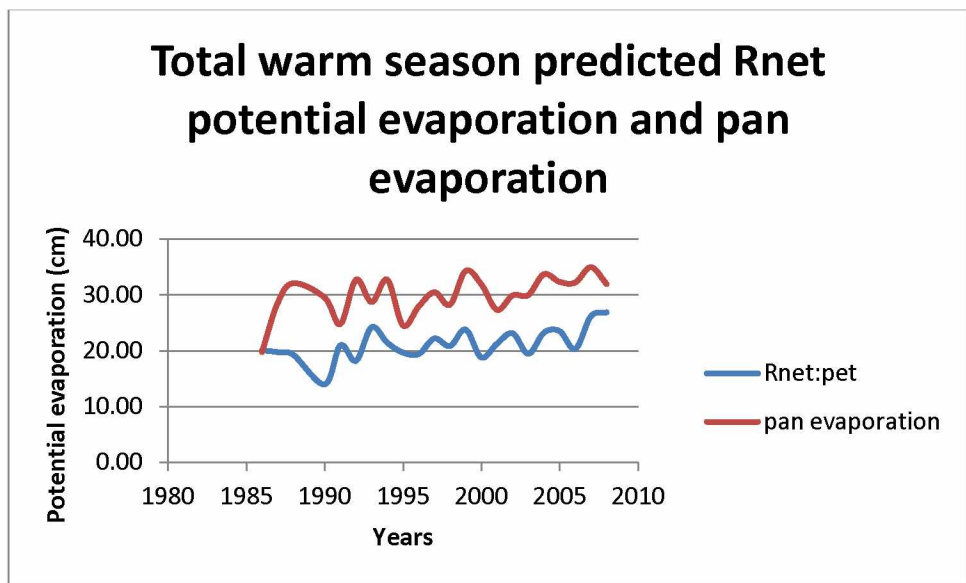
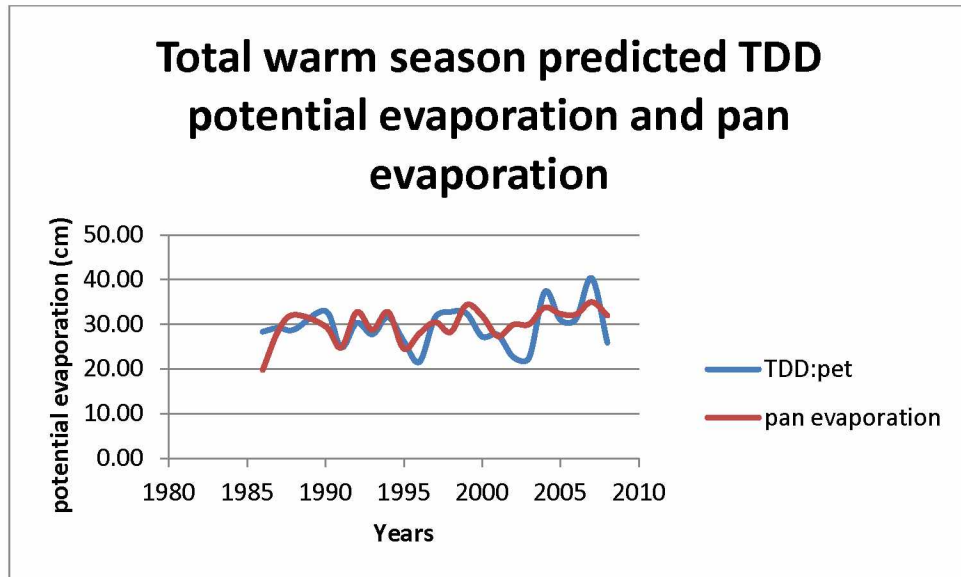
Appendix Q: Warm Season Cumulative measured pan evaporation (potential evaporation) and Calculated potential evaporation using vapor pressure deficit 2007-2008.



Appendix R: Warm Season Comparison between measured and calculated potential evaporation using vapor pressure deficit and pan evaporation 2007-2008.



Appendix S: Total warm season calculated potential evaporation using an environmental variable (TDD, Rnet, VPD) and measured pan evaporation



Total warm season predicted VPD potential evaporation and pan evaporation

